KGA 81

KÖLNER GEOGRAPHISCHE ARBEITEN

HEFT 81

Gerhard Schellmann & Ulrich Radtke

with contributions by Franziska Whelan

The Marine Quaternary of Barbados

GEOGRAPHISCHES INSTITUT DER UNIVERSITÄT ZU KÖLN

2004

KÖLNER GEOGRAPHISCHE ARBEITEN

Herausgegeben vom

GEOGRAPHISCHEN INSTITUT DER UNIVERSITÄT ZU KÖLN

durch

H. BESLER H. BREMER E. BRUNOTTE F. KRAAS J. NIPPER U. RADTKE
K. SCHNEIDER G. SCHWEIZER D. SOYEZ O. TIMMERMANN D. J. WERNER

Schriftleitung: D. WIKTORIN

Heft 81

Gerhard Schellmann & Ulrich Radtke

with contributions by Franziska Whelan

The Marine Quaternary of Barbados

GEOGRAPHISCHES INSTITUT DER UNIVERSITÄT ZU KÖLN

2004

Schellmann, Gerhard & Radtke, Ulrich:

The marine Quaternary of Barbados.

Köln: Selbstverlag Geographisches Institut der Universität zu Köln, 2004.
(Kölner Geographische Arbeiten, Heft 81)

Geographisches Institut der Universität zu Köln
- Kölner Geographische Arbeiten -
Albertus-Magnus-Platz, D - 50923 K ö l n
Telefax 0221 - 470 4917

ISSN 0454-1294
1. Auflage 2004

Layout: Gerhard Schellmann
Druck: Sutorius Printmedien GmbH & Co. KG, Köln

Preface

Today´s models of past sea-level change are complex. Although knowledge has increased enormously over the last forty years, many problems concerning the concepts of sea-level change still exist or have been detected recently. Substantial progress in this field of study is closely associated with four very successful IGCP sea-level projects, beginning with IGCP 61, and followed by IGCP 200, 274, and 367. However, this does not imply that research concerning terraces and problems of Pleistocene sea-level history in coastal geomorphology and geochronology, has lost its importance.

The 4th annual meeting of IGCP project 437 *Coastal Environmental Change During Sea Level Highstands: A Global Synthesis with Implications for Management of Future Coastal Change* (IGCP 437, President Colin Murray-Wallace, University of Wollongong, Australia) was held together with the International Conference "Barbados 2000: Quaternary Sea-level Change" (organizers Ulrich Radtke and Gerhard Schellmann) on Barbados from October 26th to November 2nd, 2002. During this conference, more than 70 scientists were introduced to key localities and issues of Quaternary sea-level research on Barbados during three days of field trips.

Barbados has been the Mecca for sea-level research since MESOLELLA's benchmark studies published in 1968. Numerous subsequent publications on the sea-level history of Barbados followed and make it difficult to keep up with newest developments in this field of research. During the conference, the organizers presented a *Field Guide,* which promised to offer more than a regular guidebook. It illustrated the history of sea-level research on Barbados and presented new geomorphic and geochronologic investigations of Barbados' fossil coral reef terraces, which have been conducted by a research group led by Prof. Ulrich Radtke (University of Cologne, Germany) and Prof. Gerhard Schellmann (University of Bamberg, Germany) since 1990. This research was initiated by advances in Electron Spin Resonance (ESR) dating of fossil coral, advances in the resolution of aerial photographs and their interpretation, and the dearth of detailed geomorphic maps depicting preserved fossil beach formations and reef terraces. This new research, based largely in the southern part of the island, has required the revision of previously published morpho- and chronostratigraphies for Barbados.

This textbook, published by „Kölner Geographische Schriften" in 2004, largely mirrors the *Field Guide,* which was accessible to conference attendees only. It comprises six chapters, ranging from a general overview to detailed morphostratigraphic descriptions. Chapter 1 provides some background information to those readers who have never been to the Caribbean or are unfamiliar with this region, its climate, tectonic setting, and the Caribbean coral reefs. Chapter 2 focuses on the geology and physical geography of Barbados and provides an overview of the hydrology, karst formations, soils, and vegetation. Chapter 3 reviews previous sea-level research carried out on Barbados and pays particular attention to the famous geological traverses across the coral deposits of South Barbados (Clermont Nose and Christchurch). This review is additionally important because many coral samples collected in the 1960's and 70´s were redated as part of the current research program. Chapter 4 resents the main research findings of our research. It includes extensive new data on the geomorphology, geology, and geochronology of southern Barbados, and details estimates of Pleistocene palaeo sea-level changes. Chapter 5 considers other localities beyond the main research area on southern Barbados, including central Barbados with its older terraces, and areas at the west, north, and southeast coast. Chapter 6 summarizes the results presented in this book and outlines perspectives of future research related to the reconstruction of palaeo sea levels on Barbados, and global aspects of Quaternary sea-level reconstruction.

We recognize that the research detailed here is incomplete in that its emphasis is mainly on the southern part of Barbados. A complete synopsis of the Quaternary of Barbados is clearly desirable, but the comprehensive chronostratigraphic mapping of all reef terraces on Barbados would require another research project of more than 10 years, and this is beyond our current remit. In addition, we note that at present the chronological framework of our work is limited to the last 600,000 years, which is the upper limit of existing dating techniques for fossil corals. Despite these limitations, we believe that this textbook provides a comprehensive coverage of the important concepts and principles of geomorphic, geochronologic, and sea-

level research on Barbados. As such, the research provides a sound basis for the discussion of coral reef stratifications and tectonics of Barbados, and palaeo sea level changes in the Caribbean more widey.

We would like to thank the Deutsche Forschungsgemeinschaft (German Research Foundation), for their generous financial support (projects Ra 383/6-1, 6-2, and 6-3) that made this research, including field work on Barbados and laboratory work at the University of Cologne, Germany, possible. We are also grateful for the financial support of our ESR research provided by the University of Bamberg, Germany (project Sch 050302-21) and the University of Essen (project FP Sch 99).

Thank you to Dr. Franziska Whelan for her contributions to this publication and for editing the manuscript. Figures and tables in Chapters 1, 2, 4, and 5 were prepared by G. Schellmann (*G. Sch.*), figures and tables in Chapter 3 by U. Radtke. The preparation of the numerous graphics included in this publication would not have been possible without the assistance of several graduate students and staff. Many thanks to Ms. Andrea Zoll, Ms. Gabriele Riedl; and Ms. Dipl.-Geog. Silke Schwieger (University of Bamberg, Germany), Ms. Dipl.-Ing. Gudrun Reichert and Ms. Anne Hager (University of Essen, Germany), and Mr. Jürgen Kubelke (University of Cologne, Germany) for their cartographic assistance.

We are grateful to Ms. Christine Ksciuczyk (University of Cologne, Germany) for her diligent and meticulous application of ESR and X-ray diffraction measuring of our numerous samples during the last five years. For helpful comments we would like to thank Dr. Ruth Lyons (Auckland, New Zealand), Dr. Antony Long (University of Durham, UK), Karen Schneider (Cologne), and Volkmar Schultchen (Wuppertal). Thank you to our graduate students and research assistants who were involved in the completion of this textbook. Thanks also to the publishers of the "*Kölner Geographische Schriften*".

We hope that this textbook on "The marine Quaternary of Barbados" will inspire new discussions about the classical Barbados model of sea-level change and help stimulate further advances in this field of research.

Gerhard Schellmann

Ulrich Radtke

List of Figures

List of Photos

List of Tables

1. Introduction

G. SCHELLMANN, F. WHELAN, U. RADTKE

The Island of Barbados is located in the eastern Caribbean Sea, approx. 150 km east of the Lesser Antilles, between 13°02' and 13°10'N latitude and 59°25' and 59°39'W longitude (Figure 1.1). The island extends approx. 32 km from north to south, 24 km from east to west, and is approx. 430 km² large. The coastline has a total length of approx. 95 km. Mt. Hillaby, which is located in central Barbados, is the island's highest point with an elevation of 343 m above sea level (asl.).

Figure 1.1: The location of Barbados.

The Caribbean side of the island is dominated by steep cliffs that are divided by bays and white sandy beaches consisting of calcareous sand and coral rubble with some pebbles and flat coral cobbles (Photo 1.1). In contrast, the Atlantic side of the Scotland District is characterized by long beaches (Photo 1.2) with darker beach sand and a higher silicate content. These are the erosive products of the sedimentary rocks present in this region.

Tides are semidiurnal; spring tides have a range of 1 m on the west coast while the amplitude of neap tides is less than 0.3 m (BIRD et al. 1979). Mean water temperatures range from 29.5°C in summer to 26°C in winter on the Caribbean side of the island, and salinity varies between 3.2% and 3.6% (SANDER & STEFFENS 1973).

Amerindians, who arrived from Trinidad or northern Venezuela, were the first settlers on Barbados about 2000 BC (DREWETT 2002). They were followed by more advanced Amerindian tribes approx. 1000 to 500 ^{14}C years ago (WHITING et al. 2001), who were killed soon after the first Europeans arrived on the island in the early 1500s. In 1536, Spanish and Portuguese sailors named the island "Isla de los Barbados" (island of beard carriers). This name derived from the ficus trees with its long aerial roots hanging in the air like long beards.

However, the Spanish and Portuguese had no interest in settling on the island, as there appeared to be no mineral resources. The British merchant Captain John Powell formally claimed Barbados for the British, and in 1625 it became a British colony. Between 1627 and 1640, British and enslaved Africans, which planted tobacco and cotton, settled on the island. The introduction of sugar in the 1650s led to the development of large plantations. Barbados had 745 plantations by the end of the 18th century. Slavery was abolished in 1833/34, after which the plantations were worked by Asian indentured laborers.

In 1639, a parliament was established on the island and became the third oldest after London and the Bermudas. The English influence, which lasted for more than 300 years, significantly affected the culture on Barbados; Caribbean's frequently call the island of Barbados "Little England". Based on English tradition, the island was divided into 11 church

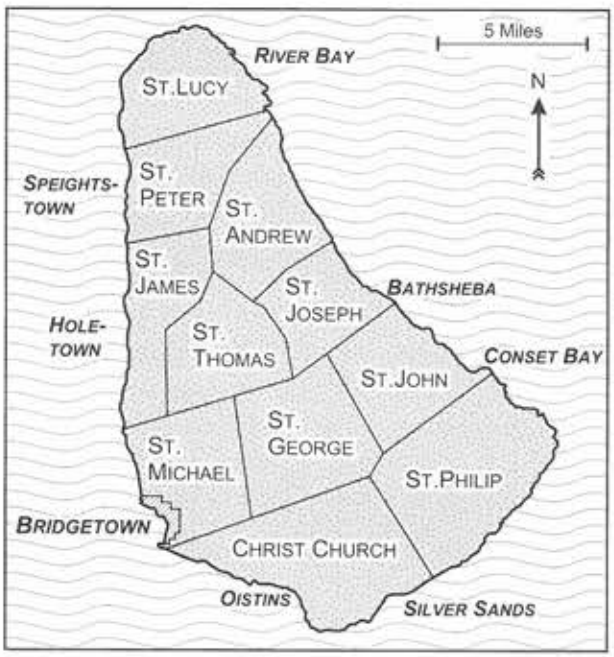

Figure 1.2:
Overview of the church districts of Barbados.

Photo 1.2:
Atlantic coast on the eastern side of Barbados (Scotland District near Bathsheba).
(Photo: SCHELLMANN 1997)

Photo 1.1:
Cave Bay is one of many bays with sandy beaches and beach rock deposits on the Caribbean coast of south-eastern Barbados.
(Photo: SCHELLMANN 1997)

districts, or parishes (Figure 1.2). Barbados gained independence on the 30th of November in 1966, when it became a full member and independent nation within the Commonwealth, and later joined the United Nations.

Barbados has more than 268,000 inhabitants (2001 estimated), with c. 100,000 of these living in the capital Bridgetown. The population density of 640 people/km^2 is one of the greatest in the Caribbean. The population growth rate is approx. 0.46% (MUNZINGER ARCHIV 2002).

Historically, the economy of Barbados has been dependent on sugar cane agriculture with the production of sugar and rum. Since the early 1990s, the economy has diversified into tourism (c. 11% of the GDP in 1999), light manufacturing and other industries (c. 16% of the GDP), sugar cane agriculture and fisheries (c. 5% of the GDP), and offshore financial services (c. 16% of the GDP in 1995) (statistics after MUNZINGER ARCHIV 2002). Tourism is the main economic source with about half a million tourists per year. Most visitors come from the United Kingdom (c. 41%, MUNZINGER ARCHIV 2002), followed by the USA and Canada.

Barbados produced approx. 24.4 million m^3 of natural gas in 1998 (MUNZINGER ARCHIV 2002). The crude oil production was approx. 328,000 barrels in 1998 (MUNZINGER ARCHIV 2002) and currently meets about one-third of the country's demand. The crude oil reserves are estimated to 3.2 million barrels (WORLD ALMANAC 2002).

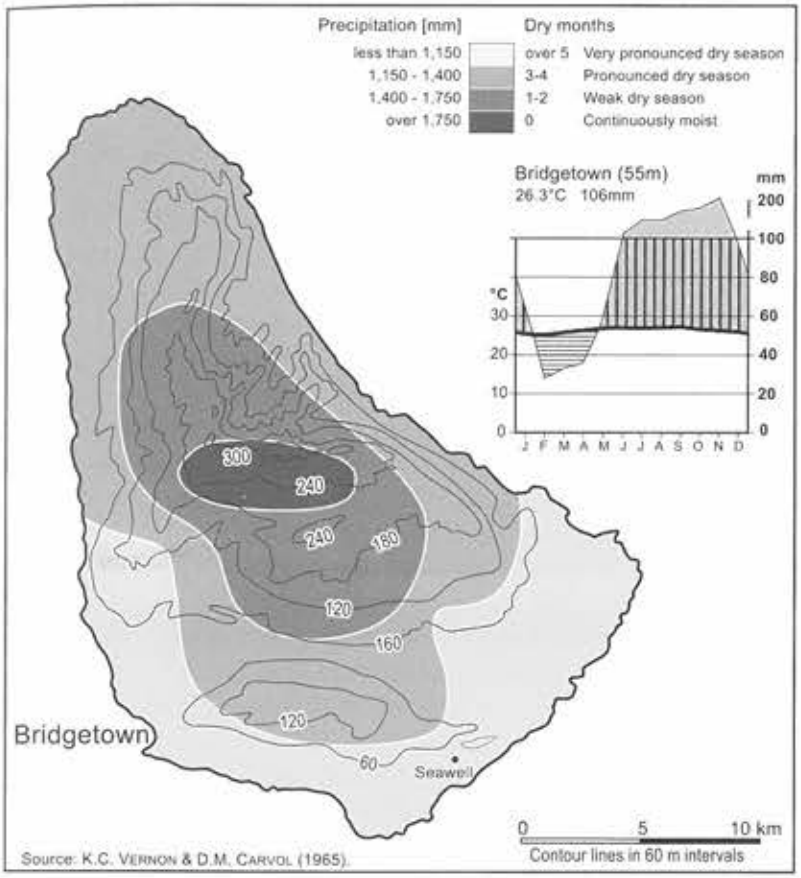

Figure 1.3: The climate of Barbados.

1.1. Climate, hurricanes, and tsunamis

Barbados is characterized by a humid to subhumid tropical maritime climate. The island lies within the belt of northeast trade winds with a mean wind speed of 16.8 km/h (RANDALL 1970). Wind energy is strongest between January and July (monthly mean velocity >18km/h) compared to the months of August to December (BIRD et al 1979). Most of the year, winds blow from northeast, east, and southeast, and determine the dominant wave action reaching the island. According to JAMES et al. (1977), wave heights are approx. 1.2 m on the east coast on calm days, and only 0.2 m on the west coast. On rough days, waves may reach heights of 4 m on the east coast and of approx. 0.3 m on the west coast.

Mean monthly temperatures range from 24° to 28°C with little seasonal variability. Mean daily temperatures are between 28° and 31°C. Night temperatures rarely fall below 20°C. Mean annual precipitation ranges from 1,100 to 1,250 mm in the coastal regions but reaches more than 1,750 to 2,000 mm at the higher central parts of the island (240 to 340 m) (Figure 1.3). Due to orographic effects, precipitation varies widely across Barbados. Barbados' driest areas are located along the south and southeastern coast in the lee of the more elevated central part of the island. Except for central Barbados, the island experiences a pronounced dry season during the winter months (January to May) with highest rainfall occurring at the center of the island, and a rainy season from September to December with highest rainfall on the western, leeward side of the island. Approximately 60% of the average annual rainfall occurs during the wet season (JONES & BANNER 2003). Rainfall is predominately caused by tropical depressions and hurricanes passing the island, or by the proximity of the northward shifted Innertropical Convergence Zone (ITC). The dry season is dominated by a strong trade wind inversion, which causes thermal convection to be weak. Therefore, rainfall is restricted to local con-vection cells, especially at the more strongly heated and elevated center of the island.

In contrast to the islands of the Lesser and Greater Antilles located to the west and to the north, Barbados is not located in a major hurricane region. However, the island experiences one hurricane during the rainy season approx. every 10 to 25 years, resulting in the loss of human lives and severe economic damage. According to RAPPAPORT & FERNANDEZ-PARTAGAS (1997), approx. 40% of all destructive Caribbean hurricanes occur in September, 30% in August, and 20% in October.

Hurricane Marilyn (September 13th 1995) was the last hurricane affecting Barbados. It passed the island directly to the north with 75 mph winds and created minor damages (WILSON 1997). Barbados was strongly affected by Hurricane Allen on 4th August, 1980 with 125 mph winds, which also passed the island on its northern side and damaged coral reefs near the west coast (MAH & STEARN 1986). Severe damages and the loss of lives were caused by Hurricane Janet on the 22nd of September in 1955 (Figure 1.4), which passed the island with 120 mph winds not far from the south coast. Hurricane Janet

Photo 1.3:
Cliff destroyed by hurricane wave action at 'The Spoud', north-eastern coast of Barbados.
(Photo: SCHELLMANN 2000)

Photo 1.4:
Geomorphic evidence for hurricane impacts. Boulders and sand were deposited at 4 to 5 m asl. on a destroyed cliff near 'The Spoud', northeast coast of Barbados.
(Photo: SCHELLMANN 2000)

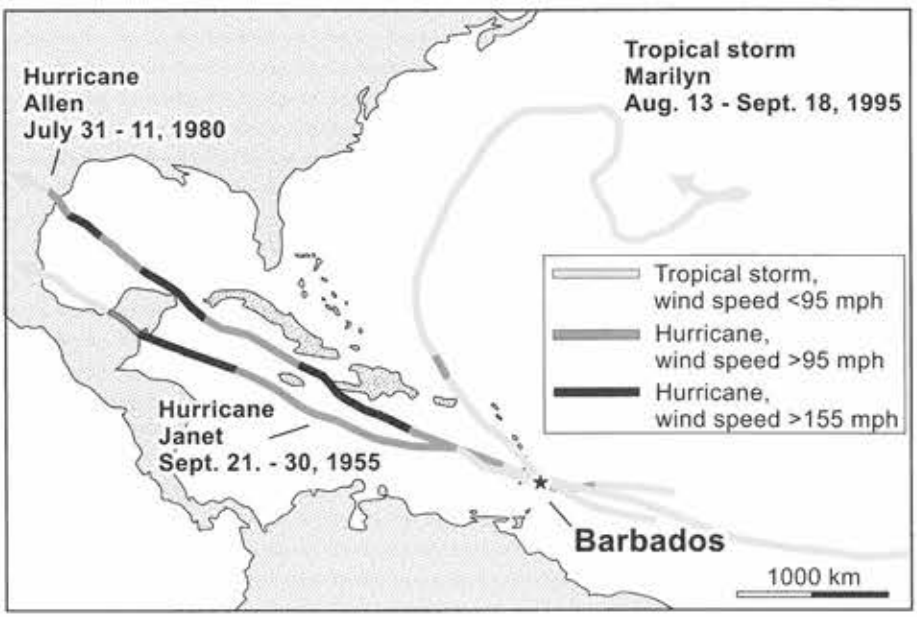

Figure 1.4:
Pathways of some important hurricanes since 1950.

Table 1.1: Catastrophic hurricane damages on Barbados since 1492 (source: RAPPAPORT & FERNANDEZ-PARTAGAS 1997).

Hurricane	Fatalities
Sept. 10 – 11, 1898	283 deaths
July 22 – 23, 1813	at least 18 deaths and 8 missing
Sept. 2 – 3, 1786	many persons were killed in the ruins of their own houses
The Great Hurricane of Mid-October 1780 (Oct. 10 - 16)	4326 deaths
Sept. 27, 1694	>1000 deaths in Barbados and offshore
Sept. 10, 1675	>200 deaths
Aug. 10, 1674	>200 deaths

killed 35 people and destroyed 1,800 homes.

The strongest and most destructive hurricanes that affected Barbados in recent history are listed in Table 1.

The cliffs located on the northeastern coast of Barbados along 'The Spoud' headland were most likely destroyed by such an event. The deposition of a 1 to 3 m broad rampart of boulders at 6 to 10 m asl. could also have originated from one of these strong hurricane events (Photo 1.3, Photo 1.4).

However, not all boulder deposits in the Barbadian littoral zone can be explained by hurricane impacts. The large boulder ridges along the eastern and southeastern coast of Barbados (Photo 2.27 and 2.28) suggest transport energies from mega-waves like tsunamis (Chapter 2.3). It is not astonishing that the geologically extremely active Caribbean bears a great risk of tsunamis, which are commonly generated by submarine slides, volcanic eruptions, or earthquakes in the Caribbean region itself, or far away in the Atlantic area. A less destructive tele-tsunami, observed in the Caribbean in historical time, originated from the 1755 Lisbon, Portugal, earthquake. The waves were only 1.5 to 1.8 m high at Barbados (LANDER et al. 2002). Regarding the compilation of historical tsunamis in the Caribbean by LANDER et al. (2002), at least 27 tsunamis have affected the various coastlines of the Caribbean during the past 500 years (time period 1498 to 1998). Many of them caused significant damages of local infrastructure and losses of lives. Barbados was affected by tsunamis at least three times during this time period: in 1755 (waves 1.5 to 1.8 m), in 1761 (waves of 1.2 m), and in 1767.

Additionally, impacts of earlier Holocene and Pleistocene palaeo-tsunamis, some of them with extreme magnitudes, were described for other Caribbean shorelines. SCHEFFERS (2002a; 2002b) reported three young Holocene palaeo-tsunami events on the islands Aruba, Bonaire, and Curaçao and the distinctive formation of boulder ridges, ramparts, and boulder assemblages at up to 12 m asl. The deposition of large boulders by hurricane or tsunami waves in historical time (approx. 1662 AD) was described by JONES & HUNTER (1992) for the south coast of Grand Cayman. HEARTY (1997) and HEARTY et al. (1998) reported extreme boulders with weighs exceeding 2,000 t at up to 20 m asl. on the coast of Eleuthera Island, Bahamas, suggesting an extreme wave event (tsunami or storm) during the end of the last interglacial sea-level maximum (Late MIS 5e).

1.2. Geologic and tectonic setting

From a geographic point of view, Barbados belongs to the Lesser Antilles, which are the "islands above the wind", located in the trade wind zone (Figure 1.5). In terms of tectonis and geology, Barbados is unique in the Lesser Antilles. Barbados does not belong to the presently active volcanic island chain of the Lesser Antilles such as Saba, St. Eustatius, St. Christopher, Nevis in the northwest, and Basse Terre (western half of Guadeloupe), Les Saintes, Dominica, Martinique, Santa Lucia, St. Vincent, the Grenadines, and Grenada in the south.

Nor does it belong to the older volcanic island arc, which was active from the Eocene to the Oligocene (MACDONALD et al. 2000, MARTIN-KAYE 1969) and extends from Anguilla, Barbuda, St. Mar-

tin, and St. Bartholemew in the northwest, to Barbuda, Antigua, Grande Terre (eastern Guadeloupe), Désirade, and Marie-Galante (Figure 1.5). This older volcanic arc is no longer characterized by volcanic landscapes, since the volcanoes have been eroded and the volcanic rock is covered by thick layers of shallow-marine limestone. Since the Miocene, the center of volcanic activity has moved further to the west, and the outer chain of the Lesser Antilles has now reached a relatively stable tectonic situation. Consequently, there is very little evidence of recent uplift on these islands. Like Barbados, the limestone islands of the outer chain of the Lesser Antilles are relatively flat and low.

Barbados is distinguished from the other Antilles Islands

1) by its location far east of the islands of the Lesser Antilles Arc, and

2) by its extraordinary tectonic position.

The island is located in the subduction zone of the Atlantic oceanic crust of the North American Plate where it slides under the Caribbean Plate in westward direction (Figure 1.6). Due to this plate motions thick sediment layers have been scraped off the ocean floor since the late Eocene in the vicinity of Barbados. These sediments have been piled up to form an elongated accretionary complex known as the 'Barbados Ridge Accretionary Prism' (e.g. SPEED 1990, SPEED 1981). This significant submarine ridge is approx. 20 km thick and almost 300 km wide. It extends from the Atlantic Abyssal Plain to the eastern flank of the Tobago Trough and parallels the subduction zone up to 17° N (Figure 1.5).

Barbados represents the highest elevation of this ridge and is the only emergent part of it, which reaches above sea level. The existence of tectonic mud diapirs is the most probable reason for this local anomalous elevation of Barbados (see Chapter 2). South of the island, the Barbados Ridge bends towards the west and disappears north of Tobago on the wide continental shelf of South America (SENN 1948). The Barbados Ridge is bordered by deep basins to the west (Tobago Trough) and southeast (Barbados Basin), which were generated by the mass loss of the ocean floor due to plate subduction. The Tobago Forearc Basin is more than 2,000 m deep. Its deepest point is located between Barbados, St. Lucia, Grenada, and Tobago, and reaches 2,730 m below sea level (SENN 1948). The Barbados Basin, which is also more than 2,000 m deep, marks the steep decline of the ocean floor to the southeast of Barbados.

1.2.1. Plate tectonics and volcanism

The Caribbean Plate originated from the divergent movement of North and South America, which occurred during the end of the Jurassic and the Cretaceous period 80 to 160 Ma ago. There are different tectonic models, which describe the plate tectonic evolution of the Caribbean. The classic 'Pacific' model proposes that the Caribbean crust originated from the Pacific region near the Galapagos hot spot, and later drifted eastward between the two Americas (e.g. PINDELL & BARRET 1990).

Another model favors a plate tectonic evolution generated by spreading processes between North and South America, which were initiated by the opening of the Central Atlantic Ocean (e.g. MESCHEDE 1998; MESCHEDE & FRISCH 1998; GIUNTA et al. 2002). The Caribbean Plate used to be the eastern part of the Pacific Plate, which moved towards the Northern Atlantic Ocean. A subduction zone developed in the vicinity of the present Central American land bridge 100 Ma ago and generated the oldest prototype of the Caribbean Plate (Figure 1.7, MESCHEDE & FRISCH 1998). Then, the plate was probably enlarged by the formation of new oceanic Caribbean crust and expanded towards the northeast during the Cretaceous and to the east during the Early Tertiary (Figure 1.7). The easternmost extent of the plate was most likely reached during the older Tertiary (Eocene to Oligocene). During this time period, the oldest volcanic island arc was formed in the region of the Lesser Antilles (Figure 1.5). This chain is a reminder of the active subduction of the Atlantic oceanic crust of the North American Plate sliding underneath the eastward drifting Caribbean Plate. With the formation of this first volcanic island arc, the Caribbean Plate probably reached its greatest size. During the Miocene, volcanic activity shifted westward and initiated the formation of a younger volcanic island arc (approx. 800 km in length) in the area of the inner chain of the Lesser Antilles (Figure 1.5).

At present, the Caribbean Plate is bordered by active subduction zones to the west and east, and by significant transform faults to the north and south (Figure 1.7). The oceanic Cocos Plate submerges under the Caribbean Plate at a rate of approx. 11.9 cm/a. This convergence-forced subduction zone is located to the west of the present Central American land bridge. At the same time, the Cretaceous crust of the Atlantic oceanic floor submerges under the younger oceanic crust of the Caribbean Plate by gravity-induced subduction. The rate of subduction

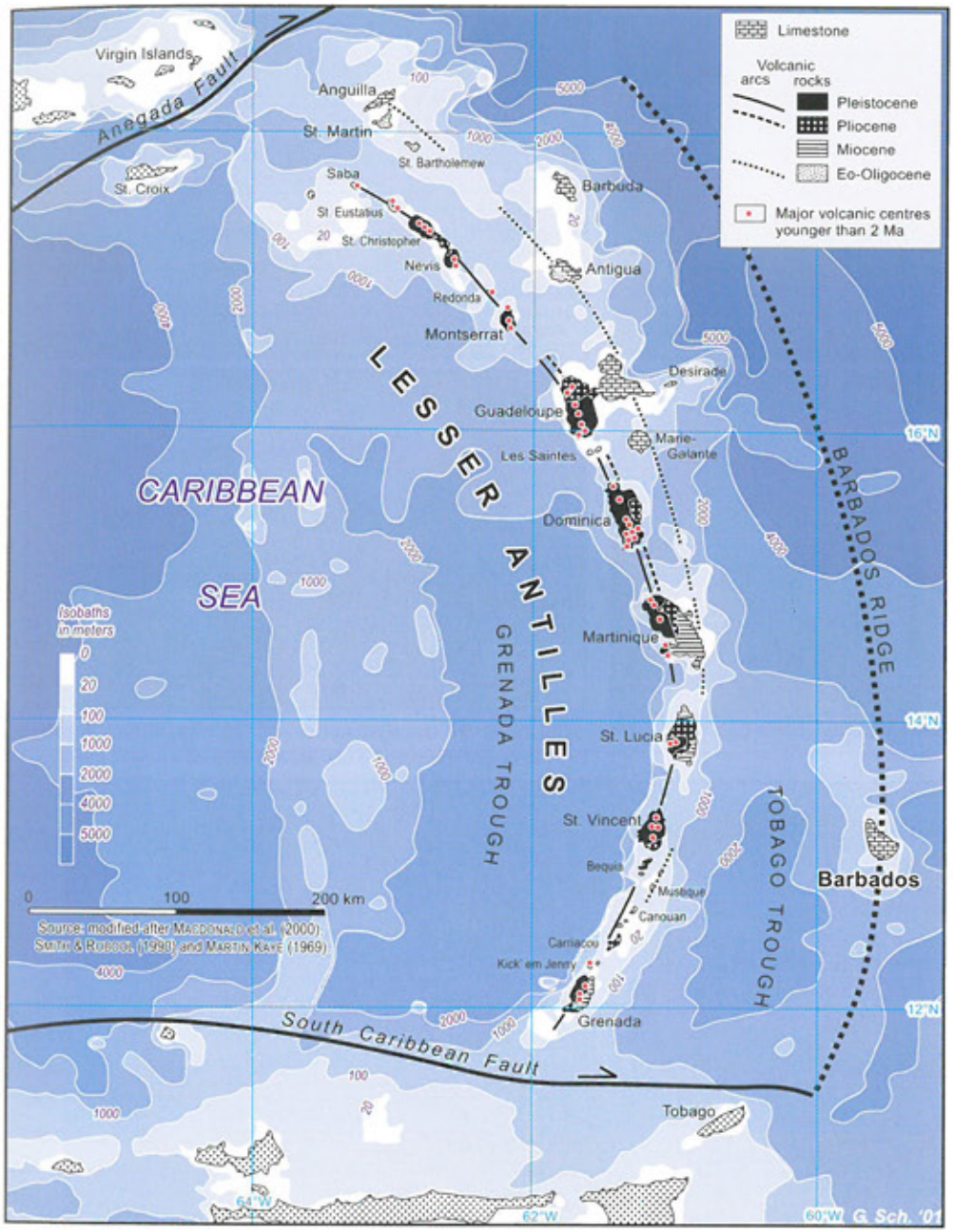

Figure 1.5: The eastern Caribbean Plate.

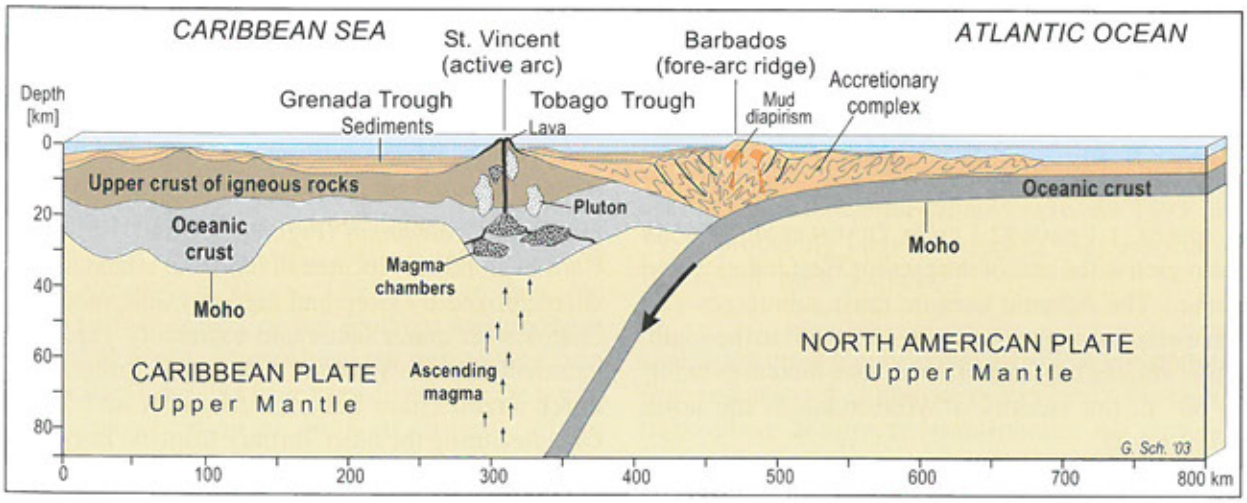

Figure 1.6: Cross section of the subduction zone in the vicinity of Barbados (strongly modified after BOTT 1982).

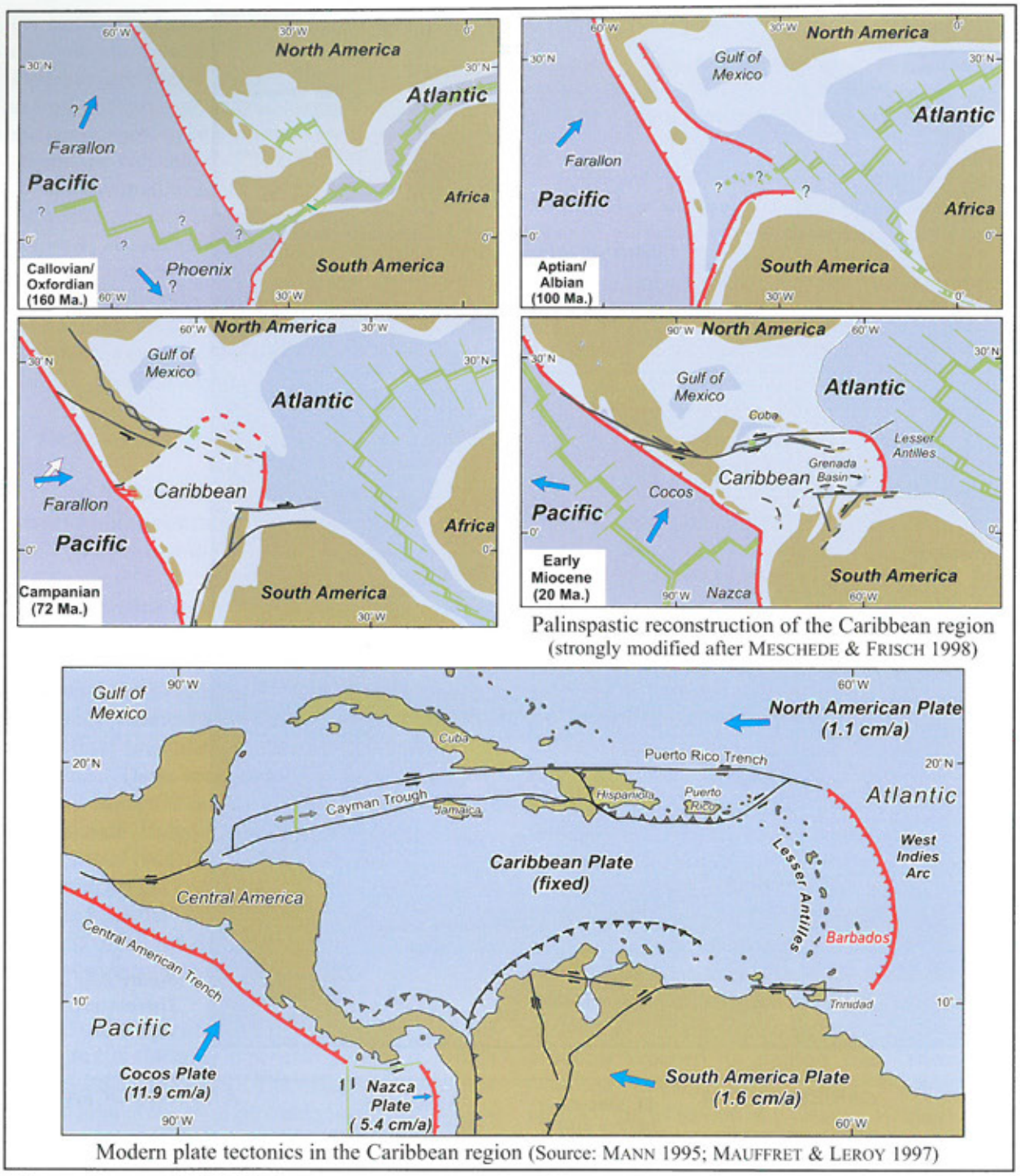

Figure 1.7: History of plate tectonics in the Caribbean.

is approx. 1.1 cm/a (2.1 cm/a, DIXON et al. 1998) in the region to the east of the present West Indies island chain. The Atlantic oceanic crust submerges at a relatively flat angle of approx. 45° to 50° in the south. However, the angle of submergence increases to 50° to 60° in the vicinity of Martinique in the north (Figure 1.8).

Active subduction is generally associated with earthquakes (e.g. SMITH & ROOBOL 1990, MANN 1995) and volcanism (Figures 1.8 and 1.5). The Caribbean Islands located in the inner island arc are characterized by steep and high volcanic mountain chains with crater lakes and extremely explosive stratovolcanoes. Volcanic activity occurred in the outer island chain between Anguilla and Marie Galante during the older Tertiary from the Eocene to the Oligocene. However, volcanism has been limited to the inner island chain since the Miocene. Three regions have displayed considerable volcanic activity

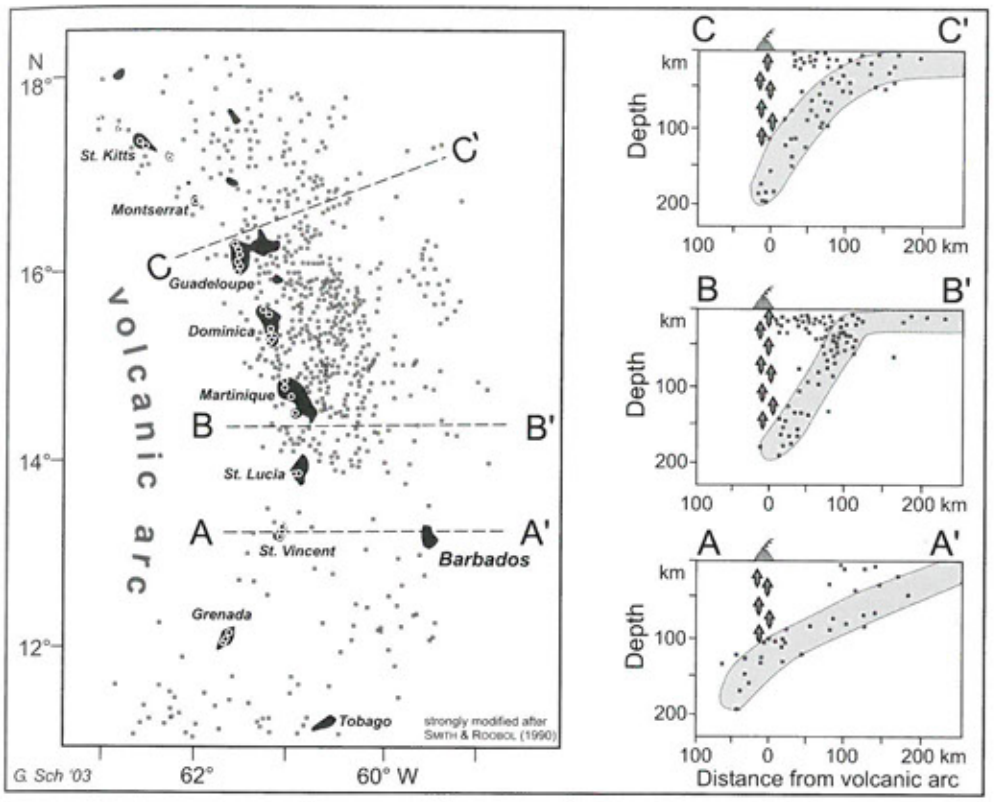

Figure 1.8: Earthquake hypocenters of the volcanic arc of the Lesser Antilles (strongly modified after SMITH & ROOBOL 1990).

during the last 2 million years: the regions between Saba and Montserrat, between Guadeloupe and Martinique, and between St. Lucia and Grenada (Figure 1.5).

From a plate tectonics point of view, the Caribbean has existed since the late Mesozoic. However, the relatively isolated Caribbean Sea, which is separated from the Atlantic Ocean by the southern Florida Peninsula, the Greater Antilles, and the numerous islands of the Lesser Antilles, was not formed until the uplift of the Panama Isthmus during the younger Tertiary around 9 to 13 million years ago. The gradual closing of the Central American seaway ended any major exchange of deep ocean water between the Pacific and the Atlantic Oceans, and Caribbean Loop Current and Gulf Stream became more and more established at this time (e.g. ROTH et al. 2000; DUQUE-CARO 1990). However, the Panama Isthmus was not completely closed until approx. 2.7 to 3.7 million years ago (KAMEO 2002, KAMEO & SATO 2000, NESBITT & YOUNG 1997). Since then, the warm surface waters of the southern and northern equatorial ocean currents have not moved west into the Pacific Ocean, but have been diverted to the north. This intensification of the Gulf Current, which contributed to the warming of the higher latitudes, is generally attributed to the establishment of the present oceanic and atmospheric currents and climate zones on earth.

1.2.2. Historic volcanic eruptions and the deposition of volcanic ashes on Barbados

It is generally assumed that approx. 13 Antilles volcanoes have been active during the last 100,000 years. At present, volcanic activity is revealed in form of solfataras on the islands of Dominica and St. Lucia. Recent volcanic eruptions occurred on St. Vincent (Mt. Soufrière volcano, last eruption in 1979), on Guadeloupe (Mt. Soufrière volcano, last eruption in 1977), and on Martinique, where the well-known eruption of Mt. Pelée in 1902 destroyed the harbor town of St. Pierre and killed approx. 30,000 inhabitants (SIGURDSSON & CAREY 1991). Soufrière volcano on Montserrat erupted between 1995 and 1998, producing large amounts of ash, pyroclastic flows, and much publicity.

During these highly explosive volcanic eruptions, fine volcanic ashes and gases can reach the higher troposphere and lower stratosphere. Air currents, including the northeastern and eastern trade winds in the lower and middle troposphere up to 6 to 9 km and west winds in the upper Troposphere (Figure 1.9),

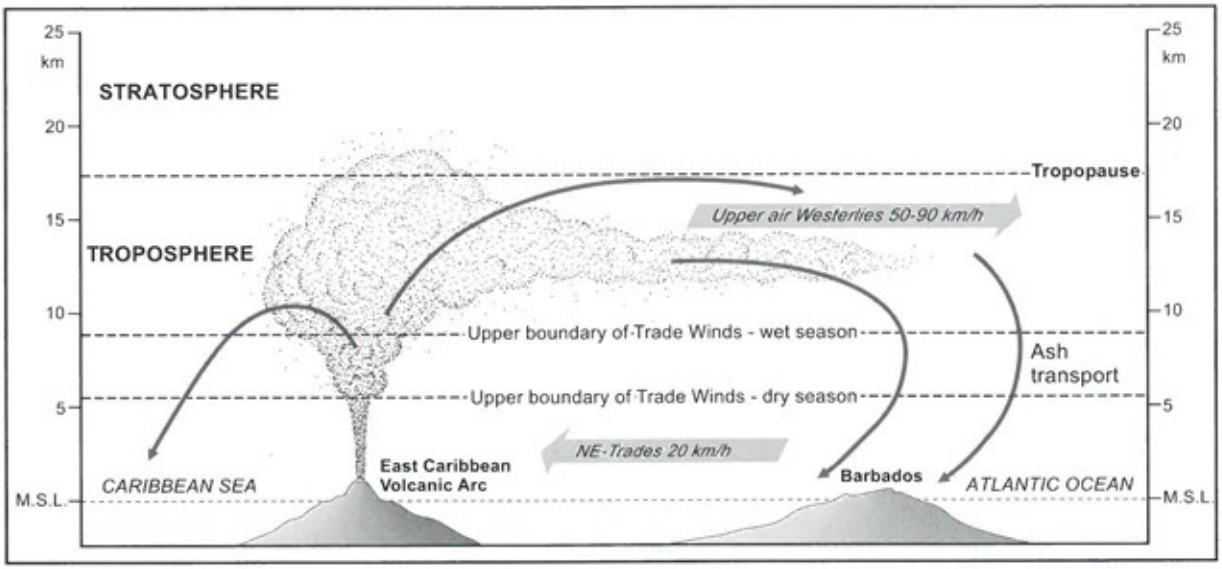

Figure 1.9: Wind systems and the transport of volcanic ash in the eastern Caribbean (modified after SEALEY 1992, and SIGURDSSON et al. 1980).

disperse them. The ashes and gases may become widely dispersed before being precipitated by gravity and rain.

Barbados also received silicate ashes through these processes. According to HARRISON et al. (1980), approx. 40% to 60% of these ashes consists of volcanic glass, 20% to 40% are composed of plagioclase, 5% to 20% contain hypersthene, and less than 5% consist of zircon and apatite. Barbados' volcanic dust deposits originated from eruptions on the volcanic islands of the southern Antilles, ranging from Dominica in the north to Grenada in the south. For example, the eruption of the Roseau Volcano on Dominica, approx. 28,000 years ago, generated a 5 to 6 cm thick ash deposit on Barbados (Fig-

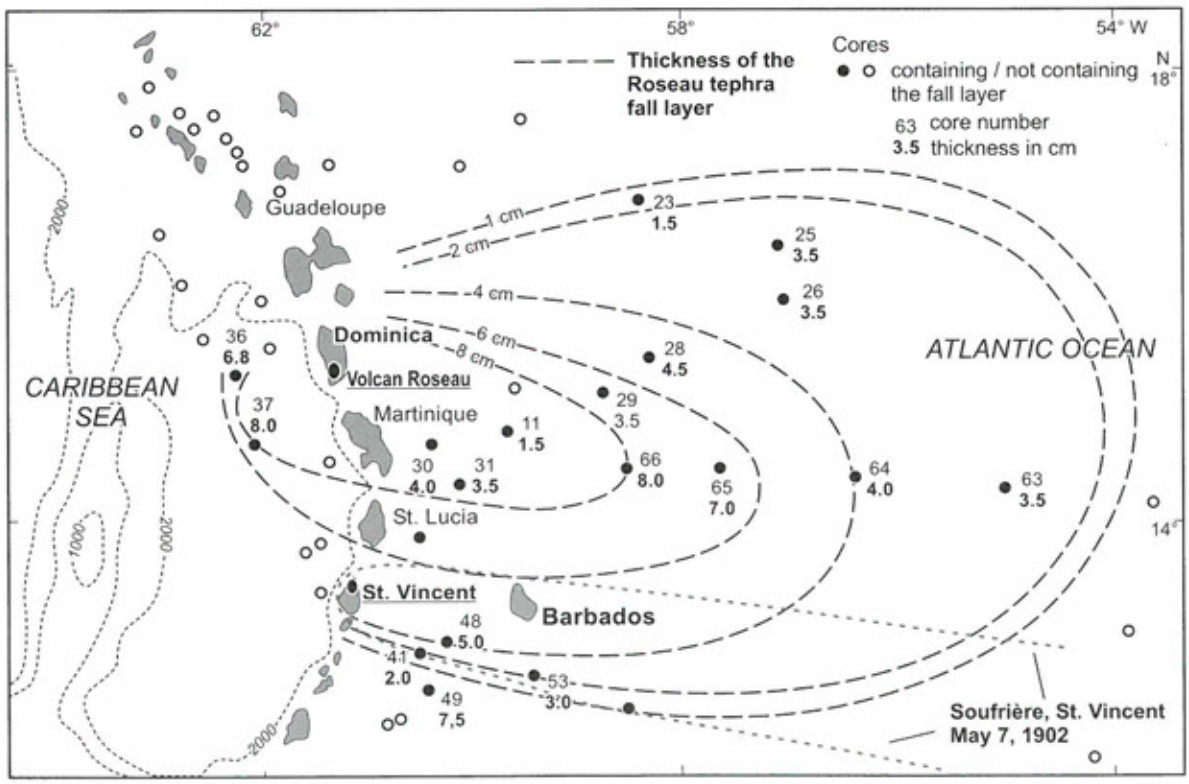

Figure 1.10: Deposition and thickness of Quaternary Roseau tephra fall layers, and dispersal of tephra fall from the 1902 eruption of Soufrière St. Vincent (modified after SIGURDSSON et al. 1980; SIGURDSSON & CAREY 1991)

ure 1.10). Other ash deposits originated from the phreatomagnetic eruptions of Mt. Soufrière volcano on St. Vincent in 1718, 1812 (deposit of 25 mm), 1902 (5 to 10 mm), and 1979 (SIGURDSSON & CAREY 1991).

Further information on the deposition of volcanic ashes on Barbados was provided by DILLER & STEIGER (1902), FLETT (1902), HARRISON et al. (1980), and SIGURDSSON & CAREY (1991).

Other siliclastic particles in soils and sediments on Barbados originated 1.) from the atmospheric deposition of Saharan dust (PROSPERO et al. 1970; PROSPERO & NEES 1986), which was transported by trade winds; and 2.) to a lesser degree, from the erosion of Tertiary sandstone and mudstone and subsequent fluvial and marine transport of silica grains. BORG & BANNER (1996) estimated that approx. 30% to 85% of the silicate fraction in soils originated from volcanic ashes from the Lesser Antilles. In contrast, MUHS et al. (1987) assumed that African dust was the most important source for soil clay on Barbados. PROSPERO & NESS (1986) stated that the periods of unusually high dust concentrations (especially during summer) in Barbados corresponded to times of rainfall deficits in the sub-Sahara area, and were associated with ENSO events.

Further aerosol measurements on Barbados was published by TODD et al. (2003), PROSPERO & CARLSON (1972), DELANY et al. (1967), and others.

1.3. Coral reefs, reef-building coral, and coralline algae in the Caribbean

Coral reefs generally form prominent high topographic areas on the sea floor and are characterized by their growth towards sea level and by their lateral seaward extension. A coral reef body mainly consists of colonies of hermatypic coral and calcareous red algae.

The reef grows faster in height than the surrounding level of sedimentation. Calcareous sediments are generated in the vicinity of reefs and deposited on the surrounding sea floor. Waves and ocean currents transport and accumulate coral rubble into more protected back reef areas and adjacent shallow lagoons. A fore reef talus develops at the reef slope exposed to the open sea. Both fore reef talus and lagoon are closely associated with the actual reef body, and form a coral reef or coral reef complex in a morphological sense.

Coral reefs may be differentiated into several geomorphic units as, for example, reef types defined by their shape, size, and location in relationship to the coastline. These reefs include, among others, fringing reefs, barrier reefs, atolls, banks, platform reefs, and patch reefs. Reefs may further be classified based on their position in relation to sea level, for example, drowned reefs, shallow-water reefs, and emerged reefs. The position of the reef in relation to the prevailing wind direction allows for a differentiation between windward and leeward reefs. The number of parallel reef tracts determines the reef type, such as simple reef, double reef, or multiple reef.

The assessment of the relationship between sea level rise and reef response allows for the differentiation between a) 'give up' reefs, which are relics drowned by sea-level rise, noncarbonate sedimentation etc.; and b) 'catch up' reefs, which sea-level rise initially left behind, but which recover with accelerated vertical reef growth during times of slower sea-level rise; and c) 'keep up' reefs, which are able to maintain their reef crest at or near the rising sea level throughout their growth history (SPENCER & VILES 2002, NEUMANN & MACINTYRE 1985). Further reef types and corresponding examples from the West Indies were described by GEISTER (1983).

Apart from platform reefs, such as the Bahama Banks and other reefs in close proximity to the largest Caribbean Islands (Cuba, Hispaniola, Puerto Rico), the most common reef types in the Caribbean Sea are single or double fringing reefs, which can be found throughout most of the Caribbean Islands. Fringing reef growth starts offshore on the shelf and generates an elongated reef that parallels the coastline in close proximity and is generally separated from the beach by a shallow lagoon. A fringing reef is further characterized by a fore reef slope with a reef talus, and a reef platform or reef flat zone of varying width with a reef crest as its highest top (Chapter 2.2. and 4.2).

The most important Caribbean reef-builders are colonies of different species of stony coral (see below). Calcareous algae are a secondary integral element for reef building processes. Various coral communities generally predominate in different vertical zones. The formation of coral reef zones largely de-

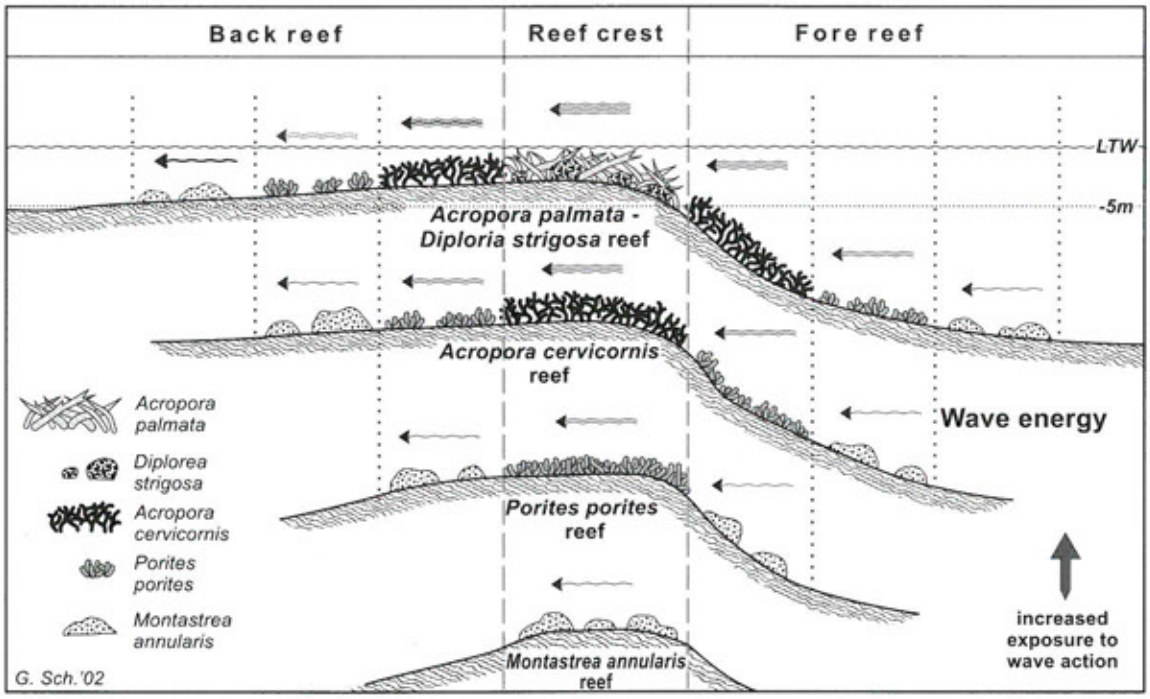

Figure 1.11: Correlation of wave energy and the variations in coral facies zones (strongly modified after GEISTER 1983 and GEISTER 1980).

pends on species competition for light intensity, temperature, salinity, water current, sedimentation, and wave action.

Broadly speaking, the most common reef zones or reef facies in the Caribbean are

(a) the *Acropora palmata* (elkhorn coral) zone and the *Diplora sp.* dominated brain coral zone located in shallow water with depths of down to 5 m,
(b) the *Acropora cervicornis* (staghorn coral) zone in moderately deep water ranging from 4 to 7 m in depth, and
(c) the *Montastrea annularis* and *M. cavernosa* zone in deeper water with depths reaching down to 10 m.

However, this rudimentary classification of coral facies zones is strongly modified by local ecological conditions. For example, wave strength is one important environmental factor for the distribution of coral species. Wave action depends on reef morphology and varies between fore reef, reef slope, reef crest, reef lagoon, inner reef channels, etc. This leads to wave-dependent changes in coral reef zones as illustrated in Figure 1.11.

1.3.1. The most important reef-building coral species

Since the Miocene the Caribbean Sea has been a marginal sea of the Atlantic Ocean and developed a unique fauna of reef forming coral. It hosts approx. 27 genera with almost 70 coral species. Compared to the Indo-Pacific fauna, the Caribbean coral fauna is much less species-abundant. Ninety percent of all Caribbean coral reefs are composed of the following six genera: *Acropora, Montastrea, Diploria, Porites, Agaricia,* and *Siderastrea* (SCHUMACHER 1991, Figure 1.12). Due to the light requirements for photosynthesis, living coral reefs are only present in water depths of less than approximately 30 m.

BUDD (2000) presented a detailed description of the development and dispersion of Caribbean reefs during the last 50 million years. PANDOLFI (2002) stated that Quaternary coral reef communities in the Caribbean showed a remarkable similarity in coral species assemblages during the last 500 ka. Shallow reefs were dominated by large species of branching *Acropora* coral. This pattern of coral species distribution, which was stable over a long time period, differs considerably from modern, anthropogenically altered coral community compositions (PANDOLFI 2002).

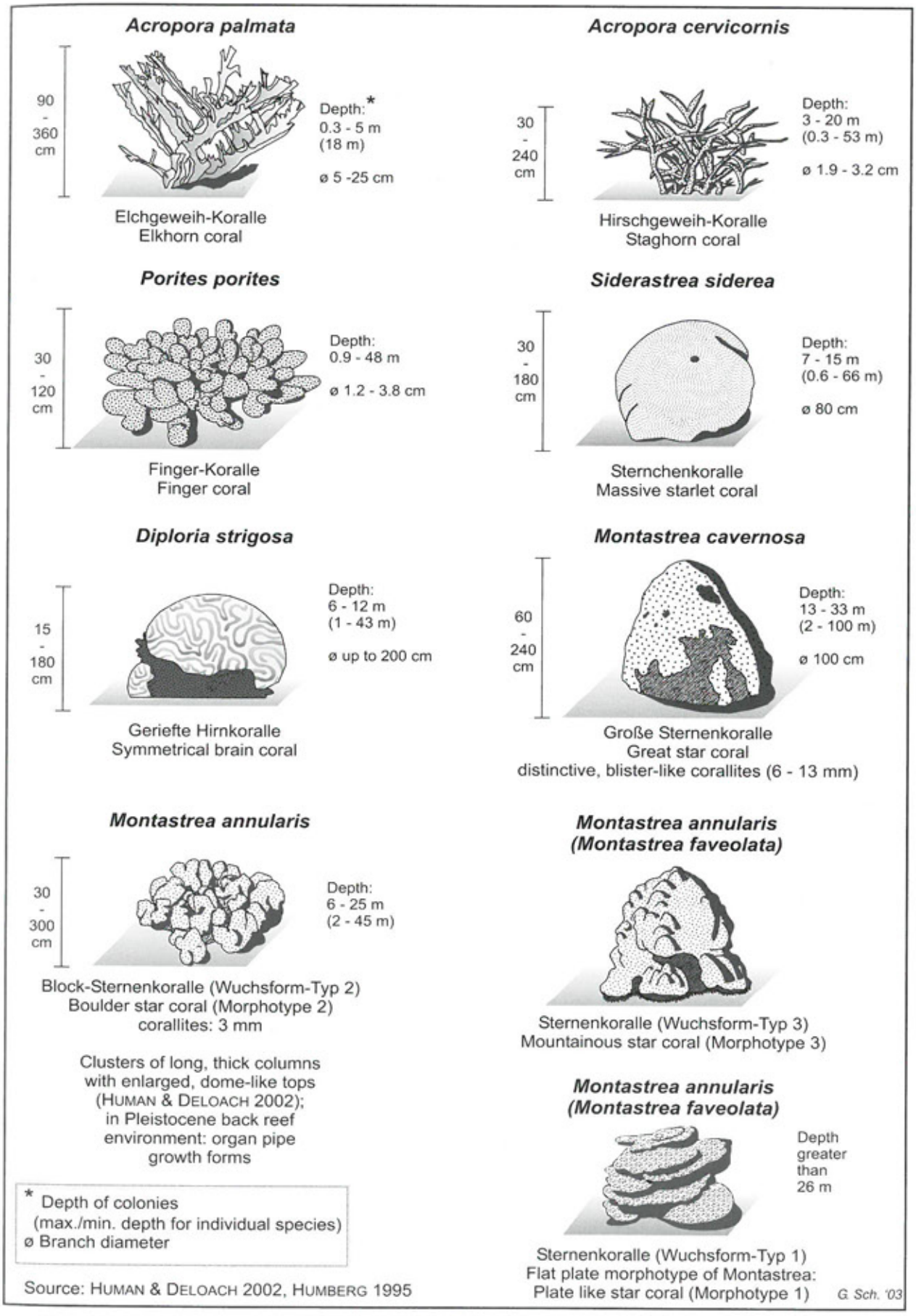

Figure 1.12: Some important Caribbean coral reef species distributed in Pleistocene coral limestone of Barbados.

The species composition of a coral reef is largely dependent on two abiotic factors: light availability and wave energy. Even though reef-building coral does not photosynthesize, it is dependent on sunlight because it lives in endosymbiosis with zooxanthellae (algae endosymbionts), which supply the coral's energy demand with their photosynthesis. Coral polyps consume substances dissolved in water, including nitrates, amino acids, and other organic matter. They provide carbon dioxide and matter containing phosphate and nitrogen for the zooxanthellae. The latter use the carbon dioxide for photosynthesis and, in turn, provide products of assimilation, such as sugar, glycerin, and amino acids. Zooxanthellae create conditions for calcium crystallization at the lower outside wall of the coral polyps. It is for this reason that zooxanthellae increase the formation of the aragonite coral structure ten-fold, compared to algae-free coral (SCHUMACHER 1991).

Only coral species that live in endosymbiosis with zooxanthellae are reef-forming coral. They are the only organisms with calcium deposition rates that support reef growth that is faster than the accumulation of sediment on the surrounding sea floor. Due to their fast growth rates, they are also able to restore damage caused by wave action in a relatively short time (e.g. LIRMAN 2000).

Since sunlight is reduced by 60% to 80% within the upper 10 m of clear tropical seas, it is not surprising that the growth rates of many reef-building coral species, including *Porites astreoides*, *Montastrea annularis*, and *Siderastrea siderea* (HUSTON 1985), decrease with increasing water depth, and structural reefs are restricted to the upper c. 40 m of water depth (SPENCER & VILES 2002).

Acropora palmata is one of the most important reef-building coral in the Caribbean and one of the fastest growing stony coral species. Dense, reef building A. *palmata* communities live in water depths between 0 m to 5 m only (LIGHTY et al. 1982). They are known to reach annual growth rates of up to 10 cm (BAK 1976) or of 5-6 inches (c. 13 to 15 cm) (HUMANN 1996). In comparison, the growth rate of *Porites astreoides* amounts to approx. 5 mm per year in well-lit flat water areas (HUSTON 1985). The fine branches of *Acropora cervicornis,* which frequently dominates in water depths between 5 and 15 m, reach growth rates of 10 to 20 cm/year (HUSTON 1985, SCHUMACHER 1991). Annual growth rates of 26 cm were observed on Barbados. In contrast to the coral species mentioned above, *Montastrea annularis* does not reach its maximum upward growth near the water surface but in water depths between 5 to 15 m. There, growth rates range from 7 to 10 mm/year (HUSTON 1985).

Coral growth does not only depend on light conditions but also on water temperature and other abiotic and biotic factors. Optimal water temperatures range from 23° to 29°C. Coral growth is negatively impacted by suspended sediment. Water quality and chemical conditions also play a role in coral development. Optimal salinity ranges from 2.8% to 4.8%. Fresh water input causes a considerable decrease in growth and may initiate coral death (GEISTER 1983).

Many stony coral species show significant growth bands, which may be compared to tree rings. Isotope studies ($^{16}O/^{18}O$, $^{13}C/^{14}C$) suggested that coral growth is seasonal and reflects changes in ecological conditions such as water depth, water temperature, wave stress, salinity, and other factors. DULLO & MEHL (1989) described seasonal growth lines in modern and Pleistocene coral on Barbados. DUNBAR & COLE (1993) provided a general overview on coral records for climate variability. The use of isotopic ratios for recording environmental changes in *Montastrea* samples from the Caribbean was evaluated by WATANABE et al. (2002). MATTHEWS (1990) summarized results of mean delta ^{18}O data from some Pleistocene coral reef tracts on Barbados, and GUILDERSON et al. (2001) generated a detailed oxygen isotope time series since the last glacial maximum from offshore Barbados.

The long-term growth rate of a coral reef is largely dependent on the following factors: the individual growth rates of the different reef-forming coral species; the population density of coral on the reef; the intensity and duration of erosive processes (bioerosion, abrasion, storm damage, etc.), and phases of periodic coral death due to catastrophic environmental change, such as input of fresh water or sediment, diseases, sea-level change, etc. As stated in GEISTER's (1983) literature review, Caribbean coral reefs with *Acropora palmata* as the predominant reef-forming coral have reached long-term mean vertical growth rates of 0.7 to 15 m/1,000 years during the Holocene. In comparison, long-term mean vertical growth rates are 1 to 12 m/1,000 years for *Acropora cervicornis* reefs, and approx. 1 to 4 m/1,000 years for *Montastrea annularis* and *Montastrea cavernosa* reefs.

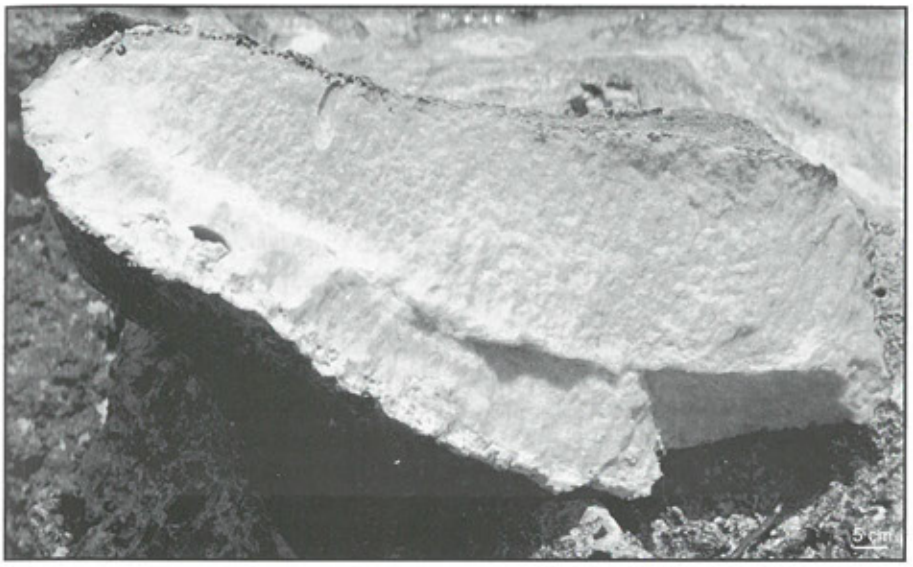

Photo 1.5:
Last interglacial (MIS 5a) *Acropora palmata* with central growth line (Inch Marlowe Point, south coast of Barbados).
(Photo: SCHELLMANN 2000)

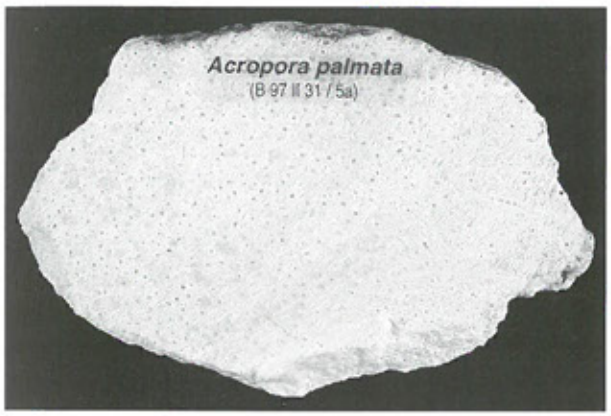

Photo 1.6: Cross section of last interglacial (MIS 5a) *Acropora palmata*.

Vertical reef growth, which is associated with the building of framework-dominated reef flats and reef crests, occurs under the conditions of an increasing or a stable sea level only. Based on MONTAGGIONI (2000), fast-growing reefs can reach growth rates of up to 10 m/1,000 years, which can be sustained for 3,000 to 5,000 years. A maximum growth rate of 20 m/1,000 years may be reached for periods of approx. 500 years.

Fast-growing reefs form expanded vertical accretion sequences. Vertical aggradation is lower than lateral reef growth. Moderately growing reefs reach growth rates of 0.5 to 0.7 m/1,000 years, and relate to either aggrading sequences or backstepping parasequences, whereas slowly growing reefs (0.1 to 0.4 m/1,000 years) form series of backstepping units (MONTAGGIONI 2000). During periods of sea-level stillstands, reefs progress seaward at various rates, which are generally higher than their vertical growth rates. Upward reef growth begins to decrease and changes into lateral reef accretion before the beginning of a sea-level fall (KENNEDY & WOODROFFE 2002, STODDART 1990, and others). Therefore, the reconstruction of sea-level changes based on estimates of long-term mean vertical reef accretion requires considerable caution.

Species composition in a coral reef depends on a complex interplay of ecological factors, including light intensity, wave energy, strength of underwater currents, sediments, substrates on the sea floor (sand, rocks, etc.) and others. Therefore, reasons for variations in fossil coral communities are hard to identify. Even though reef morphology and zonation vary in the Caribbean Sea, some commonality has been observed. Most reefs display a shallow lagoon and back reef zone colonized by *Diploria sp., Porites sp., Montastrea sp., Siderastrea sp.*; a wave-exposed *Acropora palmata* reef crest zone; and a deeper water fore reef zone with *Acropora cervicornis* and/or *Montastrea annularis* as the most dominant species. Beside these coral communities, encrusting coralline algae (see below) are important calcifying organisms in shallow areas with rough water conditions and in deep water areas with depths of more than 40 m, where coral cover is strongly reduced (BAK 1977).

Acropora palmata (*A.p.*)

Acropora palmata ("elkhorn coral") plays an important role in dating and estimating Quaternary sea-level change (Photos 1.5 and 1.6). *A. palmata* has been the most common shallow water coral species in the Caribbean over a long Quaternary time

period before anthropogenic influences altered coral community composition.

Since *A. palmata* is relatively resistant to strong wave action, it grows on the upper reef slopes, reef crests, and reef flats. *A. palmata* colonizes habitats ranging from water depths of -5 m to low tide water level, and is commonly associated with *Diploria strigosa*. Sometimes local *A. palmata* reef colonies grow in water depths of up to -12 m as for example at different locations at the east coast of St. Croix (ADEY & BURKE 1977), and at the exposed northwest coast of Curaçao (BAK 1977). Individual coral reef bodies of *A. palmata* have been observed in great depths of up to 27 m below sea level (LIGHTY et al. 1982).

According to LIGHTY et al. (1982), *A. palmata* species does not form an interlocking framework in depths greater than 5 m. One of the reasons why *A. palmata* does not inhabit greater water depths is its requirement for water movement for the purpose of cleanliness, as it lacks the ability to clean itself (BAK 1977). Branches of *A. palmata* reach heights of 2 m to 3.5 m and colonies may cover areas of many square meters (GREENBERG 1992). According to MESOLELLA (1968), fossil *A. palmata* branches reach diameters of up to 60 cm.

A. palmata grows very quickly (see above). It reaches growth rates of up to 15cm/year and may produce up to 10^5g $CaCO_3$ per m^2 per year under optimal ecological conditions (BAK 1977). Under rough water conditions, coralline algae, especially *Porolithon pachydermum*, play an important role in the encrustation and cementation of unconsolidated coral and algal fragments, which contribute substantially to the formation of the reef. Drill samples of preserved fossil *A. palmata* reefs show that their growth correlated with the Late Glacial and Holocene sea-level rise of approx. 114 m during the last 19,000 years (FAIRBANKS 1989, BARD et al. 1990a).

As for many reef-building coral species, the skeleton of *A. palmata* consists of aragonite. Due to the fast growth of this species, only the outermost surface layer may experience the submarine diagenetic change into magnesium-calcite (LIGHTY et al. 1982). Because of the mass and compact body of aragonite needles, *A. palmata* is not particularly susceptible to diagenetic solution and recrystallization processes. Even fossil *Acropora palmata* older than 500,000 years may consist of largely unaltered skeletal aragonite, as shown by the macroscopic characteristics of the aragonite structure and by X-ray diffraction (RDA) and Electron Spin Resonance (ESR) measurements. Even though the latter do not directly prove calcification, they indicate its presence through Mn^{2+} lines, generated by the diagenetic change of aragonite, as displayed in the ESR spectrum of aragonitic coral samples (SCHELLMANN & KELLETAT 2001).

LIGHTY et al. (1982) presented radiocarbon (^{14}C) dating results for living *A. palmata* from samples collected at Florida and the Bahamas in 1884 and 1912, respectively, which yielded values of 195 ± 50 years BP (before 1950) for the sample collected in 1884, and 205 ± 65 years BP for the sample collected in 1912. It may therefore be assumed that the marine ^{14}C reservoir effect is approx. 150 years for the Caribbean Sea for the recent past (see also RADTKE et al. 2003). This estimate is considerably younger than the commonly referred to mean global reservoir effect of approx. 400 years. According to DRUFFEL (1997), the Suess effect with its anthropogenically lowered atmospheric ^{14}C content in the top 400 m of surface water could not be detected in the Caribbean Sea. However, the ^{14}C level varied considerably within a few decades. Overall, the variability of ^{14}C values reached up 20 to 30 per mil between 1885 and 1953 (DRUFFEL 1997: Figure 1), which would affect age estimates by up to 240 years, since a variation of 1 per mil ^{14}C equals approx. 8 years. This indicates that ^{14}C values may be greatly influenced by short-term vertical exchange processes between deep sea currents (deeper than 400 m) and surface water in the Caribbean Sea. It may be deduced that greater variations, perhaps by an order of magnitude, in the ^{14}C reservoir effect occur within time spans of a few years only.

Acropora cervicornis (*A.c.*) (LAMARCK 1816)

Acropora cervicornis ("staghorn coral") also belongs to the fast growing and colony-forming Caribbean coral reef species (Photos 1.7 and 1.8). It is characterized by noticeably long branches of up to 3 cm in diameter and up to 2.4 m in length (GREENBERG 1992).

Due to its fragility, it grows in calm water only. Therefore, it inhabits deeper fore reefs and reef slopes at water depths below wave action and forms part of reef crests under extremely calm surf conditions only (GEISTER 1983). *A. cervicornis* prefers water depths

Photo 1.7:
Last interglacial (MIS 5a) *Acropora cervicornis* back reef facies (Inch Marlowe Point, south coast of Barbados).
(Photo: SCHELLMANN 1997)

Photo 1.8:
Last interglacial (MIS 5e) *Acropora cervicornis* reef slope facies exposed at Clermont Nose traverse (Bridgetown, University of the West Indies).
(Photo: SCHELLMANN 2002)

between 3 and 22 m below sea level (HUMANN 1996). SCATTERDAY (1974) reported dense living colonies of *A. cervicornis* in water depths between 4 and 10 m off Bonaire. Isolated colonies of *A. cervicornis* have also been observed on a sandy sea floor in shallow water areas of the back reef zone with moderate surf conditions.

Porites sp. (P.sp.) (LINK 1807)

Porites porites ("finger coral") is a coral species that may easily be distinguished by its morphology and short branches. It is relatively frequent in the Caribbean and inhabits great water depths.

P. porites is related to branching coral "*Porites divaricata*" (thin finger coral) and *Porites furcata* (branched finger coral), which has branches comparable to fingers (HUMANN 1996). The branches of *P. porites* can reach up to 3.8 cm in diameter. *Porites sp.* is a reef forming coral and grows in dense colonies under calm surf conditions in reef crest areas. Under moderate surf conditions, *Porites sp.* is replaced by *A. cervicornis* and settles in the calmer back reef and reef slope areas (GEISTER 1983). *Porites sp.* is generally observed in water depths ranging from 1 to 53 m below sea level (HUMANN 1996).

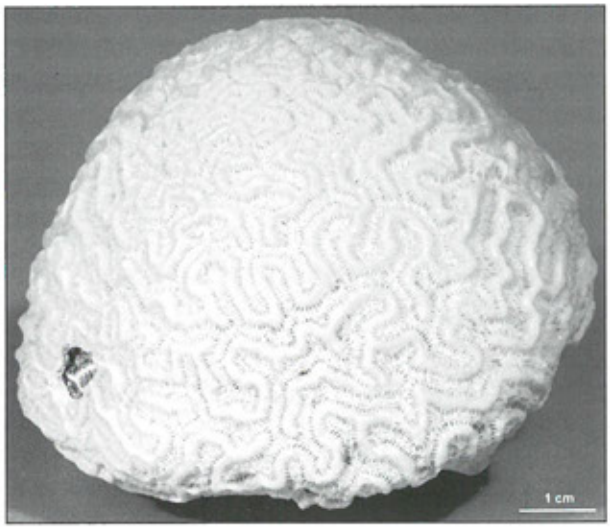

Photo 1.9:
Holocene *Diploria strigosa* sample from Curaçao, Netherlands Antilles. *(Photo: SCHELLMANN 2000)*

Diploria strigosa (D.s.) (DANA 1848)

The surface structure and body of *Diploria strigosa* look like a brain (Photo 1.9), which is why this coral is commonly called "brain coral". This massive coral reaches more than 30 cm in thickness and up to 2 m in diameter. *D. strigosa* inhabits reef slopes in water depths ranging from 1 to 43 m below sea level and, most commonly, between 6 and 13 m (HUMANN 1996). It also occurs in shallow waters of the shore zone (BAK 1977). Due to its compact body, *D. strigosa* withstands extreme surf and is frequently found on reef crests in association with *A. palmata* (GEISTER 1983; BAK 1977).

Acropora palmata-Diploria strigosa reefs have been observed on the leeward sides of Barbados, the Netherlands Antilles, Jamaica, Hispaniola, Marie Galante, and other islands.

Montastrea annularis (M.a.) (ELLIS and SOLANDER 1786)

The stony coral *Montastrea annularis* ("boulder star coral" or "mountainous star coral") is one of the most important reef building coral species in the Caribbean. It may adopt three distinct morphological types (HALL 1999, MESOLELLA 1968). *M. annularis* forms massive discoid or plate-like colonies in deep water habitats ranging from 10 to 30 m (45 m) below sea level (Photo 1.10). The plate-like formations are adapted to the reduced light flux. In shallower water, *M. annularis* grows in massive boulder-shaped colonies or in columnar forms with annual growth rates of approx. 12 cm. Some *M. annularis* growth types have the appearance of organ pipes with diameters of approx. 1.5 m and heights of more than 3.4 m (GREENBERG 1992). For example, an organ-pipe growth form of *M. annularis* reaches heights of up to 5 m in the back reef zone of a last interglacial coral reef terrace in River Bay on the northeastern coast of Barbados (Photo 2.15).

M. annularis is unable to grow under strong surf conditions. It generally inhabits shallow and calm water of the back reef area or deeper inner reef channels, and fore reef areas at water depths of 6 to 25 m. Individual *M. annularis* colonies may reach water depths of up to 60 m (DUNCAN 1975). Growth rates of *Montastrea* change significantly with depth. As described by DUNCAN (1975), *Montastrea*

Photo 1.10:
Plate-like growth form of *Montastrea annularis* in last interglacial (MIS 5c) fore reef facies (Batts Rock Bay, west coast). *(Photo: SCHELLMANN 2002)*

annularis shows an upward growth of 6.7 mm/year in 10 m of water, but rates of 2.1 mm/year or less in water depths below 27 m.

M. annularis is frequently associated with *Montastrea cavernosa*, *Diploria strigosa*, *Diploria labyrinthiformis*, and *Siderastrea siderea* (HUMANN 1996, GEISTER 1983, BAK 1977, SCATTERDAY 1974).

Siderastrea siderea (S.s.) (ELLIS AND SOLANDER, 1786)

Siderastrea coral species have massive coral heads (Photo 1.11). *Siderastrea siderea* has the most pronounced coral heads, which may reach diameters of more than 60 cm. It is, therefore, called "massive star coral". *S. siderea* is related to *Siderastrea radians* ("lesser starlet coral"), which has smaller and flatter coral heads with diameters of approx. 30 cm (GREENBERG 1992). The shape of corallites also helps distinguish these two species, as the corallites of *Siderastrea siderea* are steeper and have dark centers (HUMANN 1996).

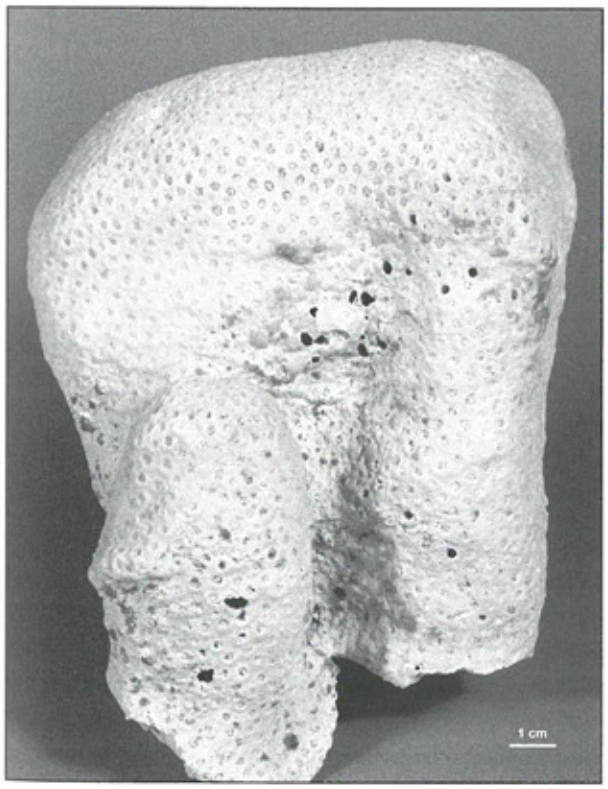

Photo 1.11:
Holocene *Siderastrea siderea* sample from Curaçao, Netherlands Antilles. *(Photo: SCHELLMANN 2000)*

While *Siderastrea siderea* prefers water depths of 8 m to 14 m below sea level, *Siderastrea radians* generally inhabits shallow water with wave movement and water depths ranging from 1 m to 7 m below sea level. According to DEBROT et al. (1998), *Siderastrea siderea* has distinct yearly density bands with growth rates of 3.5 to 5.5 mm/year.

1.3.2. Crustose coralline algae

Caribbean fringing and barrier reefs that are strongly exposed to wave action are frequently encrusted by red calcareous algae (*Melobesiodeae*, dominated by *Porolithon pachydermum* and *Lithophyllum congestum),* encrusting vermetid gastropods, and crust-forming foraminifers, such as *Homotrema rubrum* (GEISTER 1983, ADEY 1978). They are present on subtidal to intertidal reef crests and reef platforms (Photo 1.12), in lagoons, and along rocky cliffs. Crustose coralline algae may be limited to a strong encrustation of the coral detritus, but may also build elongated intertidal and wave-beaten ridges and rims (benches), isolated boiler reefs, and boiler platforms (e.g. ADEY 1986, ADEY 1978). The latter can be found in the uppermost meter of sea water, near the mean sea level (ADEY 1986; KELLETAT 1997). Calcareous algae ridges grow only a few meters thick but can reach up to 20 km in length (with breaks) and 50 m in width (ADEY 1987). Individual algae boiler reefs may reach diameters of more than 30 m. Their size largely depends on sea-level change and wave energy. ADEY (1986) cored present day calcareous algae walls in the Lesser Antilles and measured thickness between 1 and 8 m. However, these enormous thickness values may have resulted from positive sea-level movement. ADEY (1978) presented a summary table for algal ridge areas in the Caribbean.

MARTINDALE (1992) described a zonation model for encrusting coralline algae on recent reefs on Barbados and used the model to interpret the palaeoecological condition of Pleistocene reefs. According to PERRY (2001), both depth and species composition of calcareous encrustations on Pleistocene *Acropora palmata* reef facies on Barbados differ with the exposure to storm waves and surf. For example, encrustations are generally 3 mm to 4 mm thick on the wind-protected west coast. In comparison, they reach depths of up to 20 mm on the storm-exposed northeastern coast of Barbados (PERRY 2001).

Photo 1.12:
Coralline algae is encrusting penultimate interglacial *Acropora palmata* reef crest facies. Sample location: last interglacial $T\text{-}4_{[7]}$ wave-cut platform at Salt Cave Point, south coast of Barbados. Note camera lens for scale. *(Photo: SCHELLMANN 1997)*

Calcareous algae and vermetid gastropods frequently build elongated intertidal rims along the rocky coasts of Barbados. Depending on wave action, these rims develop within a few decimeters around mean sea level. Calcareous algae can live several meters below sea level under the condition of constantly strong wave action (Chapter 2.3). However, the base of geomorphologically significant calcareous algae skeletons does not reach more than 2 m below sea level. In general, calcareous algae extend from their base to low tide water level. They may exceed high tide water level and reach the higher intertidal zone in locations with consistently high surf. Furthermore, they can reach a maximum intertidal height of up to 2 m asl. in areas with high wave energy, such as the windward coastlines of the Antilles (ADEY 1978, ADEY 1986, GEISTER 1983).

2. General geology and physical geography of Barbados

G. SCHELLMANN, U. RADTKE, F. WHELAN

Barbados consists of two principal natural regions, the Scotland District in the east, and the coral reef terraces in the northern, western and southern parts of the island (Figure 2.1). The Scotland District is dissected by gullies and is largely shaped by mass movement (Photo 2.1). The coral reef terraces (Photo 2.2) have a step-like appearance, are altered to an undulating surface by dolines (DAY 1983, WANDELT

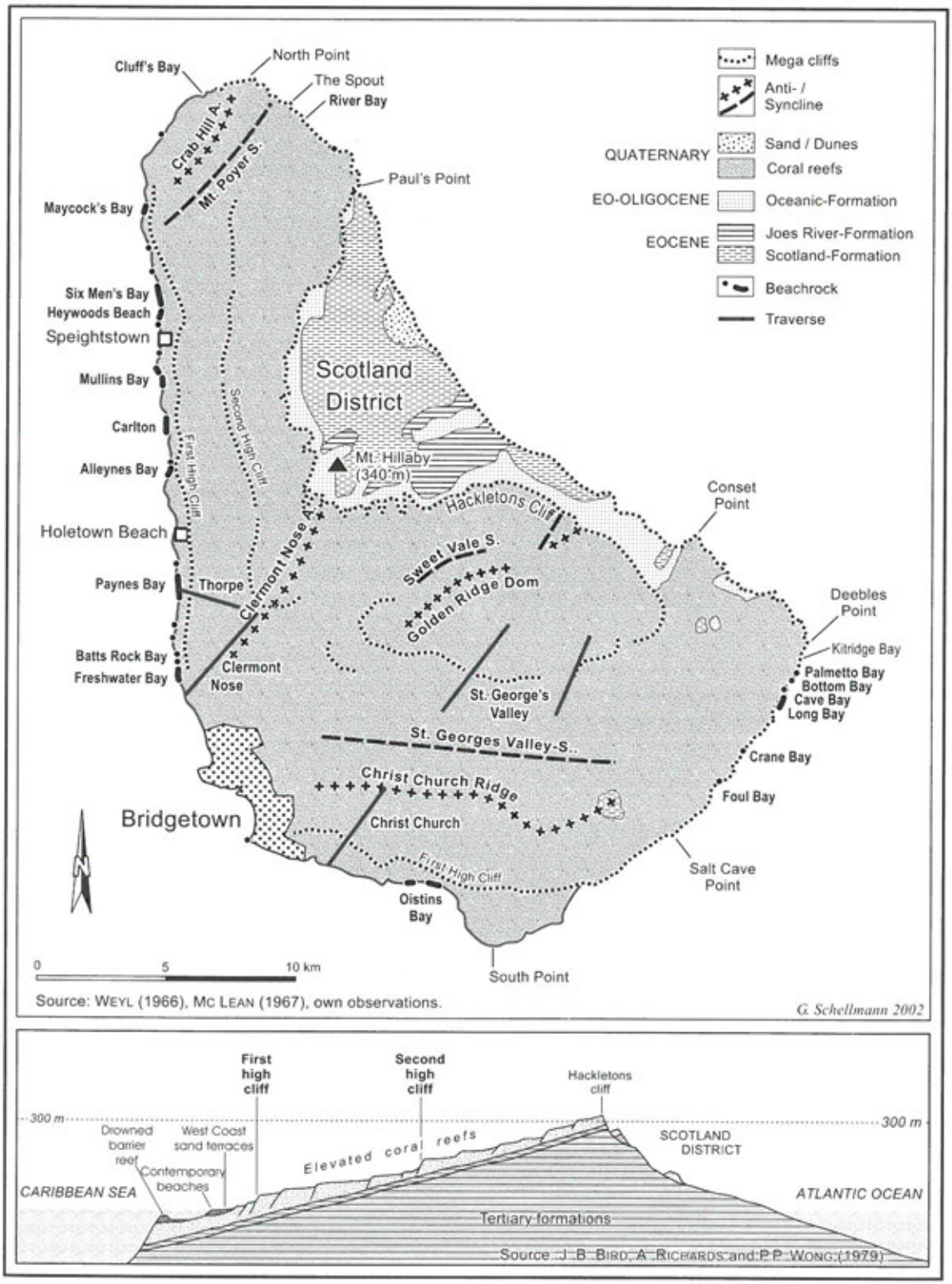

Figure 2.1: The geology of Barbados.

Photo 2.1:
View of Scotland District looking north.
(Photo: SCHELLMANN 1997)

Photo 2.2:
Aerial photograph of the higher elevated coral reef terraces located north of Bridgetown. Note the dolines (elongated or round depressions) and gullies (dense woody vegetation).

2000), and are dissected by dry valleys (FERMOR 1972) and gullies (SPENCER 1902). The island's highest elevations are marked by Mt. Hillaby, which is 343 m high, and by Hackletons Cliff, which is slightly higher than 300 m (Figure 2.1).

A significant escarpment, as displayed at Hackletons Cliff, forms the boundary between Scotland District and the coral limestone terraces (Figure 2.1, Photo 2.3). The cliff is continually being eroded back by fluvial processes, rock falls, and mass movements. Individual coral boulders slowly slide downhill towards the coastline (Photo 2.4), where they become erratics in a new environment, and where they are slowly being destroyed by waves of the Atlantic Ocean, chemical weathering, and littoral bio-erosion.

Except for minor ash layers, volcanism is absent on Barbados due to the thickness of the Earth´s

Photo 2.3:
Viewpoint at Hackletons Cliff.
(Photo: SCHELLMANN 1994)

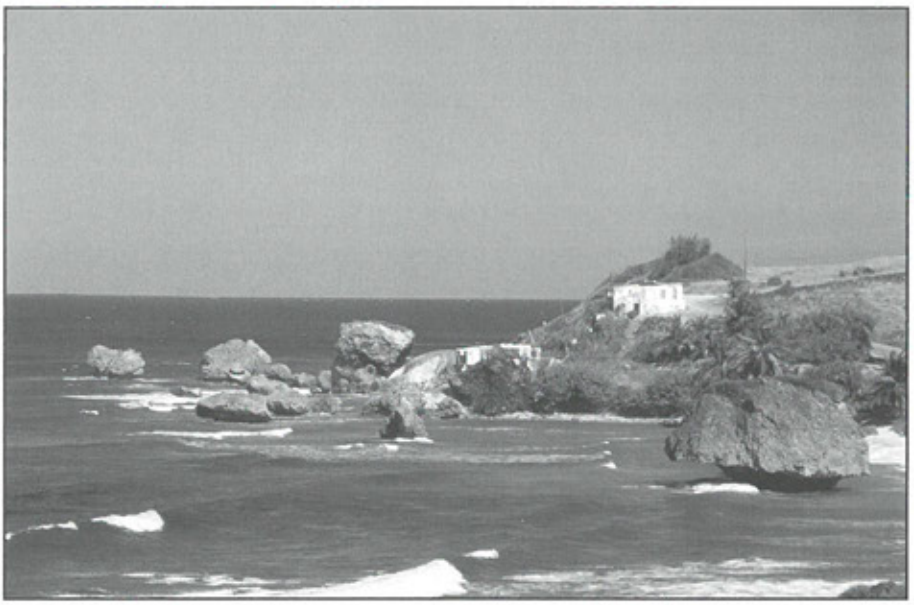

Photo 2.4:
Migrated "erratic" coral limestone boulders located on the Atlantic coast of Scotland District.
(Photo: SCHELLMANN 1997)

mantle at the Barbados Ridge, a reduced convective mantle current, and the relatively low degree of descent of the Atlantic oceanic crust in this area. Instead of volcanic material, Pleistocene coral limestone reaches a thickness of up to 130 m and covers the folded, broken, shifted, and only weakly consolidated oceanic sedimentary rock originating from the Eocene to Miocene (TORRINI 1986, SPEED 1981, WEYL 1966).

2.1. The Tertiary basement and the Scotland District

The Tertiary basement, which lies underneath the Pleistocene coral cap, is subject to significant erosion in eastern Barbados (Figure 2.1). It determines the landscape of the Scotland District. Minor outcrops of Tertiary sedimentary rock are restricted to some small areas in southern and southeastern Barbados (Figure 2.1) and to some individual locations near Cluff's Bay, located in northern Barbados. The Tertiary basement consists of rocks that are very susceptible to landslides, earth flows, and fluvial erosion, forming v-shaped valleys. The Tertiary rocks are composed of radiolarian earth, clay and mudstone, intercalated by sandstone and conglomerate.

Table 2.1:
Tertiary rock types of Scotland District (generalized after WEYL 1966, and TORRINI & SPEED 1989).

Pleistocene	Coral Rock Formation			Coral reef limestone
Pliocene				
Miocene	Globigerina marl	1000 m	"Oceanic Allochton" (moderately folded and faulted)	Globigerina marl, clay
	Bissex Hill Formation	20 m		Foraminiferal arenite
Oligocene	Oceanic Formation	570 m		Radiolarian earth, clay, ash
Eocene	Joes River Formation	0 - 300 m	"Basal Complex" (strongly folded and faulted)	Organic mudstone
	Scotland Formation	> 1300 m		Mudstone, Quartz sandstone, conglomerate

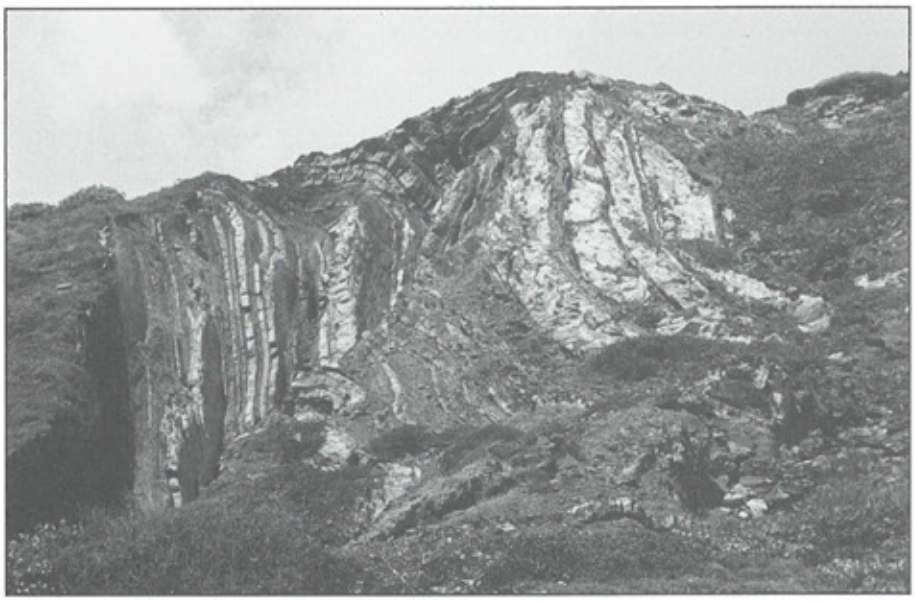

Photo 2.5:
This folded sandstone of the Eocene Scotland Formation was observed in Scotland District, northern Barbados. *(Photo: SCHELLMANN 2000)*

Photo 2.6:
Woodburne Oil Field in St. George's Valley.
(Photo: SCHELLMANN 1994)

Layers in the Eocene formations "Scotland" and "Joes River" (Table 2.1), which have a high clay and montmorillonite (swelling clay mineral) content, function as slip planes (DEGRAFF et al. 1989). PRIOR & HO (1972) suggested that groundwater, which flows through the coral limestone cap after heavy rainfall, forms deep v-shaped valleys, and causes catastrophic slides on the steep slopes of the Scotland District. Intensive deforestation due to agriculture and settlement also contributes to the highly dissected erosive landscape of Scotland District (Photo 2.1), which is characterized by deep v-shaped valleys, sharp-crested ridges, significant earth flows, lobate mudflows, rotational slides, and large coral blocks that slowly slide from the coral reef escarpment to the Atlantic coast (Photo 2.4).

Seafloor off-scrape, the displacement of nappes, and the intrusion of tectonic mud diapirs (SPEED 1981, SPEED 1990) largely contributed to the strong folding and faulting of the predominantly marine sedimentary rocks of Barbados. For this reason, the landscape is strongly reminescent of alpine tectonically folded environments (Photo 2.5).

A simplified stratigraphy of the marine Tertiary sequence of Barbados is illustrated in Table 2.1. This stratigraphy consists of four major geologic units:

(1) The oldest unit is the basal complex, which is an accretionary complex mainly composed of terrigenous turbidite and gravity-flow deposits of Eocene age. This strongly faulted complex contains rocks of two lithic suites. The first suite

comprises the terrigenous rocks of Joes River and the Scotland Formation, which are mudstones, sand and sandstones. A possibly older hemipelagic suite of the Scotland Formation with radiolarian mudstone and radiolarite characterizes the second suite. According to SPEED (1990), the basal complex was deformed and accreted towards the end of the Eocene.

(2) Subsequently, the strongly deformed basal units are overlain by the shallow dipping and faulted nappes of the Oceanic and Bissex Hill Formations. The Oceanic Formation is dominated by deep-water pelagic rocks, such as radiolarian marls, which are more strongly deformed than the marls and sandstones of the Bissex Hill Formation (SPEED & LARUE 1982). The Oceanic nappes were emplaced during the Miocene approx. <16 to 20 million years ago (SPEED 1990). The glauconitic sandstones of the Bissex Hill Formation imply a deposition in shallow water, whereas the globigerina marls and clays of the Upper Miocene Globigerina Marl Formation suggest deposition in great water depths.

(3) Due to prolonged erosion, sedimentary rocks from the late Miocene and Pliocene are absent on Barbados. Instead, the unconformable overlying Pleistocene Coral Rock Formation was developed in shallow water conditions during the last 0.7 to 1.0 million years.

(4) Unlike the Pleistocene Coral Formation, all units have been intruded by tectonic diapirs consisting of an organic mud matrix. SPEED (1990) and SPEED & LARUE (1982) suggested that the Neogene and Pleistocene uplift of Barbados was partly a result of local mud diapirism. According to SPEED (1990), TORRINI & SPEED (1989), and SPEED & LARUE (1982), the central mud diapir caused the anomalous elevation of Barbados above the Barbados Accretionary Prism and is probably still active.

The Tertiary sedimentary strata contain oil and gas, which is being exploited in Woodburne Oil field, Saint George Valley (Photo 2.6). However, the oil supply is limited and Barbados is not able to meet the domestic demand for crude oil.

2.2. The Pleistocene coral reef cap

Only 15% of the surface of Barbados consists of Tertiary sedimentary rocks. Approx. 85% of the island is covered by Pleistocene coral limestone, lying discordantly over the Tertiary basement, and ranging in thickness from approx. 15 to 130 m (Figures 2.1 and 2.2). In general, the coral cap thins where the elevation of the Tertiary basement is high, and it thickens in areas with a little elevated basement (MESOLELLA et al. 1970). The coral limestone cap

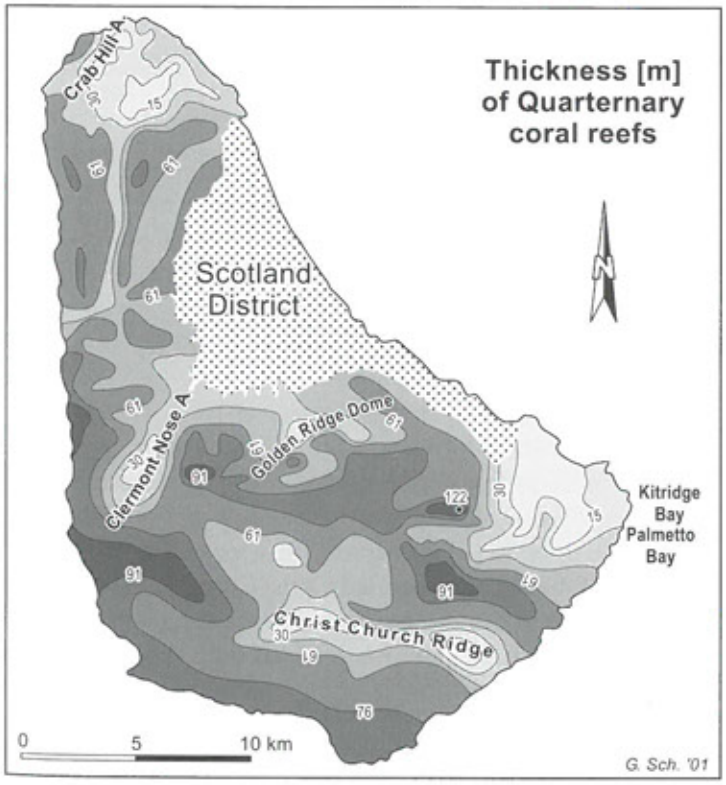

Figure 2.2:
Thickness of the Pleistocene coral cap of Barbados after MESOLELLA et al. (1970).

Photo 2.7:
View of Second High Cliff reef terraces and Sweet Vale Valley, central Barbados.
(Photo: SCHELLMANN 1999)

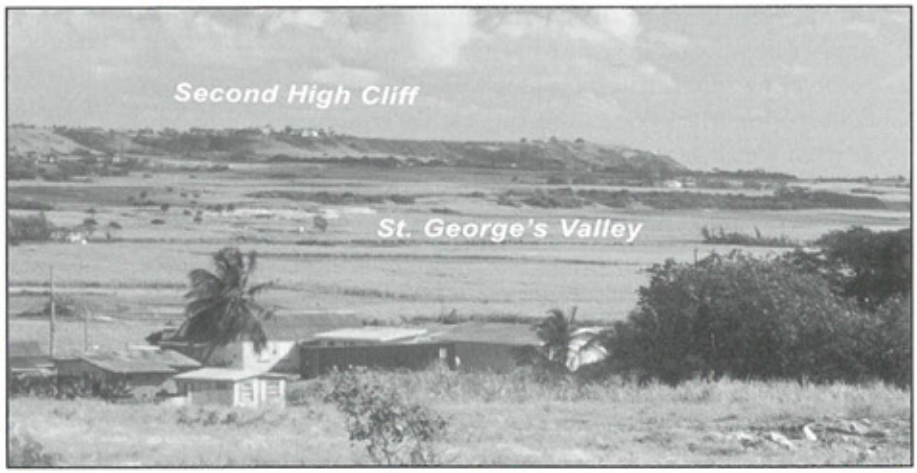

Photo 2.8:
View of St. George's Valley. Note Second High Cliff in the background of the photograph.
(Photo: SCHELLMANN 1999)

was formed during the Pleistocene emergence of Barbados. During this time, new fringing reefs were produced repeatedly under the influence of numerous sea level fluctuations. Continuing uplift locally caused them to be anticlinally or synclinally warped or to be broken (WEYL 1966, FERMOR 1972, TAYLOR & MANN 1991).

The Crab Hill Anticline is located at the northern tip of the island (Figure 2.1). There, the Tertiary base is exposed above sea level near Cluff´s Bay. Mt. Power Syncline is located to the south of the Crab Hill Anticline and extends from NE to SW. The Clermont Nose or Clermont - Mt. Hillaby Anticline parallels this syncline in the center of the island. It is in the vicinity of the Clermont - Mt. Hillaby Anticline that the coral reef terraces of the Late and Middle Pleistocene show their greatest uplift. There, First High Cliff and Second High Cliff (see below) reach their greatest elevations of 61 m and 201 m asl., respectively (TAYLOR & MANN 1991).

TAYLOR & MANN (1991) assumed that the Clermont - Mt. Hillaby Anticline has been active for as long as one million years. The direction of the strike changes to a more westerly bearing at the southeastern part of the island. However, both the Sweet Vale Syncline with the morphology of a valley-like depression (Photo 2.7), and the Golden Ridge Dome belong to the older north island, which is more than 600,000 years old. St. George Valley Syncline, with the morphology of an elongated depression (Photo 2.8), is located to the south and extends in W-E direction. This depression is located in the vicinity of the strongly uplifted Christ Church Ridge. It used to form a small seaway between the main island to the north and the south island until the penultimate interglacial.

In contrast to northern Barbados, the southern

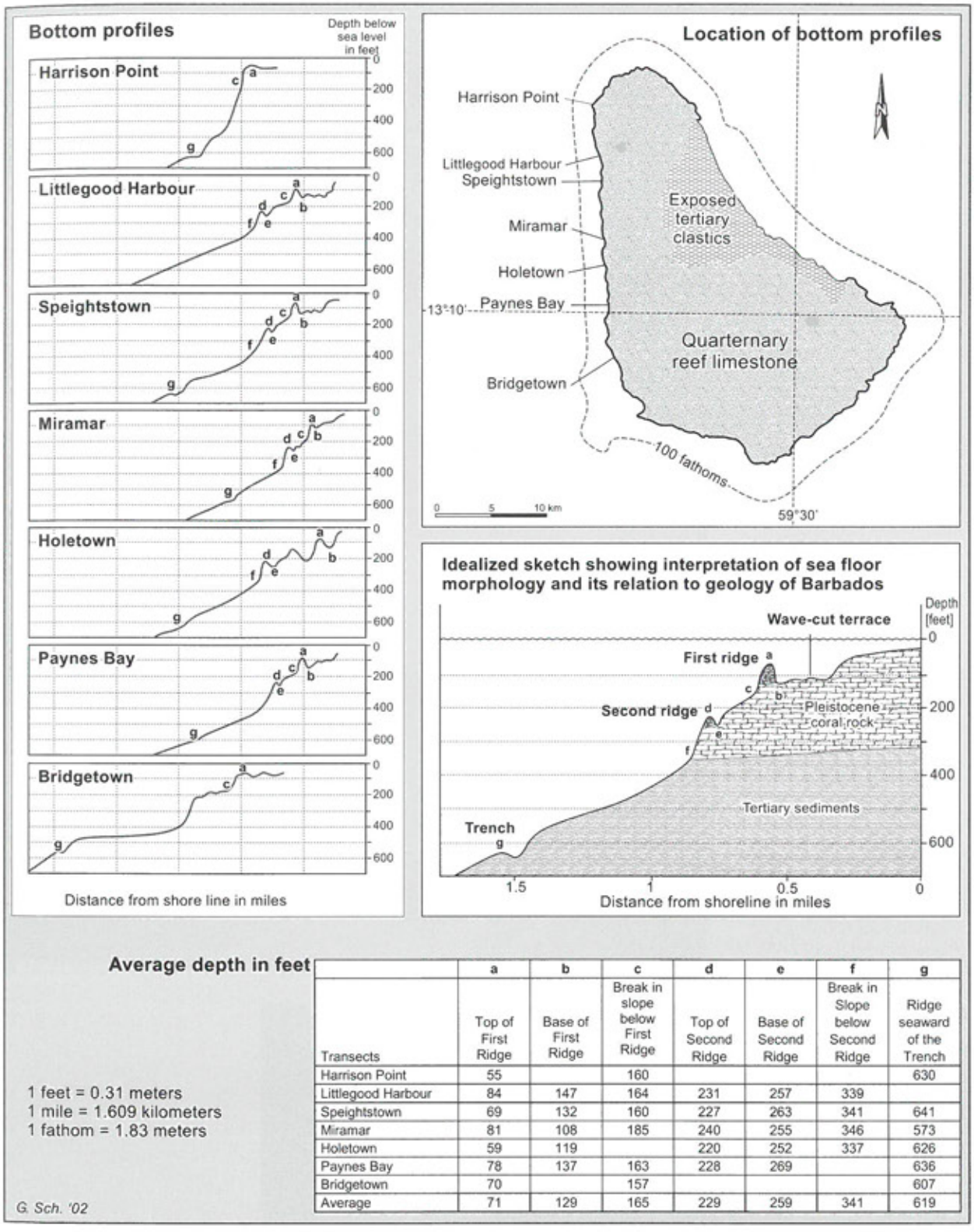

Average depth in feet

Transects	a Top of First Ridge	b Base of First Ridge	c Break in slope below First Ridge	d Top of Second Ridge	e Base of Second Ridge	f Break in Slope below Second Ridge	g Ridge seaward of the Trench
Harrison Point	55		160				630
Littlegood Harbour	84	147	164	231	257	339	
Speightstown	69	132	160	227	263	341	641
Miramar	81	108	185	240	255	346	573
Holetown	59	119		220	252	337	626
Paynes Bay	78	137	163	228	269		636
Bridgetown	70		157				607
Average	71	129	165	229	259	341	619

1 feet = 0.31 meters
1 mile = 1.609 kilometers
1 fathom = 1.83 meters

G. Sch. '02

Figure 2.3: Submerged coral reefs on the west coast of Barbados (modified after MACINTYRE 1967).

island is significantly younger and most likely emerged no more than 400,000 years ago (Chapter 4).

Due to the different rates of uplift in the vicinity of tectonic depressions and anticlines, coral reef terraces reach their greatest elevations in the center of the northern island (e.g. up to 300 m asl. at Hackletons Cliff). Hackletons Cliff is an important escarpment of the Scotland District located to the northeast. Coral reef terraces descend in several larger and smaller terrace steps from Hackletons Cliff

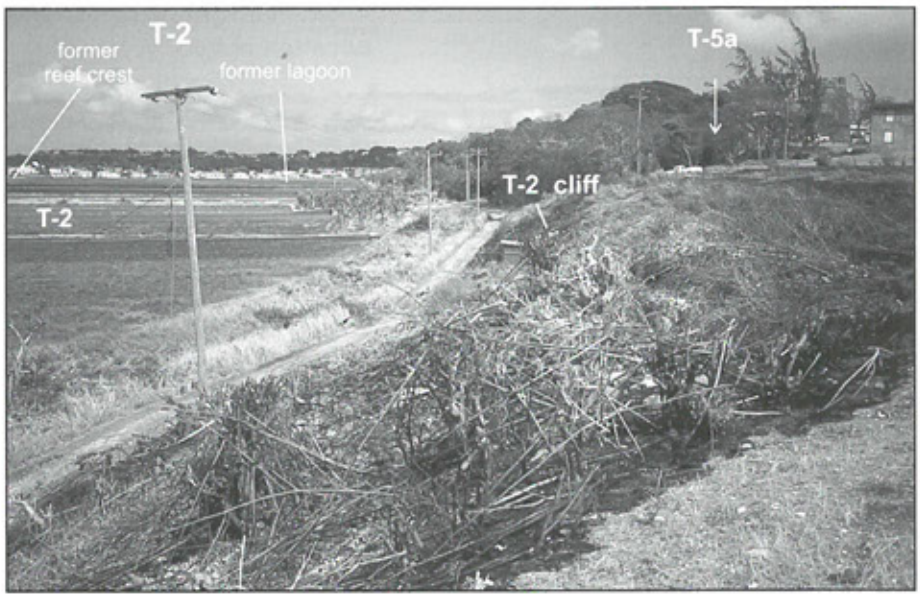

Photo 2.9:
View of First High Cliff near Rendezvous Hill, southwest coast of Barbados. The less elevated lagoonal area of the T-2 coral reef terrace is on the left side.
(Photo: SCHELLMANN 1997)

Photo 2.10:
View of Second High Cliff near Speightstown, north-western central Barbados.
(Photo: SCHELLMANN 1999)

Photo 2.11:
Large coastal section of Middle Pleistocene coral limestone sliding sea-wards near Palmetto Bay, south eastern Barbados.
(Photo: SCHELLMANN 1997)

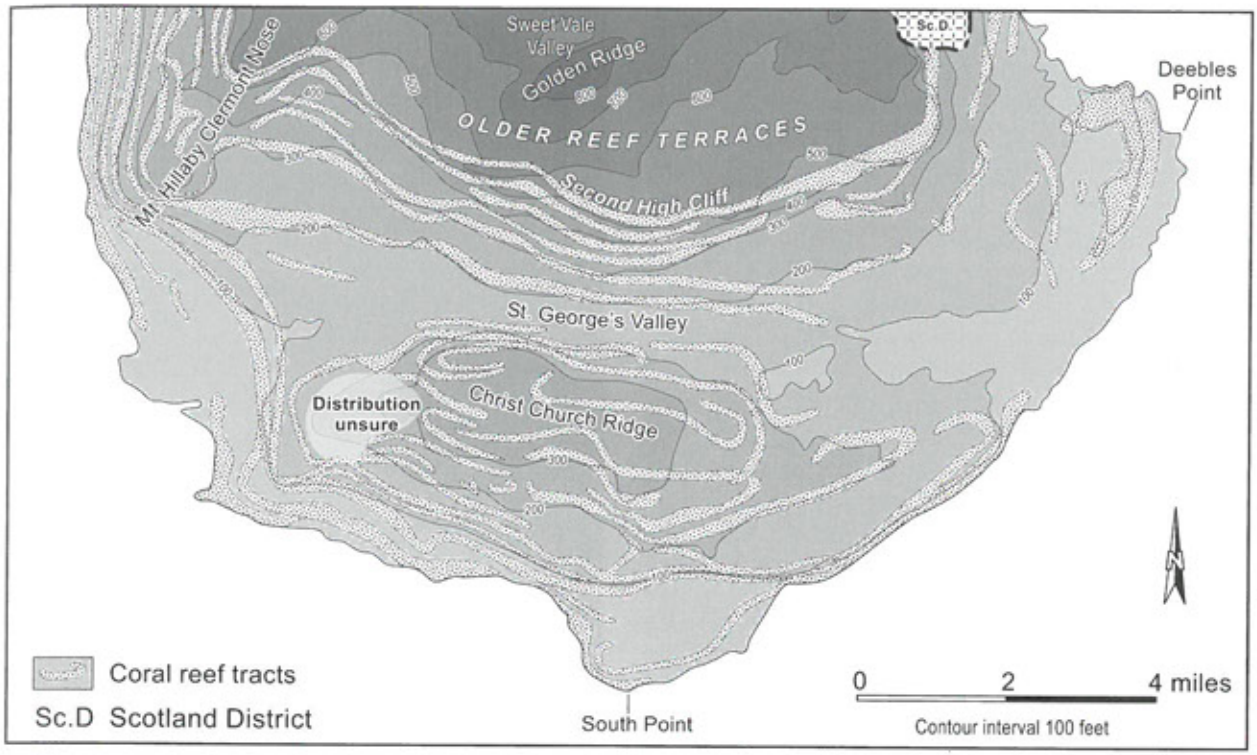

Figure 2.4: Coral reef tracts in southern Barbados modified after MESOLELLA et al. (1969).

in the northern, western, and southern directions to the Caribbean Sea or to St. George Valley. The coral reef terraces are clearly separated from each other by cliffs. Different uplift rates are not the only reason for the different levels of coral reef terraces. Sea-level fluctuations may also form terrace steps if coral growth keeps up with the changing water level.

According to MACINTYRE (1967), two submerged barrier reefs are currently observable at water depths of 17 to 26 m (55 to 84 feet) and of approx. 67 to 73 m (220 to 240 feet) on the west coast of Barbados (Figure 2.3). MACINTYRE et al. (1991) assumed that the deeper ridge was formed approx. 12,000 years BP, and was subsequently submerged in deep water due to a rapid sea-level transgression occurring approx. 10,000 years BP. Since that time, tectonic uplift has not been large enough to elevate these reefs above present sea level.

First High Cliff and Second High Cliff are the two most important cliff-steps on Barbados (Figure 2.1). First High Cliff is located close to the coastline and marks the first important step of coral reef

Photo 2.12:
Large coastal section of Middle Pleistocene coral limestone sliding seawards near Kitridge Point, south eastern Barbados.
(Photo: SCHELLMANN 2000)

terraces to elevations of more than 15 m to 61 m above present sea level (Photo 2.9, TAYLOR & MANN 1991).

Second High Cliff ranges from 72 to 201 m asl. in elevation (TAYLOR & MANN 1991), and separates the oldest and highest reef complex, which is located in the central part of the island, from the lower elevated reef terraces in northern, western, and southeastern Barbados (Photo 2.10).

Pleistocene coral reef limestones reach their greatest thickness of about 130 m in St. George Valley, located in the southeastern part of the island. This thickness implies a long-term submergence of this morphologically preserved depression. In contrast, coral limestone thickness is significantly lower in the anticlinal uplift areas of the Tertiary base, as, for example, at Christ Church Ridge, the Clermont Nose Anticline, and the Crab Hill Anticline (Figure 2.2). The coral cap is also very thin at Kitridge Point and Palmetto Bay, both located on the east coast of Barbados. There, the modern sea cliff is approx. 15 m to 20 m high and consists of coral limestone. Due to sublittoral erosion of the underlying Tertiary rock, the cliff slowly slides down towards the sea in form of large slabs that are 50 m to 120 m wide and approx. 400 m long (Photo 2.11 and 2.12).

As discussed by MESOLELLA (1967) and MESOLELLA et al. (1969), the numerous reef terraces of different heights were not abraded out of one old coral reef of uniform age (see Chapter 3), but are independent depositional coral reef bodies of different ages (Figure 2.4). Figure 2.4 illustrates the distribution of coral reef tracts on southern Barbados as presented by MESOLELLA et al. (1969). The indi-

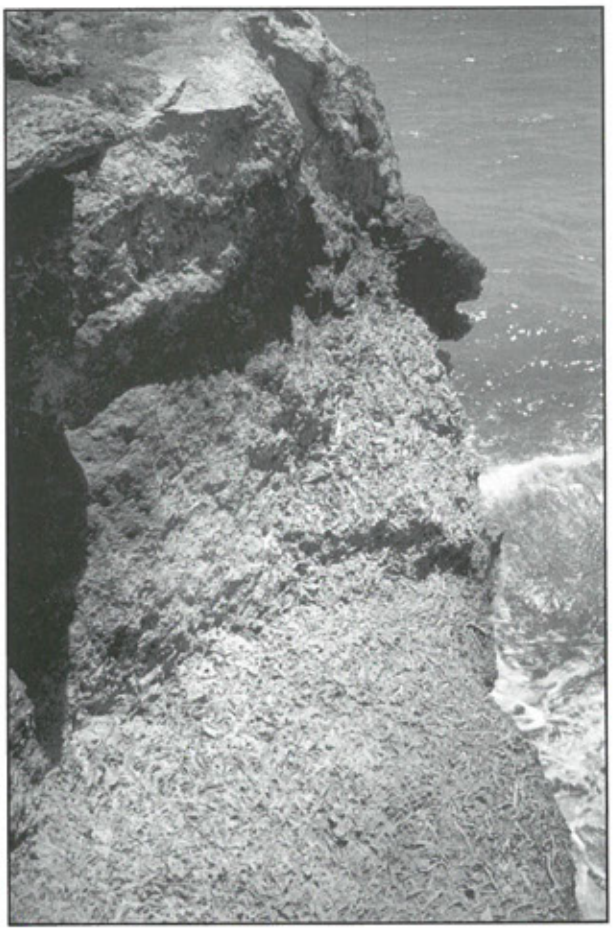

Photo 2.13:
Last interglacial (MIS 5e) *Acropora cervicornis* facies underneath massive *A. palmata* reef crest facies, exposed at the recent cliff line southwest of Bottom Bay.
(Photo: SCHELLMANN 1997)

Photo 2.14:
Penultimate interglacial *Acropora palmata* reef crest facies at Salt Cave Point, southern Barbados.
(Photo: SCHELLMANN 2002)

vidual reef tracts are comparable to the island's present active fringing reefs and have different reef zone facies, including fore reef, reef slope, reef crest, back reef, and lagoonal facies (Chapter 4.2.). A complete description of reef-associated facies within the Pleistocene coral reef cap of Barbados was provided by MESOLELLA (1967 and 1968), MESOLELLA et al. (1970), and JAMES et al. (1977).

In general, a typical Pleistocene coral reef terrace of Barbados consists of (1) a fore reef calcarenite zone located at the foot of the reef slope; (2) a reef slope, reef crest, and near back reef zone; and (3) a back reef or lagoonal facies located in the lee of the former wave-exposed reef platform (see also Chapter 4.2).

Mechanical erosion of the reef framework generates the fore reef zone, which is generally characterized by steeply dipping, laminated sands and coral fragments. Fore reef deposits are well exposed along the southeast coast of Barbados, especially at Deebles Point (e.g. HUMPHREY & KIMBELL 1990; for location see Figure 2.1). The deeper reef slope zone is composed of different head coral species, such as massive growth forms of *Montastrea annularis*, and various species of *Diploria* and *Siderastrea*.

This mixed coral facies is followed by the *Acropora cervicornis* zone in the landwards and upwards areas of the deeper reef slope facies zone. The *Acropora cervicornis* zone predominately consists of broken stags of *A. cervicornis* in a fine-grained carbonate matrix (Photo 2.13). In contrast to present day reefs on the west coast of Barbados

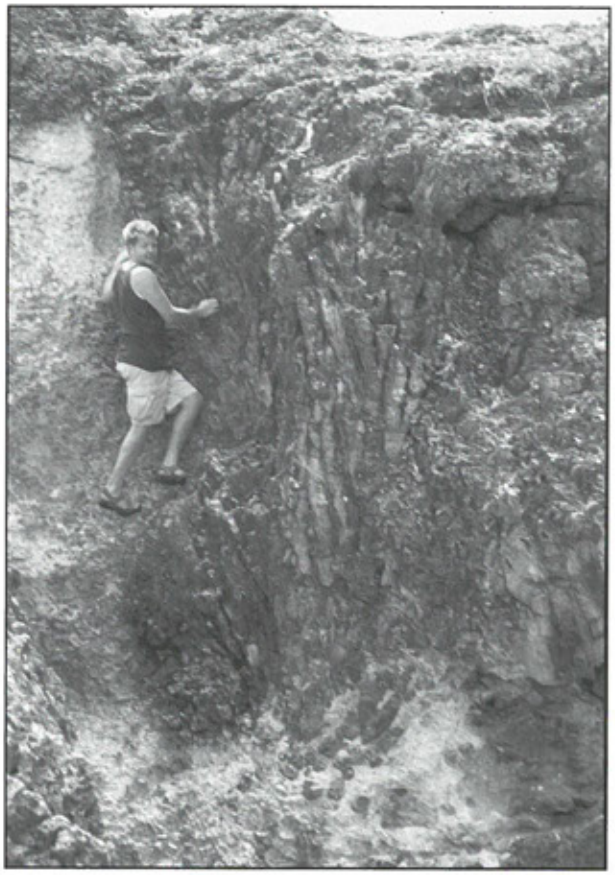

Photo 2.15:
Organ pipe growth form of *Montastrea annularis* in last interglacial (MIS 5e) back reef environment at River Bay, northern Barbados.
(Photo: SCHELLMANN 2000)

(Chapter 2.3), the crests of Pleistocene fringing reefs are dominated by *Acropora palmata* (Photo 2.14).

The former near back reef environments (rear

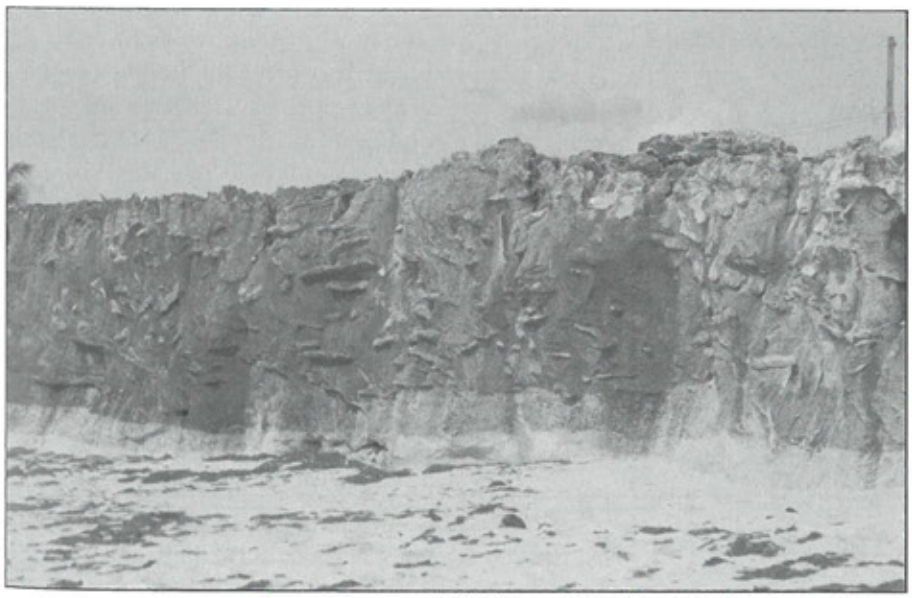

Photo 2.16:
Holocene cliff in last interglacial (MIS 5a) reef terrace, composed of sandy lagoon sediments with reworked boulders of *Acropora palmata* located at Shark's Hole, southeast coast of Barbados.
(Photo: SCHELLMANN 1999)

zone) is populated, for example, by large multilobate, pipe organ formations of *M. annularis* (Photo 2.15), and by *Diploria* and *Siderastrea* species. Small patches of *A. cervicornis* and *Porites porites* may occur locally.

The shallow back reef or lagoonal facies is characterized by calcarenites and limestone muds with scattered isolated coral in growth position, and by coral debris (Photo 2.16) and other wash-over sediments originating from the reef platform.

Beach deposits are occasionally preserved in form of gently seaward dipping or cross-stratified calcareous sandstones located at the landward margin of this zone. Beach deposits located on top of a coral reef body mark the beginning of the regression of a sea-level highstand. For example, a well exposed deposit is preserved at Bottom Bay on top of the last interglacial (stage 5e) *Acropora palmata* reef crest facies (Chapter 5.2.).

The different reef facies zones are fully or partially well exposed in numerous road cuts, quarries, and sea cliffs throughout the island. BLANCHON & EISENHOWER (2001) published some detailed information on the facies of last interglacial terraces of Barbados. HUMPHREY & KIMBELL (1990) provided a detailed description of fore reef calcarenites at the southeastern coast of Barbados. MARTINDALE (1992) and PERRY (2001) used calcareous encrustation communities for the interpretation of palaeo-ecological conditions of Pleistocene reefs on Barbados. Thin crusts are abundant and widespread, especially in reef crest communities dominated by *A. palmata*. However, MESOLELLA et al. (1970: 1904) stated "The contribution of encrusting coralline algae to the framework of the Barbados reefs is not consistent."

2.3. Modern fringing reefs, littoral forms, and tsunami deposits

Actively growing reefs are largely missing on most of the eastern and northern windward coastlines of Barbados. As described by LEWIS (1960a), Barbados' eastern coast is fringed with dead reefs located no more than several hundred meters off shore. In front of the sandy beaches of Scotland District, distinct reef flats with widths of 100 m to 200 m are preserved. Only dead coral reefs have been observed on the northern shores. Some scattered alive coral patches exist on the southern coast. A discontinuous barrier reef with few living coral colonies is present along the southeast coast (HUMPHREY 1997).

Actively growing fringing reefs have recently been restricted to the western leeward coastline of Barbados, where they were observed along a distance of approx. 18 km between Paradise Beach in the south and Six Men's Bay in the north. According to LEWIS (2002), these reefs were subject to widespread degradation from 1950 to 1991. During this time period, their surface area was reduced by 10%.

The following paragraphs describe Barbados' modern fringing reefs as presented by LEWIS (2002), LEWIS (1960a), and STEARN et al. (1977). The reefs extend as far as 100 to 150 m offshore and terminate in water depths less than 6 m to 10 m. The reefs grow on the shelf as approximately 20 narrow segments, semi-circles or curved strips. Their morphology is similar to that of modern fringing reefs elsewhere in the Caribbean. They are characterized by coral zonation including a shoreward sandy back reef zone or shallow lagoon, a reef crest area, and a seaward spur and groove zone. The latter is typified by alternating ridges and valleys located on the uppermost reef slope up to a water depth of 6 m. The reef crest zone ranges from 20 to 100 m in width and emerges during extremely low tides. The surface is covered with dead coral rubble encrusted by crustose coralline algae, and with living coral, such as *Favia fragum*, small numbers of *Porites porites* and *P. astreoides*, and scattered colonies of *Diploria clivosa*, etc. The seaward side of the reef frequently has a spur-and-groove relief with a high proportion of the coral species *Porites porites*, *Montastrea annularis*, *M. cavernosa*, *Siderastrea siderea*. *Acropora palmata*, *Diploria strigosa*, and *D. labyrinthiformis* are also present. Larger colonies of *Acropora cervicornis* grow on the seaward side in water depths ranging from 16 to 20 m. Colonies of massive coral species, including *Diploria strigosa*, *Montastrea annularis* and *Montastrea cavernosa*, as well as *Siderastrea sp.*, were observed in water depths of 20 to 30 m.

The modern reefs on the leeward coast are associated with submerged wall-reef ridges (Chapter 2.2.), which were described in detail by MACINTYRE (1967; 1972) and MACINTYRE et al. (1991).

The coastline of Barbados is relatively smooth and has no deep indentations or offshore islands. The

coastline of the Scotland District, located in the eastern part of the island, has some long sandy or pebbly beaches with massive limestone boulders. These boulders are erratics in their new environment, as they slid down from the coral limestone outcrops in the higher surrounding area. Cliffs, which are mainly composed of last and penultimate interglacial coral reef formations, rise up to elevations of 10 m to 30 m above sea level at the northern coast between Hangman's Bay to the west and River Bay to the east. A few small lowly elevated reef platforms of late last interglacial age (marine isotope stage, MIS, 5a or 5c) are preserved in front of the predominant cliff line (e.g. at Cluff's Bay, located west of North Point).

Sandy beaches are common on the western and southwestern coast between Hangman's Bay and Oistin's Bay. Last or penultimate interglacial coral limestone cliffs again predominate on the southeastern coast. They frequently rise up directly from the sea. However, some cliffs are separated from the ocean by sandy beaches (e.g. Silver Sands, Long Bay, Crane Beach) or sandy bays (e.g. Foul Bay, Cave Bay, Bottom Bay, Palmetto Bay, Kittridge Bay). The cliffs vary in height from 6 m to 15 m in the vicinity

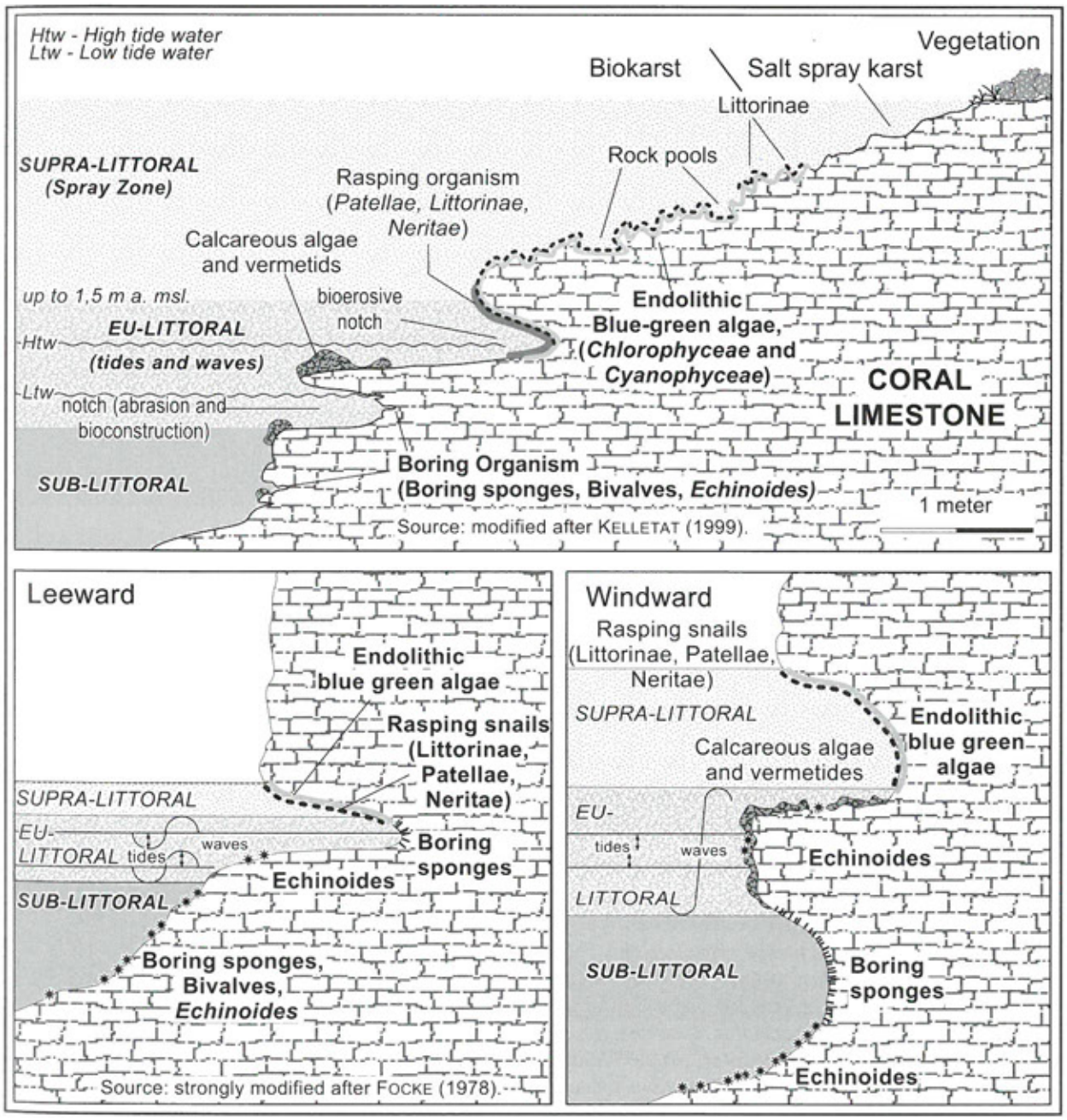

Figure 2.5: Notch morphology in dependence on tides and wave action (modified after KELLETAT 1999, and FOCKE 1978a).

of South Point, and, from 20 m to 30 m between Paragon and the eastern tip of the island.

Two impressive elements of Barbados' cliff coastlines are (1) rims (trottoirs) and solitary platforms of calcareous algae and vermetid gastropods (Photos 2.17 to 2.21); and (2) deeply incised notches (Photos 2.22 to 2.25). Both notches and calcareous bio-constructional forms are widely distributed along the wave-exposed northern and southeastern shorelines. While the bases of the notches commonly lie near mean low tide water level, their height and shape varies depending on wave height and high tide water level, as illustrated with Figure 2.5. The depths of the notches range from some decimeters to more than 2 m.

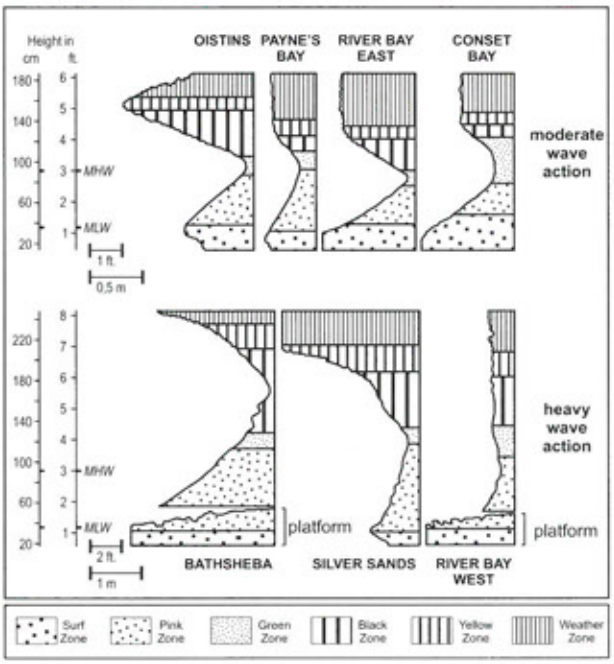

Figure 2.6:
Recent notch profiles of cliff sample sites on Barbados (modified after LEWIS 1960b). The zonation of organisms is described in the text. Zones include (1) the Surf Zone, inhabited by *Echinometra lucunter*, *Fissurella barbadensis* and others, and by sponges, *Bryozoa* and various algae species; (2) the Pink Zone, with widespread encrustations of coralline algae and the small vermetid *Spiroglophylus irregularis*; (3) the Green Zone, populated by endolithic blue green algae, which penetrate some millimetres into the rock; (4) the Black Zone, characterized by the very rough and pitted surface of the rock and inhabited by algae species, as well as *Acanthopleura granulata* and *Thais patula;* (5) the Yellow Zone, with a rough surface and yellow color due to a thin film of algae. The Yellow Zones is occupied by *Tectarius tubaculatus*, *Littorina ziczac*, *Nerita peleronta*, and *Nerita versicolor*; (6) the Weather Zone, with a very rough surface and dark brown to black color due to an algae film. *Tectarius tuberculatus*, and different species of *Littorinae* and *Neritae* populate the Weather Zone.

LEWIS (1960b) provided detailed descriptions of recent notch profiles for various cliff sample sites on Barbados. These descriptions included the zonation of organisms, as illustrated in Figure 2.6. Notch height is greater and vertical organism zones are wider on sites with stronger wave action, as for example, on the sample sites of Bathsheba, Silver Sands, and River Bay. According to LEWIS (1960b), indicator species for the Surf Zone (1) include *Echinometra lucunter*, *Fissurella barbadensis*, sponges, Bryozoa, and various algae species. The Pink Zone (2) is typified by widespread encrustations of coralline algae and the small vermetid *Spiroglophylus irregularis.* Endolithic blue green algae, which penetrate into the rock approx. 60 to 200 µm, characterize the Green Zone (3). The Black Zone (4) is the very rough and pitted surface of the rock. It is inhabited by algae species, and the fauna *Acanthopleura granulata* and *Thais patula.* The Yellow Zone (5) is distinguished by its rough surface and by the yellow color generated by a thin film of algae. Common fauna include *Tectarius tubaculatus*, *Littorina ziczac*, *Nerita peleronta*, and *Nerita versicolor.* The Weather Zone (6) has a very rough surface and is typified by its dark brown to black color caused by a film of algae. Common organisms include *Tectarius tuberculatus* and various species of *Littorinae* and *Neritae*.

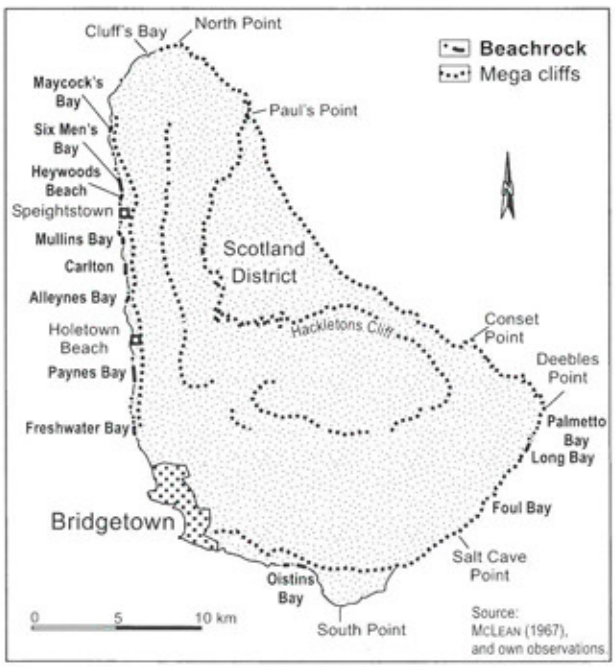

Figure 2.7: Beachrock distribution on Barbados.

Photo 2.17:
Calcareous algae pool, north-east coast of Barbados.
(Photo: SCHELLMANN 1997)

Photo 2.18:
Calcareous algae platform along the northeastern Atlantic coast of Barbados (near 'The Spoud').
(Photo: SCHELLMANN 2000)

Photo 2.19:
Calcareous algae platform (Photo 2.18. enlarged).
(Photo: SCHELLMANN 2000)

Photo 2.20:
Algae rim.
(Photo: SCHELLMANN 2000)

Photo 2.21:
Calcareous algae platform around coral limestone, which is subject to strong bioerosin ('The Spoud', northeast coast of Barbados).
(Photo: SCHELLMANN 2000)

Photo 2.22:
Bioerosive notch (diameter ca. 2 m) in last interglacial coral limestone north of 'Crane Beach' (southeast coast of Barbados).
(Photo: SCHELLMANN 2000)

Photo 2.23:
Bioerosive notch (Photo 2.22 enlarged).
(Photo: SCHELLMANN 1999)

Photo 2.24:
Bioerosive notch (Photo 2.22 enlarged).
(Photo: SCHELLMANN 2000)

Photo 2.25:
Bioerosive notch (Photo 2.22 enlarged).
(Photo: SCHELLMANN 2000)

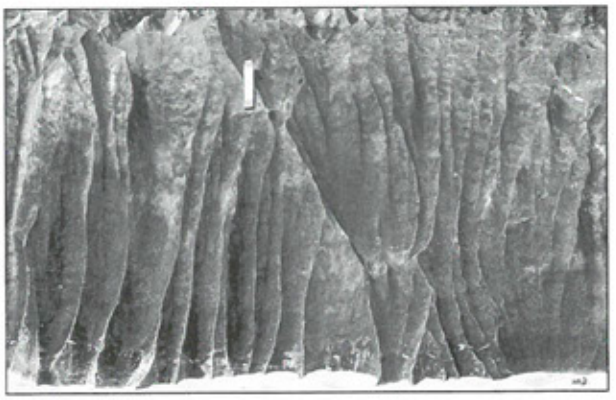

Photo 2.27:
Holocene cliff with karren solution forms in last interglacial back reef facies (calcareous sandstones) at Sharke's Hole, southeast coast of Barbados. Note tape measure (c. 20 cm in length) for scale.
(Photo: SCHELLMANN 1997)

Photo 2.26:
Salt spray micro-karst on late last interglacial (MIS 5a) coral limestone in the vicinity of South Point, located on the southern coast of Barbados. Note camera lense for scale.
(Photo: SCHELLMANN 1994)

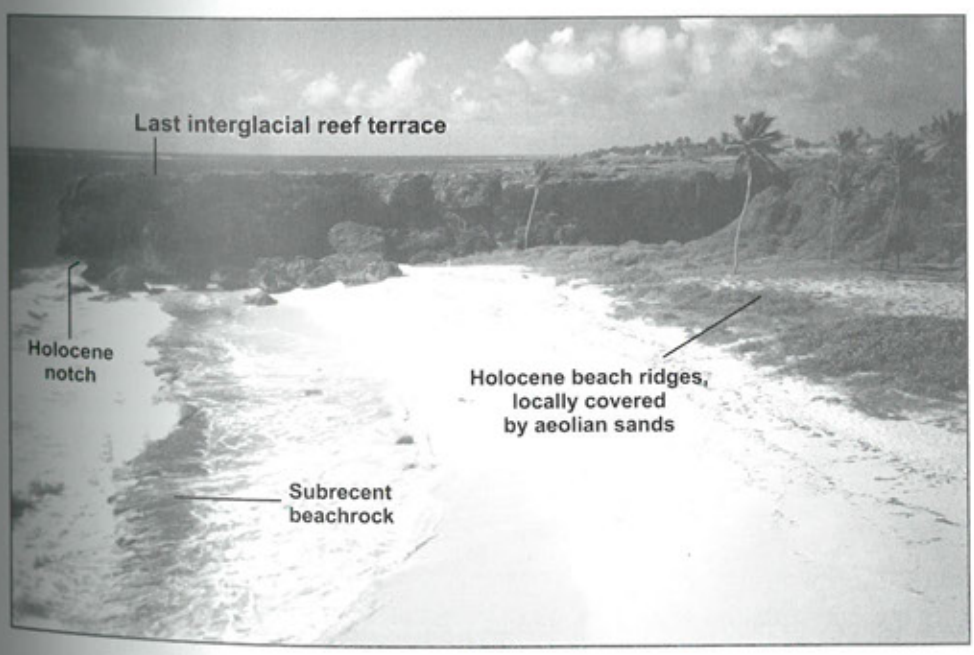

Photo 2.28:
Subrecent beachrock at Palmetto Bay.
(Photo: SCHELLMANN 1999)

As stated by BIRD et al. (1979), notch incision measurements at the west coast (Mullin Bay and Paynes Bay) indicated a notch retreat of 0.2 to 2 mm/year. If these estimates are accurate, a 2 m deep notch could have been incised during the last 1,000 to 10,000 years. This implies that Barbados' deeply incised notches have formed over long time periods during the Middle and Late Holocene sea-level high stand. Apart from minor abrasion by sand and wave action, the dominant notch forming process is bioerosion accomplished by grazing and boring organisms (Figure 2.5).

Limestone cliffs are not only affected by bioerosion but also by weathering processes. Parts of the upper cliff area that are reached by salt spray, are subject to extensive salt weathering (Photo 2.26). In areas where the cliff is composed of sandy back reef limestone, karren development may be pronounced (Photo 2.27).

A Holocene coastal sand terrace, generally 50 m to 200 m wide, is present at many localities along the western and southern coast, where sandy beaches and bays stretch along the present shoreline. A beach ridge frequently separates the deeper landward side of the terrace from the present shoreline. The beach ridge ranges from 1 m to 1.5 m above high tide water level (hTw) in altitude and is commonly covered with small dunes. A lagoon, which may be partly or completely filled with sediments, or a shallow channel is located along the external margin of the beach ridge and dune area.

Especially along the southern coast, Holocene sand terraces are bordered by former cliffs. Deeply incised notches are located at the cliff bases at approximately hTw (Chapter 4.3). In this region, cliff retreat and notch incision were active during the Mid-Holocene sea-level maximum, after which the Holocene sand terrace accumulated (BIRD et al. 1979). Reworked coral boulders, which were observed in the margin of the Holocene coastal terrace located to the west of Oistins (Dover Terrace), were dated between 2,100 and 5,000 ^{14}C years BP (Table 4.3: Locality XI-35; Chapter 4, Figure 4.14).

Beachrock is discontinuously exposed at various localities along the sandy shorelines of western, southern, and southeastern Barbados (Figure 2.7, Photo 2.28). It is usually present in the intertidal zone between the high water mark and extremely low water, where beach sand is cemented by calcite. MCLEAN (1967a, 1967b) and BIRD et al. (1979) discussed the erosion of beachrock due to organisms and beach retreat. Barbados' beachrock has not yet been dated. A general overview of the beachrock phenomenon was published e.g. by KELLETAT (1998).

For several years, speculations about the extraordinary large limestone boulder near the Holocene cliff line between Bottom and Cave Bay, southeastern Barbados, have drawn the attention of coastal researchers. The boulder lies on the top of the last interglacial (MIS 5e) coral reef terrace at approx. 12 m asl. (Photo 2.29; location in figure 5.8). As revealed by the large head coral *Montastrea sp.* in the middle of the limestone boulder, the bolder is turned up-side-down. The coral is inverted relative to its former growth position. Without any doubt, enormous wave energies eroded the boulder from the seaward cliff line, transported it several meters landward, and turned it up-side-down. The question is what kind of waves detached the boulder from the cliff, transported it, and overturned it: hurricane or tsunami waves?

Tsunami waves are likely because of the boulder's enormous dimensions. Further large boulder-ridge deposits were observed by KELLETAT & SCHEFFERS in 2002 to the south of Kitridge Point (Figure 5.4) on the east coast of Barbados (pers. communication, KELLETAT & SCHEFFERS in press). There, three distinct boulder ridges with individual boulders ranging from approx. 0.75 to 3 m in diameter parallel the coastline. Individual boulders are piled up against each other within these ridges (Photo 2.30). The first ridge is located approx. 10 to 30 m off the edge of the cliff, the second and third ridges were observed within a distance of 40 and 250 m, respectively. All boulders were deposited on a cliff at 17 to 19 m asl. The boulders originated from the upper cliff, which is composed of Pleistocene coral limestone with various fossil coral species, and some gastropod shells.

Both the pattern and the extreme dimension of these boulder-ridge deposits suggest a tsunamigenic origin. Considering the large bushes that grow in between the boulders, the age of the tsunami event exceeds a few hundred years. However, an older Holocene or Late Pleistocene age cannot be excluded. The deposits are currently being dated by D. KELLETAT and his research group at the University of Essen, Germany (pers. communication).

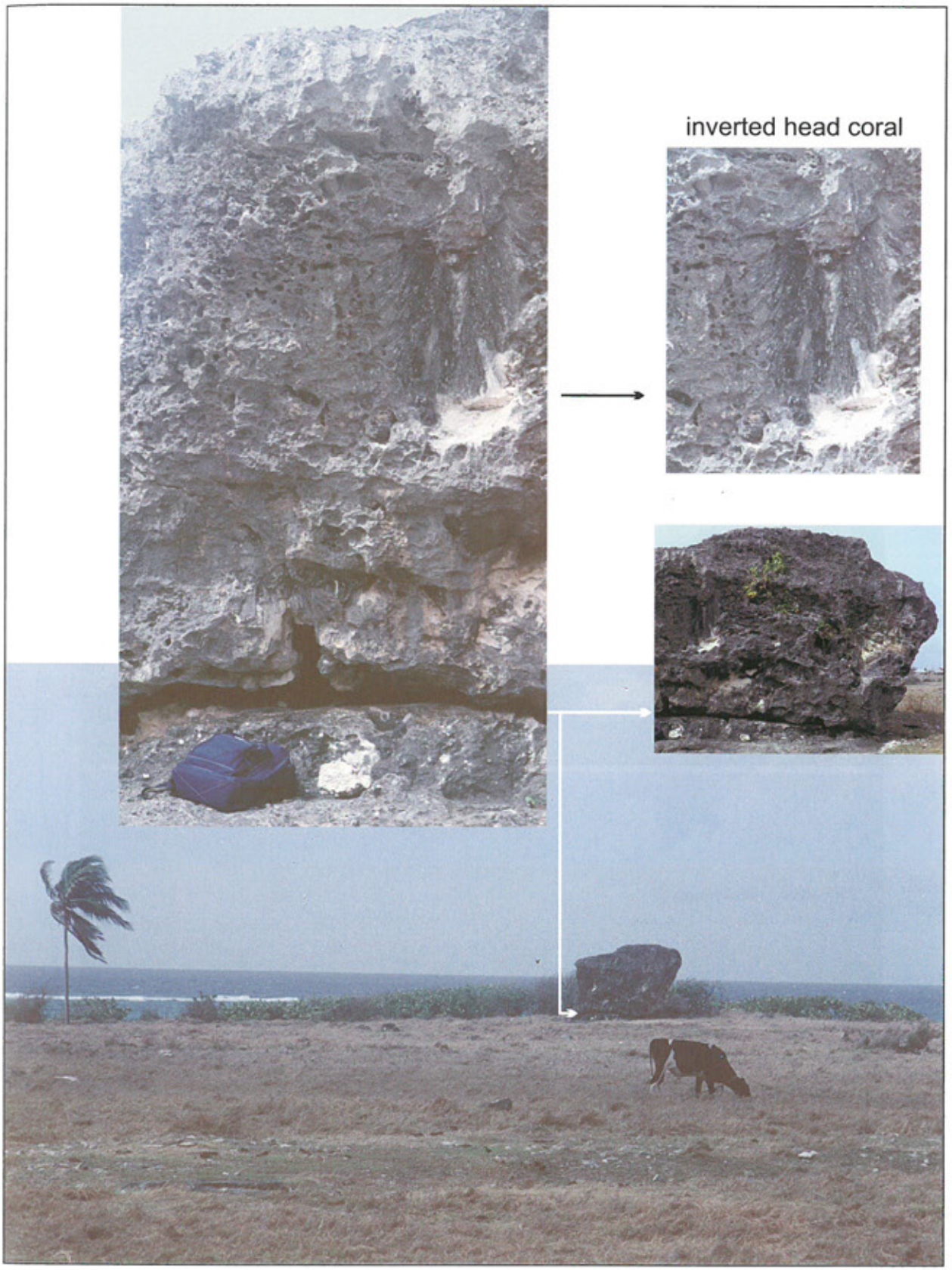

Photo 2.29: Large boulder on MIS 5e coral reef terrace near the Holocene cliff line between Bottom Bay and Cave Bay. *(Photo: SCHELLMANN 2000)*

Photo 2.30: Large boulder-ridge deposit south of Kitridge Point on the east coast of Barbados. *(Photo: SCHELLMANN 2002)*

2.4. Karst phenomena, hydrology, soils, and vegetation.

Approx. 86% of the island of Barbados consist of Quaternary coral limestone (MESOLELLA 1967; FERMOR 1972). Due to the tropical climate, this coral reef limestone is readily soluble. Limestone weathering is represented in karst morphology and hydrology on Barbados. Despite the relatively young age of the island, karst formed during the Pleistocene and included dolines and dry valleys (Photo 2.2, see below), as well as caves and other erosive formations. While karst formations are very pronounced on other West Indies Islands, for example cockpit karst in the north of Puerto Rico, larger karst formations such as poljes, cockpits, and karst cones are absent on Barbados.

Barbados' dolines (Figure 2.8) are generally round, small, discrete, and contain sinkholes (Photo 2.29) or small ponds. DAY (1983) investigated the formation and change of a subset of 1,179 dolines located within a 124.5 km² large area in northern Barbados. While the number of dolines increases with elevation up to 150 m asl., dolines are less abundant at higher elevations (DAY 1983). WANDELT (2000) investigated doline morphology on the entire island of Barbados. A total of 2,830 dolines were mapped and measured. The dolines average a depth of 6 m. The number of dolines decreases with the increasing dissection of the surface by dry valleys (Figure 2.10) above Second High Cliff. There, the transitions between dolines and dry valley are less defined (WANDELT 2000). Both cross sectional area

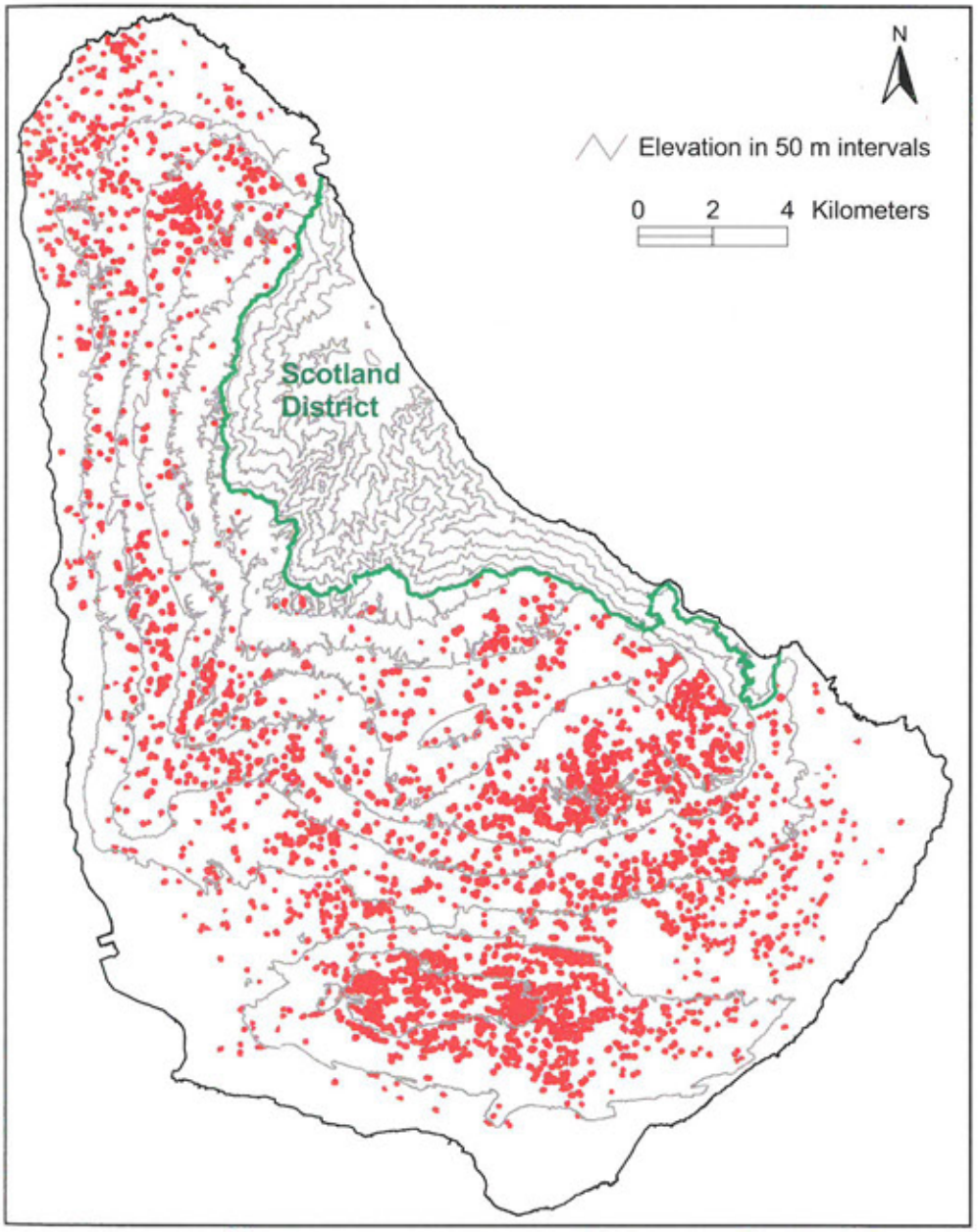

Figure 2.8: The dolines of Barbados (redrawn from WANDELT 2000).

Photo 2.31:
Sinkhole in Middle Pleistocene coral reef limestone near Adam's Castle, south coast of Barbados.

(Photo: SCHELLMANN 1990)

and the depth of dolines increase at higher elevations.

With a few exceptions, dolines are absent on the last interglacial coral reef terraces, as illustrated in Figure 2.4 for the last interglacial T-1 to T-5b terraces located in southern Barbados. Only individual dolines are present on the penultimate interglacial coral reef terraces T-6a, T-6b, and T-7 (Figure 2.9). There, they mainly occur within the vicinity of lagoonal zones, which are hydrologic drainage areas. Dolines occupy approx. 3% of the area of the older penultimate and third last interglacial T-6 to T-10 terraces, and approx. 10 to 15% of the T-11 and T-12 terraces (calculated from base data by WANDELT 2000), which are approx. 400,000 years old.

Descriptions of karst formations on Barbados were presented by JAMES (1971), DAY (1983), PFEIFFER (1993), BLUME (1973), and others.

Dry Valleys

The dry valleys (Figure 2.10) of Barbados are the island's peculiar geomorphic features. In 1972,

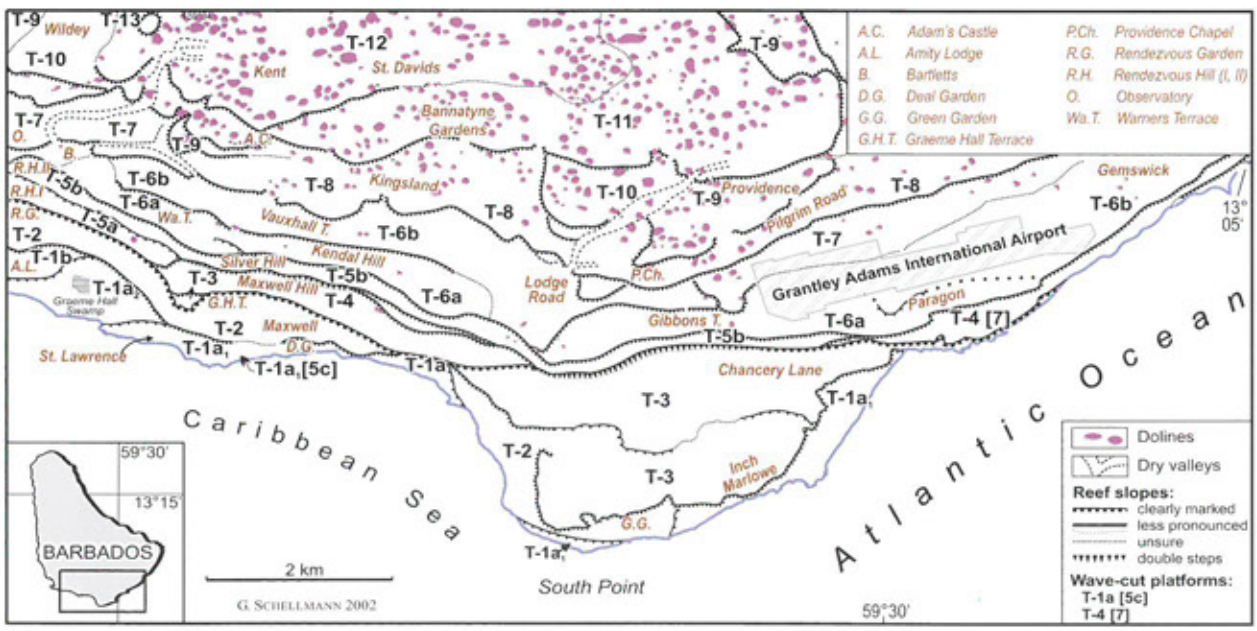

Figure 2.9:
The distribution of dolines and dry valleys on Pleistocene coral reef terraces in southern Barbados (see Chapter 4 for chronostratigraphy).

FERMOR described the dry valleys on Barbados as one continuous valley system radially extending from the highest fossil coral reef terrace at the border of Scotland District and Golden Ridge Dome. Dry valleys are usually present in semiarid and arid regions. While PFEFFER (1993) suggests that dry valleys are not limited to karst geology since they have been observed in different geologic settings, RITTER et al. (1995) argued that dry valleys are generally limited to karst hydrology.

Barbados' dry valleys are deeply incised valleys that radiate from the high elevations of Scotland District and from Golden Ring Dome. No significant dry valleys can be observed in the vicinity of Christ Church Dome. The dry valleys are frequently incised 30 m deep. Valley slopes ranging from 15° and 30° characterize the individual valleys (WANDELT 2000). WANDELT (2000) stated that the dry valley system of Barbados occupies approx. 10% of the island area. The majority of the valleys are drained by ephemeral streams, which discharge into the ocean in response to severe precipitation events, or they drain into small swamps whose outlets into the ocean are blocked by beach ridges. However, some drainages end in sinks or decrease in size and come to a sudden end, as for example those ending in Sweet Vale or St. George Valley.

Few publications have concentrated on the genesis or analysis of the dry valleys on Barbados. Early papers attempted to explain the formation of these valleys with earthquakes (SCHOMBURGK 1884), or they suggested that these valleys were remnants of

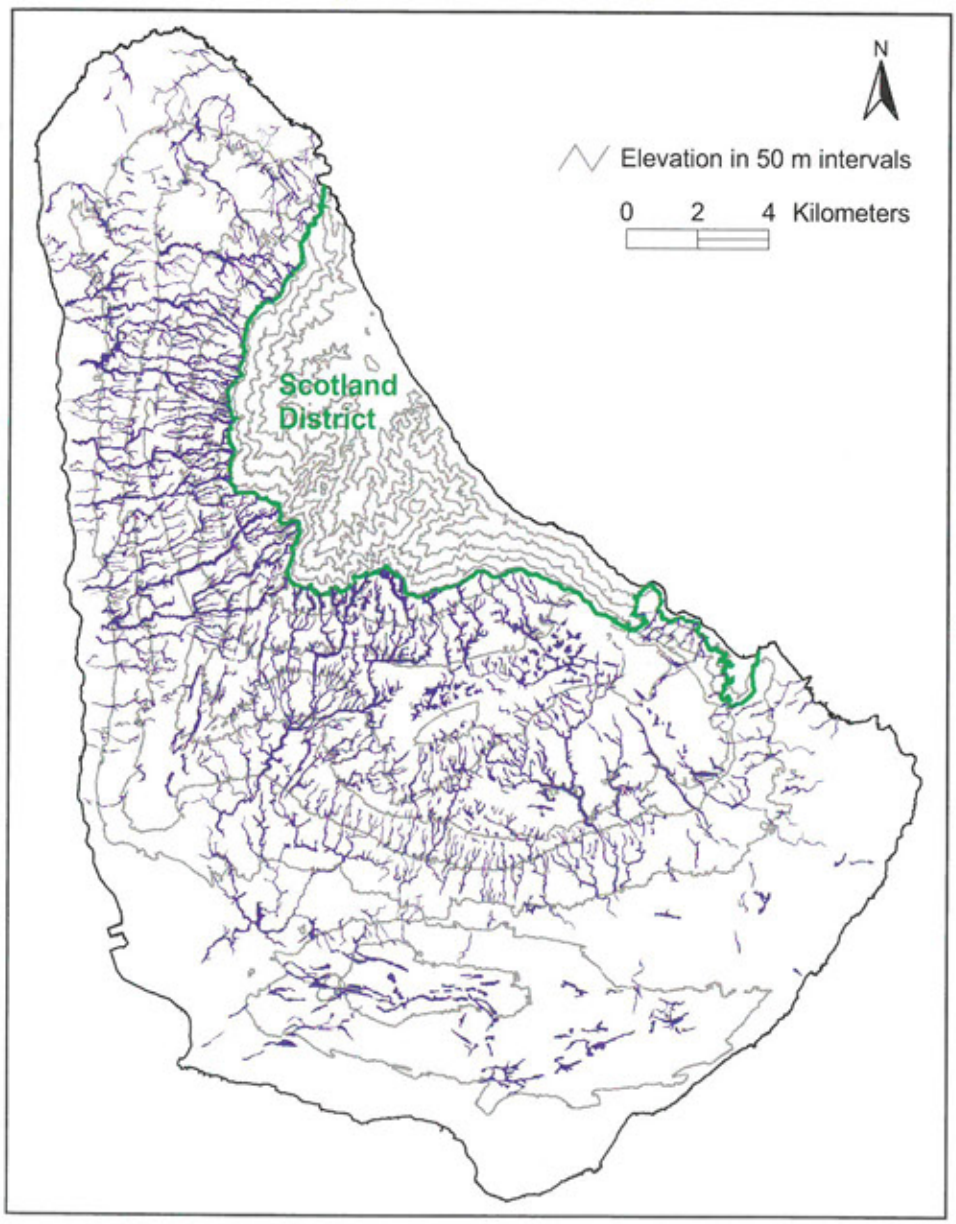

Figure 2.10:
The dry valleys of Barbados (modified after WANDELT 2000, and FERMOR 1972).

former lagoonal swamps that dried out after their uplift (HARRISON & JUKES-BROWN 1890). TRECHMANN (1955) and TRICART (1968) explained the dry valley formation on Barbados with their submarine origin. MARTIN-KAYE (1966) described the genesis of the dry valleys on Barbados with a strongly erosive surface runoff at relatively low elevations above sea level, which could be blocked by a high ground water level layered above fresh water. Holes and underwater caves would dry out due to uplift processes. FERMOR (1972) explained the genesis of the dry valleys of Barbados with inherited incisions into coral reefs due to surface water, which became dry with the decrease of surface runoff on Barbados. According to this hypothesis, the dry valleys were shaped by surface water using depressions in reef bodies. This theory is supported by the relatively small degree of karstification at the valley floors and by the heterogeneity in the formation and spatial distribution of dry valleys on Barbados. Fluvial erosion by episodic streams or the continuing incision through corrosion processes may contribute to an ongoing dry valley formation on Barbados under the current climatic conditions (FERMOR 1972).

The valley network is characterized by pinnate and perpendicular valley junctions. Pinnate junctions are common for high relief drainage systems such as those on Barbados. The genesis of the perpendicular valley junctions was explained by FERMOR (1972), who correlated the drainage network to the uplift of coral reefs. GOREAUX (1959) suggested that the drainage network extended across each new reef as it emerged. The newly emerging reef presented a barrier to the drainage causing the stream network to divert parallel to the shore until an inner reef channel, formerly a submarine channel, which served as an outlet to the sea, was reached.

The dynamics behind the genesis of Barbados' dry valleys are still unresolved, and further investigations on the age and processes of valley formation and drying out are required.

Hydrology

The extremely permeable coral limestone overlaying the dense Tertiary basement, forms the only larger groundwater aquifer for potable water on the island (Figure 2.11). Both location and replenishing of the island's freshwater reservoirs largely depend on the topography of the boundary between Pleistocene and Tertiary rocks, and on precipitation. Rainfall is most abundant in the central and highest region located above Second High Cliff. From there, ground water follows gravity and relief and flows at the base of the coral limestone towards the Caribbean Sea.

The uplifted Pleistocene coral reef terraces on Barbados constitute an aquifer that is built on low-permeability Tertiary pelagic rocks that overlie the Barbados accretionary prism (BANNER et al. 1994). According to BANNER et al. (1994), calcareous marlstone and chalk dominate the oceanic pelagic rocks. The Pleistocene coral cap forms an aquifer that is almost entirely underlain by these oceanic rocks. Groundwater flow in the coral cap is determined by the higher porosity and permeability of the coral cap compared to the underlying Tertiary rocks, and by the distribution of precipitation (BANNER et al. 1994).

Groundwater is stored in the coral cap, where the underlying Tertiary sedimentary rocks prevent downward water flow. Where these sedimentary layers are higher than sea level, groundwater creates underground streams that flow along the base of the coral cap. Close to the coast, however, the sedimentary layers are lower than sea level. There, a coastal phreatic wedge and freshwater-saltwater mixing zones developed (HUMPHREY 1997) since the heavier saltwater flows underneath the freshwater reservoirs.

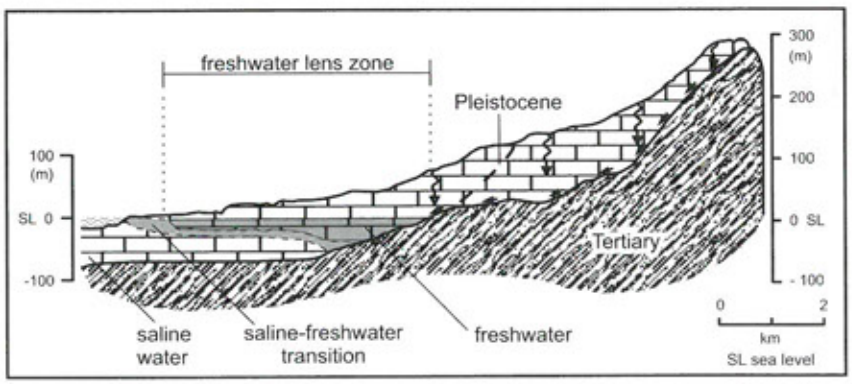

Figure 2.11:
Hydrologic cross section of Belle Catchment, located between Bridgetown and Hackletons Cliff in southwestern Barbados (redrawn after BANNER et al. 1994).

Where the base of the coral limestone lies below current sea level, larger ground water supplies are stored, as for example in St. George Valley and in the vicinity of the western coastline of Barbados. The coastal freshwater lens was investigated by STEINEN et al. (1978). It varies in thickness from 1m to 10 m, and averages approx. 7 m. The zone of mixing is between 0.1 and 12.8 m thick and separates the freshwater from the underlying saltwater.

MARTIN-KAYE & BADCOCK (1966) studied groundwater hydraulics on Barbados and divided Barbados into two hydrographic units, the stream water zone and the sheet water zone. The stream water zone was delineated where the ground water level overlies the impermeable Tertiary oceanic formation. Intermittent springs arise where the Oceanics reach the height of the valley floor (FERMOR 1972). In the sheet water zone, fresh water overlies sea water, because the interface between the Oceanics and the coral cap is below sea level near the coast. The slope of the water table is very low since it is largely dependent on the permeability of the coral rock.

Barbados relies almost entirely on groundwater as a source of supply for agriculture and industrial production. JONES & BANNER (2003) estimated that groundwater recharge for Barbados was both rapid and limited to the three wettest months of the year. Furthermore, aquifer recharge is limited to only 15% to 20% of the average annual rainfall that occurs above Second High Cliff, and to 25 to 30% of the precipitation at lower elevations. SENN (1946) estimated average evapotranspiration at 75% and runoff at approx. 5%. The remaining 20% are available for groundwater replenishment. Barbados' freshwater supplies are being increasingly reduced due to a rising water consumption caused by population growth and tourism (HUMPHREY 1997).

Water quality is at risk because of pesticides, hydrocarbons, and the extensive agricultural application of nitrogen fertilizers, as well as the lack of adequate sewage treatment. Most of the ground water supplies exceed a nitrate content of 20 ppm (BANNER et al. 1994).

Saltwater infiltrates the coastal freshwater reservoirs. Sea level rise is compounding the problem of salinization from overextraction from the aquifers. In some cases, higher salinity is experienced not only in coastal aquifers but also inland at freshwater pumping plants as the salty groundwater rises (NURSE & SEM 2001).

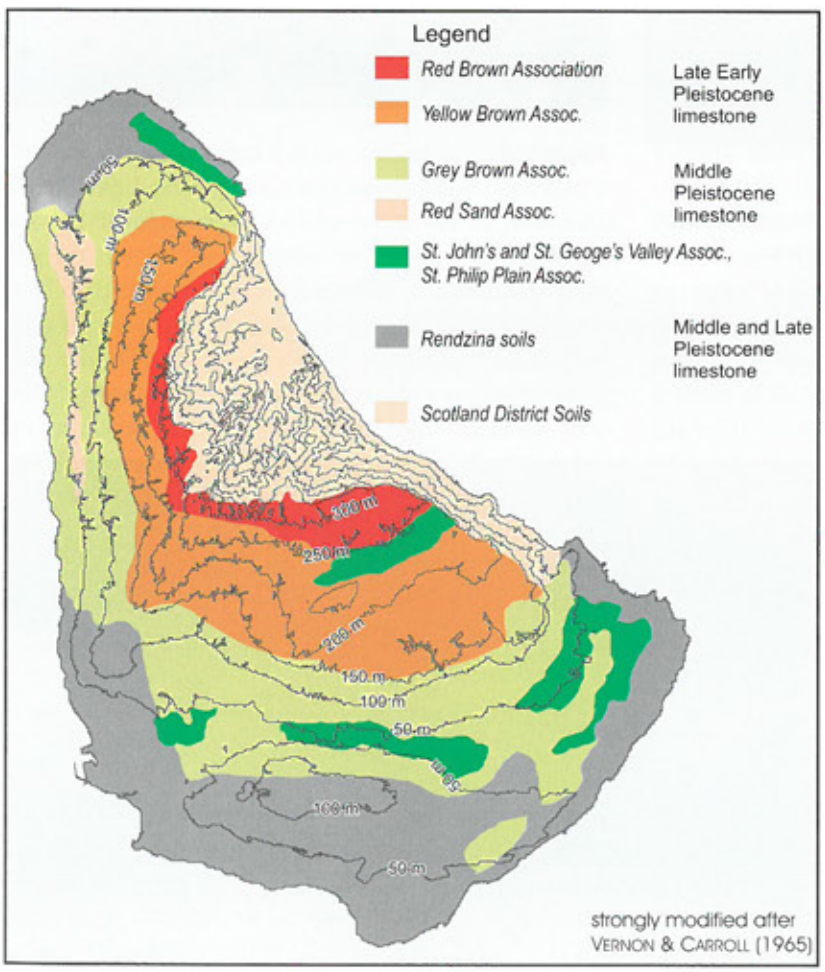

Figure 2.12:
The soils of Barbados (strongly modified after VERNON & CARROLL 1965).

Soils

Soils on Barbados (Figure 2.12) developed from Pleistocene coral limestone or Tertiary sedimentary rock; atmospheric deposits of volcanic ashes originating from volcanic eruptions in the Southern Antilles island arc; and deposits of Aeolian dust originating from the Saharan Desert and transported by northeast trade winds.

Photo 2.32:
Rendzina on last interglacial T-3 coral reef terrace (MIS 5c) near Round Rock, south coast of Barbados.
(Photo: SCHELLMANN 1994)

Photo 2.35:
Red loam on the oldest Pleistocene coral limestone of Barbados located at Horse Hill at the escarpment to Scotland District.
(Photo: SCHELLMANN 1990)

Photo 2.33:
Cambisol-Rendzina on Middle Pleistocene T-8 coral reef terrace (MIS 9) to the northeast of Providence on the south coast of Barbados.
(Photo: SCHELLMANN 1994)

Photo 2.34:
Yellowish-red sandy soil on Middle Pleistocene littoral sediment located east of Speightstown on the west coast of Barbados.

(Photo: SCHELLMANN 1994)

Soils that developed on coral limestone generally have a high clay content. According to MUHS et al. (1987), this clay largely originated from the weathering of silicate Saharan dust, as suggested by the high proportion of smectite, and from the weathering of volcanic ash from the Lesser Antilles island arc (Chapter 1.2.2), and from the weathering of the underlying reef limestone.

All soils on coral limestone are alkaline soils. Within the grain size category of sand, the quartz content is relatively high, which probably results from the erosion of the Tertiary base. Volcanic minerals and quartz from the Saharan Desert dominate silts, and clay is characterized by interstratified kaolinite-smectite (MUHS et al. 1987). According to YOUNG (1976), the smecite content decreases with increasing precipitation, which is attributed to an intensification of chemical weathering. MUHS (2001) stated that soils on the youngest terrace are dominated by smectite and mixed layer kaolinite-smectite, although these clay minerals are absent in the parent material. Intermediate terrace soils are more kaolinite-dominated, and kaolinite is the only clay mineral in soils on the highest terraces.

Overall, physical, chemical, and mineralogical properties of soils on uplifted Quaternary reef limestones on the island change with terrace age. Soils are redder (perhaps more hematite) and more clay-enriched with increasing terrace age. The total Al_2O_3 and Fe_2O_3 content, as well as the dithionite-extractable Fe content increase with age, whereas average SiO_2/Al_2O_3 values decrease with age. Primary minerals are less abundant on older terraces, and clay minerals are more strongly kaolinite dominated with increasing age (MUHS 2001).

Soils located on different coral reef terraces on Barbados generally reflect the differences in the duration of their development. For example, black soils ('Rendzina' soils) are developed on the last interglacial reef terrace (Photo 2.32). A few of these show a brown basal weathering horizon. In contrast, weakly browned black soil associations are more frequently observed on the older terraces from the Middle Pleistocene (Photo 2.33). These soils are widespread in the dry regions of southern and northern Barbados (Figure 2.12). However, more developed soils, including polygenetic soils with yellow brownish to reddish weathering horizons, are present on the older Middle Pleistocene terraces along the west coast (Photo 2.34) and above Second High Cliff (Photo 2.35, Figure 2.12), where precipitation is abundant and soils developed over longer time periods.

Despite the overall age dependancy of soil development of Barbadian coral reef terraces, which seems to form a climo- (MUHS 2001) or pedo-chronosequence, soils are extremly eroded in many limestone areas, and only poorly developed relic soils are preserved. Poorly drained black soils with an extremely high clay content are developed, where silicate and clay-rich alluvial sediments and colluvium are the parent material, e.g. in St. George's Valley. These soils contain up to 60% montmorillonite (AHMAD & JONES 1969: p. 12). Deep cracks with widths of several centimeters occur in the solum of these vertisol-like soils during dry seasons.

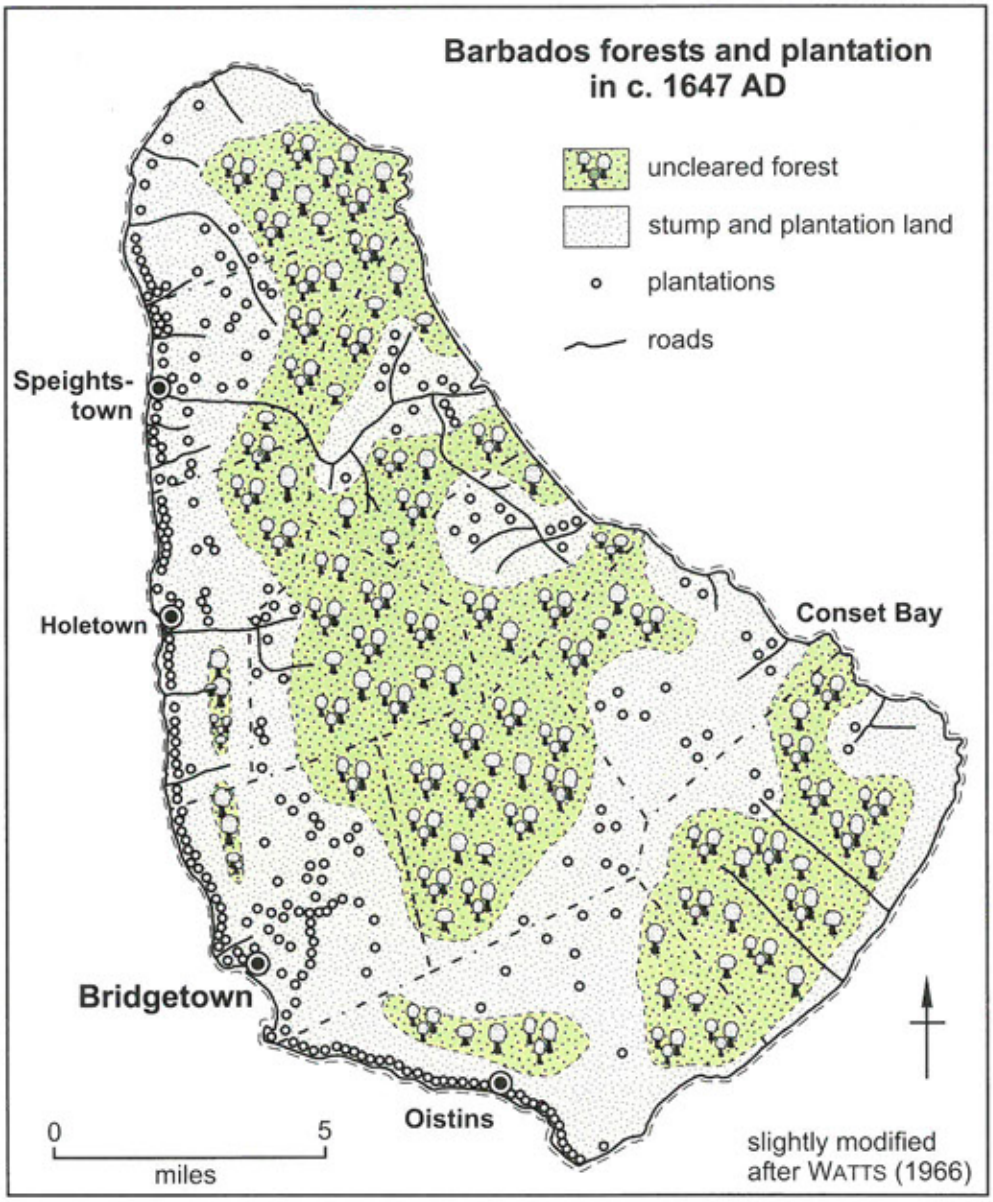

Figure 2.13: Distribution of woodland and plantation land in approximately 1647 (slightly modified after WATTS 1966).

Detailed descriptions of the soils of Barbados were presented by AHMAD & JONES (1969), BEAVEN & DUMBLETON (1966), HUDSON (1965), MUHS (2001), MUHS et al. (1987), SAINT (1934), VERNON & CARROL (1965), and YOUNG (1976).

Vegetation

The neotropical Caribbean flora may be described by species abundance and endemism (BLUME 1973). The natural vegetation of Barbados was characterized by

(1) dense seasonal rain forest in the humid interior of the island;
(2) xerophytic forest in subhumid areas; and
(3) xerophytic scrub vegetation in the semiarid coastal zone (WATTS 1966; WATTS 1970).

When English settlers arrived in 1627, a dense forest extended from the island's interior to the coast. However, Barbados' forests were completely harvested when European plantation farming began in 1647. Clear cutting was promoted by the high demand for wood and by the cultivation of sugar cane on large estates. While large areas of Barbados were still covered with forest in 1647 (Figure 2.13), the natural forest was completely removed as early as 1665, with the exception of Turner's Hall Wood in Scotland District, small areas on estates, and some small mangrove forests along the coast (WATTS 1966; 1970). Forty years of English settlement created a largely open landscape, which is dominated by large sugar cane plantations that cover approx. 80% of the island. In addition to the removal of the natural veg-

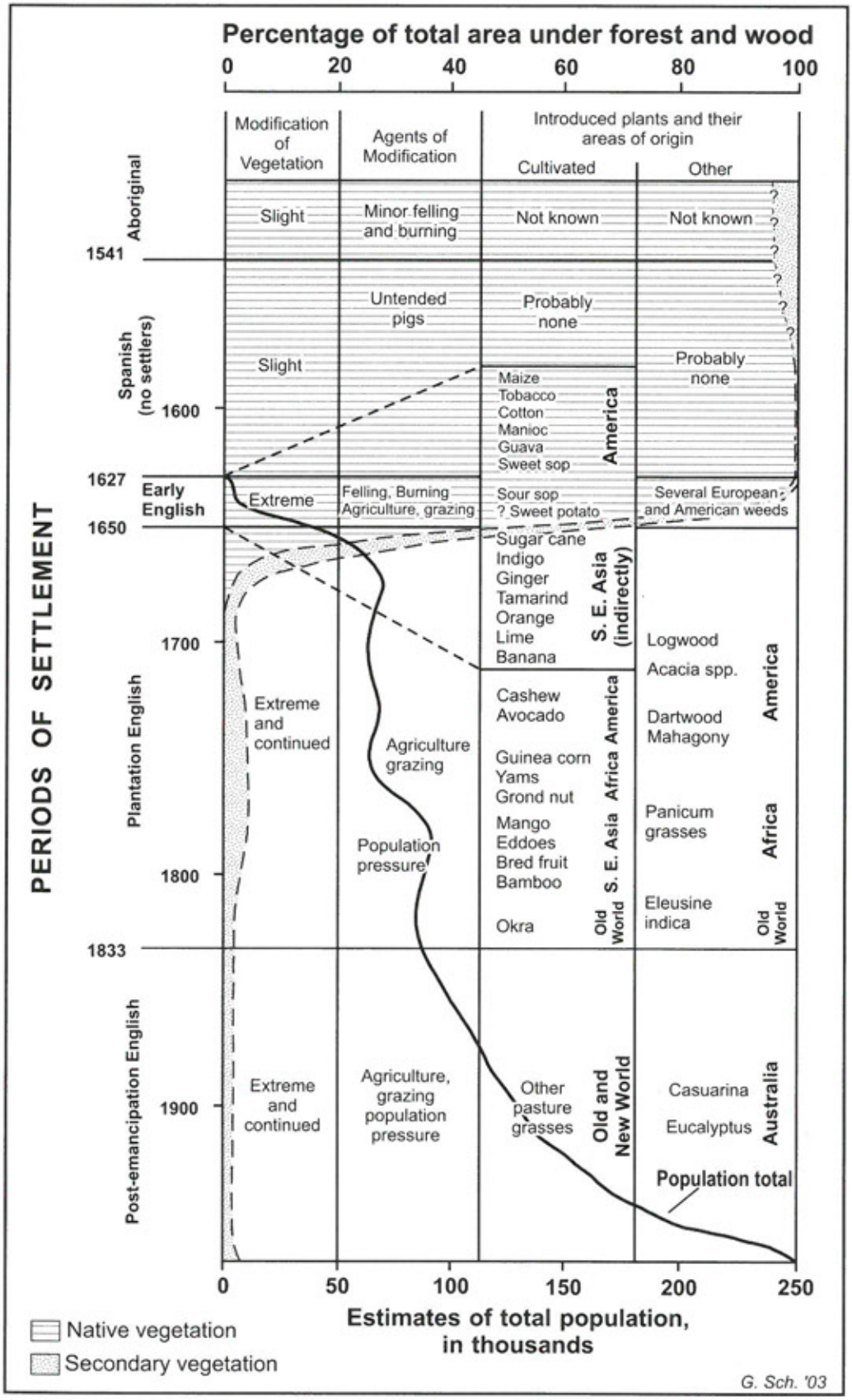

Figure 2.14:
Periods of settlement, population, and the replacement of native vegetation in Barbados (slightly modified after WATTS 1970).

etation, new alien species, such as mahogany, casuarinas, eucalyptus, grass species, and crops (e.g. manioc, maize, bananas, oranges, limes, tobacco, cotton, mangoes, avocado), were introduced (Figure 2.14).

WATTS (1966; 1970) described vegetation changes on Barbados in detail, and RANDALL (1970) illustrated the present coastal vegetation.

3. The coral reef terraces of Barbados and the development of the „Barbados Model´´– a history of research

U. RADTKE & G. SCHELLMANN

3.1. First geological studies on the coral cap of Barbados

The first geological research in Barbados was most probably that carried out by SCHOMBURGK (1848), who distinguished "Coral Limestone" from underlying "Silicious Rocks", and named the latter formation "Scotland Formation" – after the source of its discovery in the Scotland District (see Figure 2.1). These Tertiary sediments are exposed almost exclusively in the Scotland District and marginally at Cluffs Bay in the north of the island. They cover about 14% of the island surface. Made up of slate clay, weakly solidified sand, solitary sandstone and limestone banks, dark grey siltstone, embedded blocks of oil sandstones and asphalt, these sediments are extremely susceptible to earth slips and soil erosion. The resulting landscape resembles subalpine flysch areas. Along the edge of the overlying Pleistocene coral caps extensive collapses occur, with the coral blocks moving to the present coastline as erratic blocks (see Photo 2.4). Dates for the reefs, which cover about 86% of the island surface, were first provided by DUNCAN (1863), who classified various samples by Palaeontological analysis. The flat-lying Pleistocene coral reefs, which have a maximum thickness of 130 m, reach their highest altitude at Mount Hillaby (332 m). From a distance, the island looks like a flat shield made up of layers of terraces of fossil coral reefs. Fossil coral reefs exist only on the north, west and south coasts of Barbados. Recent forms can be found only on the west coast. This asymmetrical distribution of the reefs can be explained by two arguments: on the one hand, the streams and brooks of the Scotland District are rich in suspended load which prevents the growth of corals; on the other hand, the steady and occasionally strong NE-trade winds may hinder the undisturbed growth of corals on the east coast.

DUNCAN assumed the Barbados reefs to be of Miocene age, whereas GUPPY (1866) held the opinion that an age younger than Miocene is more probable as evidence of extinct species could not be found.

The first detailed geological studies of Barbados were carried out by JUKES-BROWNE & HARRISON (1891). These authors, too, questioned the corals being of Miocene age as postulated by DUNCAN (JUKES-BROWNE & HARRISON 1891, pp. 225-229). GREGORY (1895) published a comprehensive description of the fossil corals and molluscs, and came to the conclusion that the low-lying reefs must be of upper Pleistocene age and the higher reefs of lower Pleistocene (Pliocene) age. SPENCER (1902) made a distinction between three coral formations, claiming the oldest one to be of Oligocene age. This opinion was strongly contested by HARRISON & JUKES-BROWNE (1902) and HARRISON (1907). Later studies (TRECHMANN 1933, 1937; SENN 1944, 1946, 1948; WEYL 1965, 1966; RUSSEL, 1966) agreed on the Quaternary origin of the coral cap of Barbados.

3.2. Alpha spectrometric U-series dating and the development of the "Barbados Model" by MESOLELLA (1968)

Two contrary opinions on the genesis of the reefs and terraces in Barbados were being debated before MESOLELLA (1967, 1968) published the results of his research.

The so-called "erosionists" (e.g. TRECHMANN 1933, 1937; SENN 1944, 1946, 1948; WEYL 1966) claimed the coral cap of Barbados was developed in its entirety before or during the course of the uplift of the island. With the uplift of the coral shield the terraces were developed by tectonic processes and marine abrasion.

In contrast, the so-called "depositionists" (e.g. SCHOMBURGK 1848; JUKES-BROWNE & HARRISON 1891; RUSSEL & MCINTIRE 1965; RUSSEL 1966) considered these separate "terraces" to be individual coral fringing reefs which developed periodically as the island was uplifted. This means that, in contrast to the "erosionists" assumption, those fossil reefs that are highest today must also be the oldest coral formations in the island.

MESOLELLA (1967, 1968) and MESOLELLA et al. (1969) proved that the coral cap of Barbados is not made up of a more or less homogeneous body of coral limestone, and that the terraces did not develop later as erosional features. Therefore, it might be

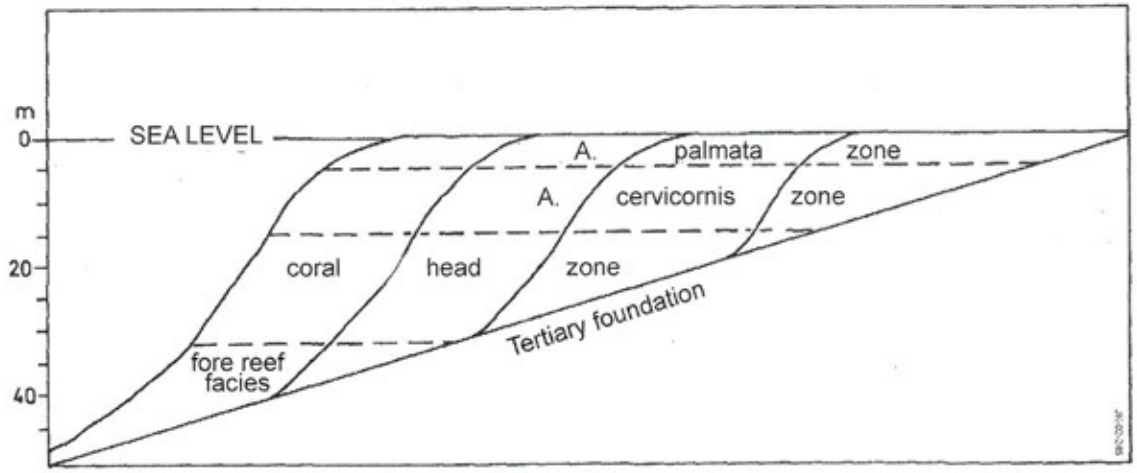

Figure 3.1: Reef migration under conditions of relative stability. Contacts of depth-sensitive coral zones are horizontal. Due to seaward migration, a terrace with a reef crest community (*Acropora palmata* zone) „pavement" is formed. The seaward migration of facies on the landward side of the *A. palmata* zone is minimal after MESOLELLA (1968: 135; in RADTKE 1989: 111).

possible, in principle, to state the "depositionists'" assumption to be true. Evidence was found to support the hypothesis that each single reef system consists of a typical zone succession ("fore-reef", "reef-crest", "back-reef"; see Figure 4.2), with individual reef units of different ages overlying each other. Each fossil reef has the same structure, which is also typical of present day reefs. The *Acropora palmata* zone represents the mean low tide at the "reef-crest" and, therefore, is a reliable indicator of the respective (palaeo-) sea level.

MESOLELLA surveyed 800 natural and man-made exposures, and came to a more detailed view than the "depositionists'". He confirmed their theory in principle, but saw the characteristic "terrace topography" not as the result of an intermittent tectonic uplift but as the result of a (relatively) continuous uplift of the island.

To prove this assumption, the relation between the velocity of reef growth and tectonic activity must be considered. This relation becomes clearly visible in the internal structure of the coral reef. With relative stability, for example, the *Acropora palmata* zone develops horizontally towards the sea (see Figure 3.1); and the exposure of a fossil reef of this origin should show a horizontal stratification of the individual species of corals. If, on the other hand, uplift rate and the rate of reef growth are balanced, a

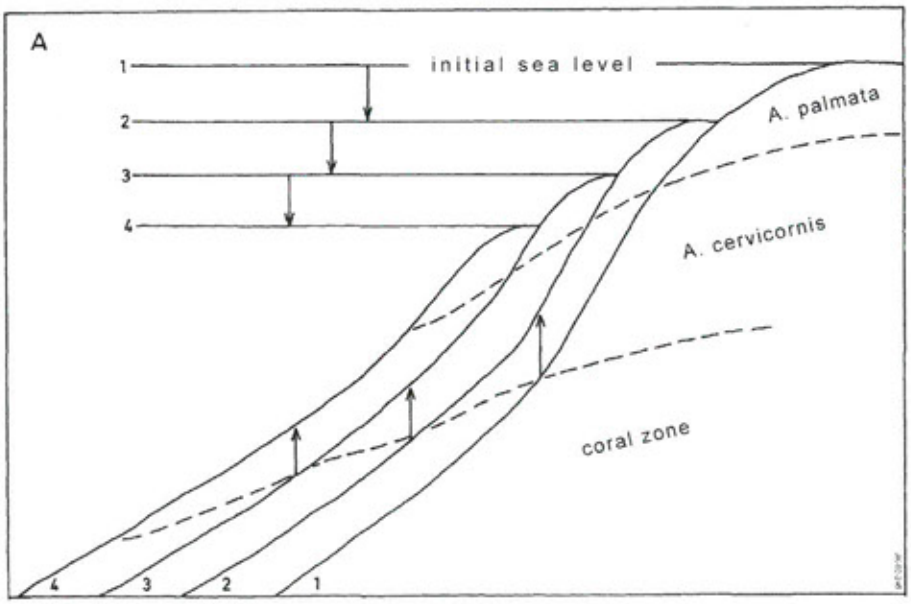

Figure 3.2:
Reef migration under conditions of emergence. Migration pattern produced when the rate of vertical reef growth equals the rate of emergence (after MESOLELLA 1968: 151, in RADTKE 1989: 112).

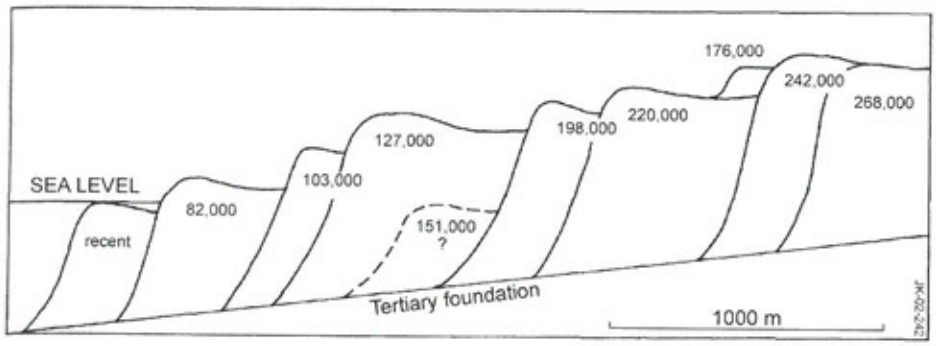

Figure 3.3: Chronological arrangement of fossil coral reefs in the vicinity of Clermont Nose, Barbados, based on radiometric data (after MESOLELLA 1968: 223, in RADTKE 1989: 112).

continious *Acropora palmata* zone which clearly slopes towards the sea should be defined (see Figure 3.2). If the velocity of uplift is higher than the velocity of reef growth, the *Acropora palmata* zone will be interrupted by the *Acropora cervicornis* zone instead of being continuous.

From the reconstruction of individual reef structures, MESOLELLA came to the conclusion that the genesis of individual reef terrace levels during constant uplift of Barbados can be verified, and it is not necessary to assume intermittent uplift. $^{230}Th/^{234}U$ analysis made it possible for the first time to prove that, in fact, reef units of different ages overlie each other, and that the uppermost reef terraces are also the oldest ones (see Figure 3.3).

Table 3.1: List of radiometric ages for terraces Barbados I, II, III and the maximum altitude of reef units (after MESOLELLA et al. 1969: 257, in RADTKE 1989: 112).

Sample	Elevation (m asl)	$^{230}Th/^{234}U$ age (a)
Barbados I		
AGA-1	13	79,000 ± 4,000
OC-26	22	82,000 ± 2,000
AEH-1	7	82,000 ± 4,000
FS-3	13	84,000 ± 4,000
Barbados II		
FT-1	23	104,000 ± 4,000
		100,000 ± 4,000
		100,000 ± 4,000
AFZ-1	20	104,000 ± 4,000
		104,000 ± 4,000
AFK-1	30	104,000 ± 6,000
AEG-2	60	110,000 ± 6,000
X-5	?	111.000 ± 6,000
Barbados III		
S-11	40	122,000 ± 6,000
AEJ-5	40	124,000 ± 6,000
AFS-1	40	124,000 ± 6,000
AFM-T-2	63	170,000 ± 6,000
AFM-B-1	63	127,000 ± 6,000
ADR-1	37	127,000 ± 6,000

In particular, MESOLELLA (1968), BROECKER et al. (1968) and MESOLOELLA et al. (1969) established the age datings for the three youngest reef units as shown in Table 3.1.

On the basis of a slightly modified set of data for three terrace profiles on the West coast, i.e. Thorpe, Clermont Nose, and a profile east of South Point area, BROECKER et al. (1968) tried to assign maximum levels of the last interglacial interval to palaeo sea levels for the first time (see Table 3.2). Since data of littoral deposits on other coasts were found to correspond to the radiometric data of Barbados I/II/III, BROECKER et al. (1968) drew the conclusion that the coral reefs were of glacial eustatic origin, which superimposed the continuous and constant uplift of the island. As the authors are of the opinion that the ages of the terraces correlate with the maxima of the summer solar irradiation in the northern hemisphere, they favour the astronomical theory (MILANKOVITCH 1941) as the explanation of Quaternary climatic oscillations.

MESOLELLA (1968) expanded this model, and correlated all the older reef units of Barbados with the so-called Milankovitch-curve. From the extrapolation of the uplift rate he concluded that the oldest reef unit in Barbados must be c. 600,000 years old. In contrast to later studies of the Quaternary reef stratigraphy of Barbados, MESOLELLA's dissertation (1968) follows ZEUNER and FAIRBRIDGE and takes into account a general lowering of the sea level during the Quaternary. By comparing a former sea level, which had an astronomical age of 484,000 years and an altitude of 35 m a.s.l, with a more recent sea level (Barbados III, 6-7 m asl.,) which had a radiometric age of 127,000 a, MESOLELLA estimated a eustatic lowering of the sea level of c. 7.6 m in 100,000 years. On this basis he calculated the palaeo sea levels of

Table 3.2:
Calculation of palaeo sea levels from BROECKER et al. 1968: 299. The estimate was established for four traverses located on Barbados and was based on the following two assumptions. First, sea level was 6 m above present sea level during Barbados III, the maximum of the Last Interglacial. Second, the uplift rate was constant (RADTKE 1989:113).

Traverse	Terrace elevation (m)	Rate of tectonic uplift (m/1000 a)	Palaeo sea-level (rel. to present sea-level) (m)
A	Barb.III 37	0.24	+6 (est.)
	Barb.I 6		-14
B	Barb.III 49	0.34	+6 (est.)
	Barb.II 26		-10
	Barb.I 12		-16
C	Barb III 55	0.38	+6(est.)
	Barb.II 27		-13
	Barb.I 18		-13
D	Barb.III 35	0.23	+6 (est.)
	Barb.I 6		-13

his sample traverses according to the following formula:

$$L = E - (RxT)$$

(L = position of maximum palaeo sea level in relation to recent sea level; E = actual altitude of coral reef (terrace) in a traverse; R = mean rate of tectonic uplift; T = age of terrace)

On the basis of these calculations, MESOLELLA established the series of Pleistocene sea levels as shown in Table 3.3.

In evaluating the results of his research, MESOLELLA deals with the advantages and disadvantages of studies of the history of Pleistocene sea level oscillations in regions of tectonic uplift. The main advantage according to MESOLELLA is the fact that the uplift uncovers "natural strip charts" (MESOLELLA 1968, 393), so that single oscillations of the Pleistocene sea level can be separated. This means that, as a rule, the age of the terraces decreases with the decrease of altitude. The main disadvantage of MESOLELLA'S approach is the assumption of a constant linear uplift rate. According to MESOLELLA, it can be verified "...that Barbados was tectonically uplifted at a near-linear rate between 500,000 and 127,000 a" (MESOLELLA 1968, 373). He admits, however, that this assumption could not be verified in Barbados in general. It cannot be verified, for example, in the interior part of the island or for the period after 125,000 a.

MESOLELLA drew the conclusion that after the maximum of the last interglacial there was a non-linear uplift rate. His conclusion was influenced by the theories set up by ZEUNER (1959) and FAIRBRIDGE (1961) which were still generally accepted in 1968. Following these theories, MESOLELLA doubted his own results concerning a Palaeo sea level of –15m c 82,00 a because, following the classical eustatic theory, this sea level should have been located at +7 to +8 m asl. during the so-called "Late

Table 3.3:
Pleistocene palaeo sea-level calculations (after MESOLELLA 1968: 286, in RADTKE 1989: 113).

Age of coral reef (a)	Palaeo sea-level (m)	Number of data
30,000	-26	(1)
82,000	-15	4
106,000	-15	2
127,000 (1st High Cliff)	+ 7(est.)	9
151,000	-25	2
176,000	+18	2
198,000	+ 6	7
220,000	-	-
242,000	+ 7	6
268,000	+ 3	1
291,000	+16	2
313,000	+19	4
334,000	+22	5
408,000	+21	2
484,000 (2nd High Cliff)	+34	5
505,000	+37	4

Monastirian". (This is, incidentally, a nice example illustrating how measured results are doubted and interpreted to match prevailing opinion; RADTKE, 1989.) As further proof, MESOLELLA quotes Th/U-dating results of molluscs in Mallorca (75,000± 5,000 a) as provided by STEARNS & THURBER (1965).

In contrast to MESOLELLA, JAMES et. al. (1972) concentrated mainly on the fossil reef units on the North coast of Barbados. JAMES et al. (1971) and JAMES (1972) accepted MESOLELLA'S results in principle. They believed, however, that for the northern part of the island a different tectonic genesis and, therefore, a fundamentally different series of fossil coral reefs must be identified. In addition to MESOLELLA'S research, JAMES describes a thin discontinuous fringing reef on the north-western coast in the Cluff's Bay and Stroud Bay area (see Figure 3.4). Four $^{230}Th/^{234}U$ ages (2 corals at 63,000 a; 2 molluscs at 59,000 a) in Cluff's Bay (see Figure 3.5) are proof for him that apart from the relative maximum levels named as Barbados I, II, III, a further Upper Pleistocene maximum sea level ("Early Wisconsian reef terrace", JAMES et al. 1971, p. 2022) does exist.

In contrast to MESOLELLA (1968) and MESOLELLA et al. (1969), JAMES still assigns the "1st High Cliff" (Barbados III) in the north-western and northern part of the island (North point shelf area) to the 104,000 a maximum (see Figure 3.4), and not to the 12,000 a level, on the basis of 5 Th/U-dating results (105,000 a; 100,000 a; 97,000 a; 110,000 a; 108,000 a; JAMES 1972, p. 237). On the north-eastern coast, though, it is not the corals of the 105,000 a level which overlie the fossil reef of 125,000 a, but those of the third Upper Pleistocene maximum sea level of c. 82,000 a. This is explained by differing neotectonics in the different areas. According to JAMES, in the northern part of Barbados, subsidence took place between 125,000 and 105,000 years ago, which was in contrast to the rest of the island. This subsidence led to the transgression of the relative maxima around 82,000 a and 105,000 a over the reef deposits of the absolute maximum sea level of the last interglacial at 125,000 a. The subsidence was followed by an intensified uplift in the north-west of Barbados which led to the above mentioned "Early Wisconsian reef terrace" forming at c. 60,000 a (see Figure 3.4).

These assumptions are no longer questioned in subsequent studies of the Quaternary stratigraphy of Barbados. Only TAYLOR (1974) criticises JAMES' dating results, when redating of samples from Cluffs Bay yielded $^{230}Th/^{234}U$-ages of 68,000 a, 77,000 a, and 82,000 a, calling in question JAMES' age dating of 60,000 a.

During subsequent years, research focussed principally on traverses which had been studied before; Clermont Nose on the central west coast,

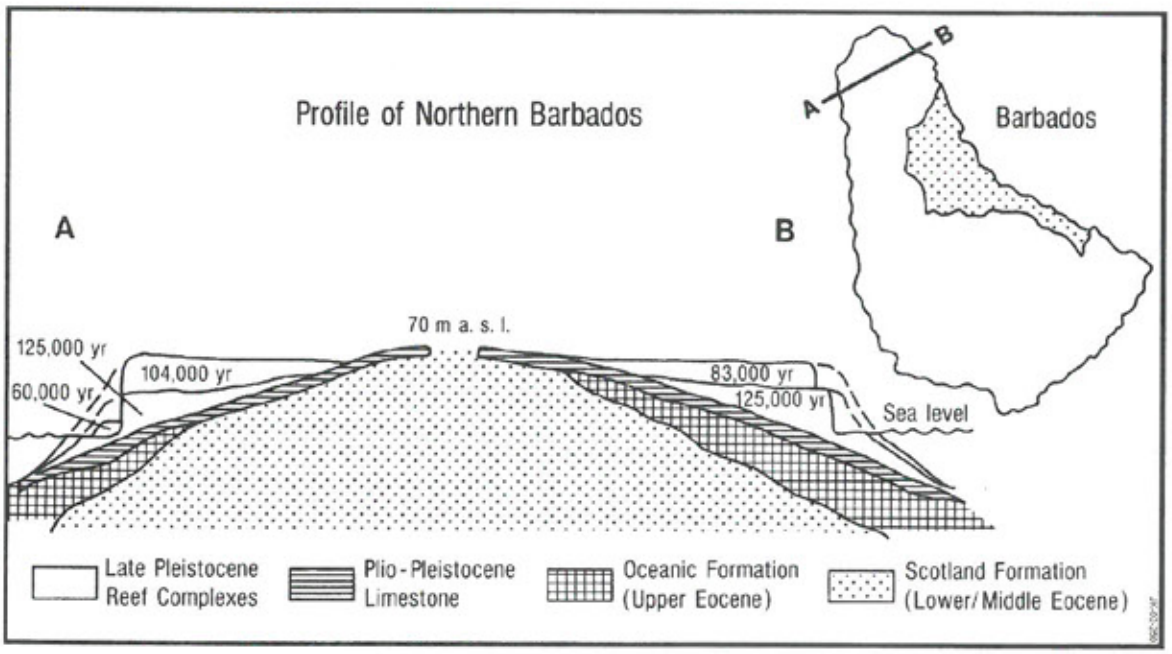

Figure 3.4: Schematic geological setting of North Barbados after JAMES (1971, in RADTKE et al. 1988: 206, RADTKE 1989: 124).

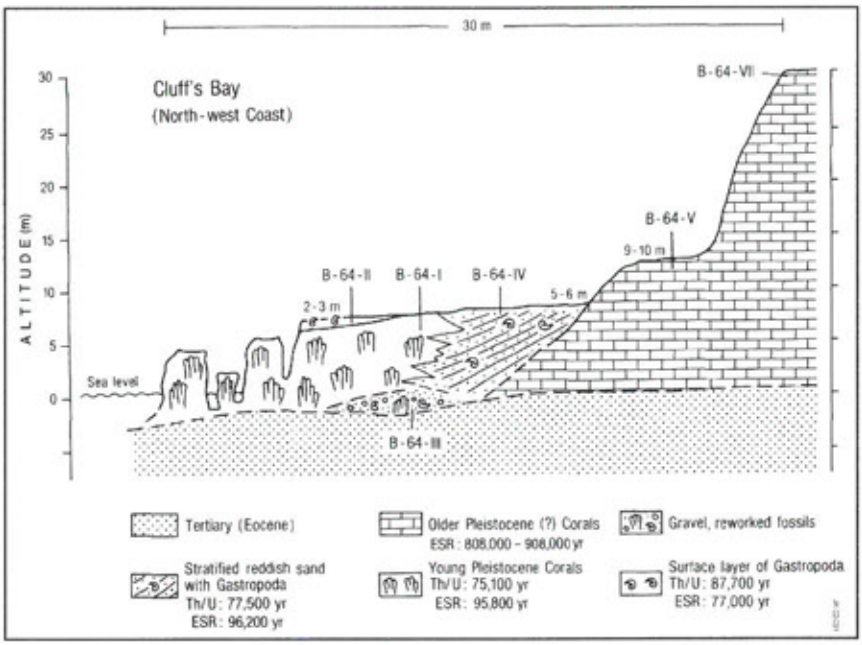

Figure 3.5:
Schematic profile of Cluff´s Bay, northwest coast (RADTKE et al. 1988: 207).

Christ Church on the south coast, and St. George's Valley in the southern central region (MATTHEWS 1973, STEINEN et al. 1973, BENDER et al. 1973, TAYLOR 1974, FAIRBANKS 1977, SHACKLETON & MATTHEWS 1977, FAIRBANKS & MATTHEWS 1978, BENDER et al. 1979)

Based on data from previous research (MESOLELLA 1968, BROECKER et al. 1968, MESOLELLA et. al. 1969), MATTHEWS (1973) once more tried to substantiate the assumption of a constant and linear uplift rate during the last 130,000 years:

"On longer time scales, the assumption of constant uplift rate must certainly break down at some point. However on shorter time scales, significant departure from constant uplift rate cannot be demonstrated. Even if it could be demonstrated, its effect on the estimates of the elevation of past sea levels would be minimal because of the short time span involved" (MATTHEWS 1973). MATTHEWS evaluated previously published data as shown in Table 3.4 but did so without communicating the parameters on which they were based.

In this context, it must be emphasized once more that calculations of palaeo sea level sites are always based on two assumptions: a sea level of +6m during the maximum of the last interglacial, and a more or less continuous linear uplift of the island at least during the last 130,000 years. Both assumptions form the basis of the "Barbados Model" which is much quoted and frequently adopted.

Among the few critics of this model, STEARNS (1976) questioned the assumption of a constant uplift between 125,000 a and 80,000 a. STEARNS considered the "Barbados Model" to be only a preliminary approach to the problem of dating Pleistocene palaeo sea levels. To him, the "Barbados Model" gave insufficient reliable information to calculate exact palaeo sea levels and to provide "standard measures" for research studies on other coasts.

Although STEARNS agrees with the conclusion that the sea level around 125,000 a was higher than those during the submaxima around 105,000 and 82,000 a, he does not take a sea level difference of 20-25 m as a basis (see MATTHEWS 1973). According to STEARNS, it is more plausible that the sea level around 125,000 a was only 6-8 m above the sea level of 105,000 a and 82,000 a.

Studies of oxygen isotopes in the corals provided a new approach to determine the absolute altitudes of maximum sea levels of the last interglacial. Following the results of studies on variations of $^{18}O/^{16}O$-relations with planktonic and benthonic foraminifers (SHACKLETON & OPDYKE 1973) the fact that molluscs and corals such as *Acropora palmata* from the reef crest of the fossil coral reefs can also record global variations of oxygen isotope relations was used (see also AHARON & CHAPPELL 1986, Papua New Guinea).

Based on oxygen isotope research, SHACKLETON & MATTHEWS (1977), FAIRBANKS (1977), and FAIR-

Table 3.4: Terrace levels and sample locations at selected standard traverses (Clermont Nose and Christ Church); calculation of respective palaeo sea levels (uplift rates assumed: Clermont 0.43/1,000 a; Christ Church 0.23/1000 a (after MATTHEWS 1973: 150, in RADTKE 1989: 115).

Locality and sample at locality	Terrace elevation (m)	Topographic elevation Elevation projected to local standard traverse (m)	Estimated elevation of Palaeo sea level-rel. to present level (m)	Radiometric age (Th/U) (a)
"Clermont standard traverse"				
Barbados I				
OC-26	20	20	-15	82,000
FS-3	14	-	-	84,000
Barbados II				
AFK-1	30	30	-15	104,000
FT-1	26	-		104,000
Barbados III-				
AFM-T-2	59	60	+6	127,000
AFM-B-1	59	-	-	127,000
"Christ Church standard traverse"				
Barbados I				
AGA-1	14	3	-16	79,000
AEH-1	6	-	-	82.000
Barbados II				
AFZ	6	6	-18	104,000
Barbados III				
S-11	36	36	+7	122,000
AEJ-5	24	-	-	124,000
AFS-1	36	-	-	124,000
ADR-1	33	-	-	127,000

BANKS & MATTHEWS (1978) calculated the palaeo sea levels shown in Table 3.5.

Unfortunately, none of the respective authors discusses the fact that there are considerable discrepancies of palaeo sea level calculations, both with the oxygen isotope model and the "Barbados Model".

With research studies on upper Quaternary coral reefs completed (for the time being), research turned to older reef units. Studies on the Quaternary stratigraphy of Barbados were able to incorporate even the oldest reef units by applying the He/U-dating method to fossil non-recrystallized corals.

Table 3.5:
Calculations of Palaeo sea level locations during the last two interglacials, based on oxygen isotope variations with molluscs and corals after FAIRBANKS & MATTHEWS (1978: 193).
Note: A variation of 0.011 % $d^{18}O$ represents a sea level change of c. 10 m. The fossil coral reefs of Kendal Hill, Kingsland, and Aberdare belong to the Christ Church Traverse.

Terrace	Age (a)	Palaeo sea-level in relation to recent sea-level (m)	
		Coral data	Mollusc data
Barbados I	82,000	-45	-47
Barbados II	105,000	-43	-28
Barbados III	125,000	+5	+10
Kendel Hill	180,000	-22	-
Kingsland	200,000	-12	-
Aberdare	220,000	-35	-

BENDER et al. (1973) first published He/U dating results for 14 samples from higher Middle Pleistocene reefs aged between 300,000 and 660,000 a. To update the "Barbados Project" which was initiated by MATTHEWS in the middle of the 1960ies, BENDER et al. (1979) tried to compile the results available, giving special consideration to Middle Pleistocene reef units. They also carried out additional He/U-dating of Middle Pleistocene corals.

To interpret the chronostratigraphy of Pleistocene coral reefs in Barbados with regard to the history of sea-level oscillations, BENDER et al. (1979) expanded models introduced by, for example, BROECKER et al. (1968) and MATTHEWS (1973). They based their calculation of palaeo sea levels on the assumption that the sea level around 125,000 a ("First High Cliff") was located c. 6 meters above the present day level, and the three standard traverses under consideration were uplifted at a constant rate. This approach was successful only at Christ Church (0.25 m/1,000 a) and Clermont Nose (0.44 m/1,000 a). At St. George's Valley both the lower sequence of fossil reefs and the "First High Cliff" are missing, so that the calculation of the uplift rate (0.34 m/1,000 a) was

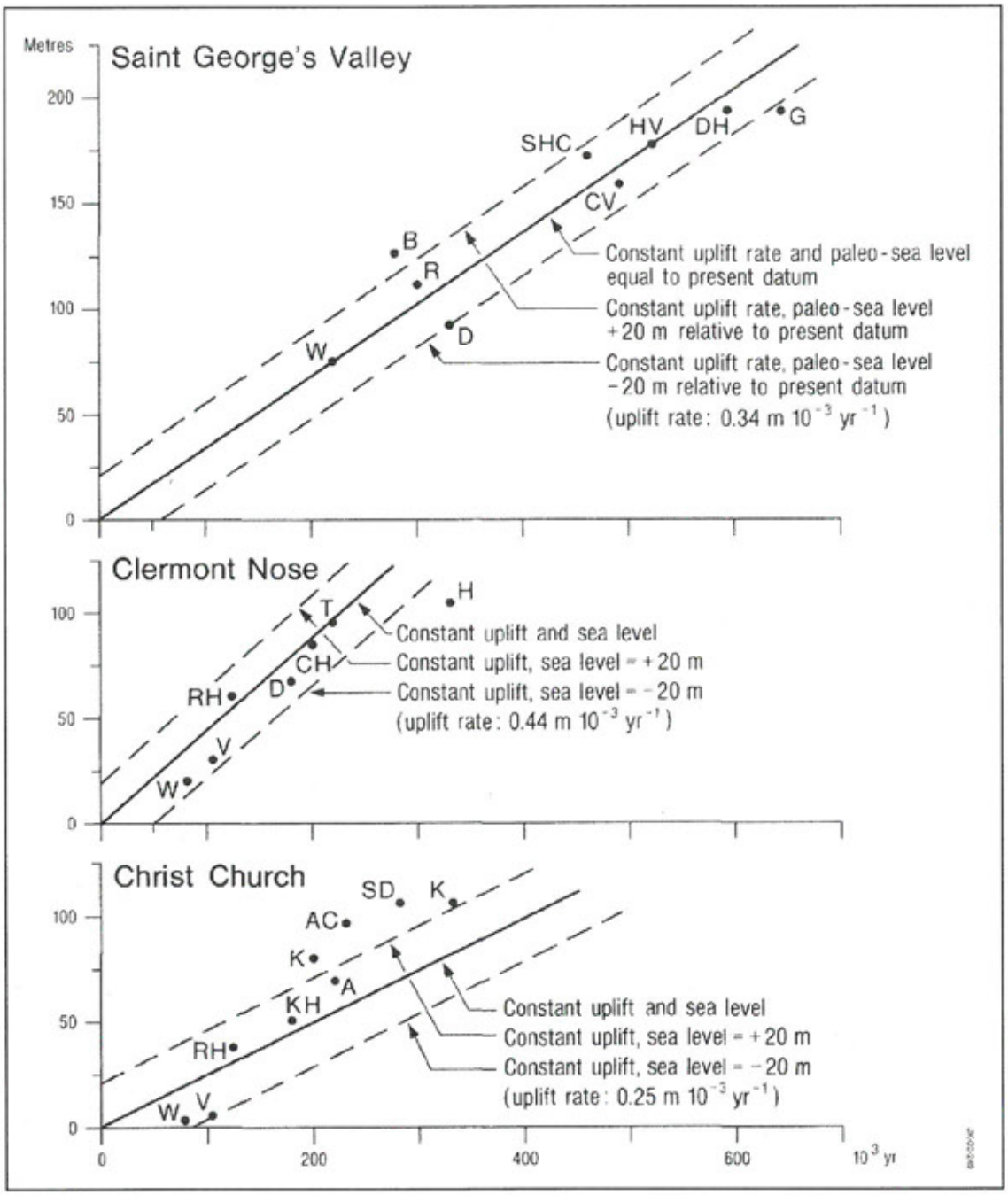

Figure 3.6: Reef tract elevation calculated using the continuous diagenesis model He^4/U age, for samples from Christ Church, Clermont Nose, and St. George´s Valley sections. Sumperimposed lines show where points would fall for three uplift models:
(1) constant uplift rate and palaeo sea level equal to present datum;
(2) constant uplift rate, palaeo sea level +20m relative to present datum;
(3) constant uplift arte, palaeo sea level –20 m relative to present datum.
Initials of terrace names are next to data point (after BENDER et al. 1979: 592, RADTKE 1989: 23).

possible only by assuming the equivalence of stages Windsor (St. George's Valley) and Thorpe (Clermont Nose traverse). Palaeo sea levels were calculated for each stage by subtracting tectonic uplift (= reef age x uplift rate) from altitude of reef crest (see Figure 3.6). The results of BENDER et al. (1979) are given in Table 3.6. From these results, the authors basically draw two conclusions:

1) Calculating Pleistocene palaeo sea levels on the basis of a constant uplift rate model can be a useful approach, although in the Christ Church area a higher uplift rate before 125,000 a must be taken into account.

2) Taking the results of the palaeo sea-level calculations around the altitude of the recent sea level as a whole, and those of St. George's Valley traverse in particular, it seems reasonable to assume that, during different Interglacials of at least the last 700,000 years, the volumes of the polar and mountain ice masses were comparable to those today.

This would mean that no depression of sea level lasting any significant time has occurred since the beginning of the Middle Pleistocene. It also implies that in regions of relative tectonic stability only maxima around 125,000 a, 300,000 a, and 500,000 a could possibly have been located slightly above recent sea level. Morphologically distinctive "steps" of marine terraces or coral reefs, therefore, could only be indications of regions of tectonic uplift.

3.3. Electron Spin Resonance dating of the coral reef tracts of Barbados

A new attempt to obtain independent age control of the fossil coral reef tracts of Barbados was begun by RADTKE et al. (1988) and RADTKE (1989), using the relatively new Electron Spin Resonance (ESR) dating technique. This first systematic ESR dating study of Quaternary corals yielded, for the last interglacial terraces Barbados I, II, and III, ages in the same range as those of the U-series dating techniques. With respect to the dating of the older coral reef tracts, ESR ages generally suggested an earlier formation of the reefs, as indicated by the studies of BENDER et al. (1979). RADTKE started his research by resampling the "classical" traverses Clermont Nose, Christ Church, Thorpe, and St. George´s Valley traverses (see Figure 4.1), which continued to play an important role in the reconstruction of the Quaternary gemorphological and geological evolution of the island in subsequent years. However, he rapidly came to the conclusion that restricting investigations to detailed examination of the Clermont Nose and the Christ Church traverses was not justifiable because of the complex geological and tectonic setting of Barbados. The projection of the one-dimensional results obtained from the traverses into the two-dimensional surface as done by, for example, BENDER et al. (1979), was based mainly on aerial photographic mapping.

The pitfalls in this procedure are numerous. It is difficult enough to follow a minor or major reef terrace during the field survey over several kilometres, but it is sometimes impossible to trace a reef on an aerial photograph. It was suggested by RADTKE (1989) that the basis for all future geological and geochronological work to be done on Barbados must be a sound morphological mapping of the island obtained by field survey studies. Such a detailed mapping is an essential basis for the development of a reliable sampling strategy.

Table 3.6: Altitude of reef units in standard traverses (Christ Church, Clermont Nose, St. George's Valley); palaeo sea levels of relative sea level maxima (each maximum represented by a reef unit). Note: Calculation is based on two assumptions: a constant uplift rate deduced from recent altitude of last interglacial reef of Barbados III (125,000 a) and that Barbados III was + 6 m above recent sea level. Individual reef units were correlated with isotope stages 5-19 of core V28-238 oxygen isotope curve (SHACKLETON & OPDYKE 1973; correlation following BENDER at al. 1979: 581, 593, in RADTKE 1989: 117).

Christ Church Traverse	Topographic elevation and estimated Palaeo sea-level surface in standard trav. (m) Uplift rate: 0.24m/ka		Clermont Nose Trav.	Topogr. elev. & est. Palaeo sea-level surf. Uplift rate: 0.44m/ka (m)		St. George´s Traverse	Topogr. Elev. & Pal. s.-l. 0.34m/ka: (m)		Mean age (ka)	$^{18}O/^{16}O$ Isotope stage
Worthing	3	-17	Worthing	20	-16				82	5
Ventnor	6	-20	Ventnor	30	-16				105	5
Rendezous Hill	37	+6	Rend.Hill	61	+6				125	5
Kendal Hill	49	+4	Durants	67	-12				180	7
Kingsland	79	-29	Cave H.	85	-3				200	7
Aberdare	67	+12	Thorpe	94	-1(-3)	Windsor	73	-2	220	7
						Rowans	110	+8	300	9
Adams Castle	91	+32	Husband	107	-33	Dayrells	92	-20	320	9
Kent	110	+28				Bourne	125	+30	280	9
St. David	110	+39				Walker	137	-	-	11
			Cott.Vale	158	-9				490	13
			Unnamed	171	+15(+18)				460	13
			Hill View		0(+2)				520	13
			Drax Hill	192	-9				590	15
			Guinea	192	-22				640	17/19

A presentation of the first ESR studies of RADTKE et al. (1988), RADTKE (1989) and RADTKE & GRÜN (1990) will not be given here as the most recent ESR dating results will be presented in detail in Chapter 4.

3.4. Mass spectrometric U-series dating

Until the mid 1980's, alpha-spectrometric U-series dating was used to date fossils or inorganic carbonates beyond the dating range of the radiocarbon method. However, because of the limitations in precision and accuracy of the $^{230}Th/^{234}U$ dating technique, it was difficult to answer the important question in palaeoclimatology of a possible double peaked sea level maximum during oxygen isotope stage 5e around 125,000 years ago. This well established age of 125,000 a was confirmed by, for example, KAUFMAN (1986), who analyzed 104 available $^{230}Th/^{234}U$ age determinations of unrecrystallized corals from stable emerged terraces. KAUFMAN (1986) used the 80 most reliable analyses, which showed surprisingly good agreement, to make an estimate of the exact duration of this period. His results showed that (1) if there was only a single rise in sea level, it probably lasted no more than 12,000 a; and (2) if there were two seperate rises of sea level, the gap between them must have been less than 7,500 a (KAUFMAN 1986). Nevertheless, the question regarding the number of last interglacial high-sea stands was not answered unequivocally.

In 1987, the new era of mass-spectrometric U-series dating (EDWARDS et al. 1987a) began; direct measurement of U and Th by mass spectrometry provided a spectacular improvement in the precision of coral dating by the U-Th disequilibrium method. The age uncertainties obtained by this new technique of U-Th measurement were comparable to those achieved by the ^{14}C method. The precision of mass spectrometry measurements for the $^{234}U/^{238}U$ ratio is typically 0.5% to 1% at the 2 sigma level, which translates into uncertainties on the order of 1.0% to 1.5% for the calculated initial $^{234}U/^{238}U$ of 70,000-140,000 a corals. Furthermore, the mass spectrometric technique provided a much better resolution for the examination of subtle diagenetic effects revealed by small variations in the $^{234}U/^{238}U$ ratio. Ages obtained by EDWARDS et al (1987a) on corals from Barbados were 87,000 a, 112,000 a and 125,000 a for the oxygen isotope (sub-)stages 5a, 5c, and 5e, respectively. The ages for the submaxima 5a and 5c were 5,000 to 7,000 a higher than the previous U-series ages obtained by alpha spectrometry.

The last major attempt of alpha spectrometric U-series was carried out in 1990 by KU et al., who published dating results of 29 samples which came from the Christ Church and Clermont Nose traverses. These samples were originially collected by R.K. MATTHEWS of Brown University and served as the basis for confirmation of oxygen isotope results of FAIRBANKS & MATTHEWS (1978). The collection was made at 10 outcrops from four morphostratigraphic units. These units included the terraces of Worthing (Barbados I), Ventnor (Barbados II), Rendezvous Hill (Barbados III) and a previously unstudied new terrace just in front of Rendezvous Hill, termed by KU et al. (1990) "Maxwell terrace". As mentioned above, the "Barbados model" has been contentious from the very beginning. A major issue is whether, during oxygen isotope stage 5e when Rendezvous Hill reef complex on Barbados Island formed, the sea rose above the present position for one relatively brief period of <20,000 a, or for two or more periods spanning from approximately 140,000 a to 115,000 a. Evidence for the latter scenario has not come from initial studies of Barbados but from elsewhere; it is also inconclusive because of the dating uncertainties involved. KU et al. (1990) have carried out redeterminations of U-series ages on a suite of 29 *Acropora palmata* samples. They also detected the high $^{234}U/^{238}U$ ratios and suggested that the anomalous ratios of samples with apparently unaltered mineralogy and trace element (Mg, Sr) chemistry may be explained by groundwater influence and isotopic exchange.

The lower-limit of the terrace ages, estimated by averaging the multiple sample measurements, are 81,000±2,000 a (Worthing), 105,000±1,000 a (Ventnor), 120,000±2,000 a (Maxwell), and 117,000±3,000 a (Rendezvous Hill). They found no evidence of previously inferred two episodes of high sea level centering around 118,000 and 135,000 a ago. No age distinction can be made between the Maxwell and Rendezvous Hill terraces which argues against any possible correlation with terraces VIIa and VIIb in Papua New Guinea. Seven samples have been dated by mass spectrometric measurements (EDWARDS et al. 1987). The two sets of ages agree within two standard deviations for the three samples from outcrop AFS, but they differ for samples at the other four outcrop locations, for which the MS ages are higher than the AS (alpha spectrometry) ages. AFS-12 is the only sample for which the comparative

measurements were made on powdered splits of the sample. For the other samples, they were done on coral fragments which were not "bona fide" splits (EDWARDS et al. 1987, KU et al. 1990) (see Table 3.7).

From these somewhat disappointing results, Ku et al. (1990) concluded that, when working close to the precision limit of dating corals using alpha-spectrometric techniques, the integrity of corals as a closed system for U isotopes is an important factor limiting our ability to resolve unambiguously the temporal relationship between climatic fluctuations and changes in the distribution of solar energy reaching the earth. With the "end" of the alpha-spectrometric epoch, KU et al. forecasted that the next step forward would require extensive application of high precision mass-spectrometric analysis.

It is notable that in the study of KU et al. (1990), no significant age difference between Rendezvouz Hill terrace (117,000 a) and Maxwell terrace (120,000 a) was detected. But, astonishingly, Ku et al. did not discuss the obvious discrepancy between their U-series ages of the maximum of the last interglacial sea-level highstand and those data obtained in earlier studies. It could be argued that a systematic error in alpha-spectrometric measurments has occurred in the dating of the last interglacial reef tracts on Barbados. However, against this speculation must be set the fact that only the ages of oxygen isotope stage 5e are significantly "rejuvenated"; the dating of stage 5a (81,000 a) and 5 c (105,000 a) are practically identical with those of the former studies (see above).

Given this background, a number of studies were published in subsequent years in which the U-series data obtained by mass-spectrometry were discussed. In these studies (e.g. KU et al. 1990, see above), many of the corals already sampled by MESOLELLA, MATTHEWS or BENDER, and dated by alpha-spectrometry U-series technique, were redated with the new technique. New sampling took places in only a few studies but even these new samples stem generally from the "classical" traverses like Clermont Nose or Christ Church. A comparison with earlier studies is sometimes complicated by the fact that the location of the sampling sites is not documented in detail. The most important results of these new geochronological studies are summarised below.

Of special interest are the offshore studies of FAIRBANKS (1989) and BARD et al. (1990a), which deal with the reconstruction of palaeo sea-level change since the glacial sea-level minimum around 18,000 a, as all former and following studies have been carried out onshore. Coral reefs drilled offshore from Barbados provided the first almost continuous record of sea-level change during the last deglaciation. FAIRBANKS chose to reconstruct glacio eustatic sea levels by coring drowned late glacial and Holocene *Acropora palmata* reefs on the south coast of Barbados. In all 16 cores were drilled. The deepest

Table 3.7: Comparison of mass-spectrometric (MS) and alpha-spectrometric (AS) results for samples collected on Barbados after KU et al. (1990).

Sample	Age (MS) (a)	Age (AS) (a)
Worthing (5a)		
FS-50A	-	78,100±1,200
FS-51	-	75,500±1,200
OC-50	-	85,200±1,300
OC-51	87,500±300	83,000±1,300
OC-53	-	83,200±1,500
Ventnor (5c)		
ANM-21	-	102,400±2,000
Maxwell Terrace		
AEJ-20	-	128,700±3,000
AEJ-21	-	127,600±2,500
AEJ-22(1)	-	-
AEJ-22(2)	-	114,200±2,000
AGP-10	-	117,600±2,300
AGP-12(1)	-	115,000±2,400
AGP-12(2)	-	114,000±2,000
Rendezvous Hill		
AFM-20A(1)	129,200±700	118,400±2,700
AFM-20A(2)	-	120,200±2,700
AFM-22A(1)	-	102,500±2,000
AFM-22A(2)	-	99,400±2,100
AFM-23(1)	-	113,500±2,400
AFM-23(2)	-	105,800±2,300
R-50(1)	-	133,700±2,700
R-50(2)	-	132,300±3.000
R-51(1)	-	116,100±2,300
R-51(2)	-	122,700±2,400
R-52(1)	128,100±900	108,500±2,000
R-52(2)	-	114,000±2,700
AFS-10	125,700±600	122,000±2600
AFS-11	122,600±700	123,800±2700
AFS-12	122,100±600	120,700±2700
	122,700±700	-
	124,400±700	-
ANM-22	-	101,500±2,100
FT-50	112,000±500	103,600±2,000
	111,800±700	-
	112,300±600	-
FT-51(1)-	110,500±2,200	-
FT-51(2)-	104,200±2,300	-
FT-53	-	102,900±1,900
BAB-10	-	103,300±1,800
BAB-11	-	108,300±2,100
BAB-12	-	129,200±2,600

Table 3.8: U-Th ages obtained by mass- and alpha-spectrometry of coral samples collected on Barbados (A = BROECKER et al. 1968, MESOLELLA et al. 1969; B = KU et al. 1990).

Sample	Locality	Age (a) BARD et al. 1990 (U/Th-mass.spec.)	Age (a) EDWARDS 1988 (U/Th-mass.spec.)	Age (a) (U/Th-alpha-spec.)
FS-13	Worthing (18m)	88,200±800	-	-
OC-51	Worthing	-	87,500±600	-
		-	87,900±700	-
AFZ2	Ventnor (6m)	100,500±1,100	-	105,000±3,000(A)
FT-50	Ventnor	-	112,000±1,000	103,600±4,000(B)
		-	111,800±1,300	-
		-	112,300±1,100	-
AFM3/1	Rendezvous Hill (55m)	125,000±1,700	-	-
AFM3/2	Rendezvous Hill (55m)	125,000±1,000	-	-

radiocarbon dated sample of *A. palmata* occured at 113.8 m below the present sea level (119.6 m if corrected for an assumed mean uplift rate of 34 cm/1000 a) and was dated to be 17,100 a in age. By dating these *Acropora* deposits for the first time, it was possible to obtain an almost complete palaeo sea-level curve for the period from 17,100 to 9,500 a (Figure 2 in FAIRBRIDGE 1989, p. 639). Almost concurrent with this publication was the construction of a second long and continuous record of the sea-level rise associated with the last deglaciation in Huon Peninsula, Papua New Guinea (CHAPPELL & POLACH 1991). This sea-level history was also based on ^{14}C dating of reef-crest corals from cores. The depths of the coral samples were corrected for a local uplift of 1.9 mm/a. These two data sets were converted from ^{14}C years to siderial years and then compared to sea-level curves predicted by different deglaciation models (e.g. TUSHINGHAM & PELTIER 1993).

BARD et al. (1990a) determined the ages of Barbadian corals using both ^{14}C and Th/U dating techniques, and thereby calibrated the radiocarbon timescale for the past 20,000-30,000 ^{14}C a (refer to BARD et al. 1990b for a detailed discussion of their techniques and results). HAMELIN et al. (1991) summarized some of the other prominent successes obtained by the U/Th dating technique. These include precise correlation of the glacial-interglacial sea-level variation with variations in solar insolation as predicted by MILANKOVITCH orbital parameters, and precise dating of historical corals for detailed studies of uplift dates of oceanic islands. Previously, such calibrations were only possible using dendrochronological methods, and could only reach back 10,000 ^{14}C a (BECKER et al. 1991). An important implication of the radiocarbon calibration curve is that the last glacial maximum, which has long been estimated to have occurred ca. 18,000 ^{14}C a BP, appears to have occurred 21,500 cal a BP. Following TUSHINGHAM & PELTIER (1993), the total sea-level rise at Barbados is 124 m, which agrees with FAIRBANKS' estimate of 121±5 m obtained from the depths of drowned reef crest corals.

After this short but very inspiring off-shore interlude with results relevant to late glacial and early Holocene sea-level history, research on Barbados focused once more on land based studies. As already discussed above, problems arising from mass spectrometric (TIMS) U-series were the main focus in subsequent studies. The problems included, for example, the discrepancy between the mass-spectrometric U-series results of BARD et al. (1990) and the data of EDWARDS (1988) as evident in Table 3.8. Note that the difference of 11,000 a between the various estimates of the age of the Ventnor terrace in particular is very substantial. Although the mass spectrometric U-series dating of corals claims a high precison and a good accuracy, the discrepancies in the first studies of EDWARDS (1988), EDWARDS et al. (1987a,b) and BARD et al. (1990) triggered subsequent studies which focused on potential sources of the age perturbations.

In 1991 HAMELIN et al. published a critical review of recent $^{234}U/^{238}U$ mass-spectrometric ages. Despite the improvement in the precision of the Th/U data, perturbations in the $^{234}U/^{238}U$ ratio may strongly affect the accuracy of the U-Th chronometer. Most data, including those from Barbados, show that most of the corals from terraces of the last interglacial have initial $^{234}U/^{238}U$ ratios higher than present-day seawater, in contrast to modern, Holocene and Last Glacial corals (see Table 3.9).

Table 3.9: Mass-spectrometric U-series dating results for last interglacial coral samples from the Christ Church Traverse and from Salt Cave after HAMELIN et al. (1991).

Sample	MS U-Th age (a)
Rendezvouz Hill (Christ Church)	
AFM3(1)	125,200±1,700
AFM3(2)	125,100±1,000
AFM9(1)	112,300±1,200
AFM9(2)	112,800±1,900
AFM8	122,300±1,300
AFS1	132,600±2,300
Salt Cave (first terrace above present sea-level)	
Salt Cave	98,400±1,200

Even apparently pristine samples have ratios higher than present-day seawater. This difference in the U initial ratios raises some uncertainty about the accuracy of the U-Th age determinations of these corals. In spite of the fact that the $^{234}U/^{230}Th$ ages cluster in a narrow range between 122,000 and 133,000 a, the data could also be interpreted as resulting from contamination of corals that are significantly older than 125,000 a. Two possible explanations are discussed by HAMELIN et al. (1991):

(1) All the samples may have been diagenetically altered, since they all come from surface outcrops which have been directly exposed to precipitation and/or soil water for 125,000 a.

2) Some of the difference in $^{234}U/^{238}U$ ratios measured in 125,000 a old corals, compared to modern seawater, may be due to a higher $^{234}U/^{238}U$ ratio in seawater 125,000 years ago.

In order to investigate these problems, BANNER et al. (1991) carried out Uranium-series isotope measurements by mass spectrometry on aragonite, dolomite and groundwater samples from Pleistocene coral-reef terraces on Barbados, in order to evaluate the behaviour of U-Th isotopes during water-rock interaction in carbonate systems. Two pristine *Acropora palmata* corals (samples GG-1 and GD-2) from the so-called Golden Grove terrace in the East Point Shelf area, yielded ^{230}Th ages of 219,000±3,000 a and 224,000±6,000 a.

The fundamental issues related to such precise data are syn- and post-depositional diagenetic changes to the concentrations of the pertinent U-series nuclides, which could shift the ages well outside the limits suggested by the analytical uncertainties. The two dated corals have high and variable initial $\delta^{234}U$ relative to values for modern seawater. This indicates that the U-series has not followed closed-system behaviour since the time of deposition. The pronounced differences in the U-Th isotope systems between the aragonitic corals, dolomites and groundwater reflect the enhanced mobility of U relative to Th during water-rock interaction. This kind of diagenesis can profoundly affect the U-Th isotopic composition and therefore the accuracay of high-precision ^{230}Th ages determined on such samples. However, diagenesis involving fluids such as the present-day groundwaters on Barbados cannot account for the elevated $\delta^{234}U$ values of the corals. BANNER et al. (1991) came to the conclusion that the mechanism by which apparently well-preserved corals become enriched in ^{234}U is yet to be identified. Early diagenetic processes involving marine porewaters could be a possible cause of these high $\delta^{234}U(t)$ values.

When dating corals of oxygen isotope stages 7 to 11(13) by mass-spectrometry, Bard et al. (1991) came to similar conclusions regarding the significant excess of ^{234}U relative to the Uranium isotopic composition which is to be expected for corals grown in present-day seawater. They proposed that the anomalies result from both diagentic addition and replacement of U and also, possibly, from global changes in the $^{234}U/^{238}U$ composition of seawater through time. Their conclusions reinforced the argument that ^{234}U anomalies cast doubt on the accuracy of the classical ^{230}Th-ingrowth dating method in old corals, and in particular for the use of measured $^{234}U/^{238}U$ ratios alone to date corals older than 150,000 a.

BARD et al. (1991) dated 12 samples from Barbados (see Table 3.10). Their statement that the dating results of the four oldest samples are very questionable seems justified. This is particularly so when it is considered that the Adams Castle terrace is morphostratigraphically (see Chapter 4) 1 to 2 interglacials younger than the reef crest of St.Davids terrace, the uppermost step of the Christ Church traverse. The age obtained for the samples of the Kingsland-Aberdare reef unit - isotope stage 7.5, the oldest of the three penultimate interglacial sea level maxima - is probably correct. On the other hand, it is not easy to understand why the samples of Kendall Hill terrace are put into stage 7.3 – morphostratigraphically, Kendal Hill is the terrace directly above the Rendevouz Hill terrace. Although BARD et al. (1991) refer to similar results from RADTKE et al. (1988), the absolute age of the Kendal Hill terrace is still highly problematic. Nevertheless, BARD et al. (1991) reached the conclusion that the TIMS

Table 3.10: Thermal ionization mass spectrometry (TIMS) results for *Acropora palmata* coral samples from Barbados. All but the two RGF samples originated from the Christ Church Traverse after BARD et al. (1991).

Sample	Location	TIMS-age (a)	Alpha-spec. age (a)
RGF1-90-22/1	Salt Cave, 40m	187,000±5,000	-
RGF1-90-22-2	Salt Cave, 40m	186,000±6,000	-
ACJ4/1	Kendal Hill	213,000±8,000	222,000±60,000
ACJ4/2	Kendal Hill	207,000±4,000	-
ACJ7	Kendal Hill	214,000±4,000	-
AGH3	Kingsland/Aberdare	228,000±4,000	-
ADI1	Kingsland/Aberdare	255,000±9,000	-
AIB2	Kingsland/Aberdare	258,000±8,000	250,000±80,000
AKF3	St. Davids Terrace	350,000±15,000	-
AKF1	St. Davids Terrace	418,000±31,000	-
AFY1	St. Davids Terrace	488,000±45,000	368,000±180,000
AHR1	Adams Castle	528,000±65,000	

technique can provide ^{230}Th-ingrowth ages with a precision of the order of a few percent for samples between 200,000 and 300,000 a.

However, the accuracy of the ^{230}Th-ingrowth chronometer in old corals appears to be limited by post-depositional disturbance of the U-Th system. As a preliminary interpretation, they proposed that the observed variations in initial ^{234}U/^{238}U ratios were due to diagenetic addition or replacement of U (and possibly Th) together with seawater ^{234}U/^{238}U variations. Nevertheless, neither meachanism alone is able to explain simultaneously the magnitude of the U isotopic anomalies, and the rather small scatter of the ^{234}Th-ingrowth ages obtained in stratigraphically equivalent samples. Moreover, no valid candidate for the fluid involved in the diagenesis has yet been identified.

In 1994 GALLUP et al., TIMS ^{230}Th ages were determined for Barbados corals which grew during interglacial periods within the last 200,000 years. Samples were collected from two transects: Clermont Nose (University Road) and Holder Hill, north of Clermont Nose (see Table 3.11).

Because it is known that inaccurate ages can result from a diagenetic remobilization from Thorium and Uranium, GALLUP et al. addressed the problem of diagenesis with a model that reproduces diagenetic trends in their own and previously published data (EDWARDS et al. 1987a/b, HAMELIN et al. 1990, 1991, BANNER et al. 1991, BARD et al. 1991 and DIA et al. 1992). To date there have been no fossil coral data sets of sufficient size or precision to support any given model. Examination of the data of GALLUP et al. (1994) in conjunction with earlier TIMS ^{230}Th data from Barbados showed that, for a given terrace, the corals with the highest initial δ^{234}U values appear to have the oldest ^{230}Th ages. The rough trend between δ^{234}U value and ^{230}Th age is explained by GALLUP et al. by net addition of ^{234}U and ^{230}Th. GALLUP et al. (1994) therefore assumed that ^{238}U concentration is constant, that initial δ^{234}U value equals the modern marine value, and that ^{234}U and ^{230}Th are continuously added during diagenesis. They determined an expression for the isotope composition as a function of time for a coral that gains ^{234}U and

Table 3.11: TIMS ^{230}Th ages of coral from the Clermont Nose and Holders Hill transects, west coast of Barbados (GALLUP et al. 1994: 797).

Sample	Height (m asl.)	TIMS ^{230}Th-age (a)
Holders Hill		
FSL-2 (modern)	0	132 ± 3,000
FS-3 (Barbados I)	12	83,300±300
FS-8 (Barbados I)	13	87,200±500
FT-1 (Barbados II)	24	104,300±400
FU-1 (Barbados III)	47	124,600±500
FU-3 (Barbados III)	40	135,400±700
FY-2 (Older terrace)	63	211,000±1,600
FW-1 (Older terrace)	64	283,700±4,200
Clermont Nose (University Road)		
Last Interglacial (Barbados III)		
UWI-2	31	129,100±800
UWI-16	40	117,000±1,000
Penultimate Interglacial		
WAN-B-2(1)	92	199,000±1,300
WAN-B-2(2)	91	201,200±2,000
WAN-B-7	91	200,800±1,000
WAN-B-1	91	193,500±2,800
WAN-B-6	91	203,600±1,700
WAN-B-8	91	203,500±1,300
WAN-B-5	91	223,300±3,800
WAN-B-sand	91	279,900 (+21,000/-19,000)
WAN-B-14	92	190,800±700
WAN-E-1	83	209,200±1,700
WAN-C1	71	203,400±400
Older Terraces		
WAN-D-3(1)	69	230,500 (+3,700/-3,600)
WAN-D-3(2)	69	230,500 (+5,500/-5,300)
WAN-D-3(3)	69	232,900 (+7,600/-7,200)
WAN-A-1	99	302,000±6,000
WAN-F-4	100	402,000 (+12,000/-11,000)

^{230}Th at constant rates from some outside source, and used the isotopic compositon of an altered coral from Barbados to solve for rates of ^{234}U and ^{230}Th addition (for details see GALLUP et al. 1994). Due to the scatter of the data about the modeled lines, GALLUP et al. did not attempt to use the model to correct ^{230}Th ages of samples. Instead, they used the lines as a guide in establishing maximum acceptable initial δ^{234}U values. For example, a sample with an initial δ^{234}U of 154 and four δ-units above the marine value, has a ^{230}Th age about 1,000 years older than its true age. GALLUP et al. came to the conclusion that for the last three interglacial and two intervening interstadial periods, sea level peaked at the same time, or after, peaks in summer insolation in the Northern Hemisphere. This overall pattern supports the idea that glacial-interglacial cycles are caused by changes in the Earth´s orbital geometry. The sea-level drop at the end of the penultimate interglacial, the last interglacial, and a subsequent interstadial period, lagged behind the decrease in insolation by 5,000 to 10,000 years.

Considering the fact that the conclusion drawn by GALLUP et al. has wide implications for palaeo sea level and palaeoclimatic research, it is crucial to have reliable information on the precise locality of samples. Samples of lower elevation (FY-2, WAN-D-3 or FW 1) than the WAN-B outcrop gave significantly higher ages; a last interglacial sample at 31 m elevation (UWI-2) was dated 117,000 a, a nearby sample at 40 m elevation gave an age of 129,100 a. Although GALLUP et al. have seen these discrepancies and suggested studying similar deposits with clearer stratigraphic relationships, special attention should be drawn to the interpretation of the localities mentioned. It is possible that the variations in the initial δ^{234}U value have produced "confusing" results and further systematic methodological studies should be carried out. Any such studies must be based on a sound morphostratigraphy.

EDWARDS et al. (1997) remeasured the samples of GALLUP et al. (1994), using both U-series and also TIMS ^{231}Pa methods (see Table 3.12). His results for those samples with concordant ages indicate that sea level was relatively high 82,800±1,000 a, 104,200±1,200 a, 121,000±2,100 a, 126,800±2,500 a, and 193,000±9,000 a ago. The sea-level highs marked by these corals correspond to oxygen isotope stages 5a, 5c, and 5e (represented by both the 121,000 a and the 126,800 a ages), and 7.1, respectively. The combined Pa/Th data support the conclusion of GALLUP et al. (1994) which was based solely on ^{230}Th ages. A comparison of the sea level constraints from EDWARDS et al. (1997) with high-latitude Northern Hemisphere summer insolation values, shows that all of the high sea levels coincide with, or slightly postdate, the times of high Northern Hemisphere insolation. EDWARDS et al. (1997) contrasted their data set with one from the Devil's Hole, where the timing of the oxygen isotope shift from glacial to interglacial values around 140,000 years ago (Termination II) generally precedes the shift in

Table 3.12: ^{230}Th, ^{231}Pa, and ^{231}Pa/^{230}Th ages for Barbados coral samples after EDWARDS et al. (1997: 784).

Sample	^{230}Th age (a)	^{231}Pa age (a)	^{231}Pa/^{230}Th age (a)
Worthing Terrace (Barbados I)			
FS-3	82,900±400	83,800±1,200	81,800±1,700
FS-8(I)	86,100±400	89,500±1,300	82,500±1,500
FS-8(II)	85,400±400	86,200±1,000	84,500±1,400
Ventnor Terrace (Barbados II)			
FT-1(I) 1	103,100±500	103,000±2,400	103,400±2,200
FT-1(II)	105,400±600	105,600±2,200	105,900±2,000
Rendezvous Hill Terrace (Barbados III)			
AFM-20	126,900±1,100	126,800±2,500	126,900±2,200
UWI-16	132,000±900	143,000±6,000	127,000±2,500
FU-1(I)	122,300±700	120,000±3,400	123,700±2,500
FU-1(II)	122,600±700	119,000±2,600	125,000±2,100
FU-3	147,300±900	No solution	119,400±2,300
„Stage 7" terraces (Penultimate Interglacial)			
WAN-B2(I)	191,700±1,600	190,000(+17,000/-12,000)	192,000±3,900
WAN-B2(II)	193,100±1,600	197,000(+15,000/-11,000)	192,300±3,300
WAN-B2(III)	190,200±1,500	195,000(+14,000/-11,000)	189,100±3,100
WAN-B-7	200,800±1,000	198,000(+15,000/-11,000)	204,900±4,000
WAN-B-8	203,600±1,800	262,000(+∞/-33,000)	197,200±3,200
WAN-B-5	217,900±2,100	No solution	204,900±4,000
FY-2	206,100±1,800	No solution	188,600±3,000

insolation from glacial to interglacial values, suggesting that Termination II did not result from insolation rise (EDWARDS et al., 1997).

A recent paper (GALLUP et al. 2002) focuses on determining the timing of the above mentioned Termination II by dating Barbados corals. The timing and cause of Termination II are particularly important because it is so closely linked to the 100,000 year cycle, of which the driving mechanism remains unclear and widely debated. The nine samples stem from a road cut at the University Road which is part of the classical Clermont Nose traverse and have been dated using ^{231}Pa and ^{230}Th dating (TIMS) (see Figure 3.7 and Table 3.13).

GALLUP et al. (2002) stated that the concordancy of ^{230}Th and ^{231}Pa dates is the best test that the ages have not been shifted by diagenetic alteration. As well, there should be no evidence of recrystallization of aragonite to calcite, and the initial δ^{234}U value should be within 0.008% of the modern value. Samples which meet all three criteria are most likely to record accurate ages; those that meet only one or two are less likely to have accurate ages, although they still may hold valuable climatic information (GALLUP et al., 2002).

For the direct determination of Termination II, precision and accuracy in chronometry are critical. Samples NU-1471/-1472/-1473 are from units below the last interglacial maximum Rendezvous Hill-terrace deposits, and all have concordant ^{231}Pa and ^{230}Th ages, clustering around 135,000 a. These ages, and initial elevations of 16-18 m below present sea level, suggest that this deposit formed during the rise to the maximum of the last interglacial sea level (Termination II). Samples NU-1471 and NU-1472 are from the mixed *Acropora palmata* and head coral unit, just below the cobble-rich of sample NU-1473. The similar ages demonstrate, after GALLUP et al. (2002), stratigraphic consistency and a genetic relationship between the two deposits. GALLUP et al. (2002) interpreted the presence of cobbles as indicating a proximity to sea level during the time recorded by the samples. Sample NU-1471 meets all three criteria mentioned above, indicating that the timing of this sea level event during Termination II was 135,800±800 a. Sample UWI-101, collected adjacent to sample UWI-2 (GALLUP et al. 1994), also meets the three criteria and confirms the age of the deposit as 129,100±500 a (GALLUP et al. 2002). GALLUP et al. (2002) were surprised that samples immediately adjacent to these samples (NU-1464, UWI-103, and UWI-107) gave ages that correspond to marine oxygen-isotope event 6.5. They admitted that the unit is not sufficiently exposed to determine whether the samples are *in situ*. So they conclude that the estimate of associated sea level of -25±3 m implied by UWI-101 and UWI-2 remains tentative. Sample OC-1 also meets all three criteria, giving an age of 113,600±400 a. GALLUP et al. (2002) interpreted the beach-like nature of the upper OC deposit as indicating a fall to 19 m below present sea level from the maximum of the last interglacial sea level (+6m). However, sample OC-2 also has concordant ^{231}Pa and ^{230}Th ages, and although its δ^{234}U value is elevated, its ^{230}Th age of 105,300±600 a puts it in substage 5c. They argued that, if the dating is correct, the sample OC-2 gives an initial sea level of 15±3 m below present sea level, and that sample OC-1 may be reworked from material during the fall from peak last interglacial sea level (for futher details see GALLUP et al. 2002). GALLUP et al. compared the results with the SPECMAP record (IMBRIE et al. 1984) and the results from Papua New Guinea, which suggested a sea-level rise peaking around 135,000 a, followed by a sea-level drop around 129,000 a

Table 3.13: ^{231}Pa and ^{230}Th ages for Barbados coral samples collected at University Road, Clermont Nose traverse after GALLUP et al. (2002).

Sample	Elev.(m)	^{231}Pa age (a)	^{230}Th age (a)	Initial elevation (m)
Ventnor (Barbados II, Stage 5c)				
OC-1	31	109,800(+2,800/-2,600)	113,600±400	-19±3
OC-2	31	103,900(+2,600/-2,500)	105,300±400	-15±3
Rendezvous Hill (Barbados III, Stage 5e)				
UWI-101	32	126,900(+2,600/-2,400)	129,100±500	-25±3
NU-1471	42	136,200±4,300	135,800±800	-18±4
NU-1472	42	134,500±5,000	136,100±800	-18±4
NU-1473	43	133,300±4,400	134,200±800	-16±4
Stage 6e				
NU-1464	36	160,400±8,500	168,000±1,300	-38±5
UWI-103	34	161,000(+24,000/-16,000)	175,300±1,400	-43±5
UWI-107	32	151,300(+8,800/-7,400)	170,300±1,300	-43±5

4. Distribution and chronostratigraphy of fossil coral reef terraces on the south coast of Barbados

G. SCHELLMANN & U. RADTKE

The fossil coral reef terraces on Barbados are one of the few type localities worldwide that provide insight into interglacial sea-level change during the Young and Middle Pleistocene. Several sea-level estimates have been established since the late 1960´s and contributed to the Barbados Model. They were published within the context of global sea-level correlations and were summarized in Chapter 3. This chapter presents our new geomorphic and geochronologic investigations of coral reef terraces in southern Barbados. This research was conducted during a time period of more than ten years and was primarily initiated by advances in ESR dating of fossil coral, by advances in aerial photo interpretation (higher resolution), and by the great deficit in detailed geomorphic maps of preserved fossil beach formations and reef terraces above present sea level. The need for a revision of previously published morpho- and chronostratigraphies can be demonstrated best in southern Barbados. The morpho- and chronostratigraphic sequences in this region appear to be more complex and diverse than previously assumed.

MESOLELLA et al. (1968) and BROECKER et al. (1968) pioneered modern research on uplifted coral reefs on Barbados. Their work focused on stratigraphic differentiations and distributions of fossil coral reef tracts using topographic maps and aerial photographs, and on geochronologic studies, as well as on the reconstruction of Late and Middle Pleistocene sea levels. Numerous subsequent studies concentrated on geochronological investigations along five „standard traverses" which cross different fossil coral reef terraces (Figure 4.1). These traverses include the traverses Thorpe and Clermont Nose on the west coast of Barbados, two traverses in the area between Windsor and Drax Hall in St. George Valley, and the Christ Church Traverse on the south coast. Different dating methods including Uranium/Thorium (U/Th) dating (e.g. GALLUP et al. 2002, BLANCHON & EISENHAUER 2001), Helium/Uranium (He/U) dating (BENDER et al. 1979), and Electron Spin Resonance (ESR) dating (RADTKE 1989; RADTKE et al. 1988; RADTKE & GRÜN 1990) were used for these and subsequent geochronological investigations (see Chapter 3). If results locally conflicted with the stratigraphic differentiation of fossil coral reef tracts originally described by MESOLELLA (1968) and BENDER et al. (1979), studies were accommodated by minor morphostratigraphic revisions for relatively small areas, as for example those for southern Barbados presented by RADTKE (1989) and KU et al. (1990). Similarly, BLANCHON & EISENHAUER (2001) did not use a clear morphostratigraphic approach in their recently published article on last interglacial reef development on Barbados. Instead, sea-level reconstruction was mainly based on two U/Th dating results, which were assumed to be accurate, and on some local field observations, which were generously extrapolated to larger areas (see Chapter 3, and SCHELLMANN & RADTKE 2001b and 2003).

The Barbados Model, frequently used for the reconstruction of Middle and Late Pleistocene palaeo sea level and global climate change, was essentially derived from studies along the standard traverses described above. In this model, the stages Barbados I, II, and III corresponded to the marine oxygen isotope stages (MIS) 5a, 5c, and 5e from the last interglacial (Chapter 3).

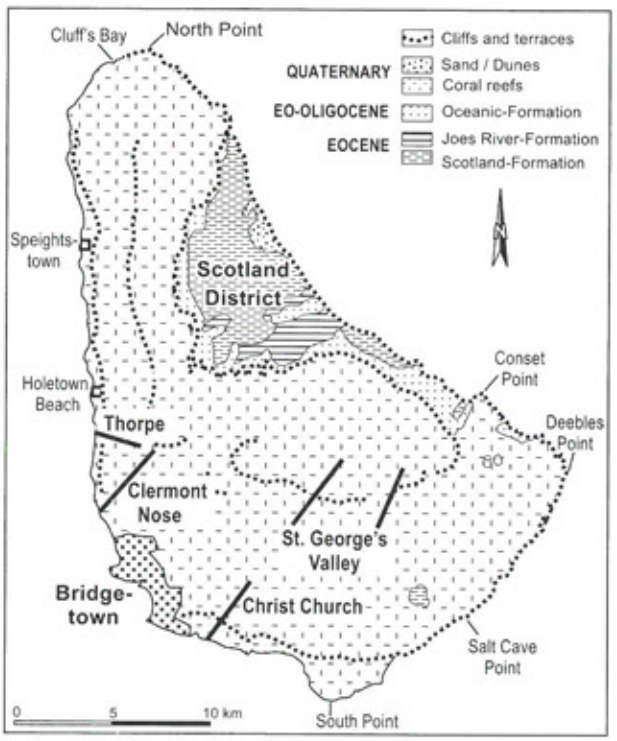

Figure 4.1:
Distribution of the standard traverses, which were traditionally used for chronostratigraphic investigations on coral reef terraces on Barbados.

Our investigations of coral reef terraces on Barbados began in 1990 and were stimulated by the impression that the existing morphological and stratigraphical model for the island did not reflect the complex evolutionary history of the Barbados coral reef terraces. In particular, no research had challenged the established morpho- and chronostratigraphic model first proposed by MESOLELLA (1968) and BENDER et al. (1979). There were no studies with detailed morphostratigraphic investigations that exceeded the generally preferred local descriptions, or which included the dating of reef terraces along traverses.

Therefore, it was necessary to conduct extensive field investigations focusing on the distribution and elevation of coral reef terraces, and to combine morphostratigraphical with geochronological research by dating a large number of sample sites.

The morphostratigraphy described below includes
1.) a differentiation of coral reef terraces, wave-cut platforms, and other erosive features, such as notches and cliffs; and
2.) an examination of various sedimentary features like coral reef facies types, discontinuities, and others.

The study of these morphostratigraphic features combined with absolute dating techniques (ESR, Th/U) allowed for estimates of tectonic uplift rates and for the identification of areas where tectonic movements vary over time. In general, these investiga-

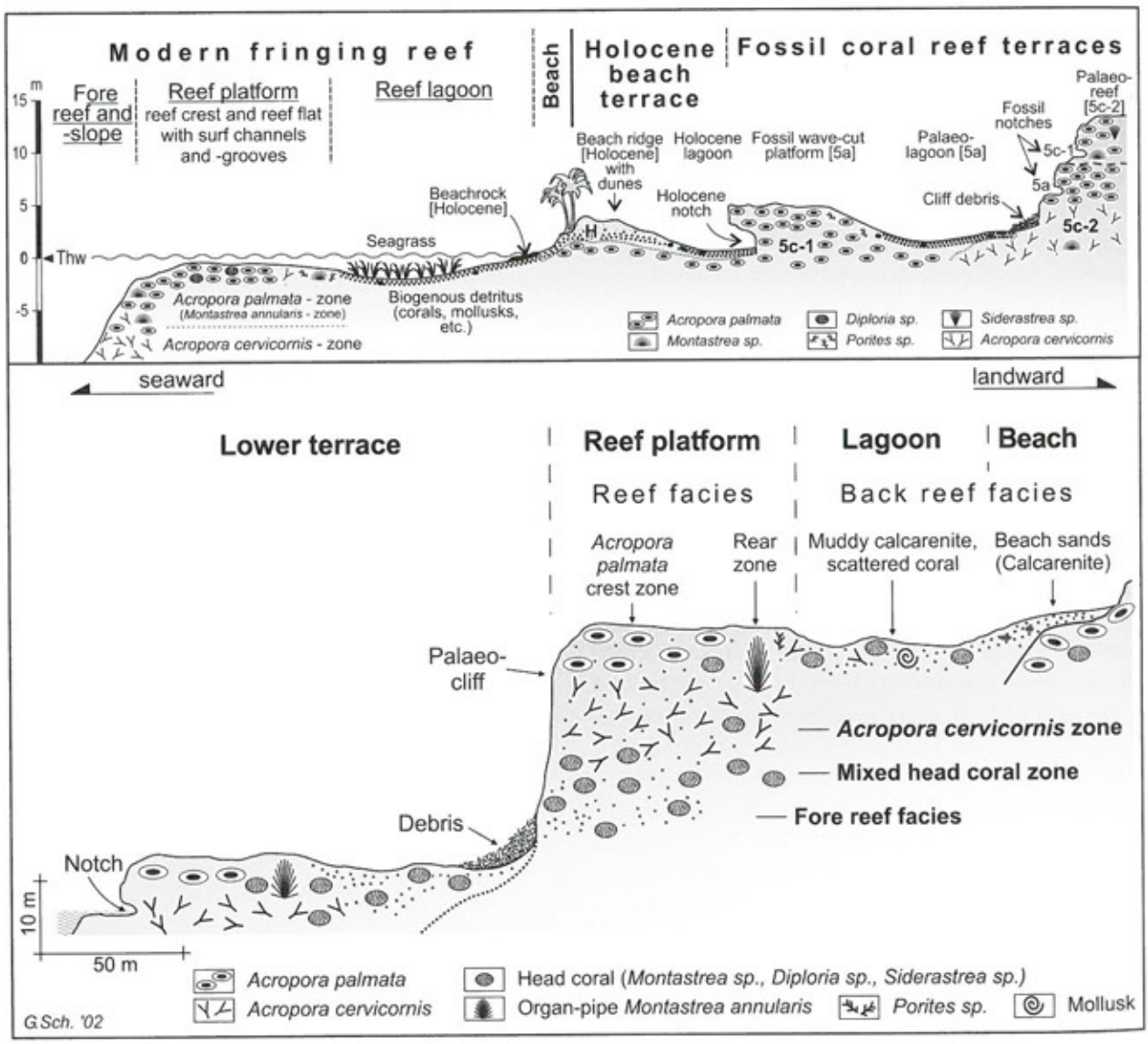

Figure 4.2:
Sketch of the morphology and coral reef zones of fossil coral reef terraces on southern Barbados (reef facies zones after MESOLLELA et al. 1970, and JAMES et al. 1977).

tions are required for precise sea-level reconstructions.

4.1. Methods

4.1.1. Morphostratigraphic methods

This research included the field mapping of former depositional coral reef terraces, former wave-cut platforms, and former cliff lines. Investigations were supported by topographic maps, aerial photographs, lithological surveys, and sampling along road cuttings, sea cliffs, and other localities.

The following important morphologic criteria determined the delineation and genetic classification of individual reef terraces (Figure 4.2):

(1) Former sea cliffs were identified based on clear morphological borders between reef terrace surfaces of different age. Younger cliffs often display deep notches at their bases.

(2) Individual reef crests and their landward reef platform areas were defined using morphological and sedimentary facies data. The specific morphological structure and coral/sediment facies distribution of depositional reef terraces with most elevated reef crests and with reef platform areas located seaward were mapped. Some reef platforms are crossed by reef channels or exhibit lower elevated reef lagoons and lagoonal channels, which extend inland.

(3) Wave-cut platforms were recognized due to their narrow width and their increasing elevation towards inland. Their surface morphology is unaffected by channels or lagoons (see below).

The elevation of coral reef terraces, including both depositional and wave-cut forms, was measured in the field using a Thommen altimeter with a vertical resolution of 1 m. In addition, morphologic and altimetric field records were checked through manual and digital aerial photo interpretation using true color aerial photographs with a scale of 1:10,000 and a Planicomp P33.

4.1.2. Electron Spin Resonance (ESR) dating method

The morphostratigraphic investigations on southern Barbados were supported by the Electron Spin Resonance (ESR) dating of over 260 coral samples from more than 80 localities (Figure 4.13). Due to methodological improvements, the quality of ESR dating results increased to such an extent that it was comparable to that of Radiocarbon (^{14}C) dating results of Holocene coral from Curaçao (Figure 4.3; RADTKE et al. 2003), and to that of mass spectrometric $^{230}Thorium/^{234}Uranium$ (TIMS Th/U) dating results for last interglacial samples (Figure 4.4, 4.4b; SCHELLMANN & RADTKE 2001a, SCHELLMANN et al. 2002; SCHELLMANN et al. 2004). Furthermore, they exceeded the accuracy of U-series dating of older coral samples. Radiocarbon dating was carried out by B. Kromer (University of Heidelberg, Germany), and TIMS U-series dating by E.-K. Potter, T. Esat, and M.T. McCulloch (Australian National University, Canberra, Australia).

ESR dating uncertainties were comparable with the variability of ^{14}C ages caused by the marine reservoir effect as illustrated by Figure 4.3. In general, the TIMS Th/U ages (Figure 4.4) also agreed well with the results of the ESR measurements for the last interglacial substages (Table 4.2: MIS 5e maxima: approx. 128 to 132 ka; MIS 5c: approx. 105 ka; MIS 5a-2: approx. 85 ka; MIS 5a-1: approx. 74 ka ago). However, a detailed comparison of dating results of MIS 5 coral reef growth calculated by both methods in Figure 4.4 showed that many ESR data are systematically 5% to 10% younger than the corresponding U-series ages (details in SCHELLMANN et al. 2004). The trend to an age under-estimation of ESR

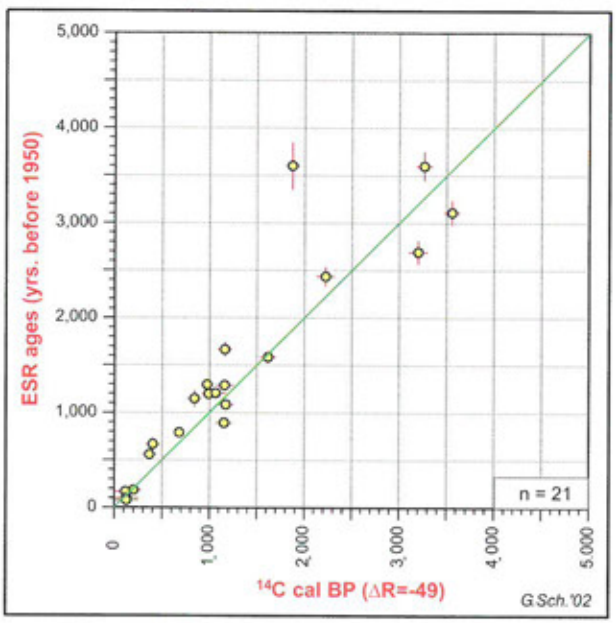

Figure 4.3:
Comparison of calibrated Radiocarbon (^{14}C) and ESR dating results for Holocene coral samples from Aruba, Bonaire, and Curaçao (Netherlands Antilles), modified after RADTKE et al. (2003).

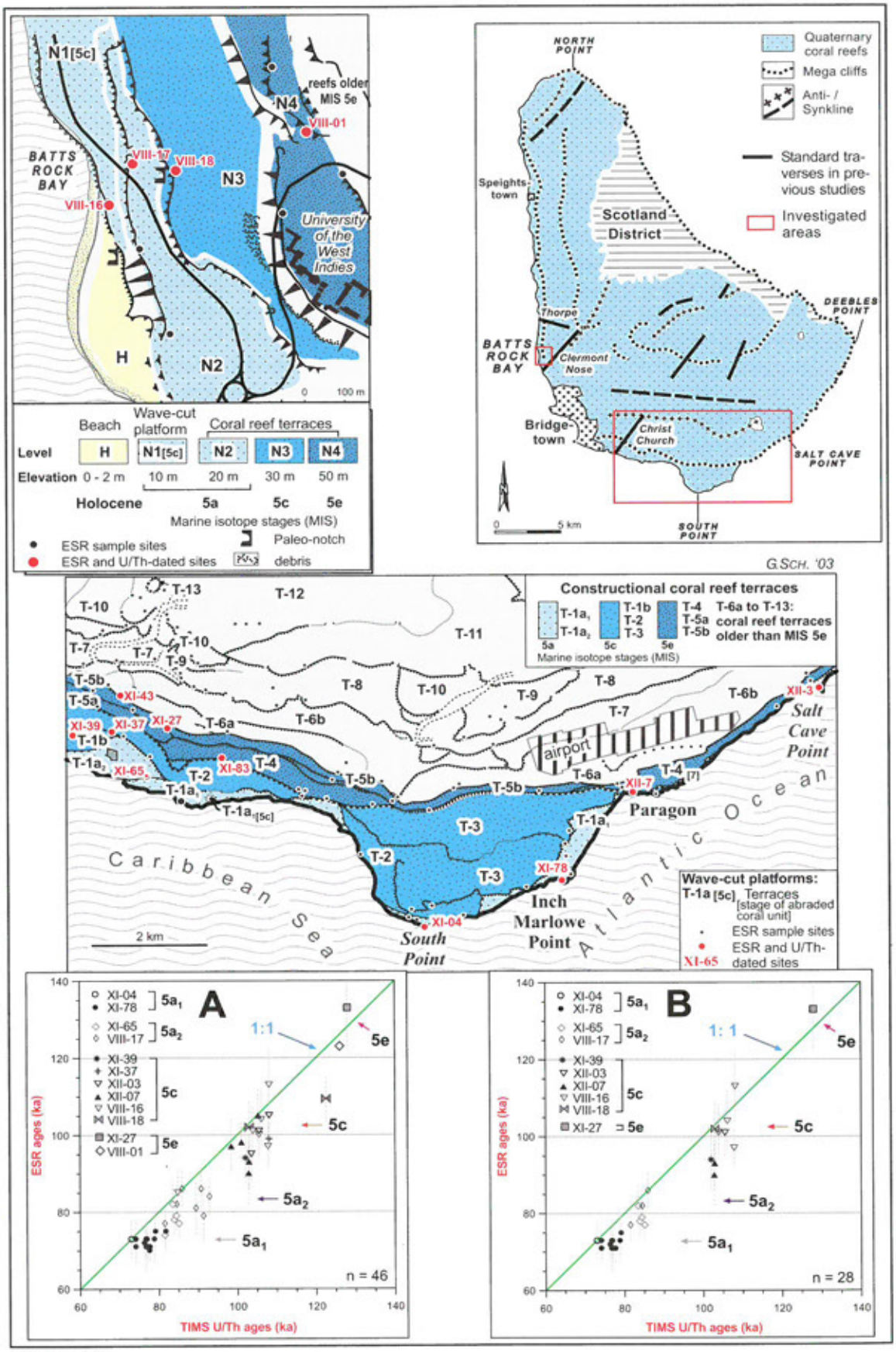

Figure 4.4:
ESR and TIMS U/Th ages of MIS 5 *in situ* coral from the west and south coast of Barbados. **A**: all U/Th data, **B**: only U/Th data with initial $^{234}U/^{238}U$ values between >141 and <157‰ (modified after SCHELLMANN et al. 2004).

in comparison with TIMS U-series data may be partially explained either by a slight overestimation of the alpha-efficiency (0.05) used for ESR age calculation, or by the slight post-depositional recrystallization of the aragonite coral structure (see below), which predominantly influences the ESR dating method. This strongly supports the view of SCHELLMANN & RADTKE (2001b, 2002, 2004), that, for an accurate ESR based chronostratigraphy, it is necessary (1) to date numerous samples from one locality, (2) to sample more than one locality in one coral reef terrace, and (3) to use only the oldest ESR dating results for chronostratigraphic interpretation (see below).

Figure 4.5 illustrates both ESR and TIMS Th/U dating results for MIS 5a-1 coral samples from Inch Marlowe Point at the south coast of Barbados (T-1a$_1$). Samples were taken from the uppermost meter of the *in situ* T-1a$_1$ *Acropora palmata* coral reef crest facies (Photo 4.2). They most likely grew within the relatively short time period of some hundred years. However, the dating results of both methods scattered from 71 to 75 ka (ESR) and from 74 to 79 ka (U/Th), respectively. Astonishingly, there was no evidence for a greater consistency in the more precise U/Th data in comparison to the ESR dating results. Although error ranges of the TIMS U-series data were much smaller (less than 1%) than the ESR ones (between 5 to 9%), the dating consistency seemed to be similar for both methods. This demonstrates that dating consistency, and therefore overall precision, is similar for both methods with the phenomenon that most ESR dating results are significantly younger than the U-series data at this locality (see SCHELLMANN et al. 2004 for more details).

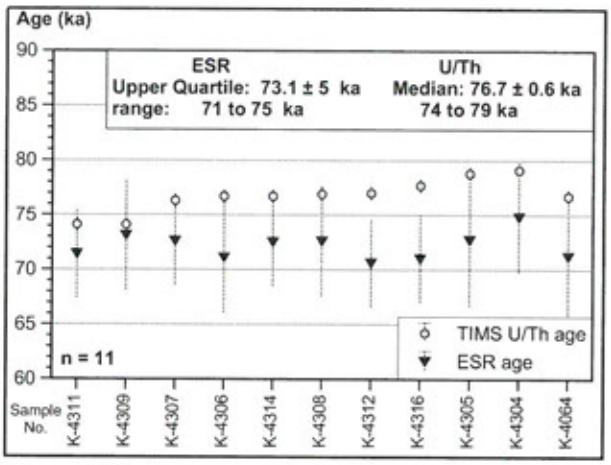

Figure 4.5:
Comparison of ESR and TIMS Th/U ages for last interglacial T-1a$_1$ (MIS 5a-1) coral samples collected at Inch Marlowe Point, south coast of Barbados (location IX-78 in Figures 4.12 and 4.17; details of ages in SCHELLMANN et al. 2004)

Therefore, it cannot be assumed that the apparently greater precision of U-series data indicates a greater accuracy of the method.

To put the results from Inch Marlowe Point into a greater context, several ESR and TIMS U/Th data sets from MIS 5a and MIS 5c sample sites from the west and south coast of Barbados were also compared (Table 4.1). ESR ages were calculated using the upper quartile values, because the number of ESR dated samples from the single localities were too small (less than 20) for a good estimate based on the 90th percentile (see below). As illustrated in Table 4.1, the ages obtained by both dating methods (ESR and its upper quartile values on the one side and the median values of the TIMS U/Th data on the other side) agree

Table 4.1:
Upper quartile values of ESR data and median values of TIMS U/Th data from MIS 5c and MIS 5a coral samples from the south (T-1a$_1$, T-1a$_2$, T-3) and west coasts (chapter 5: N1$_{[5c]}$, N2) of Barbados. Details of all data are listed in SCHELLMANN et al. (2004).

Strat.	Terrace	Sample site	ESR			U/Th			U/Th (all)		
			ka	±	n	ka	±	n	ka	±	n
MIS 5a-1	**T1a-1**	XI-04, XI-78	**73.4**	**5**	14	**76.7**	**0.6**	12	76.8	0.6	14
MIS 5a-2	**T1a-2**	XI-65	**80.9**	**5**	5	**84.2**	**0.7**	4	83.9	0.7	5
MIS 5a-2	**N2**	VIII-17	**85.5**	**6**	7	**84.5**	**0.8**	3	89.4	0.8	7
MIS 5c-3	**T3**	XII-03, XII-07	**102.6**	**6**	8	**102.9**	**1**	3	103.2	1	8
MIS 5c	**N1$_{[5c]}$**	VIII-16	**108.7**	**9**	5	**105**	**1**	7	105.4	1	8

ESR = Upper quartile value (25% of all ESR ages are ranked above this value)
U/Th = Median of U/Th data with initial delta ^{234}U values between 141 and 157 permil
U/Th (all) = Median of all U/Th data

rather well and age differences are generally smaller than 4%.

ESR dating was conducted as described by SCHELLMANN & RADTKE (2001a). All coral samples were ground manually. Twenty aliquots of 0.2 g each with particle diameters between 125 µm and 250 µm were gamma-irradiated with a ^{60}Co source at the university hospital in Duesseldorf, Germany. The irradiation dose rate ranged from 1 to 2.5 Gy/min. The aliquots of each sample were irradiated in different steps of 9 to 82 Gy up to maximum artificial radiation doses of 178 to 1780 Gy. The irradiation steps and maximum irradiations doses were adjusted depending on the ages of individual coral samples, as described in detail by SCHELLMANN & RADTKE (2001a). Typical measurement parameters were 25 mW microwave power, 0.5 G modulation amplitude, 22.972 s sweep time, 40 G scan width, 1024 points resolution, and the accumulation of 5 to 10 scans.

Figure 4.7 displays a typical ESR spectrum of a last interglacial coral sample from Barbados. Note the three dominant peaks (g-values: 2.0057, 2.0032, and 2.0006). The peak depicted at g = 2.0006 is the most suitable one for dating. It is gamma-sensitive, and it saturates much later than the rapidly dose-saturated signal at g = 2.0032, which additionally is less stable (GRÜN 1989, WALTHER et al. 1992). Figure 4.8 illustrates the ESR method for dating aragonitic coral. ESR as a dosimetric method depends on the measurement of radiation induced signals. The ESR signal at g = 2.0006 increased with irradiation by cosmic rays and other naturally occurring radiation sources, such as uranium. The response of the sample to radiation was calibrated by subjecting it to additional radiation in the laboratory. An ESR age was derived from the ratio of the past radiation dose D_E over the annual dose rate D'. Clearly, the correct determination of these two parameters is essential for any ESR age estimate.

The annual dose rate (D') of coral is dependent on uranium content and cosmic dose rate only. Due to the size of the coral from which the samples were taken, external influences by sedimentary radiation

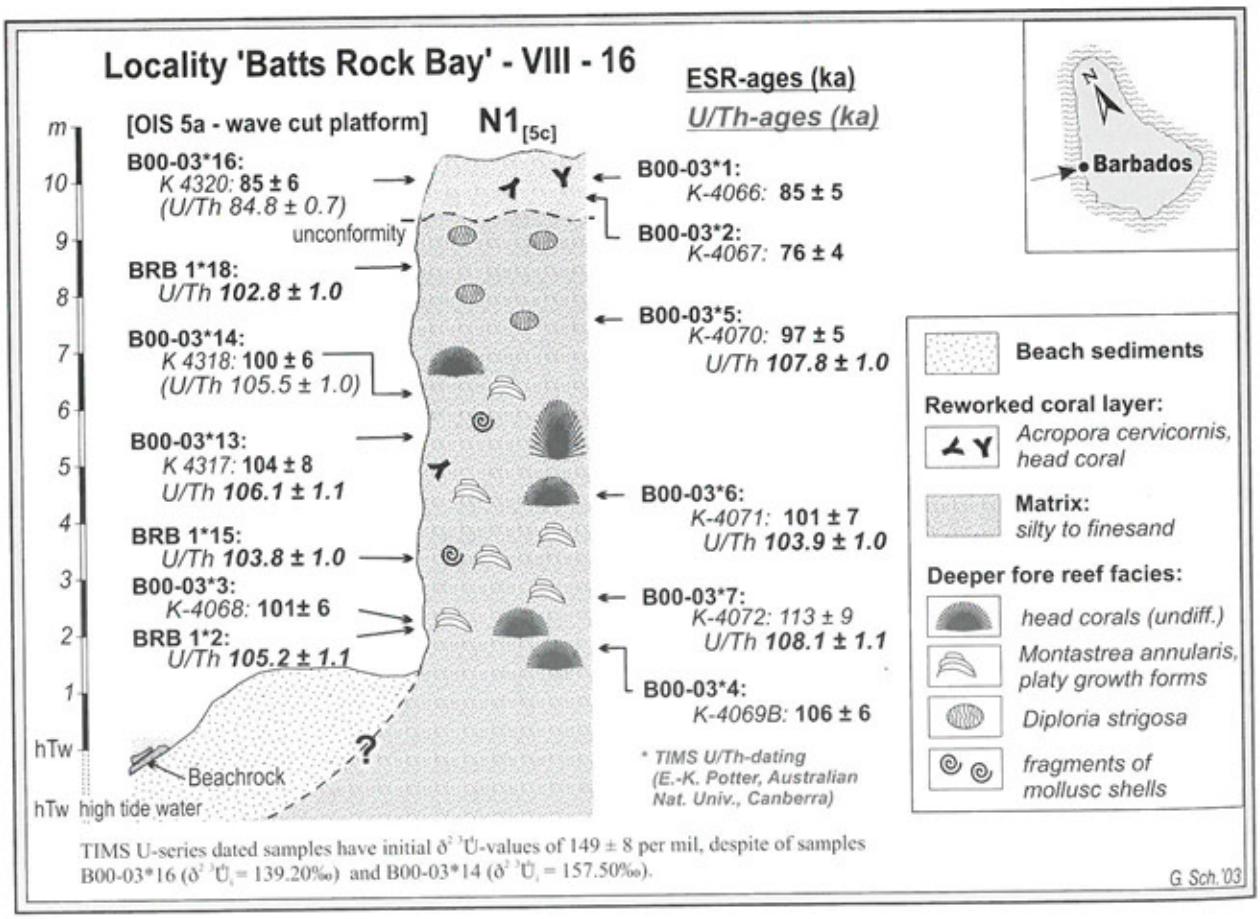

Figure 4.6:
ESR and U/Th ages of coral samples from the MIS 5a wave-cut platform (Figure 4:4: $N1_{[5c]}$) at Batts Rock Bay (location VIII-16 in Figure 4.4; details of ages in SCHELLMANN et al. 2004).

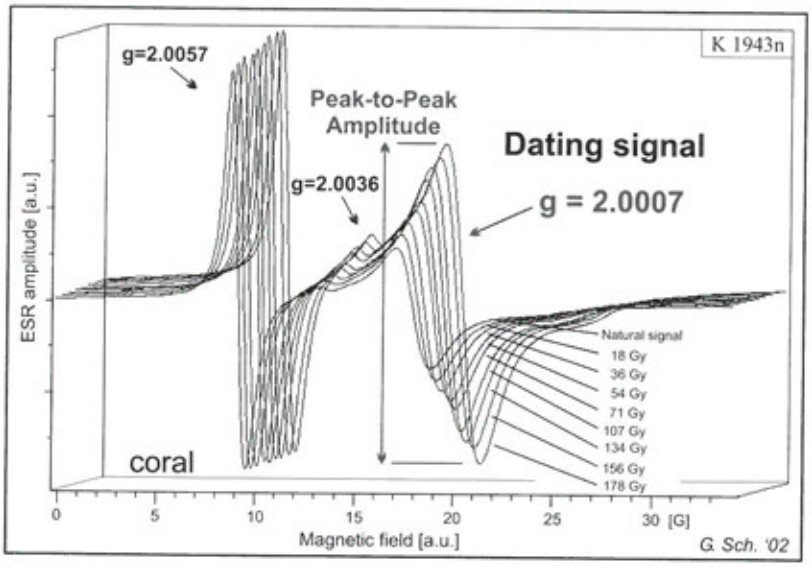

Figure 4.7:
ESR signals and signal growth of a gamma-irradiated (^{60}Co) last inter-glacial coral sample (*Acropora palmata*) collected on the south coast of Barbados (MIS 5c T-3 terrace), modified after SCHELLMANN & RADTKE (2001).

sources could be neglected. In order to establish the D' value as accurately as possible, the U content was determined for two to three aliquots of each sample using Neutron Activation Analysis (INAA: Bequerel, Australia and XRAL, Canada) and Inductive Coupled Plasma Mass Spectrometry (ICP-MS, Dept. of Geography/Dept. of Geology, University of Cologne, Germany). The resulting mean values and standard deviations were used for the ESR age calculations (Table 4.2). Although the uranium content was consistent for different measurements for many samples, the standard deviations of the mean U content ranged from 10% to 20% for a significant number of samples. This phenomenon highlights that even relatively homogenous coral sample material may display a complex uranium distribution. Therefore, it is strongly recommended to conduct at least a double, preferably a triple determination of the U content.

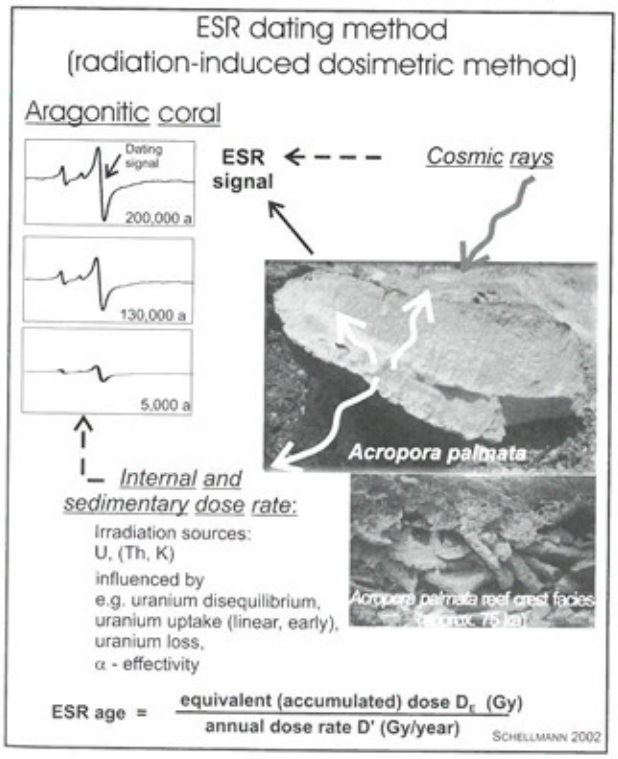

Figure 4.8:
Illustration of the ESR dating method used for dating aragonitic coral samples.

The equivalent dose (D_E) was calculated using the new D_E-D_{max} plot procedure described in detail by SCHELLMANN & RADTKE (2001a). This procedure seems to be well suited for the achievement of a more objective or transparent D_E evaluation. The D_E value is usually determined by the additive dose method. Aliquots of the sample are irradiated with a gamma source, leading to an increase in trapped electrons, which in turn leads to an enhancement of the ESR signal. The plot of the ESR intensity versus the laboratory dose is called dose response curve (Figure 4.9). The extrapolation to zero intensity yields the D_E value on the intersection with the X-axis.

However, as already reported by WALTHER et al. (1992), only the lower part of the growth curve can be described sufficiently by a single exponential saturation function. As with other carbonates, the growth curve of the dating signal g = 2.0006 of coral depicts clear inflexion points and some minor oscillations (Figure 4.10). This complicates the D_E determination. The inflexion points are characterized by a sudden increase in radiation sensitivity. They can be explained either with competition processes or with different filling mechanisms for multiple traps with similar ESR characteristics. Finally, it cannot

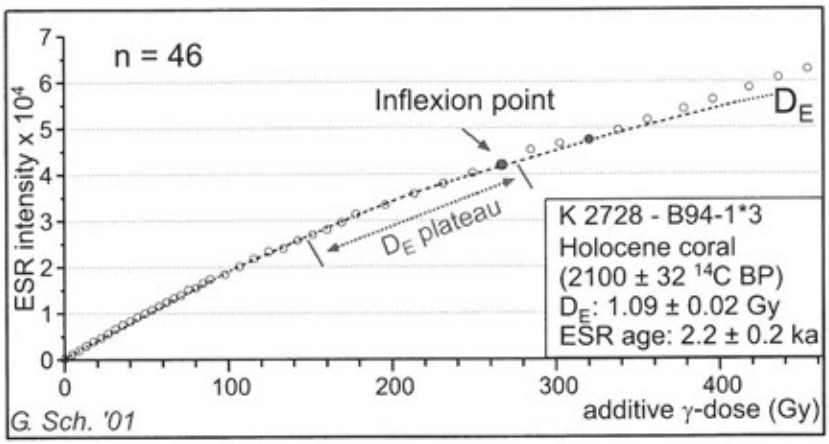

Figure 4.9:
Dose response curve for a Holocene coral sample (*Acropora palmata*) from Barbados. The coral sample was irradiated with 46 irradiation steps ranging from 4.4 to 20 Gy up to a maximum irradiation of 454 Gy (modified after SCHELLMANN & RADTKE 2001a).

be ruled out that the inflexion points are mainly a result of the strong artificial gamma-irradiation. They cannot be reduced by preheating procedures nor by changing ESR measurement parameters (e.g. JONAS 1997, SCHELLMANN & RADTKE 1999). It is necessary to use as many aliquots as possible and to narrow the distances between the data points in order to detect inflexion points or weaker oscillations in the signal growth curve.

The calculated D_E values are significantly overestimated if D_E calculation is based on the fitting of all data points onto a "disturbed" growth curve with a single exponential function (Figure 4.10). A single exponential saturation function can only describe the lower part of the additive growth curve up to the first inflexion point. There, the irradiation sensitivity of the dating signal increases monotonically, although it may have some non-linear portions or "wiggles". Therefore, the calculation of the D_E value should be solely based on the data points from the lower part of the additive dose response curve, including the natural non-irradiated first aliquot and all following aliquots up to the first inflexion point (Figure 4.10). One should use as many aliquots as possible to narrow the distances between data points in order to visualize inflexion points on the signal growth curve (for details see SCHELLMANN & RADTKE 2001a). The accuracy of ESR dating significantly improved due to using the new D_E-D_{max} plot procedure for D_E determination. Figure 4.11 illustrates the creation of D_E-D_{max} plots. The first D_E value was calculated by using all data points. Subsequently, the data set was reduced by successively eliminating the highest dose point. The resulting D_E values were plotted versus the maximum artificial gamma dose D_{max} that was used for D_E calculation (Figure 4.11: D_E-D_{max} plot). A D_E plateau, defined by the local minimum value D_{min}, occurred when the dose response curve was based on adequately small dose steps. The D_E plateau includes all values that lie within the range of uncertainty of D_{min}, and is the mean of all D_E values within the plateau range. The D_E error was derived from the mean of all individual D_E errors. The described D_E plateau should be used for all ESR age calculations (SCHELLMANN & RADTKE 2001b). D_E calculations (Table 4.3) were carried out using the software program „Fit-sim" (version 1993). ESR age

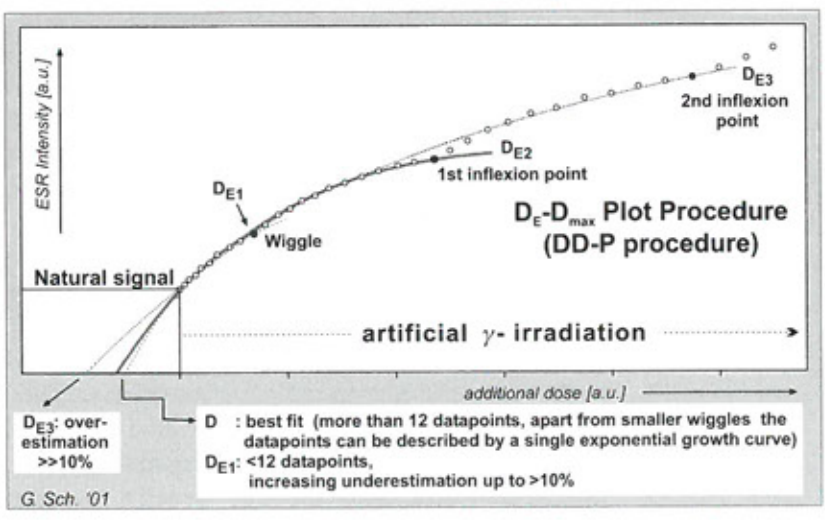

Figure 4.10:
Typical ESR signal growth curve (g=2.0006) for Pleistocene coral. Arbitrary data points were used for this illustration. Note the effects of inflexion points on D_E values, if the calculation is based on a single saturating exponential curve (modified after SCHELLMANN & RADTKE 2001a).

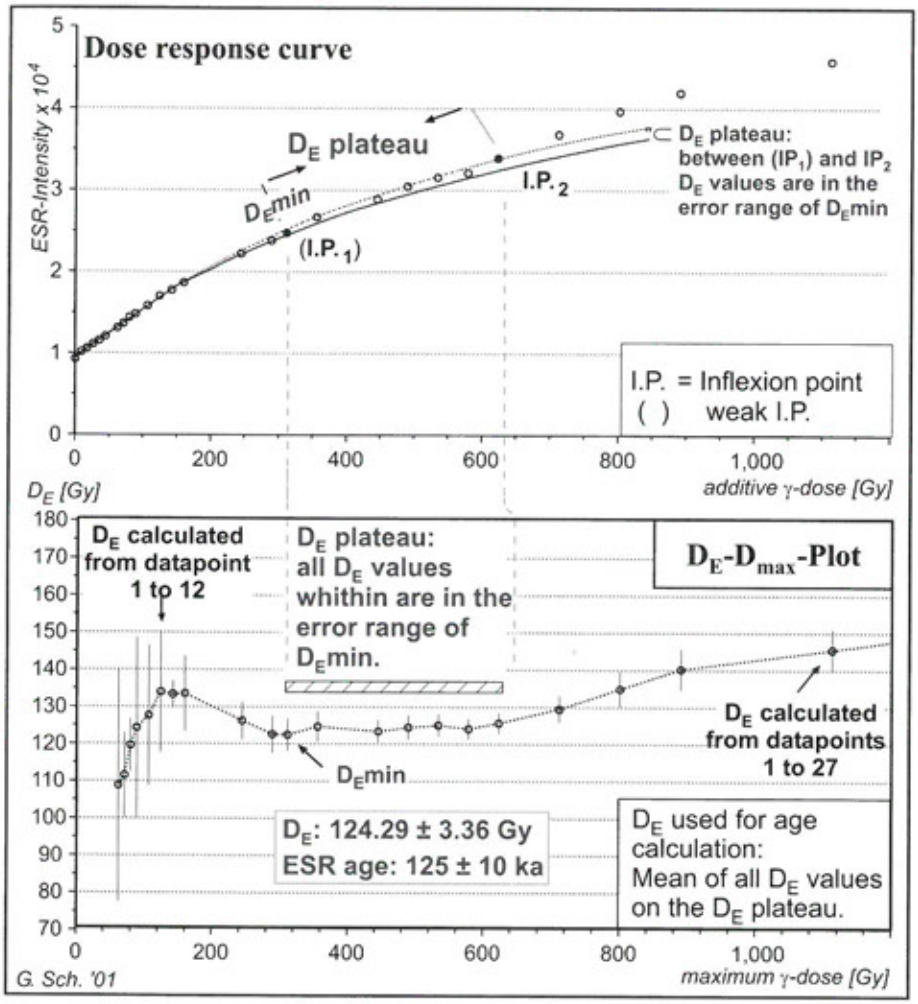

Figure 4.11:
Dose response curve and D_E-D_{max} plot of a last interglacial (MIS 5e) coral sample (*Acropora palmata*, B91-13*2) from Rendezvous Hill Terrace on Barbados (modified after SCHELLMANN & RADTKE 2001a).

calculations were conducted using the software program „Data VI" (version 1999) by Rainer Grün.

This new ESR dating methodology is sufficiently precise to allow for a differentiation between oxygen isotope stages 5a, 5c, and 5e, as well as 7, and 9 or 11. Now, last interglacial samples cannot only be classified into the main isotope stages but also into their sub-stages $5a_1$ and $5a_2$, 5c and 5e. The accurate differentiation between stages 9, 11, and older stages remains a challenge due to considerable alterations and recrystallization processes that may occur within coral samples (Figure 4.22). The problem of natural „ESR-rejuvenation", which is characterized by the recombination of electrons that increases until a natural equilibrium is reached, also needs to be considered. Physically, the upper dating limit of the ESR method is defined by this natural equilibrium limit. However, the underestimation of age progressively occurs before reaching this limit. All ESR samples were measured by X-ray diffraction (Siemens D 5000) and by an ESR screen of more than 300 Gauss in order to detect primary or secondary calcite (SCHELLMANN & KELLETAT 2001, LOW & ZEIRA 1972) and only samples with more than 95% aragonitic crystal structure were ESR dated. Nevertheless, a progressive underestimation of ESR ages, which occurred especially with the dating of coral samples from Middle Pleistocene terraces, could not be avoided. Further research is needed to develop a method that recognizes such diagenetic recrystallization and age rejuvenation effects.

The tendency to underestimate the ESR age of Middle Pleistocene coral samples was reduced by
(1) dating numerous samples from one locality,
(2) sampling more than one locality in one coral reef terrace, and
(3) using only the oldest ESR dating results for chronostratigraphic interpretations.

In the past, the extent of the age rejuvenation effects was underestimated. It was assumed that these effects did not exceed more than some thousand years. However, the age underestimation can be much larger, as illustrated most impressively by the significant change in the range of dating results for the T-8 coral reef terrace in southern Barbados. For

this terrace, preliminary ESR dating results suggested that the terrace was formed during the penultimate interglacial (SCHELLMANN & RADTKE 2001b); however, subsequent ESR dating yielded an age of approx. 300 ka BP correlating with the third past interglacial (MIS 9).

This study used the 90th percentile (if the number of ESR dated samples was greater than 20) or the upper quartile (if the number of ESR data was equal or smaller than 20) of all ESR ages from one coral reef terrace for its chronostratigraphic classification (Table 4.1 and 4.2, Figure 4.22). 90th percentile and upper quartile values are ranked values comparable to the median (50th percentile value). A 90th percentile value means that 10% of a data set is ranked above this value, whereas 25% of a data set is ranked above the upper quartile value. The error ranges of the individual ESR dating results were used for the calculation of the 90th percentile and the upper quartile value. The 90th percentile value is the mean of the 90th percentile value of the maximum ESR data set (ESR age plus error) and the 90th percentile value of the minimum ESR data set (ESR age minus error). The upper quartile value is the mean of the upper quartile value of the maximum ESR data set (ESR age plus error) and the upper quartile value of the minimum ESR data set (ESR age minus error). The error range of the resulting mean 90th percentile (upper quartile) value is the deviation from the maximum and minimum 90th percentile (upper quartile) value of an ESR data set. The oldest ESR age was used in cases, where the number of ESR dated samples was too small (less than 4 data) for a calculation of the upper quartile value (Table 4.2, Figures 4.14, 4.22, and 4.24). Nevertheless, the timing of coral reef formation calculated from the 90th percentile versus the upper quartile values differed only slightly, as illustrated by Figure 4.22. These differences lie within the ESR error ranges. All ESR dating results presented in this paper are listed in Table 4.3.

Despite the problem of Middle Pleistocene ESR age rejuvenations, these new ESR dating results provide a detailed picture of Late and Middle Pleistocene reef formation for Barbados (see below), which challenges existing chronostratigraphies based on the U/Th dating method alone. Nevertheless, important and still unsolved problems of mass spectrometric U/Th dating of Pleistocene coral include isotope movement and varying $^{234}U/^{238}U$ conditions in the ocean water (BARD et al. 1992).

4.2. Fossil coral facies patterns, coral reef terraces, wave-cut platforms, and notches as sea-level indicators

In general, the fossil coral reef terraces on Barbados consist of the morphostratigraphic units and sediment facies illustrated in Figure 4.2. The morphological characteristics are similar to those of present fringing reefs in the Caribbean. Notches, beach sand deposits, reef crests, and reef platforms, which extend up to low tide water level provide the most important indicators for the reconstruction of Pleistocene sea- level changes.

4.2.1. Coral facies patterns

The internal coral facies and zonation of raised Pleistocene reef tracts on Barbados were described by MESOLELLA et al. (1970), JAMES et al. (1977), HUMPHREY (1997), BLANCHON & EISENHAUER (2001), and others. The facies relationships in the raised reef tracts represent a generalized model, which may vary both vertically and laterally (HUMPHREY 1997).

Adjacent to the former fore reef calcarenite zone, which is dominated by coral rubble, the reef facies *sensu strictu* can be subdivided in four major units (Figure 4.2), which include

(1) the mixed head coral zone containing massive colonies of *Montastrea annularis*, brain coral of different *Diploria* species and, subordinately, species of *Siderastrea sp.* and *Montastrea cavernosa*;
(2) the *Acropora cervicornis* zone, located upwards and landwards of the former fore reef slope, most commonly containing broken branches of the staghorn coral *A. cervicornis* (Photo 4.1 and Photo 2.13);
(3) the *Acropora palmata* zone occupying the former reef crest position (Photos 4.2, 4.3, and Photo 2.14); and
(4) the near back reef rear zone, where the *A. palmata* crest facies gradually transforms into a mixed assemblage of head coral, organ-pipe growth forms of *Montastrea annularis* (Photo 2.15), and wave deposited sediments (sands, coral boulders, and rubble).

A shallow lagoon is located landwards of the rear zone, behind the reef platform, and in the back reef. The lagoon is filled with sandy sediment, some mollusk, sporadic coral boulders, and, occasionally, isolated coral in living position (Photo 2.16). Along

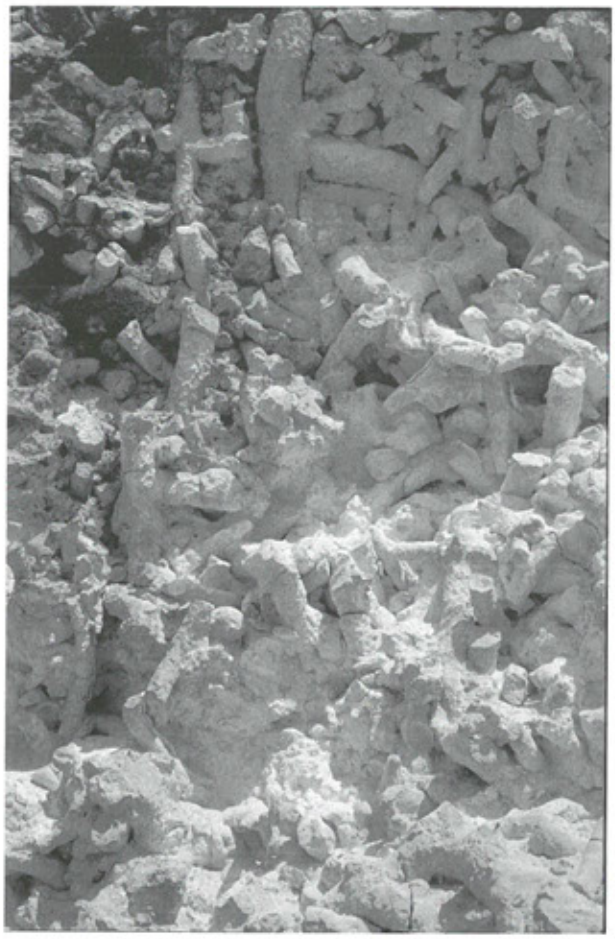

Photo 4.1:
Last interglacial (MIS 5e) *Acropora cervicornis* reef facies located at the University of the West Indies, west coast of Barbados.
(Photo: SCHELLMANN 2000)

Photo 4.3:
Last interglacial (MIS 5c) *Acropora palmata* reef crest facies with a framework predominately supported by *in situ* coral located at Round Rock, south coast of Barbados.
(Photo: SCHELLMANN 1999)

Photo 4.2:
Last interglacial (MIS $5a_1$) *Acropora palmata* reef crest facies at Inch Marlowe Point, located northeast of South Point. *(Photo: SCHELLMANN 2000)*

the former shoreline, commonly the palaeo-lagoon, is separated from an older and higher elevated reef terrace by a sea cliff, where a beach and/or a cliff-derived debris zone is sometimes preserved in front of the cliff. Beach deposits commonly lack *in situ* coral and often also larger coral rubble and boulders. Sometimes, calcarenites of beach sands are preserved on top of a coral reef body, as exemplified on top of the last interglacial *Acropora palmata* reef crest facies in Bottom Bay (Chapter 5). In this case, the beach sands mark the beginning of the regression of a sea-level highstand. Complete fore reefs, reef slopes, and reef crest facies are exposed at numerous locations in road cuttings, former cliff lines, and along steep and active cliffs at the coast.

The massive elkhorn coral, *Acropora palmata*, is the dominant reef builder of former reef crests on Barbados. It is the most common shallow water coral species in the Caribbean and the only coral species, which is an appropriate marker for palaeo sea-level reconstruction (Chapter 1.3.1). At present, this species requires strong wave movement and lives in dense colonies in shallow water ranging in depth from a maximum of -5 m to low tide water level. Fossil and compact *A. palmata* dominated reef crests (Photo 4.3) reaching vertical extensions of 4 to 5 meters are present at many localities on southern Barbados. Sometimes, the *A. palmata* crest zone reaches vertical extensions of more than 10 or 20 m as a result of a slow sea-level rise during growth. An *A. palmata* reef that is more than 20 m high and that was formed during the penultimate interglacial (MIS 7), is exposed in Foul Bay on the southeastern coast of Barbados (Chapter 5). As already stated, these extreme vertical heights of the shallow water coral zone indicate reef formation against a slow sea-level rise.

A. palmata coral facies commonly supports itself. Their framework represents a mixture of clasts and *in situ* colonies (Photo 4.2, 4.3), and the matrix is strongly reduced. Calcareous algae crusts occur within the upper areas of former reef crests, if they have been subject to strong wave action (Chapter 1.3.2). GEISTER (1983) described numerous examples for the distribution of calcareous algae on reef crest in the Caribbean.

BLANCHON & EISENHAUER (2001) used the distinctive asymmetrical thickness of calcareous algae crusts on branches as one important criterion for identifying *in situ A. palmata* dominated reef crest zones on Barbados. However, compact calcareous algae crusts are rare on both live and fossil coral on the south coast of Barbados (Photo 1.12), which is Barbados' leeward side and experiences little wave action. Nevertheless, compact *A. palmata* reef facies are clear indicators for wave-exposed shallow water conditions up to low tide water level, as mentioned by MESOLELLA (1968).

If collecting coral samples for the purpose of dating, it is important to verify that the sample was taken from an *in situ* coral formation. Hurricane and tsunami waves can deposit coral rubble and large coral boulders in the back reef area and up to several meters above sea level on top of elevated older coral reef terraces. The latter may be the reason for the anomalously young ESR dating results of coral samples collected in the area to the east of South Point (Figure 4.16: sample site XI-75). Here, samples were taken from the surface of the approx. 105 ka old T-2 terrace. The sample site is located immediately behind the sub-stage 5a cliff line of the T-1a$_1$ coral reef terrace. At that location, it was impossible to check the *in situ* nature of the samples. The two ESR dating results of 69 ± 5 and 73 ± 5 ka agree well with the age of the 4 m lower elevated T-1a$_1$ coral reef terrace immediately seaward of the sampling site. However, they are much younger than the approx. 105 ka old T-2 coral reef formation recorded elsewhere in southern Barbados.

Another example where a reworked assemblage of coral fragments (e.g. head corals lying on their surfaces) were dated, is sample site Kendal Fort located on the south coast of Barbados (location XI-80 in Figure 4.13). There, coral samples originated from 1 to 3.5 m asl, where the cliff of the T-2 terrace was undercut by waves. The extremely young ESR dating results with ages between 84 to 96 ka (Table 4.3) imply that coral samples had been relocated by former storm waves. The ages are too young when compared to dating results from the well exposed other sample sites (Figure 4.13: locations XI-36 to XI-38) on the 104 ka old T-2 coral reef terrace.

4.2.2. Coral reef terraces and wave-cut platforms

Well-preserved uplifted coral reef terraces on southern Barbados commonly have a steep slope at their seaward part, which is a cliff or former reef slope (Figure 4.2). The former reef platform, located immediately landward to this slope, typically has little relief and includes a reef crest and back reef plate,

Photo 4.4:
View of the last interglacial (MIS 5c) T-3 coral reef terrace located on the south shore of Barbados. Note the internal T-3 reef channel in the front and the built-up T-3 reef crest area in the back . *(Photo: SCHELLMANN 1994)*

Photo 4.5:
Small Middle Holocene abrasion rim in last interglacial (MIS 5c) coral limestone at Round Rock, west of South Point.
(Photo: SCHELLMANN 1997)

which may be crossed by reef channels (Photo 4.4) that end in a lagoon. The lagoon is often adjacent to a sandy beach, a rocky wave-cut platform, or a steep cliff. This morphological setting provides evidence for a constructional/depositional coral reef terrace, which has grown both seawards and upwards to the former low tide water level.

In contrast to the constructional/depositional coral reef terraces described above, some coastal terraces on Barbados were formed by cliff retreat associated with the erosion of a wave-cut platform into an older coral reef formation. These abrasional forms are younger than the eroded cliff. Commonly, these abrasion processes formed only small rims as illustrated in Photo 4.5. Generally, wave-cut terraces are typically narrower than the well-developed depositional coral reef terraces and range from 10 to 100 m in width. However, extremely wide wave-cut platforms with widths of 100 to 400 m rarely formed during Pleistocene sea-level highstands, as for example the $T\text{-}4_{[7]}$ terrace located on the south shore between Paragon and Salt Cave Point (Photo 4.6, Figures 4.13, 4.20 and 4.21). The surfaces of these platforms dip seawards by several meters from their former cliff lines and were clearly formed during slow sea-level regression.

The identification and geochronological classification of wave-cut platforms are difficult. In addition to their commonly narrow width, indicators for the identification of these terraces include
(1) the seaward dip of the terrace surface;
(2) the absence of surface channels or lagoons (Pho-

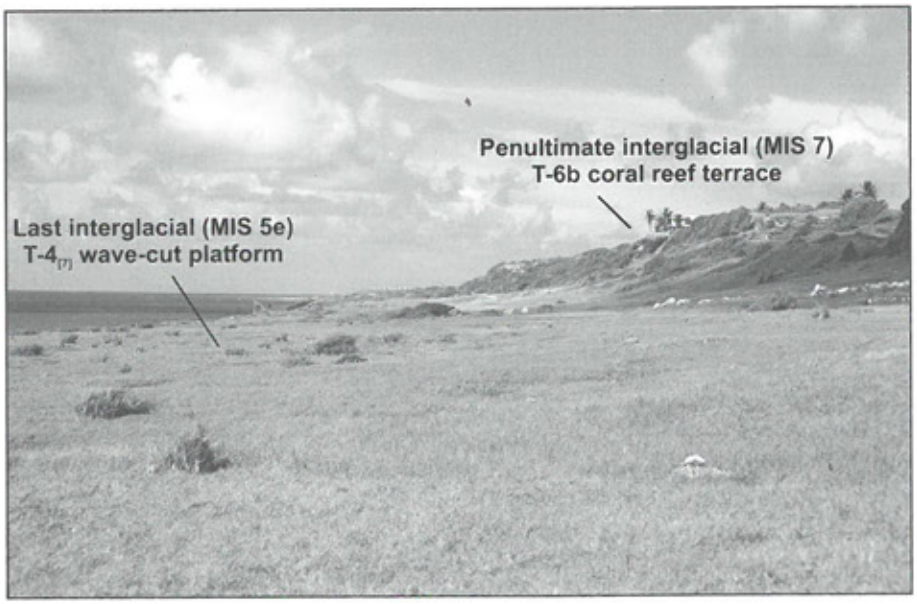

Photo 4.6:
T-4[7] wave-cut platform located on the level of the T-4 coral reef terrace to the west of Salt Cave Point. Both, the platform and the palaeo-cliff in the background were formed towards the end of the last interglacial transgression maximum (approx. 117 ka). The platform was cut into a penultimate interglacial coral reef (approx. 200 ka), which is still preserved and depicted in the background of the photograph.
(Photo: SCHELLMANN 2000)

to 4.6), and
(3) numeric dating results that are too old in comparison with the ages of depositional terraces in the surrounding morphostratigraphic context.

The third indicator is especially important at localities where small remnants of reef terraces are preserved without any additional morphological features. In these settings, it is impossible to differentiate depositional coral reef terraces from wave-cut platforms without any absolute dating results from surrounding morphological features.

An example for the use of ESR dating to distinguish between a wave-cut platform and a depositional terrace is provided by the T-1a[5c] terrace, located near Oistins at the south coast of Barbados (Figure 4.15: locality XI-34). There, ESR dates indicated that the wave-cut platform was abraded into reef crest colonies of MIS 5c-old *Acropora palmata* during the last interglacial sub-stage 5a. The platform terrace has the same elevation as the reef crest areas of the T-1a terrace dated at MIS 5a and also located along the south coast of Barbados. Both terraces occupy a similar morphological context, yet are composed of coral rocks of different ages.

Coral samples, which are supposed to be dated, should not be collected in front of former cliffs. There, a small wave-cut rim is usually developed and typically yields an age determination, which exceeds the age of corals exposed at the former cliff. Also, storm layers and cliff debris may be deposited at the foot of these cliffs and result in a mixture of ages. For example, cliff debris of *Acropora cervicornis* was sampled at the foot of the T-4 cliff near Oistins (Figure 4.15: sample site XI-21). As expected, the ESR dating results split into two groups of ages, comprising (1) ages of approx. 105 to 108 ka, which were concordant with the age of the small MIS 5c old T-2 terrace in front of the cliff, and (2) ages between 113 to 134 ka, which were similar to the age of the late MIS 5e old T-4 coral formation, which is exposed at the cliff. These dating results disagree with BLANCHON & EISENHAUER's (2001) geochronological classification of similar deposits of well-sorted stick gravel of *A. cervicornis* some hundred meters west of sample site XI-21 at the base of the First High Cliff. These authors mistakenly assumed that these gravels were intertidal deposits formed during a brief stage of reef development with a rapid sea-level fall at the end of the last interglacial maximum (MIS 5e).

Another example of sample sites to be avoided when dating coral is provided by age determinations from a small wave-cut rim in front of the T-3 sea cliff located landward of Inch Marlowe Swamp (Figure 4.18: sample site XI-59). The swamp is the former lagoon of the T-1a$_1$ coral reef terrace that was flooded during the Middle or Early Late Holocene sea-level highstand. The T-1a$_1$ coral reef is exposed at the coastline. The sample site is at the same elevation as the T-1a$_1$ reef platform located at the southern coast of Barbados. Two reworked coral boulders embedded in a sandy matrix were dated. As predicted, the two dating results of 82 ± 6 ka and 96 ± 8 ka were considerably older than the accurately dated age of the preserved T-1a$_1$ coral reef terrace located to the seaward of the sample sites. The ESR dating results for this terrace scattered between 66 ka and 75 ka

(Figure 4.18: sample sites XI-1 and XI-78).

4.2.3. Notches

Similarly to depositional terraces and wave-cut platforms, intertidal notches are also important sea-level indicators. Modern and some Late Pleistocene cliffs on Barbados have more or less well developed notches that were generated predominately by bio-erosive processes.

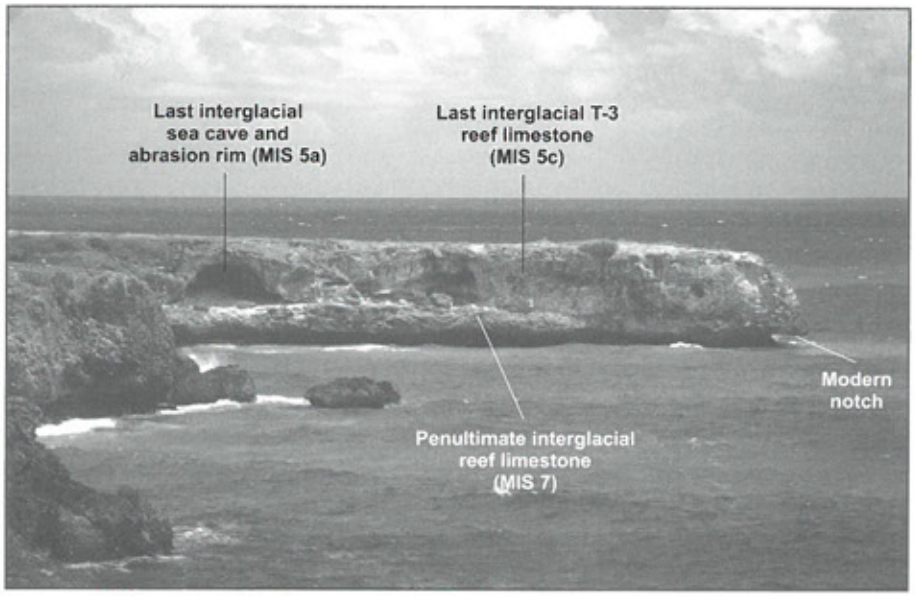

Photo 4.7:
Last interglacial T-3 coral reef terrace (MIS 5c) exposed at the recent cliff coast at 'Salt Cave Point', south coast of Barbados (Figure 4.20). The exposed former sea cave and abrasion rim at 3.5 m to 5 m asl. was formed during MIS 5a. The correlation to MIS 5a derived from the elevation of cave and rim, which is similar to that of palaeo notches at the MIS 5a cliff line at Inch Marlowe Point (Figure 4.18).
(Photo: SCHELLMANN 1999)

Holocene notches located in modern cliffs are incised up to 2 m deep into the coral limestone at the elevation of present sea level (Chapter 2.3, Photos 2.22 to 2.25). Also, Pleistocene notches and sea caves have been preserved along the modern cliff coast (Photo 4.7), and in higher elevated Late Pleistocene cliffs, mainly at locations that are protected from strong cliff retreat or cliff erosion (Photo 4.8 to 4.11; Figures 4.15 to 4.20).

It is possible to determine the age of a palaeo notch if a fossil coral reef terrace, which formed at the same time as the notch, is present in the foreland. However, the dating of palaeo notches is very problematic if the notches are located considerably higher than the coral reef terraces preserved in the foreland or if a wave-cut platform is located in front of these notches. Under these circumstances, rough age estimates may be derived from comparing the elevation of the notches to preserved coral reef crests in the greater surrounding area. When interpreting sea-level change from the ages and heights of palaeo notches, it is important to consider that tidal ranges are small

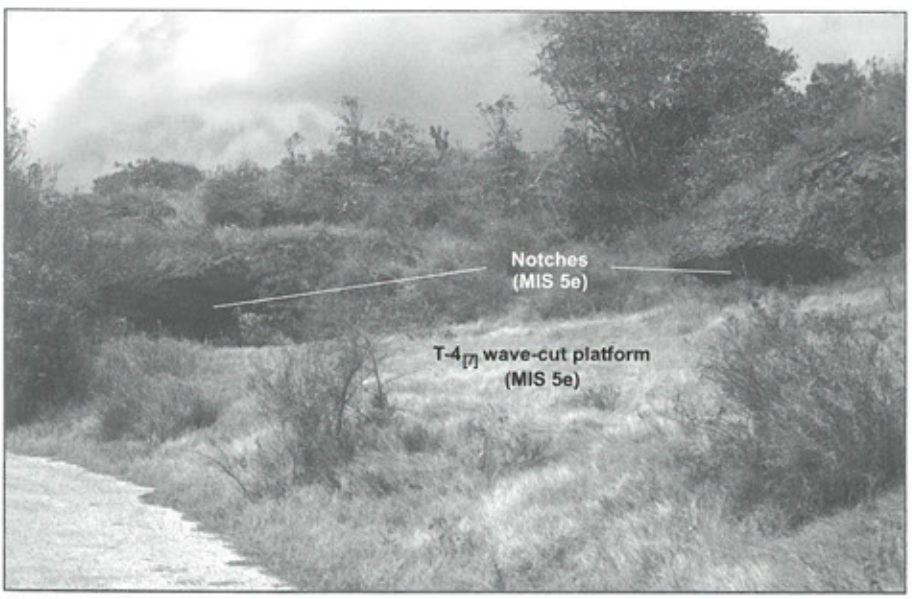

Photo 4.8:
Last interglacial notch (late MIS 5e, approx. 120 ka) in penultimate interglacial T-6a reef limestone near Paragon, south coast of Barbados (sample site XII-9 in Figure 4.19).
(Photo: SCHELLMANN 1999)

Photo 4.9:
Last interglacial notch (MIS 5a) in T-3 *Acropora palmata* reef crest facies at Chancery Lane, south coast of Barbados (samples site XI-2 in Figure 4.18).
(Photo: SCHELLMANN 1999)

Photo 4.10:
Last interglacial notch (MIS 5a) in T-3 *Acropora palmata* reef crest facies at Paragon, south coast of Barbados (sample site XII-7 in Figure 4.19).
(Photo: SCHELLMANN 1999)

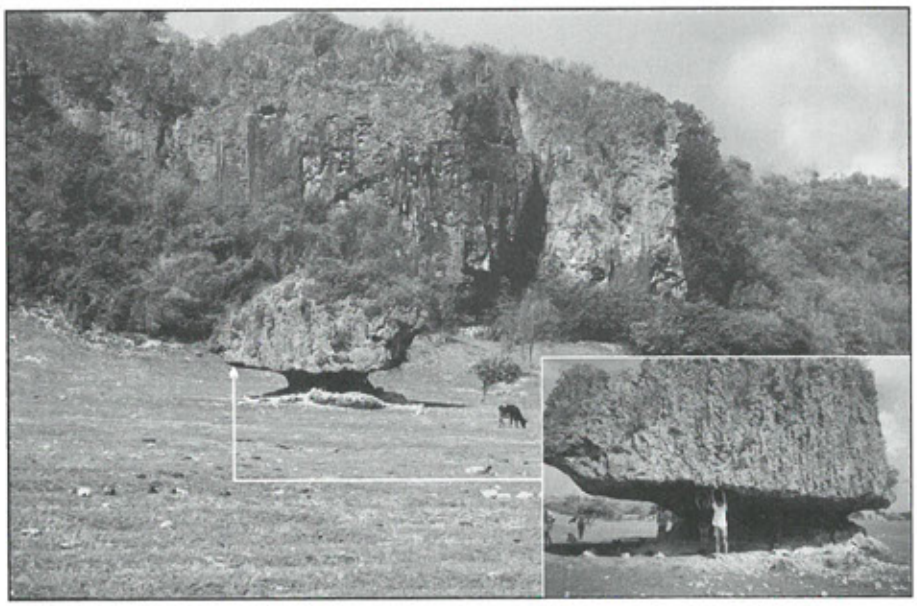

Photo 4.11:
Last interglacial notch (minimum age) in Middle Pleistocene coral limestone, northeast coast of Barbados. The approximately last interglacial terrace (MIS 5e, minimum age) is bordered by the Second High Cliff visible in the background.
(Photo: SCHELLMANN 2000)

(below 0.7 m) and that wave energies are reduced at the leeward coast of Barbados. In these regions with little surf, notches mark the elevation of the mean high tide water and are located approx. 0.5 m to 1 m higher than the highest reef crests of coral reef fringes located in front of the notches.

4.3. Distribution and chronostratigraphy of fossil coral reef terraces

Extensive areas of the south coast of Barbados were mapped using the methodology described in Chapters 4.1 and 4.2. The elevation of preserved coral reef terraces was measured, and more than 260 coral samples (mostly taken from fossil reef crest facies *Acropora palmate*) were dated using ESR (Figures 4.13 to 4.22, Table 4.2). In southern Barbados, the oldest coral reefs have been uplifted as much as c. 120 m above modern sea level. Up to 13 clearly distinguishable coral reef stages are preserved between the present coastline and the center of the southern island near St. Davids.

Since a correlation of these new morpho- and chronostratigraphic units to the traditional classification system, including the Worthing Terrace or the Ventnor Terrace, was impossible (SCHELLMANN & RADTKE 2001b), a new nomenclature was developed. This new stratigraphic nomenclature is based on letter-number-combinations (Table 4.2). The lowest and youngest main terrace level, which is located a few meters above present sea level, was called T-1 (T = terrace). The oldest and highest terrace was called T-13.

Prominent reef formations were classified into sub-levels. Sub-levels within a main level are comparable in elevation but may be separated by small fossil cliffs. For sub-levels, small letters were added to the terrace identification, such as T-5a and T-5b (Table 4.2). Sub-levels were determined along the Christ Church standard traverse. East of this traverse height differences between the sub-levels T-5a and T-5b, and T-6a and T-6b increase to some meters.

Sub-levels T-1a$_1$ and T-1a$_2$ are the only levels that were classified solely based on geochronological criteria. Reef crests of both terraces are located at similar elevation, at 2 m to m or 3 m above modern sea level (Table 4.2). The type locality for these two terraces is situated near the present coast to the west of Worthing (Figure 4.13). There, both terraces are morphologically separated by a small palaeo channel or by a wide palaeo lagoon (see below). Based on the morphological distribution, both terraces could be of similar age and may have formed simultaneously as double fringing reef terraces paralleling the coastline. However, dating results provided different times of formation, including ages of 85 ka for the T-1a$_2$ terrace, and 74 ka for the T-1a$_1$ terrace (Table 4.2 and Figure 4.22).

Reef stages preserved due to long-term tectonic uplift, such as those recorded on Barbados, typically show a positive correlation between reef elevation and age. The youngest formations are located at the lowest elevations close to the present coast, while oldest reef terraces are those situated at highest elevations and generally at a greater distance from the coast. Due to the relatively slow rate of uplift in southern Barbados (approx. 0.27 ± 0.02 m/1000a), the youngest reef terrace located above sea level (T-1a$_1$) formed at approx. 74 ka, during the end of the last interglacial sea-level highstand, and may be correlated to marine oxygen isotope sub-stage 5a (MIS 5a-1). The oldest and highest terrace formed during the interglacial sea-level maximum and was dated to approx. 410 ka (Table 4.2), which correlates to MIS 11.

Figure 4.12 compares the newly presented distribution/classification of coral reef terraces of the Christ Church area to the traditional differentiation of coral reef tracts as presented by BENDER et al. (1978). Table 4.2 illustrates the differences between the new stratigraphic classifications and dating results of reef stages presented here and previous models for the south coast of Barbados. ESR ages included in Table 4.2 represent the upper quartile (dataset >20) or the oldest age of all ESR dating results for coral samples from one terrace level (see Chapter 4.1.2.).

The youngest two reef terraces, T-1a$_1$ and T-1a$_2$, are largely comparable to the Worthing reef stage. In the literature, the Worthing stage has been correlated to marine oxygen isotope sub-stage 5a, and should be 83 ka old (EDWARDS et al. 1997). However, the terrace had never been dated on the south coast of Barbados. This is the first study to demonstrate that the Worthing stage consists of two individual depositional terraces. The first terrace T-1a$_1$ is located closer to the present coastline (Figure 4.13) and is dated approx. 74 ka; the second sub-level T-1a$_2$ occurs at a similar elevation above sea level but was dated approx. 85 ka (for details of ESR dating results see

Table 4.2: Terminology, elevation and ages of coral reef terraces in the south coast area of Barbados.

Coral reef terraces T = Terrace	$^{18}O/^{16}O$-stage	Elevation of reef crest	Average ages (ky) (n = number of samples) ESR age (maximum age) [1]	TIMS $^{230}Th/^{234}U$ ages [2]	Reef terraces after BENDER et al. (1979) $^{230}Th/^{234}U$ age (ky) after * (n = number of samples) [3]
H (Holocene)	1	1 m	3.5 (5)	1.7 ± 0.2 (1)	Holocene
T-1a$_1$	5a-1	2 m	74 ± 5 (31)	77 ± 0.6 (12)	Worthing (1 - 4 m)
T-1a$_2$	5a-2	3 m	85 ± 7 (10)	84 ± 0.7 (4)	
T-1b	5c-1	4 - 5 m	104 ± 13 (2)*	102 ± 2 (1)	
T-2	5c-2	8 - 10 m	104 ± 9 (8)		Ventnor (5 - 11 m) MS**** 101 ± 1 (1)
T-3	5c-3	15 - 17 m	105 ± 7 (42)	103 ± 1 (3)	
T-4	5e-1	21 - 23 m	118 ± 9 (8)	120 ± 1.4 (1)	Maxwell*** AS*** 114-129 (7)
T-5a	5e-2	35 - 40 m	128 ± 11 (14)		Rendezvous Hill (35 - 39 m) AS*** 121-124 (3) MS** 122-126 (3)
T-5b	5e-3	40 - 43 m	132 ± 13 (15)	128 ± 1 (1)	MS***** 129 (1)
T-6a	7-1	46 - 52 m	222 ± 21 (23)		Kendal Hill (47 - 52 m) AS* 154-310 (4)
T-6b	7-2	52 - 57 m	>200 (6)		MS***** 215 (1)
T-7	7-3	60 - 63 m	224 ± 22 (11)		Aberdare (65 - 70 m) AS* 215-230 (2)
T-8	9-1	72 - 74 m	289 ± 22 (23)		Kingsland (77 - 82 m) AS* 180-280 (5)
T-9	9-2	81 - 83 m	300 ± 40 (15)		
T-10	9-3	90 - 92 m	334 ± 34 (6)		Adams Castle (90 - 94 m) AS* 180->320 (4)
T-11	11 (?)	99 - 101 m	>310 (4)		
T-12	11	108 - 112 m	398 ± 46 (27)		Kent, St. Davids (108 - 113 m) AS* >350 (1)
T-13	11	120 - 122 m	410 ± 34 (2) *		Unnamed (120 - 122 m)

[1] Maximum ESR age: 90th Percentile value, if number of ESR data >20. Upper Quartile value, if number of ESR data≤ 20 data. * = oldest ESR age.

[2] TIMS $^{230}Th/^{234}U$ ages determined by E.K. Potter & M.T. McCulloch (Australian National University): only data with initial $\delta^{234}U$ values of >148.5± 8 permil (details in SCHELLMANN et al. 2004).

[3] MS = mass-spectr. $^{230}Th/^{234}U$ ages, AS = α-spectr. $^{230}Th/^{234}U$ ages.
Source: * BENDER et al. (1979), ** EDWARDS et al. (1987), *** KU et al. (1990), **** BARD et al. (1990), ***** BLANCHON & EISENHAUER (2001).

Figure 4.22). A complete morphological sequence, including reef crest and lagoon, is preserved for T-1a$_1$ at the St. Lawrence Swamp and Inch Marlowe Swamp areas, and for T-1a$_2$ at the Graeme Hall Swamp area. At these sites, *in situ A. palmata* reef crest facies commonly have a thickness of more than 1 to 2 m. In addition to the terraces, fossil notches and sea caves at approx. 3 to 5 m above modern high tide water level are preserved at different sites along the cliff coast between South Point and Salt Cave Point (Figures 4.16 to 4.20, Photo 4.9). These features may have formed during the development of the T-1a terraces.

The well-known reef stage Ventnor, dated at 101 ka and correlated to MIS 5c in previous studies, encompasses up to three different reef terraces (T-1b to T-3 reef terraces), which were formed before T-1a$_2$ at around 105 ka (MIS 5c). The ESR dating method does not allow for the detection of any age difference between these three terraces.

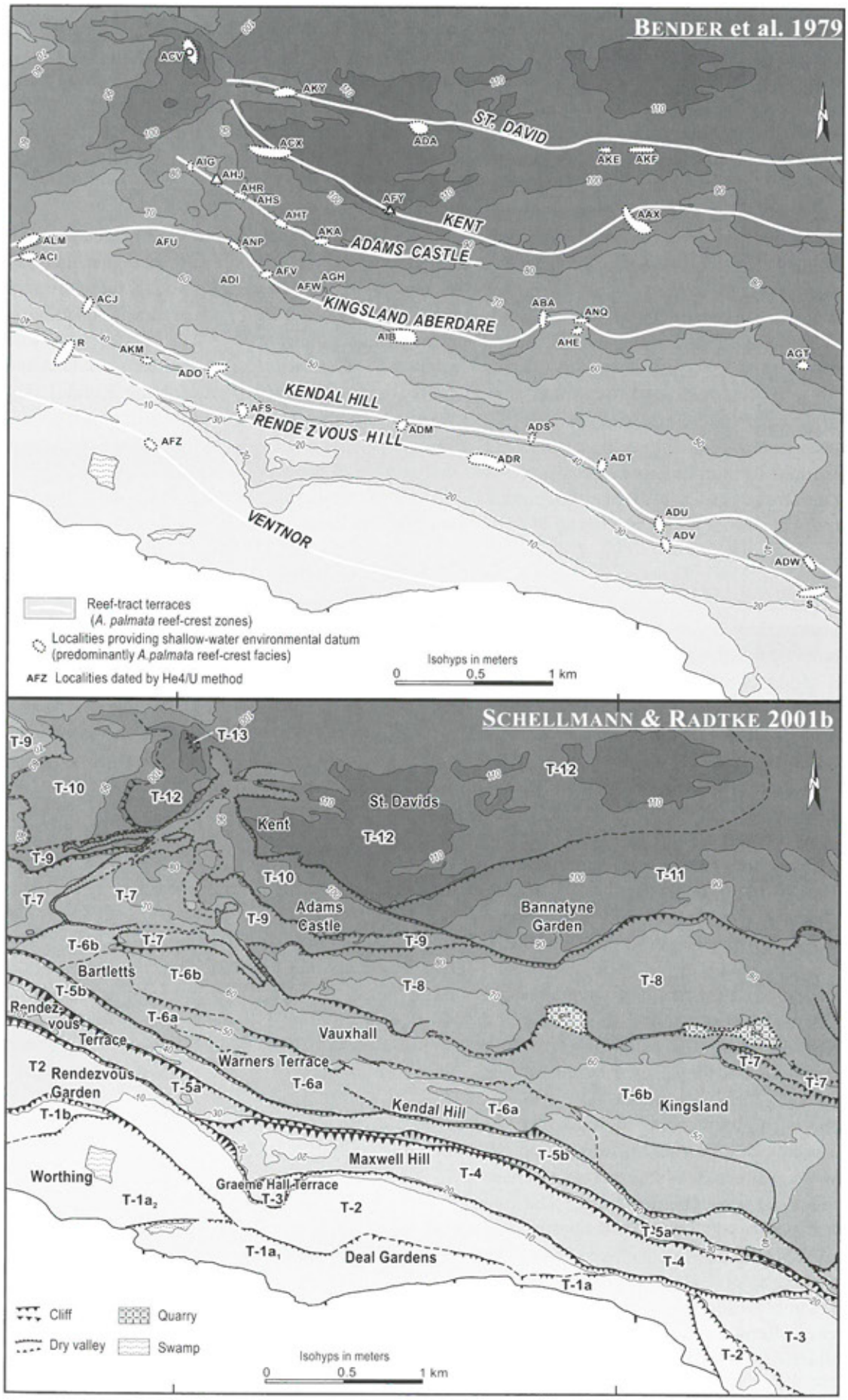

Figure 4.12:
Comparison of Pleistocene coral reef terraces at Christ Church traverse, southern Barbados, after SCHELLMANN & RADTKE (2001b), and BENDER et al. (1979).

The T-2 and T-3 terraces are widely distributed at the south coast (Figure 4.13). In general, their depositional morphology is well preserved and comprises a higher elevated, *Acropora palmata* facies dominated reef crest area associated with lagoons and channels on their landward side. The type localities for the T-2 and T-3 terraces are located east of Rendezvous Garden, and in South Point area, respectively (Figure 4.13). Notches incised during the T-2 formation are preserved at 7 to 11 m above modern high tide water level, as, for example, at the T-2 palaeo cliff line at South Point (Figure 4.16), and along the modern cliff coast between Round Rock (Figure 4.17), Paragon (Figure 4.19), and Salt Cave Point (Figures 4.20 and 4.21). In contrast to T-2 and T-3, the T-1b terrace is restricted to a small area southwest of Rendezvous Garden (Figure 4.13). Because houses and gardens cover this area, it is difficult to examine its morphology in detail and it is possible that the terrace is a wave-cut platform eroded in the previously formed T-2 reef at the end of MIS 5c.

The T-4 reef terrace is correlated to Maxwell Terrace as described by Ku et al. (1990). T-4 is best preserved morphologically at Maxwell Hill, where it displays a sequence of reef crests and lagoonal areas. Further to the east, T-4 has been strongly eroded by younger littoral cliff erosion. Locally, the terrace stretches as a small rim along the slope of First High Cliff (see "reef slope with double steps" displayed in Figure 4.13). East of Paragon, T-4 is preserved as an extensive $T\text{-}4_{[7]}$ wave-cut platform cut into penultimate interglacial coral reef limestone (Figures 4.19 to 4.21, Photo 4.6). Near Paragon, notches and a sea cave are deeply incised at the base of the former T-4 cliff line (Figure 4.19, Photo 4.8).

BLANCHON & EISENHAUER (2000) hypothesized that this terrace was a submarine fore reef ridge formed during the last interglacial transgression maximum approx. 129 ka ago. However, this terrace is the youngest of three constructional coral reef terraces, which all formed during the maximal last interglacial sea-level highstand. T-4 formed approx. 118 ka ago when sea level was several meters lower than the present sea level (Figure 4.24). The two older coral reefs T-5a and T-5b, dated approx. 128 and 132 ka (Table 4.2), were formed during the maximal last interglacial sea level (Figure 4.24). The T-5a terrace is best preserved at Rendezvous Hill I, and T-5b between Rendezvous Hill II, Silver Hill and Chancery Lane (Figure 4.13).

Coral reefs of different ages are exposed at First High Cliff (Figures 4.13 and 4.14). These include the T-5a reef in the vicinity of Christ Church Traverse, the T-3 reef to the east, followed by T-4, and finally the T-5b reef near South Point. The First High Cliff was significantly undercut during the formation of the T-2 and T-3 coral reef terraces, which are approx. 105 ka old (Table 4.2, Figure 4.22).

The T-6a to T-7 coral reef terraces originated from the penultimate interglacial sea-level highstand (MIS 7) approx. 222 to 224 ka ago. Today, these terraces are located in south Barbados at elevations ranging from 46 to 63 m asl. (Table 4.2, Figures 4.14, 4.20 and 4.21). The two younger reef terraces T-6a and T-6b are largely comparable to the Kendal Hill Terrace. In comparison, the Aberdare-Kingsland Terrace includes coral reefs from different interglacials, including reef terrace T-7 dated at approx. 224 ka (MIS 7), as well as reef terraces T-8 and T-9 dated at approx. 289 ka and 300 ka (MIS 9), respectively.

In contrast to the last and penultimate interglacial T-1 to T-7 terraces, karstification is significantly more developed on the older T-8 to T-13 reef terraces in south Barbados (Chapter 2.4). On these older terraces, both the number and area of dolines increase, and dry valleys are deeply incised locally down to the level of the penultimate interglacial T-6a and T-6b terraces near Bartletts and Providence (Figure 4.13). The latter indicates the height of former penultimate interglacial sea-level stands.

Based on its elevation, the T-10 terrace dated at approx. 334 ka (MIS 9), largely correlates to the Adams Castle reef tract of the classical Christ Church traverse. T-11 has not been mapped before. In this revised classification scheme, the highest terraces of this traverse, Kent, St. Davids, and Unnamed, (Figure 4.13), are classified as T-12 to T-13. Their ages are approx. 398 and 410 ka (MIS 11), respectively (Table 4.2 and Figure 4.22).

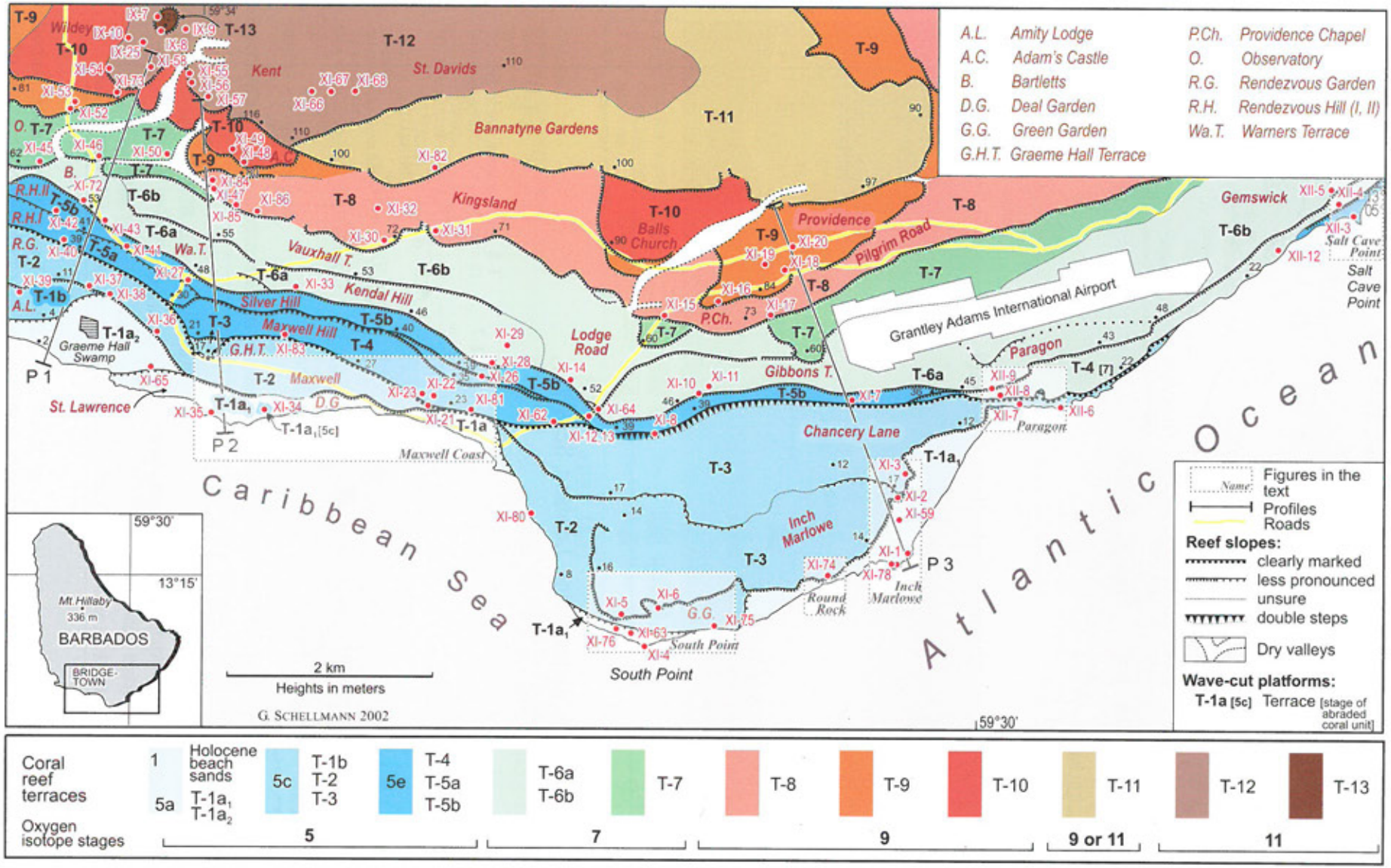

Figure 4.13: Pleistocene coral reef terraces on southern Barbados. This figure displays the locations of various sample sites, profiles, and detailed map sections referred to in Figures 4.14 to 4.21.

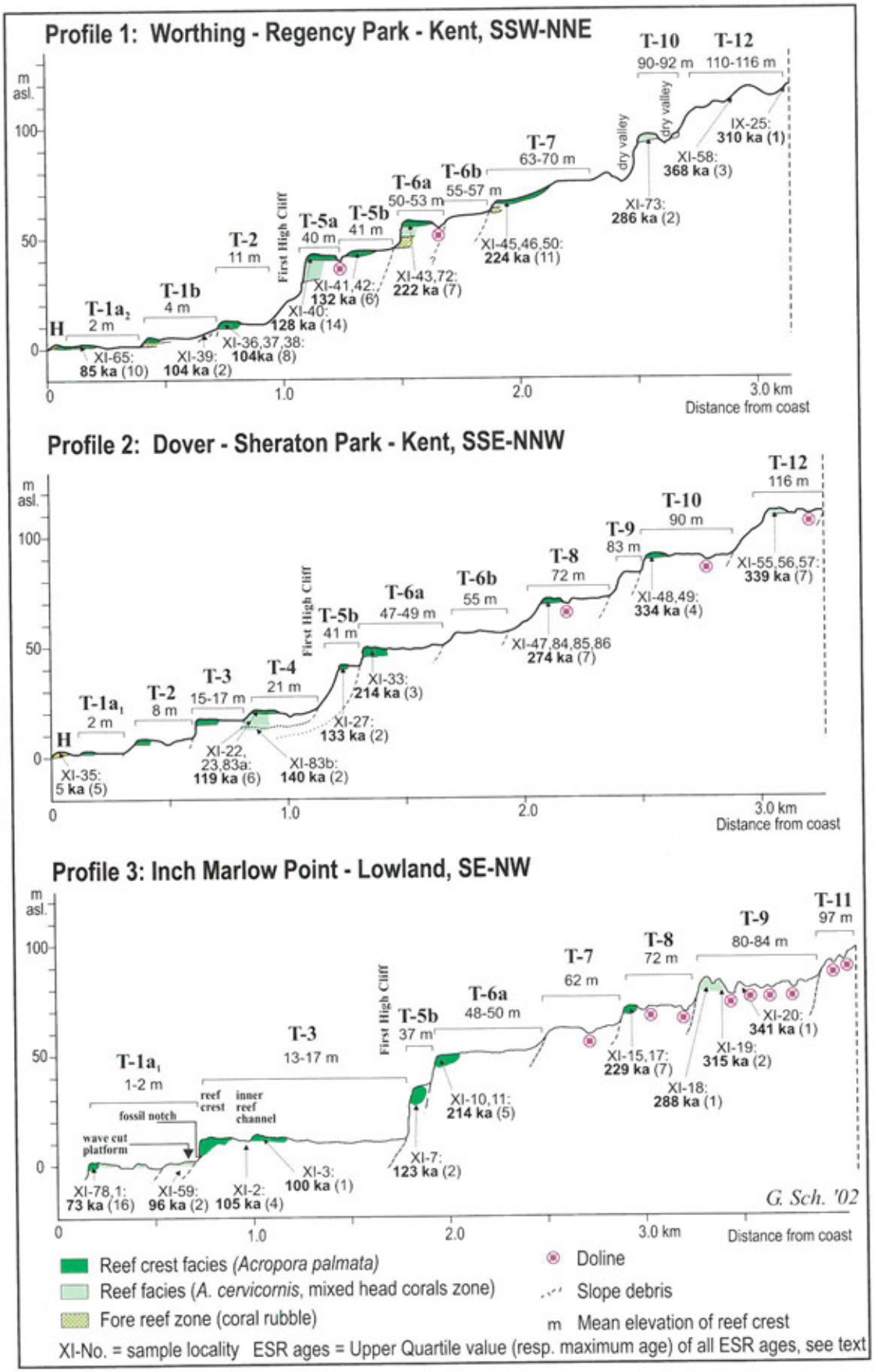

Figure 4.14:
Profiles for coral reef terraces located in the vicinity and east of Christ Church Traverse on southern Barbados; illustrating morphology, geology, and ESR dating results. See Figure 4.13 for the location of the three profiles.

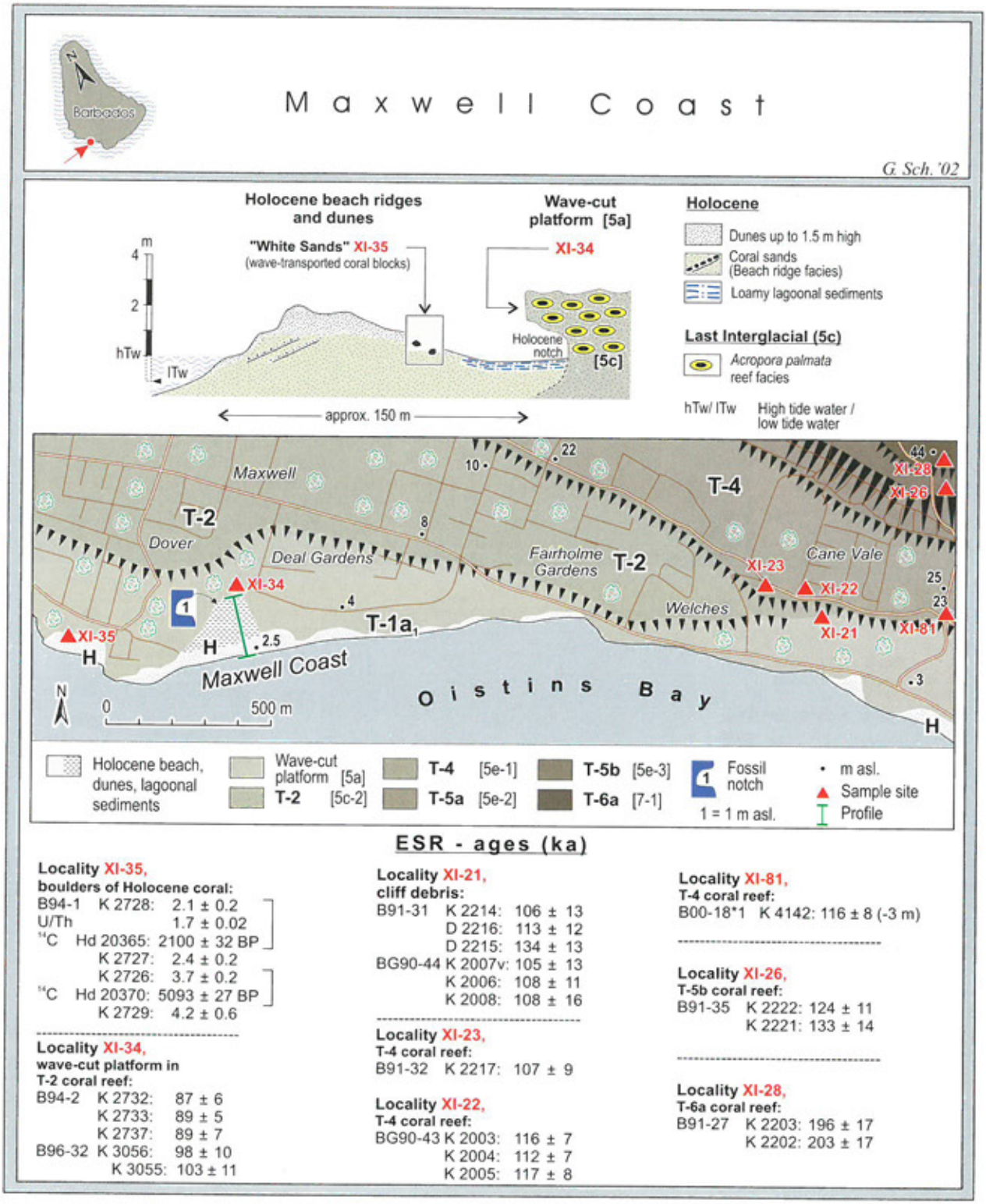

ESR - ages (ka)

Locality XI-35,
boulders of Holocene coral:

B94-1	K 2728:	2.1 ± 0.2
U/Th		1.7 ± 0.02
^{14}C	Hd 20365:	2100 ± 32 BP
	K 2727:	2.4 ± 0.2
	K 2726:	3.7 ± 0.2
^{14}C	Hd 20370:	5093 ± 27 BP
	K 2729:	4.2 ± 0.6

Locality XI-34,
wave-cut platform in T-2 coral reef:

B94-2	K 2732:	87 ± 6
	K 2733:	89 ± 5
	K 2737:	89 ± 7
B96-32	K 3056:	98 ± 10
	K 3055:	103 ± 11

Locality XI-21,
cliff debris:

B91-31	K 2214:	106 ± 13
	D 2216:	113 ± 12
	D 2215:	134 ± 13
BG90-44	K 2007v:	105 ± 13
	K 2006:	108 ± 11
	K 2008:	108 ± 16

Locality XI-23,
T-4 coral reef:

B91-32	K 2217:	107 ± 9

Locality XI-22,
T-4 coral reef:

BG90-43	K 2003:	116 ± 7
	K 2004:	112 ± 7
	K 2005:	117 ± 8

Locality XI-81,
T-4 coral reef:

B00-18*1	K 4142:	116 ± 8 (-3 m)

Locality XI-26,
T-5b coral reef:

B91-35	K 2222:	124 ± 11
	K 2221:	133 ± 14

Locality XI-28,
T-6a coral reef:

B91-27	K 2203:	196 ± 17
	K 2202:	203 ± 17

Figure 4.15:
Coral reef terraces and ESR dating results for coral samples collected along Maxwell Coast.
See Figure 4.13 for site location.

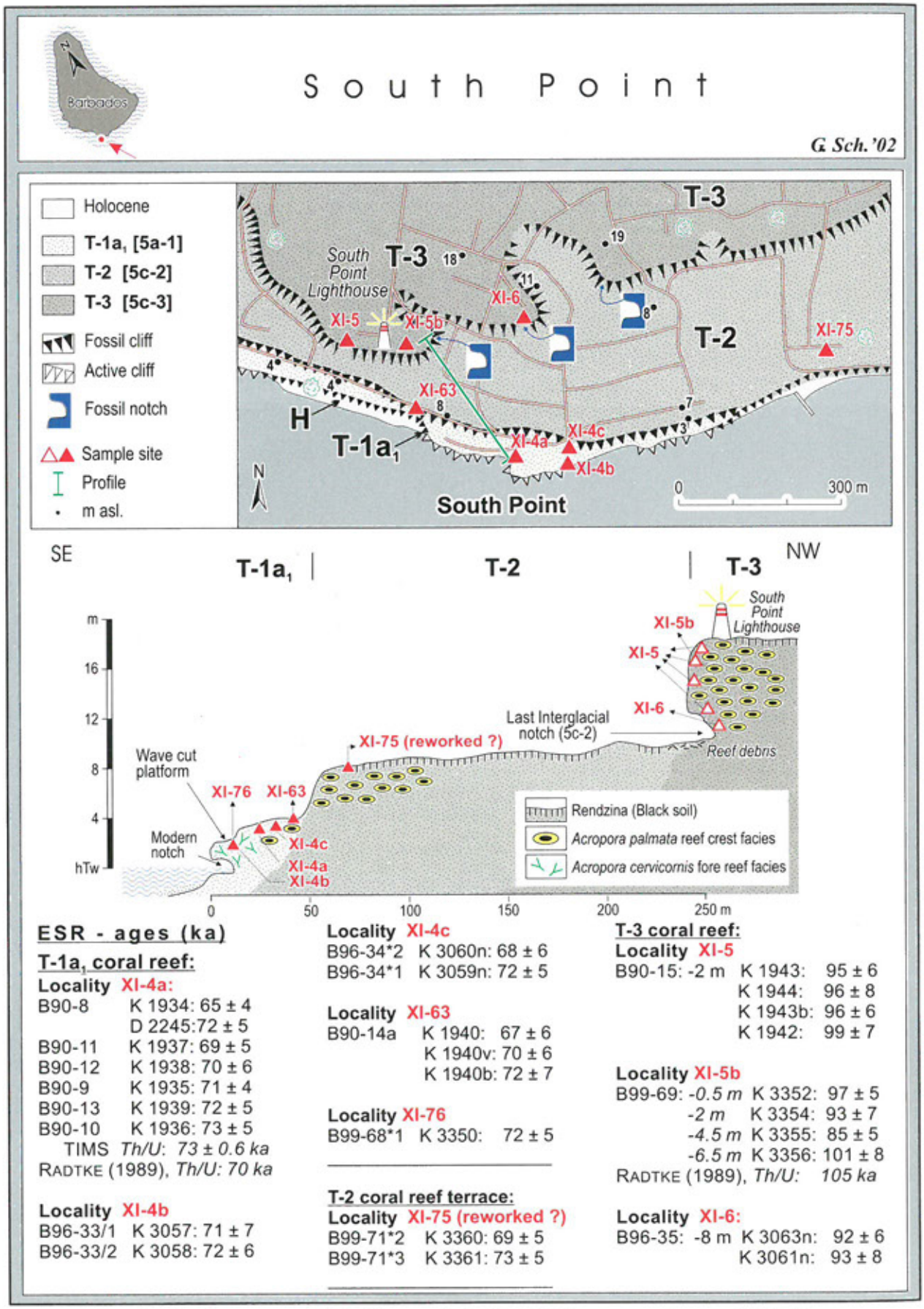

ESR - ages (ka)

T-1a1 coral reef:

Locality XI-4a:

B90-8 K 1934: 65 ± 4
D 2245:72 ± 5
B90-11 K 1937: 69 ± 5
B90-12 K 1938: 70 ± 6
B90-9 K 1935: 71 ± 4
B90-13 K 1939: 72 ± 5
B90-10 K 1936: 73 ± 5
TIMS *Th/U: 73 ± 0.6 ka*
RADTKE (1989), *Th/U: 70 ka*

Locality XI-4b

B96-33/1 K 3057: 71 ± 7
B96-33/2 K 3058: 72 ± 6

Locality XI-4c

B96-34*2 K 3060n: 68 ± 6
B96-34*1 K 3059n: 72 ± 5

Locality XI-63

B90-14a K 1940: 67 ± 6
K 1940v: 70 ± 6
K 1940b: 72 ± 7

Locality XI-76

B99-68*1 K 3350: 72 ± 5

T-2 coral reef terrace:

Locality XI-75 (reworked ?)

B99-71*2 K 3360: 69 ± 5
B99-71*3 K 3361: 73 ± 5

T-3 coral reef:

Locality XI-5

B90-15: -2 m K 1943: 95 ± 6
K 1944: 96 ± 8
K 1943b: 96 ± 6
K 1942: 99 ± 7

Locality XI-5b

B99-69: *-0.5 m* K 3352: 97 ± 5
-2 m K 3354: 93 ± 7
-4.5 m K 3355: 85 ± 5
-6.5 m K 3356: 101 ± 8
RADTKE (1989), *Th/U: 105 ka*

Locality XI-6:

B96-35: -8 m K 3063n: 92 ± 6
K 3061n: 93 ± 8

Figure 4.16: Coral reef terraces and ESR dating results for South Point area, south coast of Barbados. See Figure 4.13 for site location.

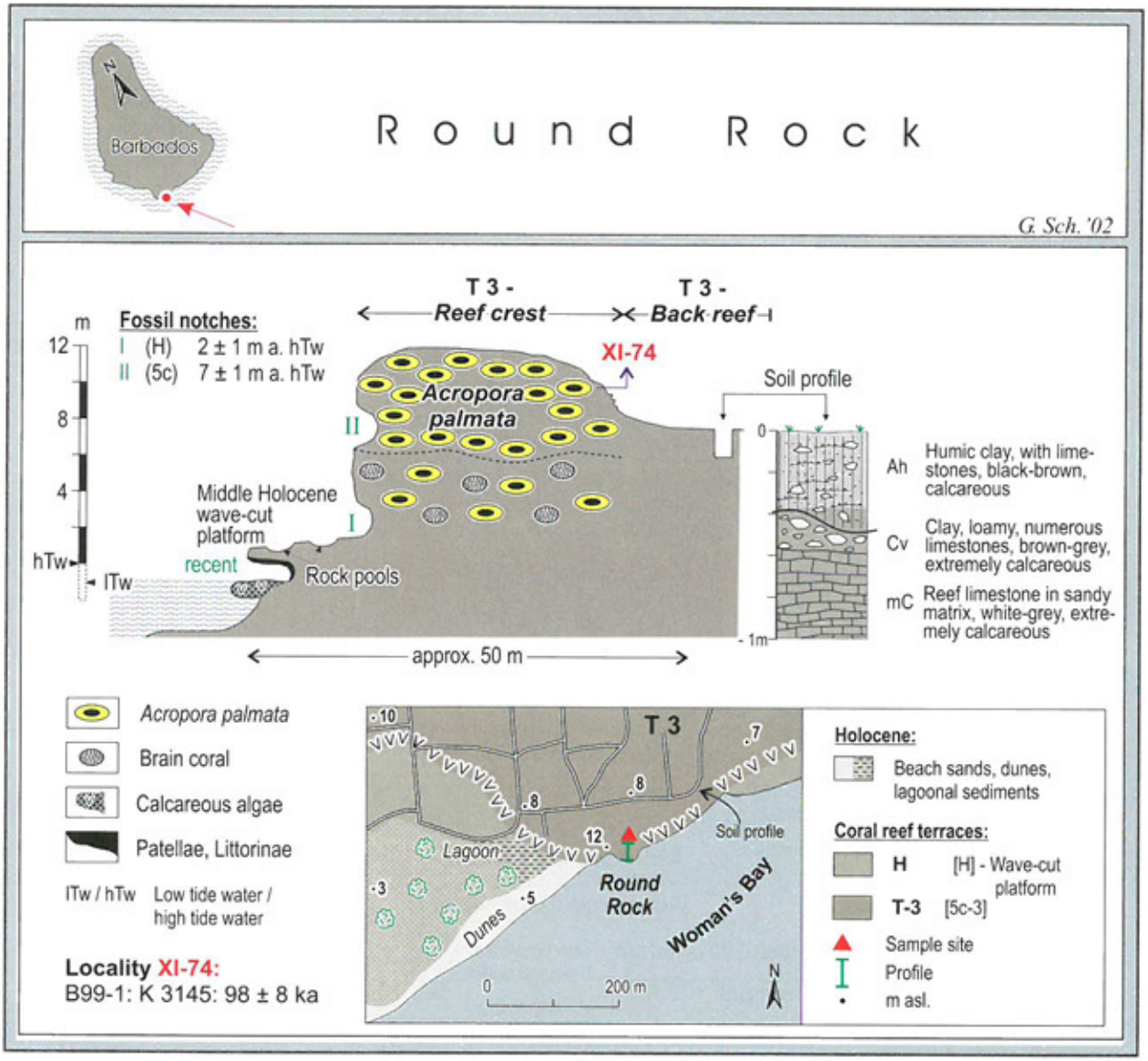

Figure 4.17:
T-3 coral reef terrace and ESR dating results for coral samples collected at Round Rock.
See Figure 4.13 for site location.

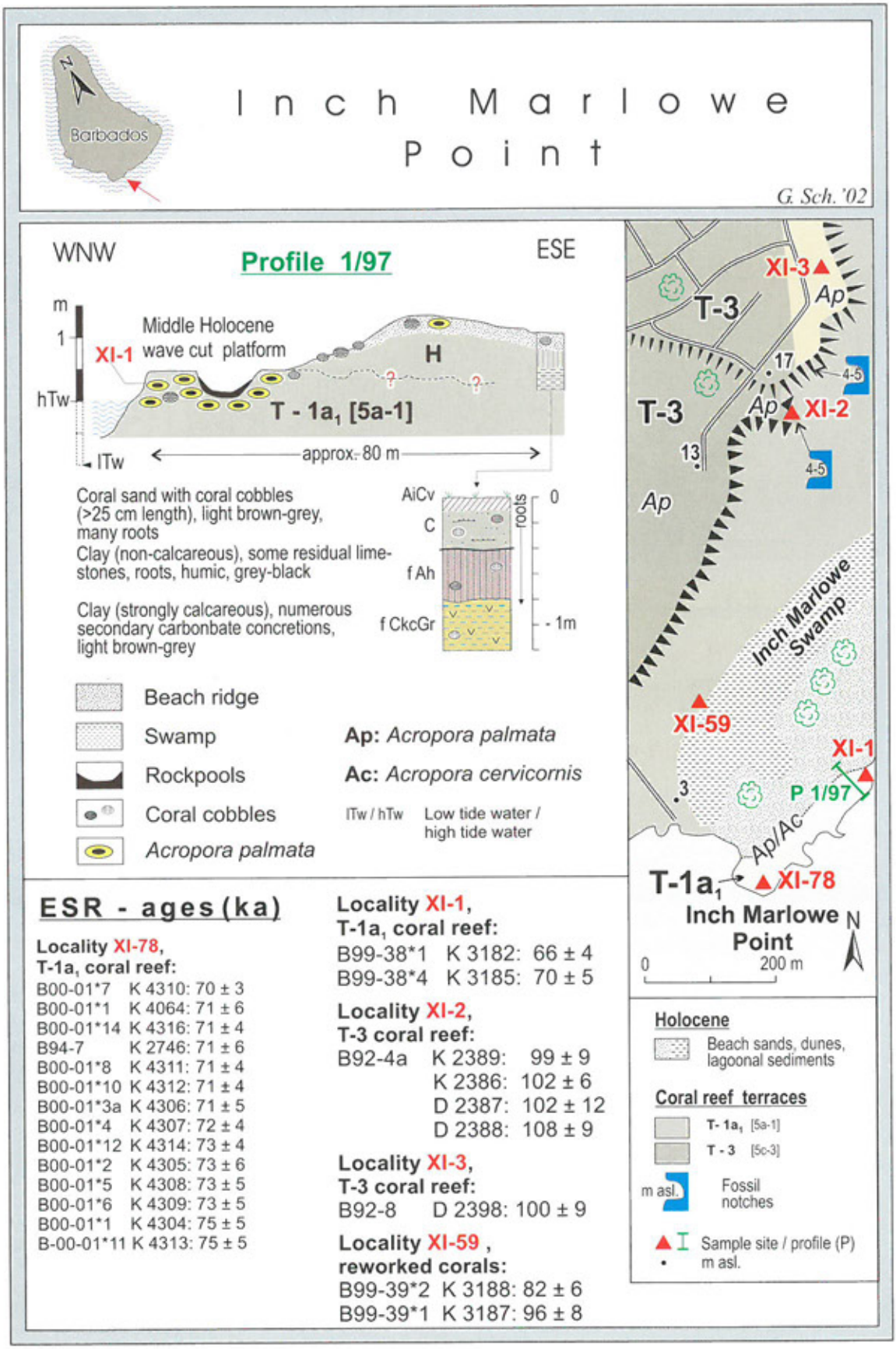

ESR - ages (ka)

Locality XI-78, T-1a$_1$ coral reef:

B00-01*7	K 4310:	70 ± 3
B00-01*1	K 4064:	71 ± 6
B00-01*14	K 4316:	71 ± 4
B94-7	K 2746:	71 ± 6
B00-01*8	K 4311:	71 ± 4
B00-01*10	K 4312:	71 ± 4
B00-01*3a	K 4306:	71 ± 5
B00-01*4	K 4307:	72 ± 4
B00-01*12	K 4314:	73 ± 4
B00-01*2	K 4305:	73 ± 6
B00-01*5	K 4308:	73 ± 5
B00-01*6	K 4309:	73 ± 5
B00-01*1	K 4304:	75 ± 5
B-00-01*11	K 4313:	75 ± 5

Locality XI-1, T-1a$_1$ coral reef:

B99-38*1	K 3182:	66 ± 4
B99-38*4	K 3185:	70 ± 5

Locality XI-2, T-3 coral reef:

B92-4a	K 2389:	99 ± 9
	K 2386:	102 ± 6
	D 2387:	102 ± 12
	D 2388:	108 ± 9

Locality XI-3, T-3 coral reef:

B92-8	D 2398:	100 ± 9

Locality XI-59, reworked corals:

B99-39*2	K 3188:	82 ± 6
B99-39*1	K 3187:	96 ± 8

Figure 4.18:
Coral reef terraces and ESR dating results for coral samples from Inch Marlowe Point. See Figure 4.13 for site location.

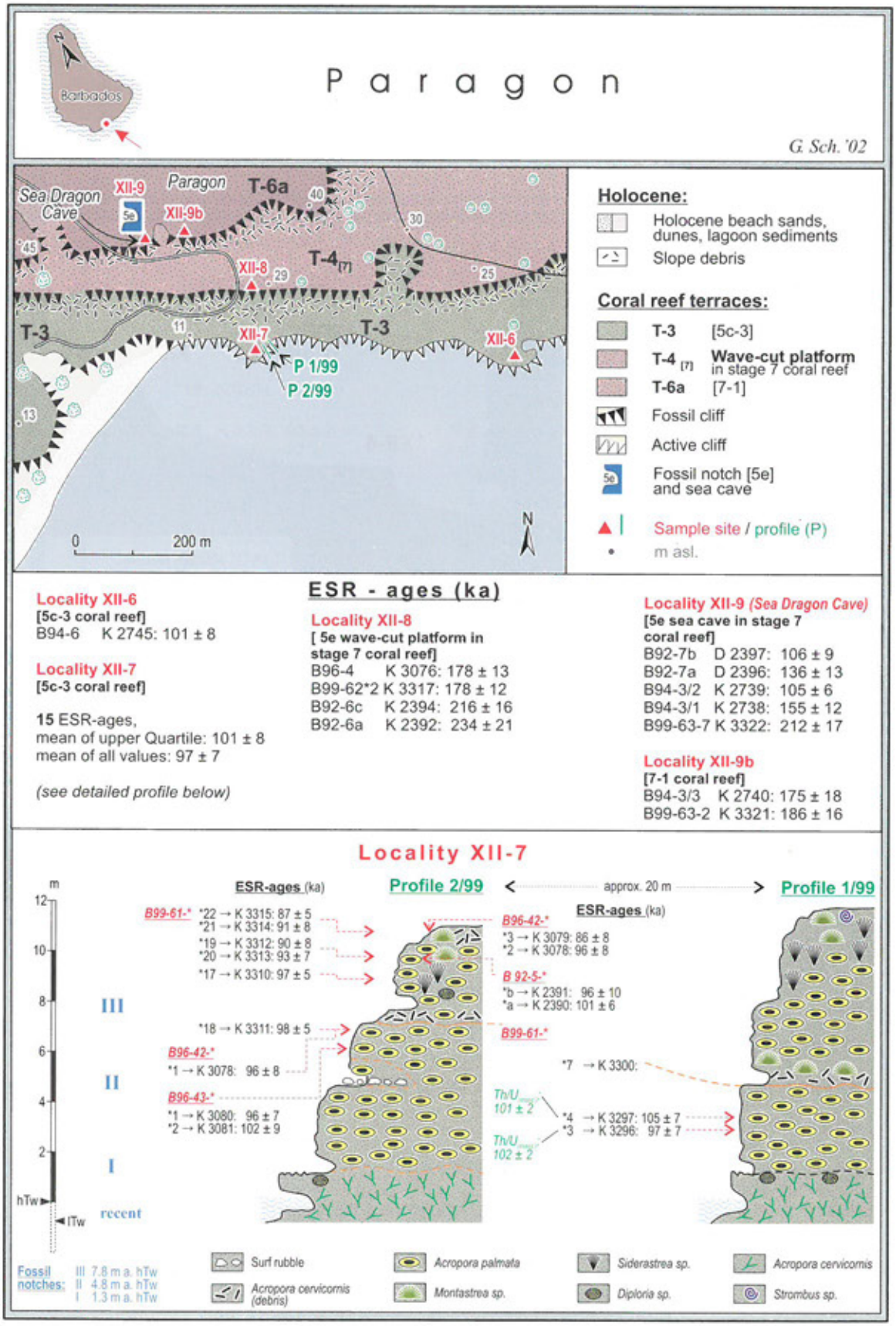

Figure 4.19:
Coral reef terraces and ESR dating results for coral samples collected at Paragon. See Figure 4.13 for site location.

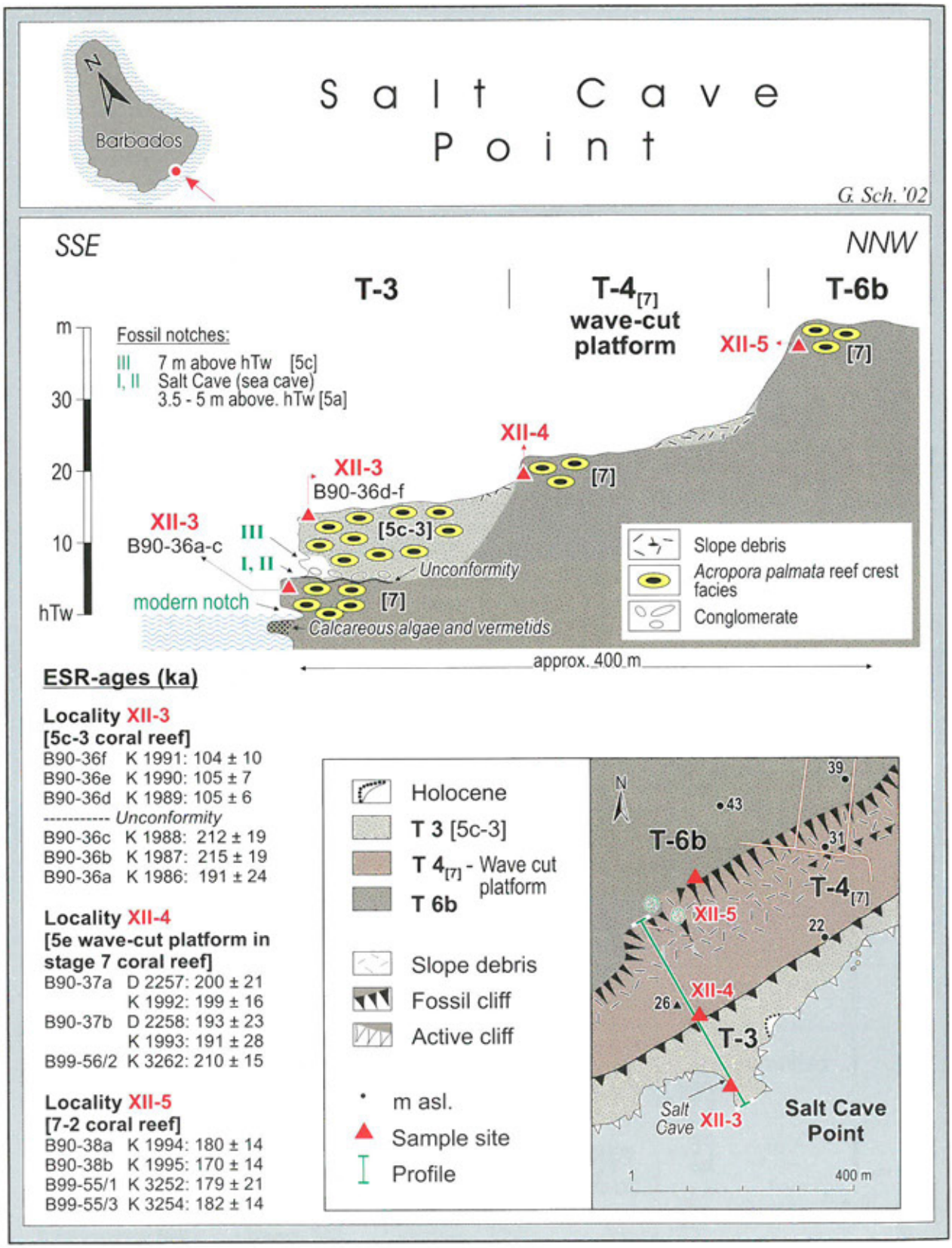

Figure 4.20:
Coral reef terraces and ESR dating results for coral samples from Salt Cave Point. See Figure 4.13 for site location, and Figure 4.21 for further dating results.

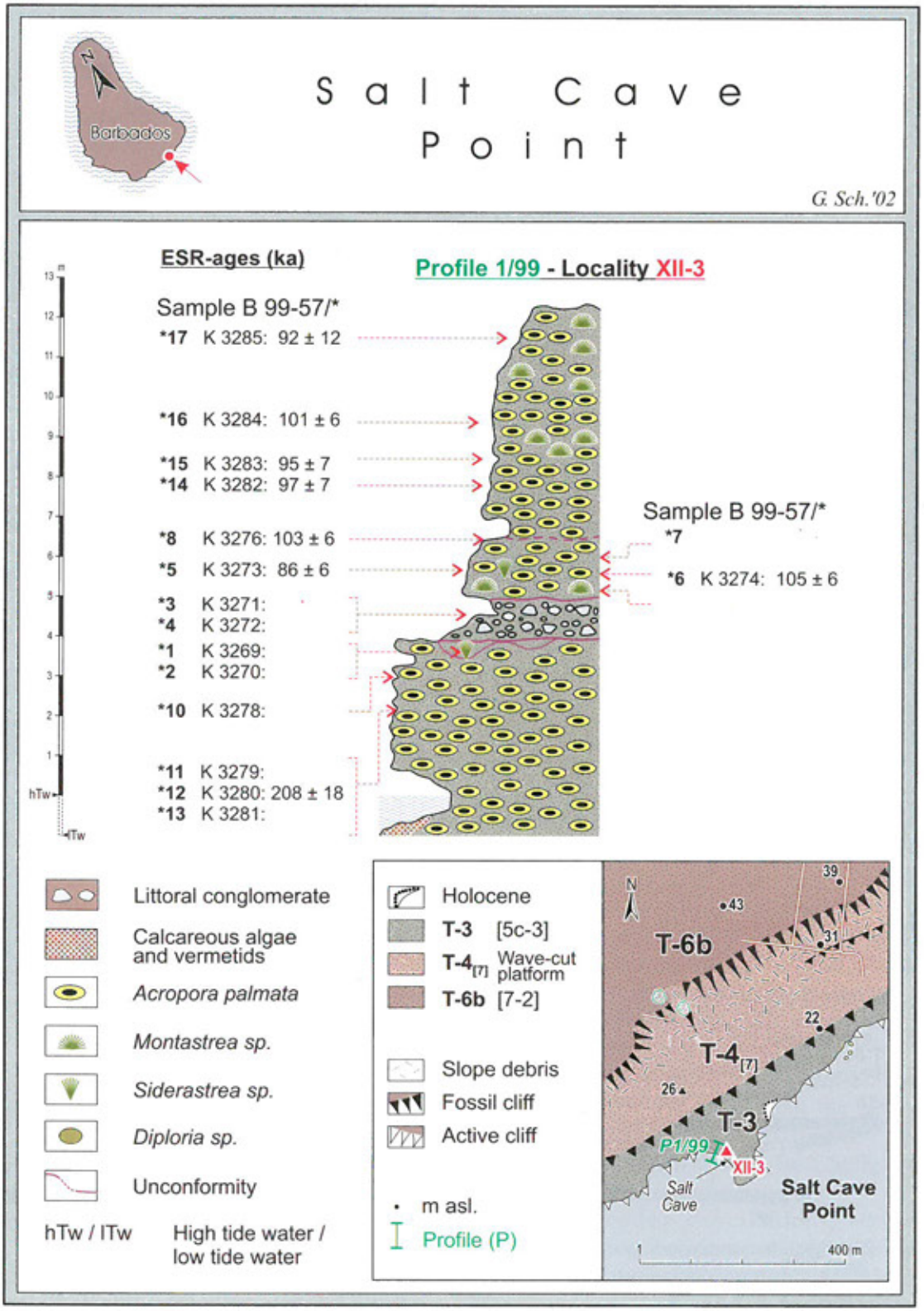

Figure 4.21:
Detailed profile depicting ESR dating results for the T-3 Terrace at Salt Cave Point. See Figure 4.13 for site location, and see Table 4.3 for details on ESR ages.

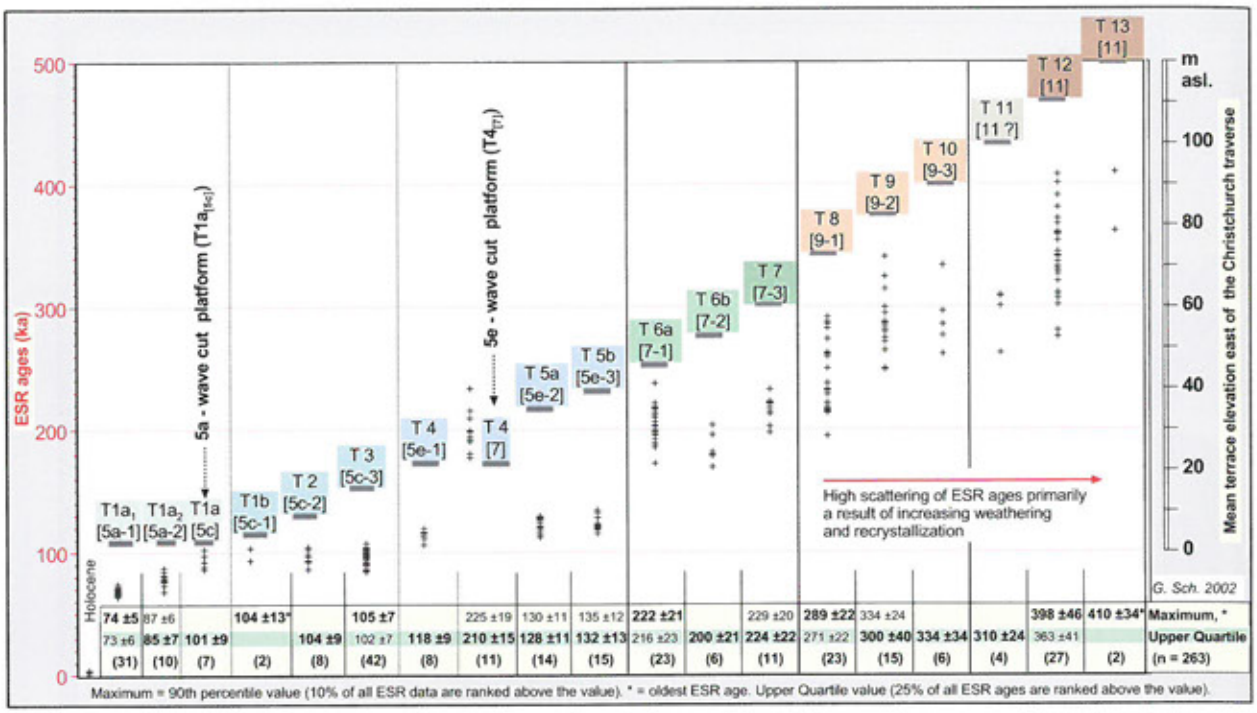

Figure 4.22:
Elevations and ESR dating results of coral reef terraces in southern Barbados.
See Table 4.3 for details on ESR ages.

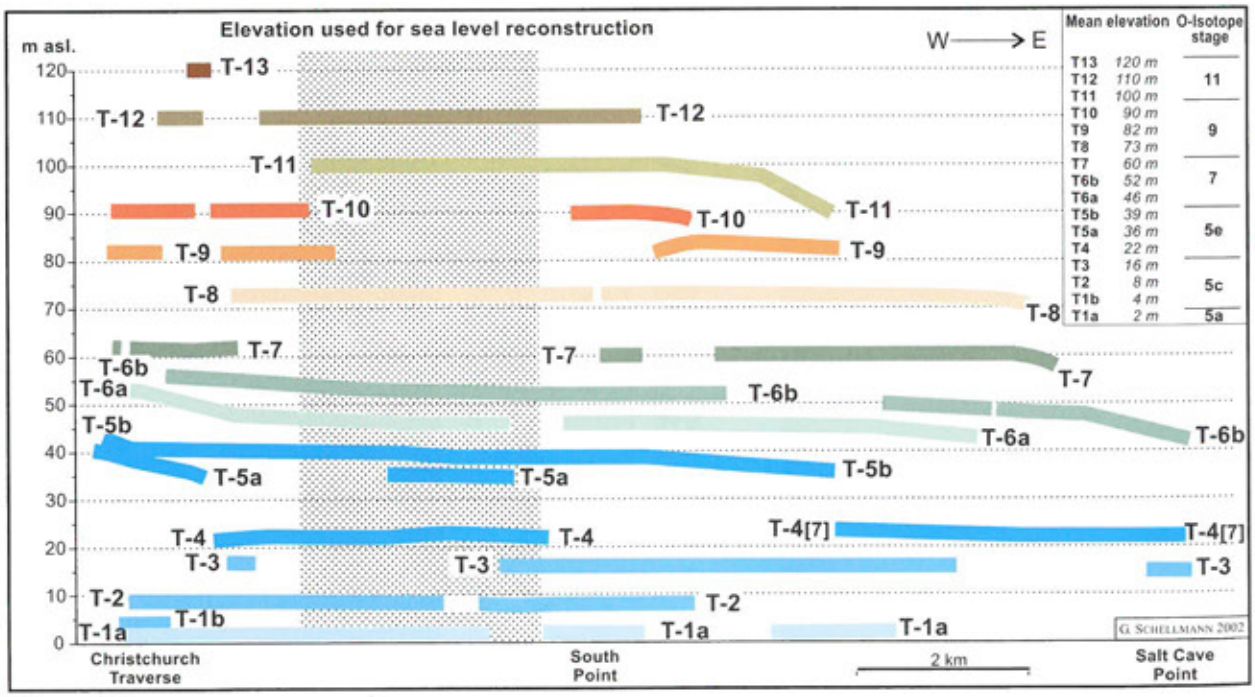

Figure 4.23:
Elevations of the Pleistocene coral reef terraces T-1 to T-13 that parallel the south shore of Barbados.

4.4. The reconstruction of sea levels during interglacial highstands of the last 400,000 years

Many scientists, who base their research on the classical „Barbados Model", assume a 6 ± 4 m higher sea level during the last interglacial c. 130 ka ago (MIS 5e) (RADTKE, 1989). Based on this assumption, sea level alternated between 10 to 20 m below present sea level during subsequent submaxima approx. 105 ka ago (MIS 5c) and approx. 80 ka ago (MIS 5a). These calculations of palaeo sea levels are based on the assumption of a constant rate of uplift for all coastal terraces and an elevation of 6 ± 4 m for the last interglacial sea-level highstand. Both assumptions require critical evaluation. Reef stages from the last interglacial transgression maximum (MIS 5e) are located at 20 m to 60 m asl. on Barbados. Assuming that these reef stages record the same sea-level highstand, it is an unavoidable conclusion that uplift rates have varied spatially and, most probably, temporally. In southern Barbados, the region located to the east of South Point is not suited for palaeo sea-level estimates, because this region has experienced differentiated tectonic uplift processes. In particular, surfaces of individual older reef terraces descend in eastern direction towards the St. George Valley syncline (Figure 4.23). The reef terraces within the vicinity of the Christ Church Traverse, which was generally used for sea-level calculations in the past, are warped anticlines (Figure 4.23). They should, therefore, not be used for sea-level calculations. For similar reasons, the terraces of the warped areas of the Clermont Nose Anticline at the west coast of Barbados should not be used for sea-level estimates either (Chapters 5 and 6). In contrast, the reef terraces preserved to the east of the Christ Church standard traverse are not affected by the Christ Church anticline. Their reef crests maintain a constant elevation above present sea level in the area to the west of South Point (Figure 4.23). This suggests that a constant uplift has affected this coastal area. However, it does not imply that the rate of uplift was constant over time.

Figure 4.24 summarizes palaeo sea-level calculations derived from the region to the east of Christ Church Traverse. These calculations assume different elevations of the last interglacial sea-level maximum including projections based on paleao sea levels at +6 m, +2 m, and at present sea level. Since the oxygen isotope content in foraminifers from the deep sea was similar for different interglacial highstands, one may hypothesize that sea levels during the transgression maxima of the previous Middle Pleistocene interglacials were broadly comparable to Holocene and last interglacial sea-level highstands. This well-accepted palaeoclimatic scenario is, however, only supported if one assumes that the last interglacial sea level was within the elevation of present sea level or up to 2 m higher (4.24). This would support the postulation of MURRAY-WALLACE & BELPERIO (1991), who report a 2 m higher sea level during the last interglacial sea-level maximum (MIS 5e). The widespread assumption that the last interglacial sea level was 6 m higher than the present sea level would result in reconstructed sea-level heights between 8 m and 18 m for the third and fourth past interglacial (MIS 9 and 11).

The following sea-level data are based on the assumption that the southern part of the island has emerged with a relatively constant uplift rate of approx. 0.27 ± 0.02 m/1000 a, and that sea level was approx. 2 ± 2 m higher during MIS 5e maximum than at present. The present heights of reef crests were used for sea-level calculations, and therefore the estimates are approximations of the former mean low tide water levels. The dating of sea-level changes was based on the ESR geochronology presented here. In general, the ESR data of last interglacial coral reefs agree well with TIMS U-series dating results from different sites on Barbados (Table 6.1 SCHELLMANN et al. 2004).

The new data presented here suggest that, during the last 400 ka, sea level seems to have oscillated more strongly than previously assumed. Evidence for strong oscillations is found, for example:

(1) in the occurrence of several sub-stages with palaeo sea-level elevations between 10 m and 25 m below present sea level, which are preserved on southern Barbados and originated from the last three interglacial sea-level highstands (Figure 4.24: E.g. sub-maxima 5a-1, 5a-2, 5c-1, 5c-2, 5c-3, 5e-1, 7-1, 9-1).

(2) in minor sea-level oscillations, which are documented by distinct coral reef terraces that were formed during the past three interglacial sea-level maxima: T-10 and T-9 during MIS 9, T-7 and T-6b during MIS 7, T-5b and T-5a during MIS 5e transgression maximum (Figure 4.24).

Due to the accuracy of dating results, sea-level history is best known for the last interglacial period. Its transgression maximum is documented in form of the two sea-level maxima MIS 5e-3 (T-5b) and MIS 5e-2 (T-5a), which are approx. 132 ka and 128

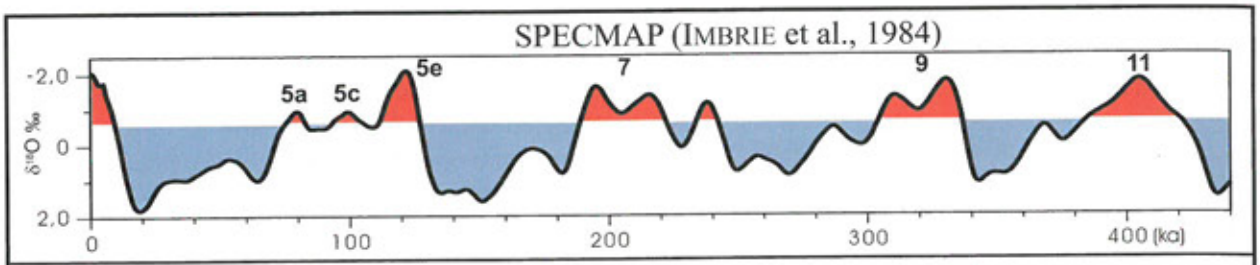

Younger and Middle Pleistocene sea level changes in the Caribbean
(based on present elevations of fossil coral reef terraces in southern Barbados)

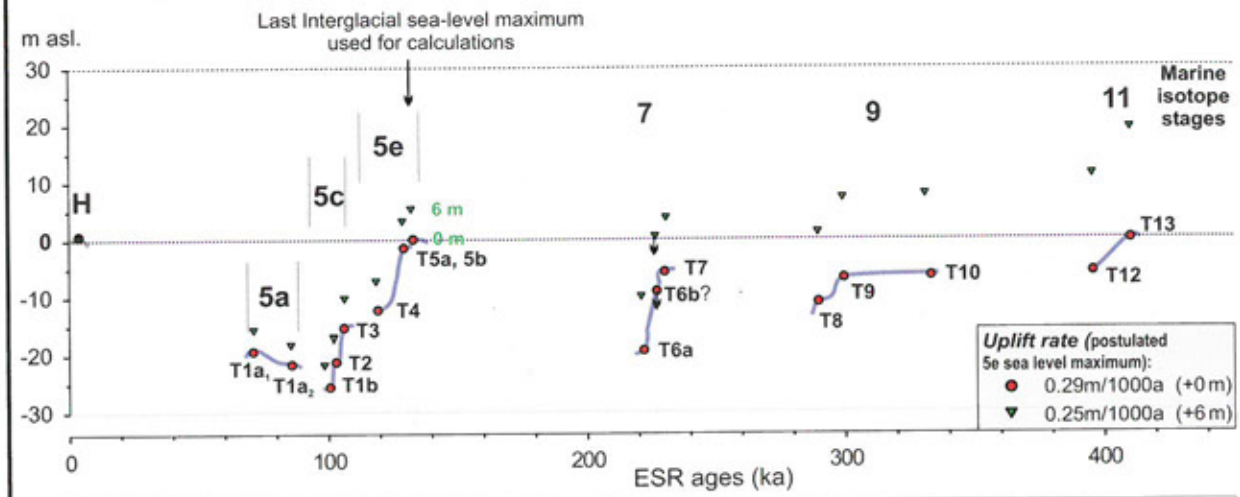

Uplift rate = (elevation of 5e coral reef terrace minus 5e sea level height (0, 6 m)) / age of the 5e terrace

Former sea level S_{Tx} = Modern elevation of reef crest Tx minus uplift rate x age of terrace Tx

Period	Terrace	Elevation	Age	$^{18}O/^{16}O$-	Sea level (0)	Sea level (+2)	Sea level (+6)
		m	ka	stage	m	m	m
Last Interglacial	T-1a$_1$	2	74	5a-1	-20	-19	-17
	T-1a$_2$	3	85	5a-2	-22	-21	-18
	T-1b	4	104	5c-1	-27	-25	-22
	T-2	9	104	5c-2	-22	-20	-17
	T-3	16	105	5c-3	-15	-13	-10
	T-4	22	118	5e-1	-13	-11	-8
	T-5a	36	128	5e-2	-2	0	4
	T-5b	39	132	5e-3	**0**	**2**	**6**
Penultimate Interglacial	T-6a	46	222	7-1	-20	-16	-10
	T-6b	52	>204	7-2	< -8	< -5	< 1
	T-7	60	224	7-3	-6	-3	4
3rd Interglacial	T-8	73	289	9	-12	-8	1
	T-9	82	300	9	-7	-2	7
	T-10	91	334	9	-8	-3	8
4th Interglacial	T-11	100	-	9 or 11			
	T-12	110	398	11	-8	-2	11
	T-13	120	410	11	-1	5	18

* sea level (m) = Last Interglacial sea level in meter used for estimations
terrace age: Upper quartile or 90th percentile value of ESR data, see text

G. SCHELLMANN 2003

Figure 4.24:
Interglacial palaeo sea level changes during the last 400 ka. Calculations were based on coral reef stages located in southern Barbados.

ka old, respectively. This means, that the last interglacial sea-level highstand most likely lasted a few thousand years only. After that, sea level dropped and reached c. -11 ± 2 m asl. during MIS 5e-1 coral reef growth (T-4) approx. 118 ka ago. Overall, the three coral reef terraces T-5b, T-5a, and T-4 were formed on south Barbados during the MIS 5e time span. This corresponds well with the established timing of MIS 5e sea-level changes in the Caribbean: Mass-spectrometric U-series data by EDWARDS et al. (1997) from Barbados and by CHEN et al. (1991) from the Bahamas indicated a maximum MIS 5e high sea stand between 132 and 128 ka ago, and a sea-level drop between 123 and 120 ka ago. KU et al. (1990) suggested that a double highstand during the last interglacial was morphologically preserved in form of the Rendezvouz Hill Terrace I (T-5a terrace), and the Maxwell Terrace (T-4 terrace). However, the Rendezvouz Hill Terrace I or T-5a reef stage was formed during the final stages of the transgression maximum approx. 128 ka ago after the formation of the T-5b reef approx. 132 ka ago. In contrast, the Maxwell or T-4 terrace was formed when sea level was significantly lower and reached a level of c. -11 ± 2 m asl. during MIS 5e-1 approx. 118 ka ago. The hypothesis of a double highstand during the last interglacial maximum is only documented with a minor sea-level oscillation, which is associated with the formation of the T5a- und T-5b coral reef terraces. Sea level was c. 2 ± 2 m above present sea level during MIS 5e-3 (T-5b), and near the present level during MIS 5e-2 (T-5a).

The three coral reef terraces T-3, T-2, and T-1b were formed on the south coast of Barbados during the last interglacial sub-stage MIS 5c. The chronostratigraphy of these various MIS 5c coral reef terraces cannot yet be differentiated - neither by the abundant ESR data nor by the relatively few U/Th data (SCHELLMANN et al. 2004). According to the ESR data, these terraces were formed approx. 104 to 105 ka ago (Figure 4.24). Sea level reached three different relative highstands during MIS 5c approx. 105 ka ago: first, c. -13 ± 2 m during MIS 5c-3; second, c. -20 ± 2 m during MIS 5c-2; and third, c. -25 ± 2 m during MIS 5c-1. Astonishingly, there are only a few TIMS U-series data that reveal timing and magnitude of sea-level changes in the Caribbean during MIS 5c. BARD et al. (1990b), and EDWARDS et al. (1997) reported a relatively high sea level (c. -18 m) approx. 101 ka and 104 ka ago, respectively. These estimates were based on samples from the discontinuously rising west coast of Barbados (Chapter 5). They generally agree with the MIS 5c sea-level changes described above.

A double sea-level oscillation with the formation of the two morphologically distinct coral reefs (T-1a$_1$ and T-1a$_2$) was recognized for the first time on Barbados during MIS 5a (SCHELLMANN & RADTKE, 2001b). Both reef terraces were identified and mapped for the south coast of Barbados. ESR dating results from 41 coral samples from different sample sites yielded ages of approx. 74 ka for T-1a$_1$ and approx. 85 ka for T-1a$_2$ (Figure 4.22; SCHELLMANN & RADTKE, 2001b, 2002, 2004). This is largely consistent with new TIMS U-series data from the south coast of Barbados, which provided median values of 76.7 ka and 84.2 ka, respectively (Table 4.1; SCHELLMANN et al. 2004). These findings suggest a double sea-level oscillation during MIS 5a, including first, an early MIS 5a-2 stand with a sea-level height of c. -21 ± 2 m dated at approx. 85 ka and second, a late MIS 5a-1 stand with a height of c. -19 ± 2 m below present sea level dated at approx. 74 ka ago. The older MIS 5a sea-level stand of approx. 85 ka is consistent with TIMS U-series data from the Worthing terrace on the west coast of Barbados. For this location, GALLUP et al. (1994), EDWARDS et al. (1997), and BARD et al. (1990b) reported approx. 83.3 ka, 82.8 ka, and 88.2 ka, respectively (Chapter 5). TOSCANO & LUNDBERG (1999) reported a MIS 5a sea-level stand of approx. -9 m below mean sea level (MSL) at 83 ka, and of approx. -15 to -11 m at 86.2 to 80.9 ka ago. This agrees well with the timing of the older MIS 5a-2 sea-level stand at Barbados, whereas the sea-level calculations differ by some meters. However, it conflicts with the assumption of LUDWIG et al. (1996) that sea level was close to that of the present at Bermuda at approx. 80 ka. CUTLER et al. (2003) recently presented data for a relatively high sea level (–24 m) approx. 76.2 ka ago (2 concordant TIMS U-series data). This correlates with the late MIS 5a-1 sea-level stand on Barbados.

Since Barbados experiences minimal glacio- or hydro-isostatic effects (PELTIER 2002), the palaeo sea levels calculated here should be close to ice-equivalent eustatic values. It is for this reason that Barbados has been the focus of research on palaeo sea levels. However, despite the excellent preservation of fossil coral reef terraces on southern Barbados, precise statements about the time and duration of palaeo sea level changes are necessarily limited by the resolution of available dating methods, as outlined in Chapter 4.1.

Table 4.3:
ESR dating results of Pleistocene coral samples from southern Barbados. See Figure 4.13 for site location.

Site	Lab. No.	Sample	Elev.	Depth		Ali.	D_{max}	Uranium		D'		D_E		ESR age	
			m asl.	cm	±	n	Gy	ppm	±	µGy/a	±	Gy	±	ka	±
IX-07	K-2383	B-92-2a	121	800	200	20	1780	2.45	0.07	918	53	376	21	**410**	**34**
IX-08	K-2385	B-92-3	121	500	300	20	1780	3.89	0.26	1408	103	509	71	**362**	**58**
IX-09	K-2380	B-92-1a	100	200	100	20	1780	3.33	0.39	1271	124	459	29	**361**	**42**
IX-09	K-2381	B-92-1b	100	200	100	20	1780	3.15	0.29	1211	99	436	33	**361**	**41**
IX-09	K-2382	B-92-1c	100	200	100	20	1780	2.80	0.14	1115	98	447	34	**401**	**47**
IX-09	K-2472	B-92-1b	100	200	100	20	1780	3.15	0.29	1210	101	435	29	**359**	**38**
IX-10	K-3011	B-96-4-1	104	300	30	20	1068	3.75	0.35	1362	114	446	32	**327**	**36**
IX-10	K-3012	B-96-4-2	104	270	30	20	1068	3.02	0.54	1131	152	374	25	**331**	**50**
IX-10	K-3013	B-96-4-3	104	320	30	20	1068	2.46	0.21	967	76	367	48	**381**	**58**
IX-10	K-3014	B-96-4-4	104	240	20	20	1068	3.25	0.08	1222	65	417	41	**341**	**38**
IX-10	K-3015	B-96-4-5	104	270	30	20	1068	4.35	0.15	1546	87	482	24	**312**	**23**
IX-25	K-3207	B-99-47-1	110	100	50	20	534	2.92	0.13	1121	63	348	13	**310**	**21**
XI-01	K-3182	B-99-38-1	1	50	30	20	267	3.19	0.14	776	37	51	2	**66**	**4**
XI-01	K-3185	B-99-38-4	1	50	30	20	267	3.29	0.20	507	42	56	3	**70**	**5**
XI-02	D-2387	B-92-4a-II	13	200	100	20	1780	3.30	0.14	872	63	88	8	**102**	**12**
XI-02	D-2388	B-92-4b-I	13	200	100	20	1780	3.30	0.14	890	66	96	3	**108**	**9**
XI-02	K-2386	B-92-4a-I	13	200	100	20	1780	3.86	0.08	994	45	102	4	**102**	**6**
XI-02	K-2389	B-92-4b-II	13	200	100	20	1780	3.93	0.47	997	86	99	2	**99**	**9**
XI-03	D-2398	B-92-8	17	100	50	19	1780	3.30	0.14	891	63	89	5	**100**	**9**
XI-04	D-2245	BG-90-8	4	100	50	20	668	3.14	0.16	770	39	55	3	**72**	**5**
XI-04	K-1934	BG-90-8	4	100	50	20	445	3.38	0.18	789	40	51	2	**65**	**4**
XI-04	K-1935	BG-90-9	4	100	50	20	445	2.85	0.07	713	31	51	2	**71**	**4**
XI-04	K-1936	BG-90-10	4	100	50	20	445	3.03	0.25	754	46	55	1	**73**	**5**
XI-04	K-1937	BG-90-11	4	100	50	20	445	2.99	0.16	732	37	50	2	**69**	**5**
XI-04	K-1938	BG-90-12	4	100	50	20	445	3.13	0.39	761	63	53	2	**70**	**6**
XI-04	K-1939	BG-90-13	4	100	50	20	445	3.09	0.30	761	53	55	1	**72**	**5**
XI-04	K-3057	B-96-33-1	4	100	50	20	356	3.53	0.35	841	60	60	4	**71**	**7**
XI-04	K-3058	B-96-33-2	4	100	50	20	356	3.35	0.21	811	44	58	4	**72**	**6**
XI-04	K-3059n	B-96-34-1	4	100	50	20	178	3.15	0.21	772	43	55	2	**72**	**5**
XI-04	K-3060n	B-96-34-2	4	50	20	20	178	3.20	0.28	760	53	52	2	**68**	**6**
XI-05	K-1942	BG-90-15a	18	200	100	19	356	2.88	0.17	774	43	77	2	**99**	**7**
XI-05	K-1943	BG-90-15b	18	200	100	20	445	3.15	0.07	820	36	78	2	**95**	**6**
XI-05	K-1943b	BG-90-15b	18	200	100	20	178	3.15	0.07	824	37	79	3	**96**	**6**
XI-05	K-1944	BG-90-15c	18	200	100	20	445	3.23	0.16	842	61	81	3	**96**	**8**
XI-05	K-3352	B-99-69-1	17	50	30	20	267	3.18	0.10	871	38	84	2	**97**	**5**
XI-05	K-3354	B-99-69-3	17	200	50	20	267	3.03	0.28	791	54	74	3	**93**	**7**
XI-05	K-3355	B-99-69-4	17	450	50	20	267	3.83	0.13	884	42	75	2	**85**	**5**
XI-05	K-3356	B-99-69-5	17	650	50	20	267	3.63	0.35	874	67	89	3	**101**	**8**
XI-06	K-3061n	B-96-35-1	18	800	50	19	178	3.57	0.38	820	68	76	3	**93**	**8**
XI-06	K-3063n	B-96-35-3	18	800	50	20	178	3.35	0.07	770	37	70	3	**92**	**6**
XI-07	D-2191	B-91-22-1	34	200	100	20	668	3.62	0.18	995	76	119	6	**120**	**11**
XI-07	K-2193	B-91-22-3	34	200	100	20	668	3.66	0.18	1013	76	124	7	**123**	**12**
XI-08	D-2194	B-91-23	39	200	100	20	668	3.43	0.17	986	74	131	9	**133**	**14**
XI-10	D-2189	B-91-21-1	46	400	100	20	668	2.65	0.13	866	70	172	18	**199**	**26**
XI-10	D-2190	B-91-21-2	46	400	100	20	668	3.23	0.16	1036	84	211	19	**204**	**25**
XI-11	D-2185	B-91-19-2	46	300	200	20	668	2.80	0.14	948	76	205	20	**217**	**28**
XI-11	D-2186	B-91-19-3	46	300	150	20	668	2.88	0.15	963	76	203	14	**210**	**23**
XI-11	K-2184	B-91-19-1	46	300	200	20	668	2.70	0.14	894	70	176	14	**197**	**23**
XI-12	K-2069	BG-90-80-1	35	150	50	20	445	3.06	0.32	887	67	110	3	**124**	**10**
XI-13	K-2070	BG-90-80-2	39	150	50	20	445	3.35	0.66	934	117	109	3	**116**	**15**
XI-14	D-2205	B-91-28-2	50	300	100	20	668	2.84	0.14	932	73	183	14	**196**	**22**
XI-14	K-2204	B-91-28-1	50	300	100	20	668	2.84	0.14	943	74	192	9	**204**	**19**
XI-15	D-2195	B-91-24-1	70	300	100	20	668	3.03	0.15	1017	82	223	22	**219**	**28**
XI-15	K-2066	BG-90-78a	70	200	50	20	445	3.18	0.16	1094	88	251	7	**229**	**20**
XI-15	K-2067	BG-90-78b	70	200	50	20	445	3.12	0.16	1082	86	252	9	**233**	**21**
XI-15	K-3064	B-96-36-1	70	100	10	20	534	3.80	0.28	1280	86	278	15	**217**	**21**
XI-15	K-3066	B-96-36-3	70	100	10	20	534	3.50	0.18	1156	61	225	13	**195**	**16**
XI-16	D-2197	B-91-25-1	80	300	100	20	668	3.82	0.19	1351	116	398	50	**295**	**45**
XI-16	D-2198	B-91-25-2	80	300	100	20	668	3.13	0.15	1125	94	323	18	**287**	**29**
XI-16	D-2199	B-91-25-3	80	300	100	20	668	3.36	0.17	1195	101	341	29	**285**	**34**
XI-16	D-2200	B-91-25-4	80	300	100	20	668	3.27	0.16	1181	102	355	40	**300**	**42**
XI-17	D-2208	B-91-29-2	70	100	50	20	668	2.83	0.14	998	77	215	19	**215**	**26**

Table 4.3 continued:

Site	Lab. No.	Sample	Elev.	Depth		Ali.	D_{max}	Uranium		D'		D_E		ESR age	
			m asl.	cm	±	n	Gy	ppm	±	µGy/a	±	Gy	±	ka	±
XI-17	K-2207	B-91-29-1	70	100	50	20	668	2.84	0.14	1006	77	220	16	**219**	**23**
XI-18	D-2229	B-91-39-2	84	300	100	20	668	2.93	0.15	1062	16	305	37	**288**	**42**
XI-19	K-3067	B-96-37-1	82	150	20	20	534	3.00	0.57	1110	92	313	23	**282**	**43**
XI-19	K-3068	B-96-37-2	82	170	20	20	534	3.04	0.05	1147	57	362	16	**315**	**21**
XI-20	K-3069	B-96-37-3	84	150	20	20	534	2.90	0.28	1125	93	383	37	**341**	**43**
XI-21	D-2215	B-91-31-2	10	100	50	20	668	3.51	0.16	1031	77	139	8	**134**	**13**
XI-21	D-2216	B-91-31-3	10	100	50	20	668	3.47	0.16	966	71	110	8	**113**	**12**
XI-21	K-2006	BG-90-44a	10	200	40	20	445	3.79	0.44	998	82	108	7	**108**	**11**
XI-21	K-2007v	BG-90-44b	10	200	40	20	445	4.05	0.21	1044	57	109	4	**105**	**13**
XI-21	K-2008	BG-90-44c	10	200	40	20	445	3.74	0.80	988	135	107	5	**108**	**16**
XI-21	K-2008v	BG-90-44c	10	200	40	20	445	3.74	0.80	1003	138	114	6	**113**	**17**
XI-21	K-2214	B-91-31-1	10	100	50	20	668	3.83	0.64	1024	111	108	7	**106**	**13**
XI-22	K-2003	BG-90-43a	23	100	20	20	445	3.41	0.16	960	48	111	4	**116**	**7**
XI-22	K-2004	BG-90-43b	23	100	20	20	445	3.31	0.13	927	44	104	4	**112**	**7**
XI-22	K-2005	BG-90-43c	23	100	20	20	445	2.99	0.16	867	45	102	4	**117**	**8**
XI-23	K-2217	B-91-32-1	21	100	50	20	668	3.24	0.16	897	65	96	5	**107**	**9**
XI-26	K-2221	B-91-35-1	35	300	100	20	668	2.99	0.15	859	65	114	7	**133**	**14**
XI-26	K-2222	B-91-35-2	35	300	100	20	668	3.06	0.15	856	63	106	5	**124**	**11**
XI-27	K-3053v	B-96-31-1	37	100	10	20	623	3.20	0.16	840	60	112	5	**133**	**11**
XI-27	K-3054i	B-96-31-2	37	200	20	20	312	3.20	0.28	921	64	119	8	**129**	**13**
XI-28	K-2202	B-91-27-1	38	300	100	20	668	2.67	0.13	894	70	182	5	**203**	**17**
XI-28	K-2203	B-91-27-2	38	300	100	20	668	2.82	0.14	925	73	181	6	**196**	**17**
XI-29	K-2201	B-91-26-1	45	300	100	20	668	2.94	0.15	1014	215	241	15	**238**	**53**
XI-30	D-2223	B-91-36-1	72	400	200	20	668	3.01	0.15	1076	92	315	37	**292**	**43**
XI-30	K-2224	B-91-36-2	72	400	200	20	668	3.10	0.16	1025	84	227	9	**222**	**21**
XI-31	K-2226	B-91-38-1	71	400	200	20	668	3.18	0.16	1042	86	226	13	**217**	**22**
XI-31	K-2227	B-91-38-2	71	400	200	20	668	3.03	0.15	995	82	213	16	**214**	**25**
XI-31	K-4162	B-00-23-1	73	300	30	20	890	3.46	0.20	1200	75	314	9	**262**	**18**
XI-31	K-4163	B-00-23-2	73	100	20	20	890	2.72	0.03	1035	49	293	14	**283**	**19**
XI-31	K-4164	B-00-23-3	73	400	40	20	890	3.79	0.04	1283	64	334	7	**260**	**14**
XI-31	K-4165	B-00-23-4	73	400	40	20	890	3.04	0.09	1085	59	317	11	**292**	**19**
XI-32	K-2225	B-91-37	72	400	200	20	668	3.42	0.17	1199	103	342	10	**286**	**26**
XI-33	D-2166	B-91-12-1	47	300	100	20	668	3.06	0.15	1017	81	216	11	**212**	**20**
XI-33	D-2167	B-91-12-2	47	300	100	20	668	2.70	0.13	898	71	180	8	**200**	**19**
XI-33	D-2168	B-91-12-3	47	300	100	20	668	2.74	0.14	927	73	198	11	**214**	**21**
XI-34	K-2732	B-94-2-1	2.5	30	20	20	1246	3.27	0.23	876	50	76	3	**87**	**6**
XI-34	K-2733	B-94-2-2	2.5	30	20	20	1246	3.38	0.11	906	40	81	3	**89**	**5**
XI-34	K-2735	B-94-2-4	2.5	30	20	20	1246	2.92	0.30	820	57	76	3	**93**	**7**
XI-34	K-2736	B-94-2-5	2.5	30	20	20	1246	3.88	0.17	1054	52	108	3	**103**	**6**
XI-34	K-2737	B-94-2-6	2.5	30	20	20	1246	3.48	0.40	913	71	83	2	**89**	**7**
XI-34	K-3055	B-96-32-1	2.5	80	8	20	623	3.15	0.49	821	87	90	4	**103**	**11**
XI-34	K-3056	B-96-32-2	2.5	75	0	20	623	2.67	0.33	756	61	74	4	**98**	**10**
XI-35	K-2726	B-94-1-1	1	80	40	20	1246	2.86	0.05	465	18	1.7	0.04	**3.7**	**0.2**
XI-35	K-2727	B-94-1-2	1	80	40	20	1246	3.82	0.45	550	47	1.34	0.06	**2.5**	**0.2**
XI-35	K-2728	B-94-1-3	1	80	40	46	470	3.50	0.28	517	34	1.09	0.02	**2.1**	**0.2**
XI-35	K-2729	B-94-1-4	1	80	40	20	1246	3.08	0.67	488	66	2.03	0.08	**4.2**	**0.6**
XI-35	K-3083	B-94-1-6	1	100	10	20	623	2.74	0.23	455	28	2.42	0.14	**5.3**	**0.5**
XI-36	K-3033	B-96-25-1	9	250	20	20	623	3.66	0.37	916	69	86	5	**94**	**9**
XI-36	K-3035	B-96-25-3	9	250	30	20	623	3.42	0.12	842	45	74	3	**87**	**6**
XI-36	K-3036	B-96-25-4	9	250	20	20	623	2.89	0.40	778	72	80	3	**103**	**10**
XI-37	K-1947	BG-90-18a	10	100	50	20	445	3.05	0.21	833	48	82	3	**99**	**7**
XI-37	K-1948	BG-90-18b	10	100	50	20	445	3.31	0.55	882	94	85	4	**97**	**11**
XI-37	K-3001	B-96-1-1	10	100	10	20	623	3.75	0.78	963	126	90	2	**93**	**12**
XI-37	K-3002	B-96-1-2	10	200	20	20	623	3.15	0.35	850	66	90	4	**105**	**9**
XI-38	K-1945	BG-90-16	10	100	50	20	445	3.39	0.16	925	48	98	4	**105**	**7**
XI-39	D-2246	BG-90-17	5	100	50	20	668	3.15	0.11	868	40	90	10	**104**	**13**
XI-39	K-1946	BG-90-17	5	100	50	20	445	3.29	0.30	872	58	82	4	**94**	**8**
XI-40	D-2172	B-91-13-1	39	100	50	20	668	3.31	0.16	949	68	114	11	**121**	**14**
XI-40	D-2172A	B-91-13-1	39	100	50	20	668	3.31	0.16	910	70	117	14	**122**	**17**
XI-40	D-2173	B-91-13-2	39	100	50	20	668	3.31	0.12	959	45	119	7	**125**	**9**
XI-40	D-2242	BG-90-20b	39	400	100	20	668	4.07	0.20	442	58	118	8	**113**	**10**
XI-40	D-2247	BG-90-20c	39	800	100	20	668	4.04	0.01	995	46	115	7	**115**	**9**

Table 4.3 continued:

Site	Lab. No.	Sample	Elev.	Depth		Ali.	D_{max}	Uranium		D'		D_E		ESR age	
			m asl.	cm	±	n	Gy	ppm	±	µGy/a	±	Gy	±	ka	±
XI-40	K-1952	BG-90-20a	39	400	100	20	445	3.25	0.22	871	53	103	4	**119**	**9**
XI-40	K-1953	BG-90-20b	39	400	100	20	445	2.93	0.15	815	63	103	3	**127**	**11**
XI-40	K-1954	BG-90-20c	39	800	100	19	356	4.17	0.18	1023	55	117	5	**115**	**8**
XI-40	K-2456	B-91-13-2	39	100	50	40	1780	3.35	0.17	982	72	128	5	**130**	**11**
XI-40	K-3003	B-96-2-1	39	200	20	20	623	3.40	0.17	968	73	125	5	**129**	**11**
XI-40	K-3004	B-96-2-2	39	200	20	20	623	3.54	0.08	980	44	119	8	**121**	**10**
XI-40	K-3005	B-96-2-3	39	200	20	20	623	3.25	0.35	927	73	118	5	**127**	**11**
XI-40	K-3006	B-96-2-3	39	200	20	20	623	2.92	0.16	851	46	109	5	**128**	**9**
XI-40	K-3007	B-96-2-F	39	200	20	20	623	3.73	0.19	1014	90	119	5	**117**	**11**
XI-41	K-1955	BG-90-21a	41	30	10	20	445	2.63	0.13	840	58	109	5	**129**	**11**
XI-41	K-1956	BG-90-21b	41	30	10	20	445	2.99	0.01	901	37	107	5	**119**	**8**
XI-42	K-1949	BG-90-19a	43	100	50	20	445	3.17	0.05	950	41	128	8	**135**	**11**
XI-42	K-1950	BG-90-19b	43	100	50	20	445	3.39	0.30	971	66	119	10	**122**	**10**
XI-42	K-1951	BG-90-19c	43	100	50	20	445	3.17	0.29	877	38	106	5	**121**	**8**
XI-42	K-3090v	BG-90-19c	43	100	10	20	623	3.09	0.01	903	37	111	5	**123**	**7**
XI-43	K-2174	B-91-14-1	52	400	200	20	668	2.94	0.15	959	77	198	16	**207**	**24**
XI-43	K-2175	B-91-14-2	52	400	200	20	668	3.01	0.26	1055	86	216	9	**218**	**20**
XI-43	K-2460	B-91-14-2	52	400	200	20	1780	3.00	0.15	993	81	217	9	**219**	**21**
XI-43	K-3092	B-91-14-2	52	400	40	20	1068	2.97	0.04	988	48	220	14	**222**	**18**
XI-45	D-2177	B-91-15-2	62	500	200	20	668	3.49	0.17	1126	94	250	19	**222**	**25**
XI-45	D-2178	B-91-15-3	62	500	200	20	668	2.82	0.11	930	50	206	19	**221**	**25**
XI-46	K-1959	BG-90-23a	64	100	20	20	445	3.46	0.17	1178	93	253	10	**215**	**19**
XI-46	K-1960	BG-90-23b	64	100	20	20	445	2.81	0.04	989	44	211	6	**213**	**11**
XI-46	K-1961	BG-90-24a	64	100	20	20	445	2.66	0.27	956	74	211	11	**221**	**21**
XI-46	K-1962	BG-90-24b	64	100	20	20	445	4.61	0.23	1473	119	292	18	**198**	**20**
XI-46	K-3030	B-96-23-2	64	200	20	20	1068	3.57	0.09	1197	60	266	20	**222**	**20**
XI-46	K-3031	B-96-23-3	64	180	10	20	1068	3.47	0.18	1190	69	278	16	**233**	**19**
XI-46	K-3042	B-96-27-1	64	130	10	20	1068	3.35	0.21	1151	72	256	15	**223**	**19**
XI-46	K-3043	B-96-27-2	64	150	10	20	1068	3.57	0.24	1179	70	240	14	**203**	**17**
XI-47	K-1964	BG-90-26a	70	150	20	20	445	3.80	0.59	1266	142	274	14	**216**	**27**
XI-47	K-1965	BG-90-26b	70	150	20	20	445	4.14	0.84	1393	198	323	14	**232**	**35**
XI-48	K-1966	BG-90-27a	89	30	10	20	445	3.62	0.40	1323	114	346	28	**262**	**31**
XI-48	K-1967	BG-90-27b	89	30	10	20	445	2.93	0.15	1145	92	340	13	**297**	**27**
XI-49	D-2164	B-91-10-1	92	300	100	20	668	3.09	0.04	1152	58	385	19	**334**	**24**
XI-49	D-2165	B-91-10-2	92	300	100	20	668	3.11	0.16	1158	101	387	36	**334**	**43**
XI-50	K-1963	BG-90-25	72	50	10	20	445	2.62	0.42	956	103	208	7	**218**	**25**
XI-52	D-2182	B-91-16-4	83	800	300	20	668	3.61	0.18	1252	115	407	22	**325**	**35**
XI-52	K-3044v	B-96-28-1	83	450	40	20	1068	3.15	0.07	1095	57	301	14	**275**	**27**
XI-52	K-3045	B-96-28-2	83	450	50	20	1068	3.34	0.23	1125	77	279	15	**250**	**19**
XI-52	K-3046v	B-96-28-3	83	450	50	20	1068	3.16	0.06	1104	56	309	16	**280**	**20**
XI-53	K-3047v	B-96-29-1	85	100	10	20	1068	3.45	0.35	1252	104	340	17	**272**	**26**
XI-53	K-3048v	B-96-29-2	85	100	10	20	1068	3.17	0.23	1158	78	307	10	**265**	**20**
XI-53	K-3049	B-96-29-3	85	250	20	20	1068	3.02	0.26	1059	79	263	9	**249**	**21**
XI-54	K-3050	B-96-30-1	100	250	20	20	1068	3.47	0.09	1274	69	408	24	**321**	**34**
XI-54	K-3051	B-96-30-2	100	250	20	20	1068	3.03	0.10	1141	98	380	27	**333**	**37**
XI-55	D-2169	B-91-11-1	105	500	200	20	668	3.83	0.19	1367	123	460	27	**337**	**37**
XI-55	K-2170	B-91-11-2	105	500	200	20	668	3.52	0.18	1269	114	433	43	**342**	**46**
XI-56	D-2249	BG-90-28a	103	400	100	20	668	3.27	0.51	1191	146	392	30	**329**	**48**
XI-56	K-1968	BG-90-28a	103	400	40	20	445	3.42	0.72	1250	111	426	22	**341**	**35**
XI-56	K-1969	BG-90-28b	103	400	40	20	445	4.28	0.36	1455	114	401	48	**276**	**40**
XI-57	K-1973	BG-90-30a	110	300	30	20	445	3.19	0.16	1158	99	350	19	**302**	**31**
XI-57	K-1974	BG-90-30b	110	300	30	20	445	3.10	0.15	1133	98	348	19	**307**	**32**
XI-58	D-2252	BG-90-29c	100	600	200	20	668	3.15	0.00	1152	61	424	48	**368**	**46**
XI-58	K-1971	BG-90-29b	100	500	50	20	445	2.63	0.13	983	88	348	26	**354**	**41**
XI-58	K-1972	BG-90-29c	100	500	50	20	445	3.15	0.16	1160	105	418	14	**360**	**35**
XI-59	K-3187	B-99-39-1	2	80	30	20	267	3.36	0.28	896	58	86	4	**96**	**8**
XI-59	K-3188	B-99-39-2	2	80	30	25	490	3.47	0.25	874	51	72	3	**82**	**6**
XI-62	K-2071	BG-90-81	20	150	50	20	445	3.16	0.57	885	102	101	3	**114**	**14**
XI-63	K-1940	BG-90-14a	4	100	50	20	445	3.43	0.38	805	62	54	3	**67**	**6**
XI-63	K-1940b	BG-90-14a	4	100	50	20	445	3.43	0.38	805	62	56	3	**72**	**7**
XI-63	K-1940v	BG-90-14a	4	100	50	20	178	3.43	0.38	818	63	57	2	**70**	**6**
XI-64	D-2187	B-91-20-1	45	200	100	20	668	2.97	0.15	1013	81	217	20	**214**	**27**

Table 4.3 continued:

Site	Lab. No.	Sample	Elev.	Depth		Ali.	D_{max}	Uranium		D'		D_E		ESR age	
			m asl.	cm	±	n	Gy	ppm	±	µGy/a	±	Gy	±	ka	±
XI-64	D-2188	B-91-20-2	45	200	100	20	668	2.98	0.15	982	76	187	15	**190**	**21**
XI-64	K-2068	BG-90-79	45	200	50	20	445	3.15	0.33	999	79	173	4	**173**	**14**
XI-65	K-3037	B-96-26-1	3	20	10	20	623	2.69	0.13	775	35	68	3	**88**	**6**
XI-65	K-3038w	B-96-26-2	3	20	10	20	623	2.57	0.17	744	45	63	4	**85**	**8**
XI-65	K-3039	B-96-26-3	3	20	10	20	623	3.60	0.18	957	69	82	5	**81**	**7**
XI-65	K-3040w	B-96-26-4	3	20	10	20	623	3.39	0.12	908	41	78	3	**85**	**5**
XI-65	K-4183	B-00-27-1	3	150	20	20	267	2.63	0.07	673	28	49	2	**74**	**4**
XI-65	K-4184	B-00-27-2	3	150	20	20	267	3.60	0.09	868	37	66	2	**77**	**4**
XI-65	K-4185	B-00-27-3	3	150	20	20	267	3.10	0.06	775	32	60	2	**78**	**4**
XI-65	K-4186	B-00-27-4	3	150	20	20	267	2.90	0.01	749	30	61	4	**82**	**6**
XI-65	K-4187	B-00-27-5	3	150	20	20	267	3.15	0.04	789	33	62	2	**79**	**4**
XI-67	K-1975	BG-90-31	112	100	30	20	445	2.73	0.14	1084	90	374	23	**345**	**36**
XI-68	D-2254	BG-90-32a	102	100	100	20	668	2.64	0.15	1079	68	422	34	**391**	**41**
XI-68	D-2255	BG-90-32b	102	100	100	20	668	3.71	0.23	1453	101	593	56	**408**	**49**
XI-68	K-1976	BG-90-32a	102	100	50	20	445	2.64	0.15	1008	61	283	21	**281**	**27**
XI-68	K-1977	BG-90-32b	102	100	100	20	445	3.83	0.40	1469	134	546	35	**372**	**42**
XI-72	K-1957	BG-90-22a	53	100	20	20	445	3.24	0.16	1081	83	209	25	**193**	**27**
XI-72	K-1958	BG-90-22b	53	100	20	20	445	3.24	0.16	1073	83	202	10	**188**	**17**
XI-72	K-3091	BG-90-22b	53	200	20	20	1068	2.85	0.07	988	48	219	12	**222**	**16**
XI-73	K-3009	B-96-3-2	90	200	20	20	1068	3.80	0.01	1355	66	388	28	**286**	**25**
XI-73	K-3010	B-96-3-3	90	200	20	20	1068	4.46	0.23	1549	96	429	31	**277**	**26**
XI-74	K-3145	B-99-1	12	200	30	20	267	3.50	0.30	905	61	89	3	**98**	**8**
XI-75	K-3360	B-99-71-2	8	50	30	20	267	3.77	0.28	891	53	61	2	**69**	**5**
XI-75	K-3361	B-99-71-3	8	50	30	20	267	3.49	0.25	856	49	62	3	**73**	**5**
XI-76	K-3350	B-99-68-1	2	20	10	20	267	3.42	0.11	869	38	63	3	**72**	**5**
XI-78	K-2746	B-94-7	2	30	10	20	1246	3.37	0.33	841	57	59	3	**71**	**6**
XI-78	K-4064	B-00-01-1	1	50	10	20	267	3.41	0.23	1064	48	60	3	**71**	**6**
XI-78	K-4304	B-00-01*1	1	15	5	20	267	2.44	0.12	703	31	53	2	**75**	**5**
XI-78	K-4305	B-00-01*2	1	15	5	20	267	2.58	0.21	724	41	53	3	**73**	**6**
XI-78	K-4306	B-00-01*3a	1	15	5	20	267	2.40	0.15	686	33	49	3	**71**	**5**
XI-78	K-4307	B-00-01*4	1	15	5	20	267	2.27	0.11	663	29	47	1	**72**	**4**
XI-78	K-4308	B-00-01*5	1	15	5	20	267	2.26	0.13	664	30	48	2	**73**	**5**
XI-78	K-4309	B-00-01*6	1	15	5	20	267	2.39	0.23	689	42	50	2	**73**	**5**
XI-78	K-4310	B-00-01*7	1	50	10	20	267	2.51	0.03	665	25	47	1	**70**	**3**
XI-78	K-4311	B-00-01*8	1	15	5	20	267	2.93	0.03	786	29	56	2	**71**	**4**
XI-78	K-4312	B-00-01*10	1	15	5	20	267	2.23	0.07	653	25	46	1	**71**	**4**
XI-78	K-4313	B-00-01*11	1	15	5	20	267	3.77	0.19	957	47	72	3	**75**	**5**
XI-78	K-4314	B-00-01*12	1	15	5	20	267	3.37	0.17	872	41	63	2	**73**	**4**
XI-78	K-4316	B-00-01*14	1	30	5	20	267	3.39	0.17	864	42	60	2	**71**	**4**
XI-80	K-4149	B-00-19-3	4	300	30	20	267	2.65	0.13	692	36	65	2	**93**	**5**
XI-80	K-4150	B-00-19-4	4	300	30	20	267	2.68	0.13	694	37	64	3	**92**	**6**
XI-80	K-4151	B-00-19-5	4	300	30	20	267	2.51	0.13	668	35	64	2	**96**	**6**
XI-80	K-4152	B-00-19-6	4	300	30	20	267	3.02	0.16	753	40	66	3	**88**	**6**
XI-80	K-4154	B-00-19-8	4	50	20	20	267	2.45	0.14	687	34	58	2	**84**	**5**
XI-81	K-4142	B-00-18-1	20	300	100	20	267	3.06	0.15	267	43	97	8	**116**	**8**
XI-82	K-4167	B-00-25-1	95	250	50	20	890	3.75	0.02	1301	63	342	18	**263**	**16**
XI-82	K-4168	B-00-25-2	95	250	50	20	890	3.60	0.26	1305	94	403	18	**309**	**26**
XI-82	K-4169n	B-00-25-3	95	250	50	20	890	3.17	0.15	1160	69	349	14	**301**	**22**
XI-82	K-4170	B-00-25-4	95	250	50	20	890	2.65	0.01	1001	48	310	16	**310**	**22**
XI-83	K-4136	B-00-17-3	20	700	30	20	267	2.55	0.09	717	36	102	3	**142**	**8**
XI-83	K-4137	B-00-17-4	20	700	30	20	267	2.28	0.05	643	30	89	4	**138**	**9**
XI-83	K-4140	B-00-17-7	20	600	30	20	267	2.56	0.16	681	41	80	4	**117**	**9**
XI-83	K-4141	B-00-17-8	20	250	50	20	267	2.57	0.13	267	38	89	5	**120**	**9**
XI-84	K-4156	B-00-20	77	100	20	20	890	3.39	0.17	1216	70	313	5	**263**	**16**
XI-85	K-4157	B-00-21	70	250	50	20	890	3.80	0.06	1347	68	388	13	**288**	**18**
XI-86	K-4158	B-00-22-1	70	200	20	20	890	3.05	0.08	1105	56	300	14	**274**	**19**
XI-86	K-4159	B-00-22-2	70	200	20	20	890	3.34	0.13	1153	62	274	10	**238**	**15**
XI-86	K-4161	B-00-22-4	70	200	20	20	890	2.95	0.18	1051	64	262	9	**250**	**17**
XII-03	K-1986	BG-90-36a	13	700	100	20	445	3.54	0.08	985	117	188	8	**191**	**24**

Table 4.3 continued:

Site	Lab. No.	Sample	Elev.	Depth		Ali.	D_{max}	Uranium		D'		D_E		ESR age	
			m asl.	cm	±	n	Gy	ppm	±	µGy/a	±	Gy	±	ka	±
XII-03	K-1987	BG-90-36b	13	700	100	20	445	3.34	0.27	1048	77	225	10	**215**	**19**
XII-03	K-1988	BG-90-36c	13	700	100	20	445	3.12	0.15	980	83	208	7	**212**	**19**
XII-03	K-1989	BG-90-36d	13	250	50	20	445	3.54	0.17	925	48	97	3	**105**	**6**
XII-03	K-1990	BG-90-36e	13	250	50	20	445	3.45	0.21	904	52	95	3	**105**	**7**
XII-03	K-1991	BG-90-36f	13	250	50	20	445	3.63	0.43	940	80	98	3	**104**	**10**
XII-03	K-3273A	B-99-57-5	13.5	630	30	50	2670	5.07	0.16	1113	56	95	4	**86**	**6**
XII-03	K-3274x	B-99-57-6	13.5	690	30	50	2670	3.84	0.16	926	49	97	2	**105**	**6**
XII-03	K-3276	B-99-57-8	13.5	660	30	20	534	4.03	0.06	970	45	100	4	**103**	**6**
XII-03	K-3280	B-99-57-12	13.5	1030	30	20	534	3.17	0.24	963	69	200	10	**208**	**18**
XII-03	K-3282	B-99-57-14	13.5	470	30	20	534	3.67	0.10	853	42	87	4	**97**	**7**
XII-03	K-3283x	B-99-57-15	13.5	390	30	50	2670	3.72	0.25	906	56	86	3	**95**	**7**
XII-03	K-3284	B-99-57-16	13.5	300	30	20	534	3.38	0.13	864	43	87	3	**101**	**6**
XII-03	K-3285x	B-99-57-17	13.5	60	30	50	2670	3.50	0.71	918	115	84	3	**92**	**12**
XII-04	D-2257	BG-90-37a	22	200	100	20	668	3.08	0.09	1024	51	205	19	**200**	**21**
XII-04	D-2258	BG-90-37b	22	300	100	20	668	3.03	0.09	980	48	189	20	**193**	**23**
XII-04	K-1992	BG-90-37a	22	100	50	20	445	3.32	0.25	1114	74	222	9	**199**	**16**
XII-04	K-1993	BG-90-37b	22	100	50	20	445	3.38	0.59	1116	133	213	19	**191**	**28**
XII-04	K-3262	B-99-56-2	29	50	30	26	534	3.47	0.21	1189	70	249	10	**210**	**15**
XII-05	K-1994	BG-90-38a	39	50	20	20	445	3.00	0.15	1011	75	182	2	**180**	**14**
XII-05	K-1995	BG-90-38b	39	50	20	20	445	3.33	0.17	1080	81	183	6	**170**	**14**
XII-05	K-3252	B-99-55-1	39	100	50	20	267	3.00	0.08	993	46	178	19	**179**	**21**
XII-05	K-3254	B-99-55-3	39	100	50	26	534	3.19	0.00	1048	46	190	12	**182**	**14**
XII-06	K-2745	B-94-6	13	30	10	20	1246	2.80	0.14	817	55	83	3	**101**	**8**
XII-07	K-2390	B-92-5a	13	100	50	20	1780	3.49	0.13	934	44	94	4	**101**	**6**
XII-07	K-2391	B-92-5b	13	100	50	20	1780	3.88	0.54	1000	93	96	4	**96**	**10**
XII-07	K-3078	B-96-42-2	13	400	40	20	356	3.80	0.28	925	60	89	5	**96**	**8**
XII-07	K-3079	B-96-42-3	13	20	10	20	356	3.55	0.35	942	66	81	5	**86**	**8**
XII-07	K-3080	B-96-43-1	13	500	50	20	356	3.32	0.12	808	40	77	4	**96**	**7**
XII-07	K-3081	B-96-43-2	13	20	10	20	356	3.10	0.42	809	78	92	6	**102**	**9**
XII-07	K-3296	B-99-61-3	11.5	870	20	20	267	3.59	0.28	830	57	80	2	**97**	**7**
XII-07	K-3297	B-99-61-4	11.5	830	20	20	267	3.00	0.14	730	40	76	3	**105**	**7**
XII-07	K-3307x	B-99-61-14	11.5	110	30	50	2670	2.56	0.08	740	33	78	3	**105**	**6**
XII-07	K-3310x	B-99-61-17	11.5	170	30	50	2670	3.04	0.14	810	40	79	2	**97**	**5**
XII-07	K-3311	B-99-61-18	11.5	390	20	20	267	3.57	0.06	883	39	86	2	**98**	**5**
XII-07	K-3312x	B-99-61-19	11.5	90	20	50	2670	3.72	0.45	949	80	86	2	**90**	**8**
XII-07	K-3313	B-99-61-20	11.5	90	20	20	267	2.96	0.24	785	50	75	3	**93**	**7**
XII-07	K-3314x	B-99-61-21	11.5	50	20	50	2670	3.01	0.38	819	68	75	2	**91**	**8**
XII-07	K-3315x	B-99-61-22	11.5	90	20	50	2670	3.38	0.18	870	44	76	3	**87**	**5**
XII-07	K-4065A	B-00-02-1	11.5	1100	50	20	267	2.89	0.15	773	36	121	4	**153**	**10**
XII-08	K-2392	B-92-6a	29	100	50	20	1780	2.90	0.15	1041	82	243	9	**234**	**21**
XII-08	K-2394	B-92-6c	29	100	50	20	1780	2.91	0.16	1022	58	221	10	**216**	**16**
XII-08	K-3076	B-96-41	29	100	20	20	356	3.26	0.06	1061	49	189	11	**178**	**13**
XII-08	K-3317	B-99-62-2	22	60	20	20	267	3.41	0.02	1112	49	189	13	**178**	**12**
XII-09	D-2396	B-92-7a	41	100	50	20	1780	2.80	0.14	864	63	118	7	**136**	**13**
XII-09	D-2397	B-92-7b	41	100	50	20	1780	3.30	0.18	908	66	97	4	**106**	**9**
XII-09	K-2738	B-94-3-1	41	100	50	20	1246	3.24	0.25	1012	65	157	7	**155**	**12**
XII-09	K-2739	B-94-3-2	41	100	50	20	1246	3.03	0.13	845	40	88	3	**105**	**6**
XII-09	K-2740	B-94-3-3	41	100	50	20	1246	2.99	0.41	983	94	172	7	**175**	**18**
XII-09	K-3321	B-99-63-2	41	400	100	26	534	2.93	0.25	925	67	172	8	**186**	**16**
XII-09	K-3322	B-99-63-7	41	400	100	20	267	2.94	0.21	965	65	204	9	**212**	**17**
XII-12	K-3288	B-99-59-1	19	50	30	26	534	3.44	0.17	1157	89	226	6	**195**	**16**
XII-12	K-3289	B-99-59-2	19	50	30	20	267	3.18	0.17	1060	59	191	9	**181**	**13**

5. Chronostratigraphical results from selected localities of Barbados (west, north, southeast coast, and central part)

U. RADTKE & G. SCHELLMANN

Last but not least, Chapter 5 presents some preliminary chronostratigraphical results from localities outside our main research area of southern Barbados. At this stage of our investigations we cannot yet draw a complete picture of the distribution and facies geometry of coral reef terraces in these parts of the island. However, some ESR dating results and initial morpho- and sedimentological evidence are presented here, which give some insight on the distribution, elevations, and ages of coral reef terraces in these areas of Barbados.

5.1. West coast of Barbados: Clermont Nose standard traverse

Coral reef terraces stretch roughly south to north along the west coast of Barbados between Batts Rock Bay (Clermont Nose standard traverse north of Bridgetown) and Speightstown. They run parallel to the modern shoreline, and are several hundred meters wide along. North of Speightstown, the orientation of the reef tracts changes first to the northeast and then to the east, indicating a lateral growth of the island in this direction. Terrace distributions, sediment facies structures and absolute dating results have been published by, among others:

- MESOLELLA (1968) for different sites along the west coast,
- STEINEN et al. (1973) and BLANCHON & EISENHOWER (2001) for the vicinity of Holetown,
- RADTKE et al. (1988) and RADTKE (1989) for the Thorpe and Clermont Nose traverses,
- GALLUP et al. (1994) for Clermont Nose and Holders Hill,
- MESOLELLA et al (1969), BENDER et al. (1979), EDWARDS et al. (1997), BARD et al. (1990b), KU et al (1990), and GALLUP et al. (2002) for the Clermont Nose area.

These and other geochronological investigations were discussed in detail in Chapter 3.

The Clermont Nose area has the highest uplift rate on Barbados (approx. 0.44 to 0.49 m/ka). The MIS 5e coral reef terrace, which is commonly referred to as First High Cliff or Rendezvous Hill terrace, rises to 61 m asl., and declines to less than 40 m asl. in northern and southern direction. This warping indicates an anticlinal deformation of the coral reef terraces in this area. It is commonly referred to as the Clermont Nose or Clermont Mount Hillaby anticline (BENDER et al 1979, TAYLOR & MANN 1991). Thus, this area has the best potential for observing preserved uplifted coral reef terraces that developed during interglacial sea-level sub-maxima.

Numerous researchers described and dated a sequence of constructional coral reef terraces in the Clermont Nose area. (The TIMS U-series ages by EDWARDS et al. (1997) are cited below; a map was published by BENDER et al. (1979).) This sequence includes:

- Worthing terrace at 20 m asl., dated at approx. 83 ka (MIS 5a);
- Ventnor terrace at 30 m asl., dated at approx. 104 ka old (MIS 5c);
- Rendezvous Hill terrace at 61 m asl., dated at approx. 121 to 127 ka (MIS 5e);
- Durants terrace at 67 m asl., dated at approx. 206 ka (MIS 7).

For the more elevated older terraces, ages were reported by MESOLELLA et al. (1969) based on U-series dating by alpha-spectrometry; by BENDER et al. (1979) based on Th/U and He/U dating, also by alpha-spectrometry; and by RADTKE et al. (1988) and RADTKE (1989) based on ESR dating. These studies provided the basis for the following commonly used subdivision of coral reef terraces on the Clermont Traverse:

- Cave Hill terrace at 78 to 85 m asl., dated at approx. 227 ka (ESR), corresponding to MIS 7;
- Thorpe terrace at 94 to 100 m asl., dated at approx. 220 to 300 ka (Th/U), and 307 ka (ESR), corresponding to MIS 7, or, more accurately, to MIS 9;
- Husband or Lodge terrace at 107 to 113 m asl., estimated at 360 or 380 ka based on He/U dating by BENDER et al. (1979);
- so-called "Unnamed" terrace at 122 m asl., age unknown.

Mapping and sampling along the Clermont - Nose standard traverse was conducted during our field trips in 1999 and 2000. Samples were collected for ESR

dating and for TIMS Th/U dating by E. K. Potter, T. Ezat, and M. McCulloch (Australian National University, Canberra). The ESR dating results are presented below.

Figure 5.1 shows a preliminary field map, including sample sites, different terrace levels (N = Niveau), and ESR dating results. Field mapping is still in progress, especially in the regions of the oldest and highest elevated reef terraces. A correlation of the terraces to the commonly used terminology is also illustrated in the legend of Figure 5.1. All ESR dating results are listed in Table 5.1.

The lowest coastal terrace in this area is the beach sand terrace at up to 2 m asl., assumed to be Mid-Holocene. A partly destroyed beach rock is preserved along the sandy beach of this terrace, and a deep MIS 5a notch in c. 7 m asl. is cut into MIS 5c coral limestone of the N1[5c] wave cut platform at the proximal landward margin of the former Mid-Holocene cliff line. The N1[5c] wave cut platform is approx. 10 m asl. It is well developed northeast of Batts Rock Bay, where it reaches a width of up to 180 m. The profile in Figure 5.2 shows that the abrasion terrace is cut into a deeper fore reef coral facies, which is approx. 106 ± 8 ka old (MIS 5c). The younger ESR ages of 76 ± 4 and 85 ± 5 ka (MIS 5a), derived from samples embedded in the uppermost 1 m of the profile, indicate that the uppermost layer consists of reworked coral fragments, which were deposited during the abrasion process. However, due to dense vegetation and the height of the profile, it has not been possible yet to confirm the existence of an unconformity at the base of the presumed upper MIS 5a layer. Nevertheless, the morphostratigraphic context implies that the platform was formed during late MIS 5a (see below).

The N1[5c] wave cut platform is younger than the MIS 5a coral reef formation of the N2, or Worthing, terrace at 18 to 20 m asl. The seaward part of the N2 terrace consists of an *Acropora palmata* reef crest facies that is at least 2 - 3 m thick. A deep notch is developed at the base of the former N2 cliff line at the proximal landward side of the N2 terrace. The notch was cut into the *A. palmata* reef crest facies of the N3 or Ventnor terrace during the growth of the N2 coral reef. The N2 terrace was ESR dated at three localities: VIII-17, VIII-27, and VIII-08 (Table 5.1). The ESR ages range between 76 ± 5 ka and 88 ± 6 ka, with a mean age of 82 ± 5 ka; the mean of the upper 10% of all ages is 88 ± 7 ka. As described in Chapter 4, only the maximum ESR ages should be used for chronostratigraphy. The maximum ESR ages indicate an early MIS 5a age of the N2 terrace. This terrace correlates to the T-1a2 terrace at the south coast of Barbados, which was ESR dated at 85 ± 7 ka (Table 4.2). A late MIS 5a terrace with an ESR age of 74 ± 5 ka is preserved at the southern coast of Barbados (Chapter 4). The N1[5c] wave cut platform at approx. 10 m asl. may correlate to this late MIS 5a terrace, if a stronger uplift rate is considered for the Clermont – Nose area (approx. 0.44 to 0.49 m/ka).

The N3 terrace at approx. 30 m asl. is located landwards of N2. An *A. palmata* reef crest is preserved on the seaward part of N3, which is approx. 100 m wide and more than 3 m thick. East of sample site VIII-18, a broad lagoon is developed behind the N3 reef crest and is filled with sand and coral rubble. Five ESR ages were determined for sample site VIII-18. They range between 102 ± 6 ka and 109 ± 6 ka. Mean age is 106 ± 7 ka, and the mean of both maximum values is 108 ± 7 ka. Therefore, N3 was formed during MIS 5c and correlates to one of the three MIS 5c terraces at the south coast of Barbados.

Rendezvous Hill, or N4 terrace, located at 60 m to 61 m asl., is the next oldest coral reef terrace east of Batts Rock Bay. The University of the West Indies is largely situated on this terrace, and the N4 coral reef facies are exposed along Gordon Cummins Highway below the University. The uppermost 3.5 m are composed of a compact *A. palmata* reef crest facies, which is underlain by an *A. cervicornis* reef slope deposit, at least 6-8 m thick, with some rounded boulders of *A. palmata, Siderastrea sp. and Montastrea sp.* Pebbles of rounded *A. cervicornis* predominate in its basal part. This continuous reef facies sequence overlies a second *A. palmata* reef crest facies at 45 asl., which is more than 4 m thick and mixed with different species of head coral. The precise age of this sequence is still unknown. ESR ages of four *A. palmata* samples from the uppermost reef crest facies range between 103 ± 8 ka and 123 ± 10 ka. The mean of the two oldest ages is 122 ± 9 ka, indicating that N4 (including *A. palmata* reef crest and underlying *A. cervicornis* reef slope facies) was formed during late MIS 5e. This particular road cutting was also described and U-series dated by GALLUP et al. (2002), as discussed in Chapter 3.

North of University Road, a higher sub-level of N4 is preserved at 61 m to 62 m asl. It was ESR dated at sample sites VIII-01 and VIII-19 (Figure 5.1). Neglecting the extreme age value of sample B99-64*4, which may have been a reworked sample, the maximum

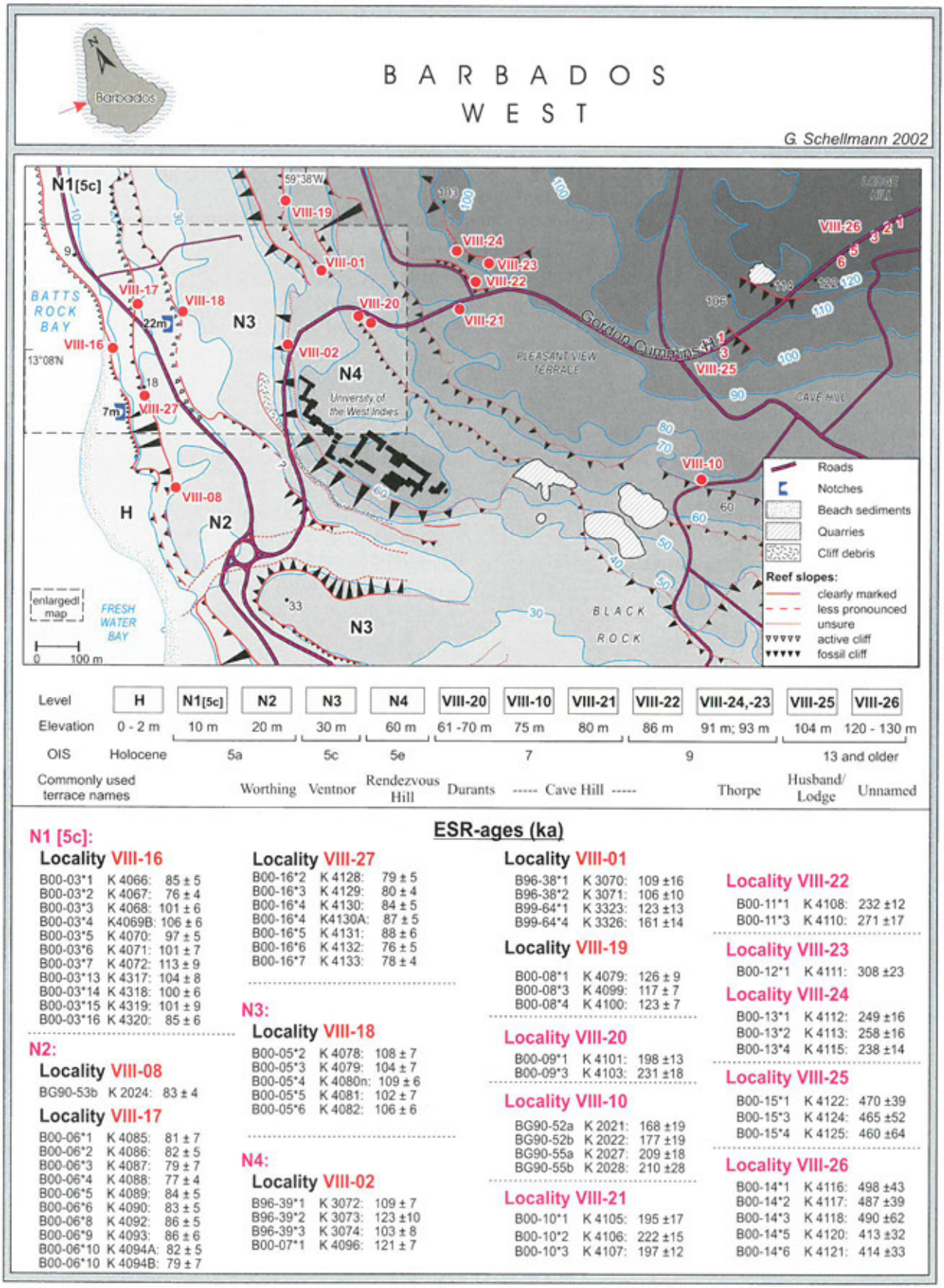

Level	H	N1[5c]	N2	N3	N4	VIII-20	VIII-10	VIII-21	VIII-22	VIII-24,-23	VIII-25	VIII-26
Elevation	0 - 2 m	10 m	20 m	30 m	60 m	61 -70 m	75 m	80 m	86 m	91 m; 93 m	104 m	120 - 130 m
OIS	Holocene	5a		5c	5e		7		9		13 and older	
Commonly used terrace names			Worthing	Ventnor	Rendezvous Hill	Durants	----- Cave Hill -----			Thorpe	Husband/ Lodge	Unnamed

ESR-ages (ka)

N1 [5c]:

Locality VIII-16

B00-03*1	K 4066:	85 ± 5
B00-03*2	K 4067:	76 ± 4
B00-03*3	K 4068:	101 ± 6
B00-03*4	K4069B:	106 ± 6
B00-03*5	K 4070:	97 ± 5
B00-03*6	K 4071:	101 ± 7
B00-03*7	K 4072:	113 ± 9
B00-03*13	K 4317:	104 ± 8
B00-03*14	K 4318:	100 ± 6
B00-03*15	K 4319:	101 ± 9
B00-03*16	K 4320:	85 ± 6

N2:

Locality VIII-08

BG90-53b	K 2024:	83 ± 4

Locality VIII-17

B00-06*1	K 4085:	81 ± 7
B00-06*2	K 4086:	82 ± 5
B00-06*3	K 4087:	79 ± 7
B00-06*4	K 4088:	77 ± 4
B00-06*5	K 4089:	84 ± 5
B00-06*6	K 4090:	83 ± 5
B00-06*8	K 4092:	86 ± 5
B00-06*9	K 4093:	86 ± 6
B00-06*10	K 4094A:	82 ± 5
B00-06*10	K 4094B:	79 ± 7

Locality VIII-27

B00-16*2	K 4128:	79 ± 5
B00-16*3	K 4129:	80 ± 4
B00-16*4	K 4130:	84 ± 5
B00-16*4	K4130A:	87 ± 5
B00-16*5	K 4131:	88 ± 6
B00-16*6	K 4132:	76 ± 5
B00-16*7	K 4133:	78 ± 4

N3:

Locality VIII-18

B00-05*2	K 4078:	108 ± 7
B00-05*3	K 4079:	104 ± 7
B00-05*4	K 4080n:	109 ± 6
B00-05*5	K 4081:	102 ± 7
B00-05*6	K 4082:	106 ± 6

N4:

Locality VIII-02

B96-39*1	K 3072:	109 ± 7
B96-39*2	K 3073:	123 ±10
B96-39*3	K 3074:	103 ± 8
B00-07*1	K 4096:	121 ± 7

Locality VIII-01

B96-38*1	K 3070:	109 ±16
B96-38*2	K 3071:	106 ±10
B99-64*1	K 3323:	123 ±13
B99-64*4	K 3326:	161 ±14

Locality VIII-19

B00-08*1	K 4079:	126 ± 9
B00-08*3	K 4099:	117 ± 7
B00-08*4	K 4100:	123 ± 7

Locality VIII-20

B00-09*1	K 4101:	198 ±13
B00-09*3	K 4103:	231 ±18

Locality VIII-10

BG90-52a	K 2021:	168 ±19
BG90-52b	K 2022:	177 ±19
BG90-55a	K 2027:	209 ±18
BG90-55b	K 2028:	210 ±28

Locality VIII-21

B00-10*1	K 4105:	195 ±17
B00-10*2	K 4106:	222 ±15
B00-10*3	K 4107:	197 ±12

Locality VIII-22

B00-11*1	K 4108:	232 ±12
B00-11*3	K 4110:	271 ±17

Locality VIII-23

B00-12*1	K 4111:	308 ±23

Locality VIII-24

B00-13*1	K 4112:	249 ±16
B00-13*2	K 4113:	258 ±16
B00-13*4	K 4115:	238 ±14

Locality VIII-25

B00-15*1	K 4122:	470 ±39
B00-15*3	K 4124:	465 ±52
B00-15*4	K 4125:	460 ±64

Locality VIII-26

B00-14*1	K 4116:	498 ±43
B00-14*2	K 4117:	487 ±39
B00-14*3	K 4118:	490 ±62
B00-14*5	K 4120:	413 ±32
B00-14*6	K 4121:	414 ±33

Figure 5.1:
Distribution and ESR dating results of coral reef terraces along the Clermont Nose standard traverse between Batts Rock Bay and Cave Hill. See Table 5.2 for details on ESR ages.

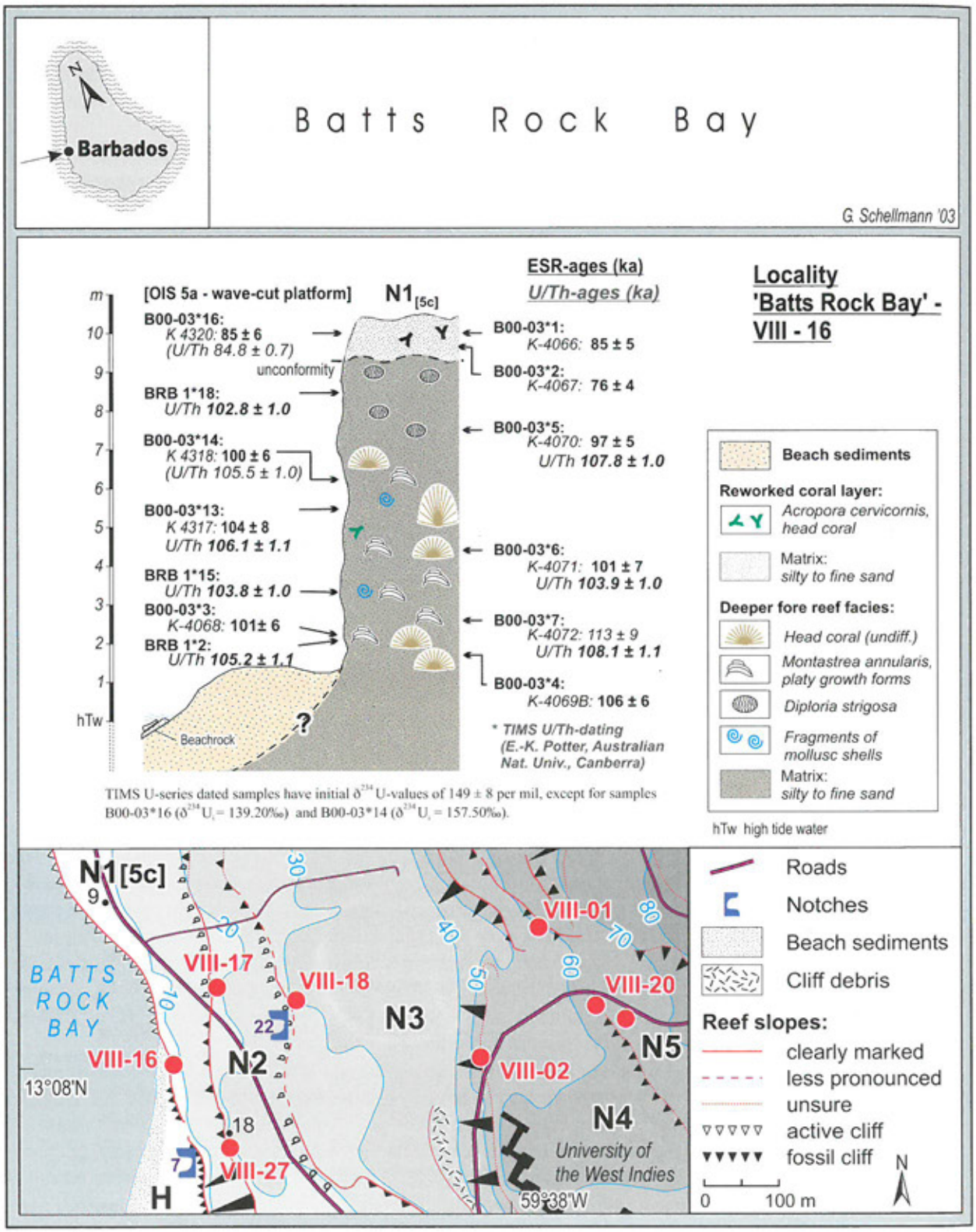

Figure 5.2:
ESR dating results from MIS 5a wave-cut platform terrace, which has been abraded in MIS 5c coral reef. The site is exposed along the modern cliff line at Batts Rock Bay, west coast of Barbados. See Table 5.2 for details on ESR ages.

ESR ages are similar to those determined for sample site VIII-02, located at University Road, and indicate an MIS 5e age for this small terrace rim.

As already stated, the mapping of the higher and older terraces in this area of the island is still in progress. However, the ESR dating results presented in Figure 5.1 indicate an MIS 7 age for both the coral

reef terraces located east of the university; the first at 61 m to 70 m asl. (Figure 5.1: sample site VIII-20) and the second at approx. 75 to 80 m asl. (Figure 5.1: sample sites VIII-10 and VIII-21). These results agree well with former penultimate interglacial U-series and ESR dating results (see above) from Durant Terrace (67 m asl.) and Cave Hill Terrace (78 to 85 m asl.).

Two higher coral reef tracts were most probably formed during MIS 9 and appear at approx. 86 m asl. (Figure 5.1: sample site VIII-22) and 91-93 m asl. (Figure 5.1: sample sites VIII-23, VIII-24). Sample sites VIII-23 and VIII-24 correspond to the Thorpe Terrace, dated at approx. 307 ka (ESR) by RADTKE et al. (1988) and RADTKE (1989).

Remarkably, the most elevated coral reef terraces, located at 104 and 122 m asl., seem to be as old as 470 and 500 ka, respectively (Figure 5.1: sample sites VIII-25 and VIII-26). The lower elevated sample site VIII-25 at 104 m asl. corresponds to the Husband or Lodge terraces, for which BENDER et al. (1979) estimated an age of 360 or 380 ka based on He/U dating. Sample site VIII-26 at 122 m asl. may correlate to the so-called Unnamed Terrace level, which has not been dated as yet. Reef terraces of sea-level highstand MIS 11 are to be investigated in more detail in the future.

The relatively low elevations of the coral reefs MIS 9 to MIS 13 situated in this region provide substantial evidence for a much stronger uplift of the Clermont Nose area during the time period beginning with the last interglacial maximum compared to the preceding time period. For example, if we assume a constant uplift at the rate rate calculated from the present height of the last interglacial terrace at 61 m asl. (c. 0.47 m/ka), the oldest MIS 13 coral reef tract, which is preserved at sample site VIII-26 (122 m asl.), should have an elevation of approx. 220 to 245 m asl. Instead of this, its present height is only 120 to 125 m asl. It follows, therefore, that uplift was has not been constant over the period of the last 500,000 years. However, there is no evidence to suggest that the uplift rate has not been constant over the last 130,000 years so the calculations made by GALLUP et al. (2002) may still be valid. Nevertheless the data from Clermont Nose supports the argument presented in Chapter 4, that anticlinal warped areas, may have a complex tectonic history and are not necessarily suitable for Pleistocene sea-level reconstruction.

Table 5.1: ESR dating results from localities on the west coast of Barbados. See Figure 5.1 and Figure 5.2 for sample site locations.

Site	Lab. No.	Sample	Elev.	Depth		Ali.	Dmax	Uranium		D'		DE		ESR age	
			m asl.	cm	±	n	Gy	ppm	±	µGy/a	±	Gy	±	ka	±
VIII-01	K-3070	B-96-38-1	61	100	10	20	356	3.55	0.64	970	112	105	10	**109**	**16**
VIII-01	K-3071	B-96-38-2	61	100	10	20	356	3.85	0.21	1026	56	108	6	**106**	**10**
VIII-01	K-3323	B-99-64-1	62	150	20	20	267	3.00	0.25	871	56	107	9	**123**	**13**
VIII-01	K-3326	B-99-64-4	62	150	30	20	267	2.65	0.13	859	63	139	6	**161**	**14**
VIII-02	K-3072	B-96-39-1	54	230	20	20	356	3.58	0.25	949	58	103	3	**109**	**7**
VIII-02	K-3073	B-96-39-2	54	230	20	20	356	3.51	0.30	973	67	120	5	**123**	**10**
VIII-02	K-3074	B-96-39-3	54	230	20	20	356	3.38	0.17	888	46	92	6	**103**	**8**
VIII-02	K-4096	B-00-07-1	53	200	50	20	267	2.90	0.13	841	42	101	2	**121**	**7**
VIII-08	K-2024	BG-90-53b	16	150	30	20	445	2.67	0.09	701	30	58	1	**83**	**4**
VIII-10	K-2021	BG-90-52a	75	100	20	20	445	3.35	0.52	1067	112	180	8	**168**	**19**
VIII-10	K-2022	BG-90-52b	75	100	20	20	445	3.41	0.50	1098	112	194	8	**177**	**19**
VIII-10	K-2027	BG-90-55a	76	100	20	20	445	3.34	0.19	1133	66	237	15	**209**	**18**
VIII-10	K-2028	BG-90-55b	76	100	20	20	445	3.48	0.64	1176	148	247	10	**210**	**28**
VIII-16	K-4066	B-00-03-1	10	50	10	20	267	3.28	0.11	865	35	72	3	**85**	**5**
VIII-16	K-4067	B-00-03-2	10	80	30	20	267	3.14	0.01	789	32	60	2	**76**	**4**
VIII-16	K-4068	B-00-03-3	10	850	30	20	267	2.47	0.07	608	29	62	2.1	**101**	**6**
VIII-16	K-4069B	B-00-03-4	10	890	30	20	267	2.83	0.04	692	32	73	2	**106**	**6**
VIII-16	K-4070	B-00-03-5	10	300	30	20	267	2.83	0.08	739	34	72	2	**97**	**5**
VIII-16	K-4071	B-00-03-6	10	600	30	20	267	2.53	0.13	641	40	65	2	**101**	**7**
VIII-16	K-4072	B-00-03-7	10	780	30	20	267	2.51	0.07	655	36	73	5	**113**	**9**

Table 5.1 continued:

Site	Lab. No.	Sample	Elev.	Depth		Ali.	Dmax	Uranium		D'		DE		ESR age	
			m asl.	cm	±	n	Gy	ppm	±	µGy/a	±	Gy	±	ka	±
VIII-16	K-4317	B-00-03*13	10	450	20	20	267	2.56	0.13	757	37	79	3	**104**	**8**
VIII-16	K-4318	B-00-03*14	10	430	50	20	267	2.67	0.00	690	36	69	2	**100**	**6**
VIII-16	K-4320	B-00-03*16	10	50	20	20	267	2.64	0.19	727	40	61	3	**85**	**6**
VIII-17	K-4085	B-00-06-1	19	50	20	20	267	3.86	0.11	958	43	78	5	**81**	**7**
VIII-17	K-4086	B-00-06-2	19	50	20	20	267	2.72	0.07	736	30	60	2	**82**	**5**
VIII-17	K-4087	B-00-06-3	19	50	20	20	267	3.65	0.04	910	38	72	6	**79**	**7**
VIII-17	K-4088	B-00-06-4	19	50	20	20	267	2.92	0.14	759	37	58	2	**77**	**4**
VIII-17	K-4089	B-00-06-5	19	50	20	20	267	3.68	0.10	933	41	78	2	**84**	**5**
VIII-17	K-4090	B-00-06-6	19	50	20	20	267	4.10	0.07	1011	44	84	4	**83**	**5**
VIII-17	K-4092	B-00-06-8	19	50	20	20	267	3.67	0.23	936	52	80	2	**86**	**5**
VIII-17	K-4093	B-00-06-9	19	50	20	20	267	2.94	0.19	791	43	68	2	**86**	**6**
VIII-17	K-4094A	B-00-06-10	19	50	20	20	267	3.05	0.17	802	40	66	2	**82**	**5**
VIII-17	K-4094B	B-00-06-10	19	50	20	20	267	3.08	0.06	798	33	63	5	**79**	**7**
VIII-18	K-4078	B-00-05-2	29	320	30	20	267	3.34	0.08	876	42	95	4	**108**	**7**
VIII-18	K-4079	B-00-05-3	29	240	30	20	267	3.24	0.13	857	43	99	3	**104**	**7**
VIII-18	K-4080n	B-00-05-4	29	20	10	20	267	3.55	0.09	1017	45	111	3	**109**	**6**
VIII-18	K-4081	B-00-05-5	29	40	10	20	267	3.11	0.14	876	42	89	5	**102**	**7**
VIII-18	K-4082	B-00-05-6	29	100	20	20	267	3.38	0.01	924	38	98	3	**106**	**6**
VIII-19	K-4097	B-00-08-1	59	50	10	20	267	3.02	0.24	911	56	115	4	**126**	**9**
VIII-19	K-4099	B-00-08-3	59	50	10	20	267	3.28	0.09	949	42	111	4	**117**	**7**
VIII-19	K-4100	B-00-08-4	59	50	10	20	267	3.22	0.11	950	43	117	4	**123**	**7**
VIII-20	K-4101	B-00-09-1	61	150	20	20	267	2.77	0.08	945	46	187	8	**198**	**13**
VIII-20	K-4103	B-00-09-3	61	200	20	20	267	3.46	0.28	1179	85	272	8	**231**	**18**
VIII-21	K-4105	B-00-10-1	80	120	20	20	890	2.83	0.29	965	75	188	7	**195**	**17**
VIII-21	K-4106	B-00-10-2	80	200	20	20	890	2.58	0.13	911	49	202	9	**222**	**15**
VIII-21	K-4107	B-00-10-3	80	200	20	20	890	2.26	0.13	791	44	156	5	**197**	**12**
VIII-21	K-4106	B-00-10-2	80	200	20	20	890	2.58	0.13	911	49	202	9	**222**	**15**
VIII-21	K-4107	B-00-10-3	80	200	20	20	890	2.26	0.13	791	44	156	5	**197**	**12**
VIII-22	K-4108	B-00-11-1	86	100	20	20	890	3.03	0.04	1076	50	249	7	**232**	**12**
VIII-22	K-4110	B-00-11-3	86	100	20	20	890	2.38	0.14	920	53	249	6	**271**	**17**
VIII-23	K-4111	B-00-12-1	93	100	20	20	890	2.98	0.17	1139	70	351	14	**308**	**23**
VIII-24	K-4112	B-00-13-1	91	100	20	20	890	2.77	0.14	1019	56	253	9	**249**	**16**
VIII-24	K-4113	B-00-13-2	91	100	20	20	890	2.71	0.06	1009	49	260	10	**258**	**16**
VIII-24	K-4115	B-00-13-4	91	100	20	20	890	3.03	0.08	1084	54	258	8	**238**	**14**
VIII-25	K-4122	B-00-15-1	104	300	20	20	1068	2.20	0.16	913	68	429	16	**470**	**39**
VIII-25	K-4124	B-00-15-3	104	450	20	20	1068	2.15	0.25	870	89	405	18	**465**	**52**
VIII-25	K-4125	B-00-15-4	104	450	20	20	1068	2.30	0.28	922	97	425	39	**460**	**64**
VIII-26	K-4116	B-00-14-1	122	100	20	20	1068	2.09	0.12	925	58	460	27	**498**	**43**
VIII-26	K-4117	B-00-14-2	122	100	20	20	1068	2.38	0.03	1025	52	499	31	**487**	**39**
VIII-26	K-4118	B-00-14-3	122	100	20	20	1068	2.09	0.29	923	100	452	30	**490**	**62**
VIII-26	K-4120	B-00-14-5	122	200	20	20	1068	2.58	0.03	1046	53	432	25	**413**	**32**
VIII-26	K-4121	B-00-14-6	122	200	20	20	890	2.63	0.20	1058	79	440	12	**414**	**33**

5.2. North point area between Cluff's Bay and River Bay

The northernmost part of the island, the North Point shelf area, has a flat relief with only minor height differences between reef tracts of different ages. This area lacks the clear step-like terrace morphology of the western and southern coastlines of Barbados.

MESOLELLA et al. (1969) attributed the fossil coral reef facies of the North Point area to the maximum sea-level stand of the last interglacial (MIS 5e, marine oxygen isotope stage 5e) approx. 125 ka. JAMES (1972) and JAMES et al. (1971) doubted this interpretation and assumed that the northern part of the island, north of Holetown (Potters Fault, 13°11´ to 13°12´), experienced a tectonic history during the Late Pleistocene which was completely different from that of the rest of Barbados. In addition to the previously identified terraces of MIS 5a, 5c, and 5e (80 ka, 105 ka, and 125 k a, respectively), JAMES suggested a sea-level highstand at 60 ka (Early Wisconsin reef terrace). This has been a frequently cited reference for a positive Early Wisconsin temperature change. Based on JAMES, the tectonic history is described as follows. Firstly, a submergence occurred between 125 ka and 80 ka. Secondly, highstands transgressed over the 125 ka reef on the Northwest and Northeast coasts at 105 ka and 80 ka, respectively (Figure 3.4). Subsequent research could neither confirm this tectonic history nor the existence of the 60 ka reef (TAYLOR 1974, RADTKE et al. 1988).

Cluff's Bay

JAMES (1971) reported evidence of a 60 ka sea-level highstand for Cluff's Bay (Figure 3.5, Photo 5.1) and Stroud Bay. Although, there is only one U-series date available for Stroud Bay (97,4 ka), a systematic study was carried out at Cluffs Bay. There, several dates were obtained from the mollusc *Cittarium* from beach deposits. KAUFMAN et al (1971) showed that mollusc shells may provide invalid dates, which are typically younger than the correct dates due to post-mortem U uptake.

Nevertheless, neither the ESR nor the U-series dates of molluscs and corals confirmed a high sea level prior to the 80 ka sea-level stand. The dates by RADTKE et al. (1988; Fig. 3.5) strongly implied a correlation of these sediments with sub-stages 5a or 5c. Despite the lack of deposits, a sea-level highstand at 125 ka may be represented by a notch cut into the older calcarenites. The findings do not seem compatible with JAMES´ hypothesis of tectonic uplift after 105 ka or 80 ka, and tectonic lowering subsequent to the 125 ka highstand. However, it is possible that the topographic situation and climatic conditions during the last sea-level highstand did not allow for coral growth, as it is presently the case along the east coast of Barbados. Recent ESR studies confirmed the dating results of Cluff's Bay presented by RADTKE (1989) (sample site I-03 in Table 5.2 and Figure 5.3) with ESR ages of 84 ka, 83 ka, 73 ka, 76 ka and 84 ka (mean 80 ka; mean of maximum ESR ages 84 ± 7 ka). The deposits may correspond with the oldest MIS 5a coral reef tract T1a2 at the southern coast of Barbados, which was ESR dated at 85 ± 7 ka (Table 4.2).

Animal Flower Cave, North Point, and River Bay

The area around Animal Flower Cave (Figure 5.3), located on the north coast of Barbados, seems to be rather complex. JAMES (1971) assumed that deposits of the 125 ka sea-level maximum were covered by coral from the 80 ka highstand, caused by tectonic lowering subsequent to the 125 ka maximum and an uplift approx. 80 ka ago. Data presented by RADTKE et al. (1988) suggested a different stratigraphy. The base was certainly formed by Older Calcarenites, as stated by MESOLELLA et al. (1969); these calcarenites are at least as old as MIS 11, and the reef complex may be correlated to the reef formation of Second High Cliff, which is distributed at an altitude of 120 m approx. 3.5 km southeast of North Point (RADTKE et al. 1988). U-series and ESR dating results for the overlying complex in the Animal Flower Cave area (18 to 20 m asl.) support a reef formation during MIS 5e approx. 125 to 130 ka ago. The sample sites, located at 23 and 27 m asl., and several hundred meters south of the cave at the road junction (Figure 5.3), provided inconsistent ESR and U-series ages. Therefore, RADTKE et al. (1988) concluded: "A final resolution of the stratigraphy of northern Barbados remains as the subject of future investigations".

While recent ESR studies confirm the dating results of RADTKE (1989) and RADTKE et al. (1988) (Figure 5.3: Animal Flower Cave), the new data set gives a greater insight into the genesis of North Point

Photo 5.1:
Last interglacial (MIS 5a) coral reef platform at Cluff's Bay, north coast of Barbados.
(Photo: SCHELLMANN 1999)

area (Table, 5.2; Figure 5.3).

The suggested evolution of North Point area and its overlying complex during MIS 5e is supported by the ESR dating of fossil reef deposits at 7 to 10 m asl. at River Bay on the northeast coast (sample site II-2 in Figure 5.3 and Table 5.2), and by the ESR dating of an *Acropora palmata* reef crest at 22.5 m asl. at sample site I-15 east of North Point (Figure 5.3). The flat North Point area ends with a clearly visible bipartite terrace step at the road junction approx. 600 m south of Animal Flower Cave (Figure

Table 5.2: ESR dating results from localities near North Point. See Figure 5.3 for site locations.

Site	Lab. No.	Sample	Elev.	Depth		Ali.	Dmax	Uranium		D'		DE		ESR age	
			m asl.	cm	±	n	Gy	ppm	±	µGy/a	±	Gy	±	ka	±
I-03	K-2033	BG-90-57c	3	200	100	20	445	2.26	0.11	612	41	52	2	**84**	**7**
I-03	K-2034	BG-90-57d	3	200	100	20	445	2.24	0.11	604	42	50	1	**83**	**7**
I-03	K-2035	BG-90-57e	3	200	100	20	445	2.79	0.14	686	49	50	1	**73**	**6**
I-03	K-2037	BG-90-57g	5	400	200	20	445	3.22	0.16	778	56	59	2	**76**	**6**
I-03	K-3160	B-99-16	5	80	30	20	267	2.62	0.25	710	47	59	3	**84**	**7**
I-08	K-2038	BG-90-58a	20	200	100	20	445	3.17	0.16	854	62	90	6	**105**	**10**
I-08	K-2039	BG-90-58b	20	200	100	20	445	3.19	0.16	852	63	88	5	**103**	**10**
I-08	K-2040	BG-90-58c	20	300	100	20	445	3.38	0.17	863	65	86	4	**100**	**9**
I-09	D-2041	BG-90-59a	23	200	100	17	312	3.44	0.17	963	73	119	5	**123**	**11**
I-09	K-2042	BG-90-59b	23	100	50	20	445	3.45	0.17	988	73	121	9	**123**	**13**
I-09	K-2043	BG-90-59c	23	200	100	20	312	3.63	0.18	1002	77	122	8	**122**	**12**
I-15	K-4073	B-00-04-1	22.5	790	30	20	267	3.57	0.10	931	48	117	3	**127**	**7**
I-15	K-4074x	B-00-04-2	22.5	800	30	20	267	3.30	0.05	852	39	104	6	**123**	**9**
I-15	K-4075	B-00-04-3	22.5	370	30	20	267	3.09	0.02	848	37	103	2	**122**	**6**
I-15	K-4076	B-00-04-4	22.5	300	30	20	267	3.35	0.04	907	40	107	7	**118**	**10**
II-2	K-4171	B-00-26-1	7	650	50	20	267	4.49	0.06	1166	55	153	5	**131**	**8**
II-2	K-4174	B-00-26-4	7	600	50	20	267	3.42	0.01	896	40	111	3	**123**	**7**
II-2	K-4175	B-00-26-5	7	600	50	20	267	2.97	0.22	820	54	112	6	**137**	**12**
II-2	K-4178	B-00-26-8	7	250	25	20	267	3.11	0.06	895	41	118	5	**132**	**8**
II-2	K-4179	B-00-26-9	7	250	25	20	267	3.01	0.08	853	39	105	3	**124**	**7**
II-2	K-4180	B-00-26-10	7	100	20	20	267	3.33	0.05	978	42	128	7	**130**	**9**
II-2	K-4181	B-00-26-11	7	100	20	20	267	3.42	0.10	972	44	116	4	**120**	**7**
II-2	K-4182	B-00-26-12	7	100	20	20	267	3.55	0.05	971	42	106	5	**109**	**7**

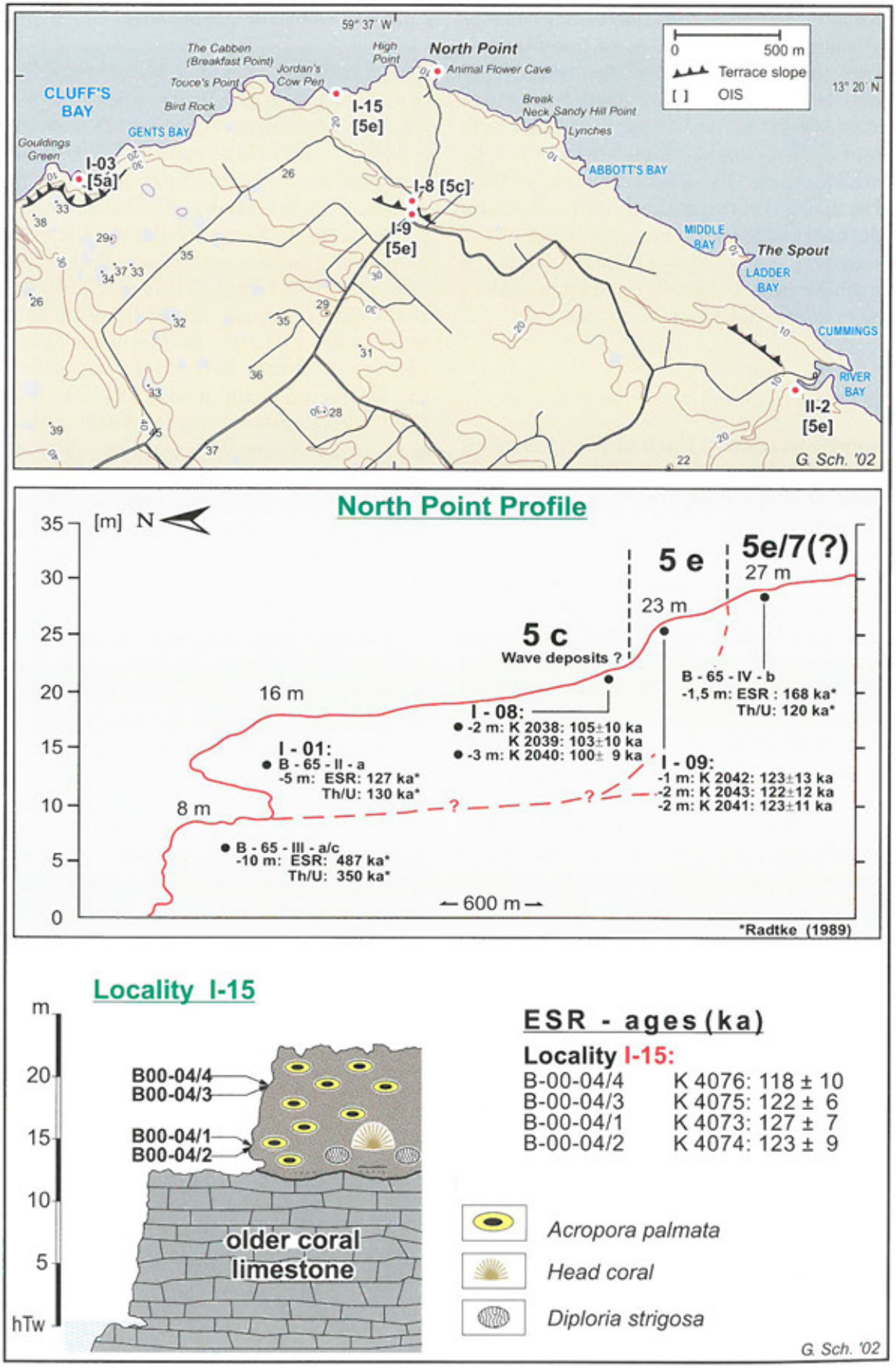

Figure 5.3:
ESR dating results and profiles of coral reef terraces near North Point. See Table 5.2 for details on ESR ages.

5.3). Samples were taken from road cutting outcrops at 20 m (sample site I-8) and 23 m asl. (sample site I-9). There, the lower elevated sediments were ESR dated at 105 ka, 103 ka, and 100 ka (MIS 5c), whereas the higher sub-littoral or back reef sediments with *Acropora palmata* coral, which were not *in situ*, yielded ESR ages of 123 ka, 123 ka, and 122 ka (MIS 5e). The poorly consolidated, less elevated deposit (MIS 5c) can be explained as transgressive sediments overlying the 125,000 a reef of North Point area. It was possibly transported into its present position by a tsunami or a very strong hurricane event.

5.3 Southeast coast of Barbados between Salt Cave Point and Deebles Point, and the oldest coral reef tracts north of St. George's Valley

The depression of St. George's Valley was flooded during interglacial times until at least the ante-penultimate sea-level highstand (MIS 9), after which this area was uplifted above sea level. The eastern entrance of the depression was closed with penultimate interglacial coral reef terraces that now range from 20 m to 40 m asl. in elevation. They were ESR dated at the locations Deebles Point (samples sites VII-1 to VII-3 in Figure 5.4 and Table 5.3) and Foul Bay area (samples sites XII-1, XII-2, XII-10 in Figure 5.4 and Table 5.3, Figure 5.5). The MIS 7 ESR ages agree well with two U-series dating results of Golden Grove terrace west of Deebles Point by BANNER et al. (1991).

In the vicinity of the modern coastline, less elevated last interglacial reef terraces are preserved, for example, at Shark's Hole (Figure 5.6), Bottom and Palmetto Bay (Figure 5.7). At the latter localities, MIS 5e coral reefs are superimposed on MIS 7 and MIS 9 coral limestone (Figure 5.7).

In St. George's Valley the ancient reef structures are more dominant on the north than on the south side of the valley. Not all reef tracts can be detected continuously from the valley's western (east of Bridgetown) to eastern part (East Point/Deebles Point). The reef tracts Windsor, Dayrells, Rowans, and Walkers are generally clearly preserved, with the exception of the eastern shelf area where they converge. Bourne is a fossil reef of minor significance, while Cottage Vale follows the foot of Second High Cliff (The Mount) discontinuously.

The dominant feature of Second High Cliff can be traced easily throughout the whole island from East Point area to the north of Scotland District. Second High Cliff is not only composed of depositional elements, such as reef crest, coral stock, etc., but also exhibits erosional features. The initial chronostratigraphy of the St. George´s Valley traverse was based on very few samples per terrace, which were dated using He/U (BENDER et al. 1979) and ESR (RADTKE 1989). The He/U ages ranged from 290 ka (Rowans) to 640 ka (Guinea, the reef above Drax Hall). ESR ages (RADTKE 1989) varied from 310 ka to 642 ka. Due to recrystallization (ESR) or Helium loss (He/U), both methods have the potential to significantly underestimate the actual ages. BENDER et al. (1979) correlated the lowest terrace (Windsor) of St. George´s Valley with both the Thorpe terrace of the Clermont Nose profile, and the Aberdare terrace of Christ Church traverse (penultimate interglaciation, MIS 7).

RADTKE (1989) criticized this correlation, and new ESR dating results support his point of view. Windsor terrace displays an ante-penultimate age of 312 ka (Figure 5.8). Both the Bourne (445 ka) and Rowans (384 ka) terraces possibly belong to the "mega"-interglacial of MIS 11 at approx. 400 ka. In the field these terraces are separated from the much older reef facies (Dayrells terrace, 581 ka) by an erosional feature. The age of Dayrells corresponds to the age of Second High Cliff, which was dated for the first time at MIS 15, approx. 600 ka ago (Figure 5.8). Due to possible problems of recrystallization, the ESR ages represent minimum ages. Therefore, it cannot be ruled out that Second High Cliff is even older. Drax Hall terrace, located at 175 m asl., is the highest reef tract that has been dated so far. It is most likely at least as old as MIS 17 (Figure 5.8).

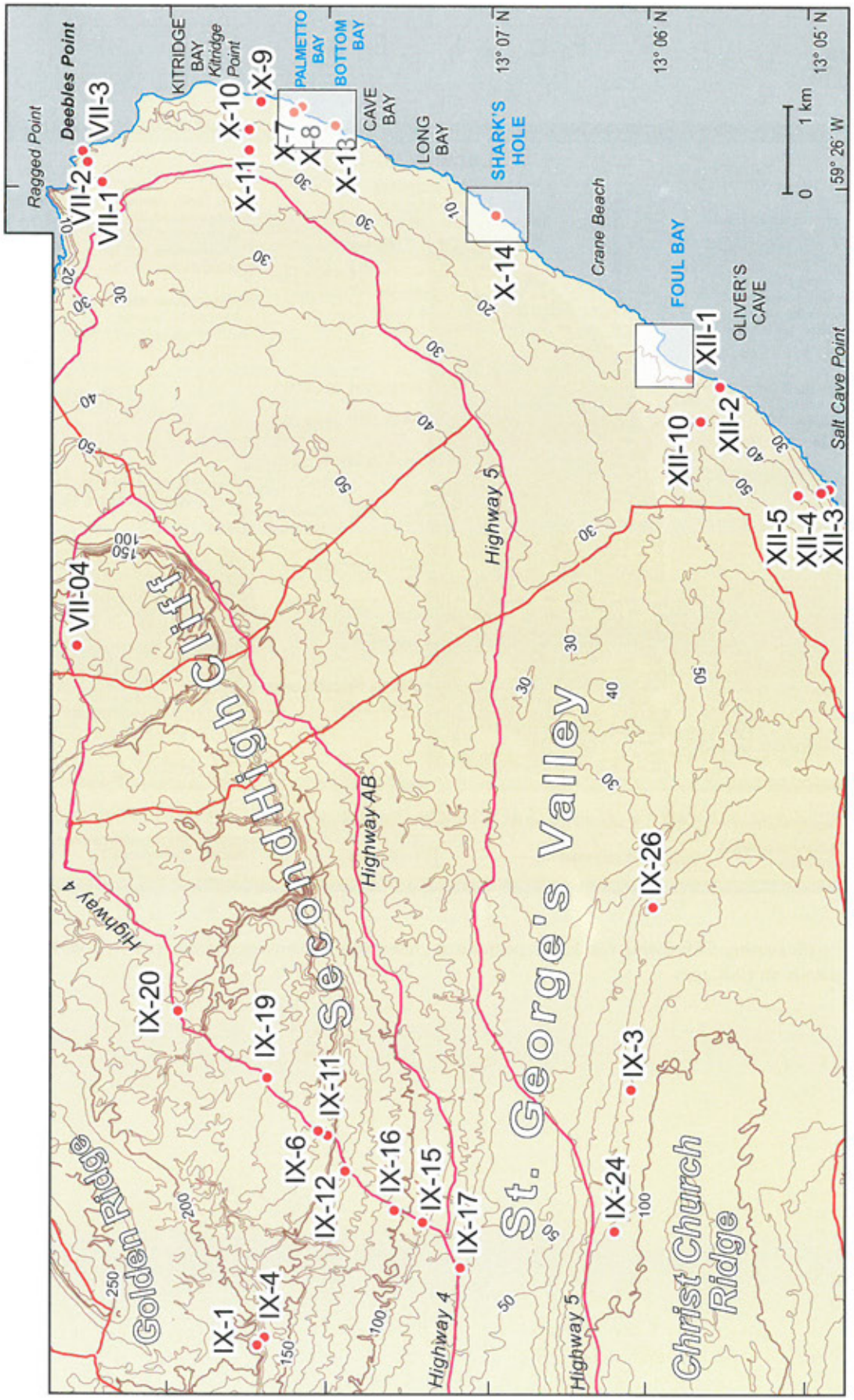

Figure 5.4:
Sample sites on eastern Barbados. See Table 5.3 for details on ESR ages.

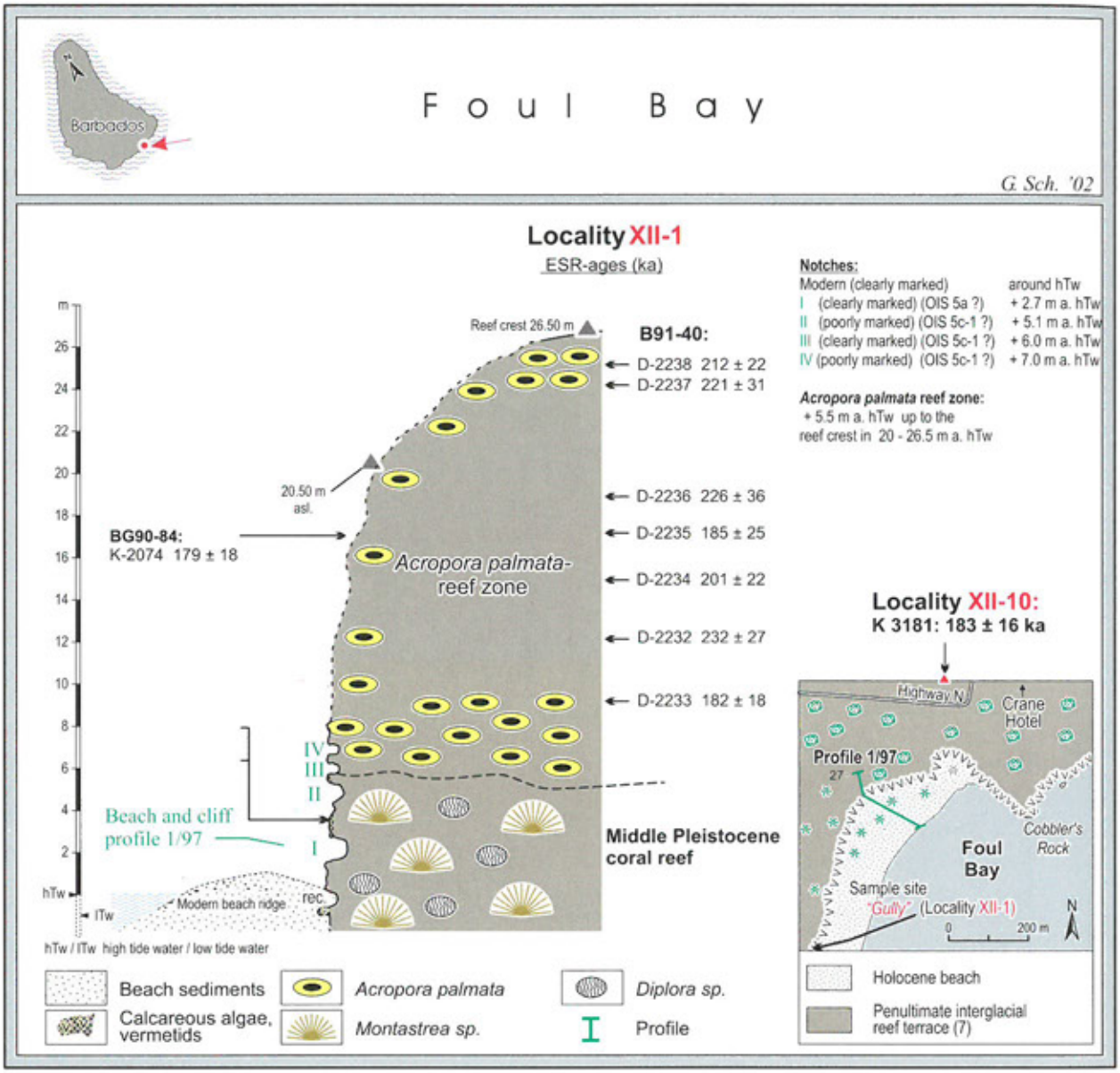

Figure 5.5:
Detailed profile illustrating ESR dating results for penultimate interglacial *Acropora palmata* reef at Foul Bay. See Table 5.3 for details on ESR ages.

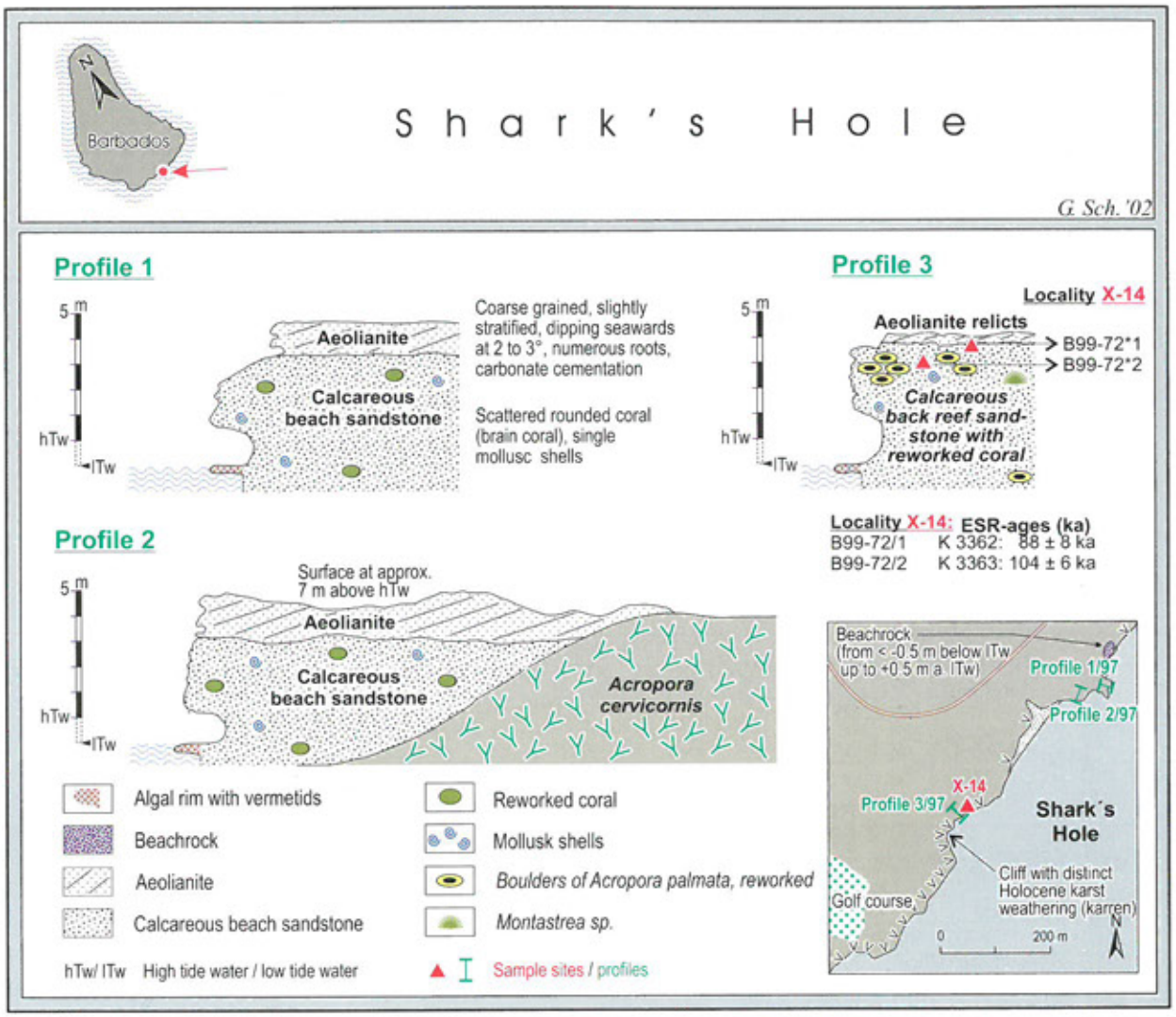

Figure 5.6: MIS 5a beach and back reef deposits at Shark's Hole. See Table 5.3 for details on ESR ages.

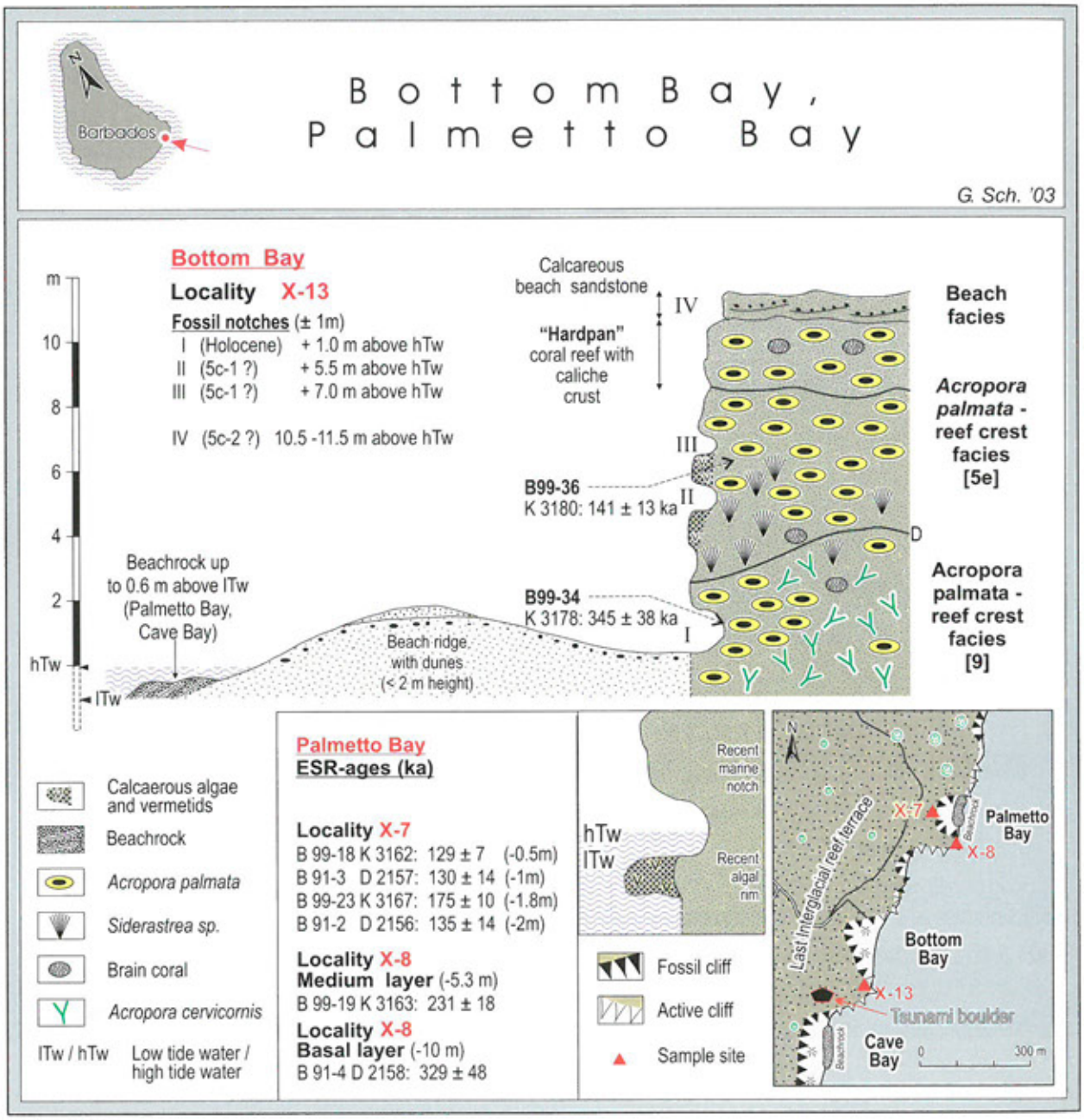

Figure 5.7:
Profile illustrating ESR dating results for Last Interglacial coral reef terrace at Bottom Bay and Palmetto Bay. See Table 5.4 for details on ESR ages.

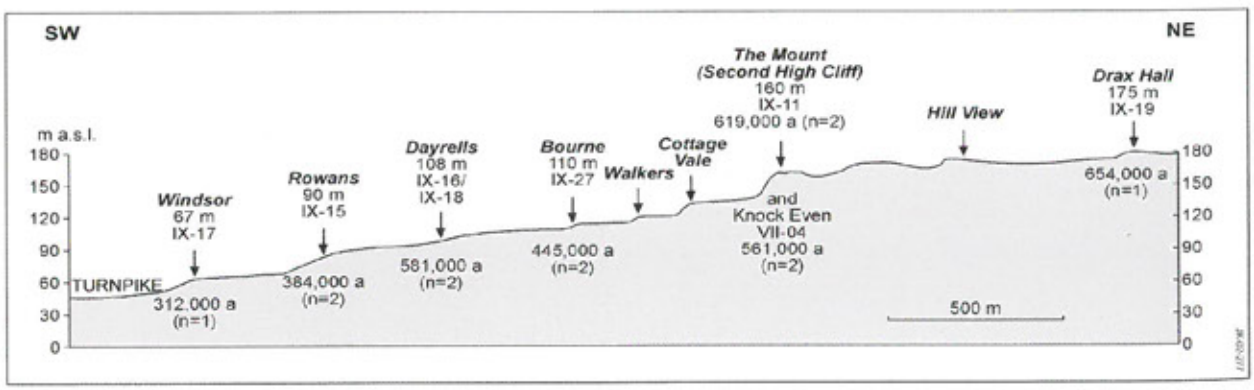

Figure 5.8:
Profile of coral reef terraces with ESR ages along the eastern St. George's Valley Traverse.

Table 5.3: ESR dating results from localities at Eastern Barbados. For locations of sample sites see Figure 5.4.

Site	Lab. No.	Sample	Elev.	Depth		Ali.	Dmax	Uranium		D'		DE		ESR age	
			m asl.	cm	±	n	Gy	ppm	±	µGy/a	±	Gy	±	ka	±
VII-01	K-3219	B-99-49-4	30	50	20	20	534	2.68	0.06	937	42	178	15	**190**	**18**
VII-02	K-3220	B-99-50-1	25	50	20	20	289	3.56	0.13	1156	58	205	16	**177**	**17**
VII-03	K-3224	B-99-51-1	18	50	20	20	289	3.62	0.00	1156	50	196	10	**169**	**11**
VII-04	K-3364	B-99-73-1	182	100	50	20	1424	3.92	0.17	1537	94	655	69	**426**	**52**
VII-04	K-3365	B-99-73-2	182	100	50	20	1424	3.87	0.05	1574	88	852	90	**543**	**65**
VII-04	K-3366	B-99-73-3	182	100	50	20	1424	3.01	0.15	1275	119	737	76	**578**	**81**
VII-04	K-3367	B-99-73-4	182	100	50	20	1424	3.65	0.35	1481	135	748	80	**505**	**71**
VII-04	K-3369	B-99-73-6	182	100	50	20	1424	4.40	0.15	1713	102	757	59	**442**	**44**
IX-01	K-3021	B-96-8-2	197	350	50	20	534	2.99	0.01	1128	57	405	38	**359**	**39**
IX-03	K-3200	B-99-43-1	86	200	30	20	890	2.62	0.19	1009	69	326	29	**323**	**39**
IX-04	K-3023	B-96-9-2	180	2000	200	30	1472	2.70	0.13	1011	73	601	40	**594**	**58**
IX-06	K-1932	BG-90-6	172	1000	200	28	1135	3.07	0.50	1165	169	625	31	**536**	**82**
IX-06	K-1933	BG-90-7	172	100	50	28	1335	2.79	0.48	1206	170	758	46	**629**	**96**
IX-06	K-3017	B-96-6-1	172	600	60	40	1068	2.66	0.35	1024	117	458	21	**447**	**55**
IX-11	K-1930	BG-90-4	160	800	200	28	1335	3.00	0.29	1154	111	613	46	**532**	**65**
IX-11	K-1931	BG-90-5	160	800	200	20	445	2.41	0.05	896	50	351	36	**392**	**46**
IX-12	K-1985i	BG-90-35	130	200	100	36	712	1.78	0.10	792	67	393	34	**497**	**62**
IX-15	K-1978	BG-90-33a	108	700	100	20	445	2.85	0.15	999	89	306	11	**306**	**29**
IX-15	K-1979	BG-90-33b	108	700	100	20	445	2.95	0.57	1063	160	370	20	**348**	**56**
IX-15	K-1980	BG-90-33c	108	700	100	20	445	3.74	0.26	1284	93	392	22	**305**	**28**
IX-15	K-1981	BG-90-33d	108	700	100	20	445	3.67	1.65	978	95	502	22	**379**	**39**
IX-15	K-1982	BG-90-33e	108	700	100	20	445	3.60	0.18	1308	122	508	30	**389**	**43**
IX-16	K-2015	BG-90-49a	90	200	100	30	1362	3.24	0.31	1342	125	812	49	**605**	**68**
IX-17	K-1929	BG-90-3	67	200	100	20	445	2.33	0.12	910	52	284	16	**312**	**26**
IX-19	K-2013	BG-90-48a	175	600	200	30	1362	3.25	0.33	1273	127	722	43	**567**	**66**
IX-19	K-2014	BG-90-48b	175	600	200	30	1388	3.46	0.17	1371	139	896	49	**654**	**76**
IX-20	K-3016	B-96-5	164	200	50	20	534	2.74	0.06	1100	59	454	29	**412**	**35**
IX-24	K-3205	B-99-46-1	91	120	20	20	890	2.94	0.06	1110	54	327	27	**295**	**28**
IX-26	K-3215	B-99-48	70	50	20	20	534	2.90	0.00	1142	54	370	35	**324**	**35**
X-07	D-2156	B-91-2	10	200	100	201	668	2.79	0.14	836	61	113	7	**135**	**14**
X-07	D-2157	B-91-3	10	100	50	20	668	2.62	0.13	808	57	105	8	**130**	**14**
X-07	K-3162	B-99-18	10	50	10	20	267	3.10	0.06	937	40	121	5	**129**	**7**
X-07	K-3167	B-99-23	10	180	20	20	267	2.98	0.08	961	45	168	6	**175**	**10**
X-08	D-2158	B-91-4	10	1000	200	20	668	2.64	0.13	924	84	304	34	**329**	**48**
X-08	K-3163	B-99-19	10	530	30	20	534	4.94	0.27	1562	99	361	15	**231**	**18**
X-09	K-3168	B-99-24	20	50	30	20	267	2.70	0.44	776	78	77	7	**99**	**12**
X-10	K-3169	B-99-25	25	50	20	20	534	2.82	0.69	871	126	114	7	**130**	**20**
X-10	K-3171	B-99-27	25	50	20	20	267	2.80	0.16	819	43	89	4	**109**	**7**
X-11	K-3174	B-99-30	28	50	20	20	534	2.94	0.01	896	36	115	5	**128**	**7.5**
X-13	K-3178	B-99-34	12	1000	40	26	534	3.35	0.01	1168	62	403	39	**345**	**38**
X-13	K-3180	B-99-36	12	500	30	20	267	3.17	0.24	890	60	125	7	**141**	**13**
X-14	K-3362	B-99-72-1	4	50	30	20	267	2.75	0.07	756	31	66	5	**88**	**8**
X-14	K-3363	B-99-72-2	4	100	30	20	267	2.81	0.13	794	38	82	3	**104**	**6**
XII-01	D-2232	B-91-40-12	12	1800	200	20	668	2.99	0.15	915	81	213	16	**232**	**27**
XII-01	D-2233	B-91-40-8.5	8.5	2150	200	20	668	3.16	0.16	884	76	161	9	**182**	**18**
XII-01	D-2234	B-91-40-15	15	1500	200	20	668	3.28	0.17	962	83	193	13	**201**	**22**
XII-01	D-2235	B-91-40-17.5	17.5	1250	200	20	668	3.15	0.16	909	78	168	17	**185**	**25**
XII-01	D-2236	B-91-40-19	19	1100	200	20	668	3.02	0.15	941	81	213	28	**226**	**36**
XII-01	D-2237	B-91-40-24	24	600	100	20	668	2.95	0.15	953	80	210	24	**221**	**31**

Table 5.3 continued:

Site	Lab. No.	Sample	Elev.	Depth		Ali.	Dmax	Uranium		D'		DE		ESR age	
			m asl.	cm	±	n	Gy	ppm	±	µGy/a	±	Gy	±	ka	±
XII-01	D-2238	B-91-40-25	25	500	100	20	668	2.71	0.14	886	72	187	12	**212**	**22**
XII-01	D-2265	BG-90-88	26	2400	200	20	668	2.80	0.14	842	74	190	26	**225**	**37**
XII-01	K-2074	BG-90-84	26	1600	100	20	445	3.10	0.16	874	75	157	8	**179**	**18**
XII-01	K-3018	B-96-7-1	24	2100	100	20	356	2.83	0.32	785	73	138	11	**175**	**21**
XII-01	K-3019	B-96-7-2	24	2100	100	20	356	2.65	0.21	727	53	123	7	**169**	**16**
XII-02	D-2209	B-91-30-1	2.5	250	50	20	668	2.76	0.14	929	73	189	18	**203**	**25**
XII-02	D-2210	B-91-30-2	0	50	30	20	668	2.96	0.15	975	73	164	7	**168**	**15**
XII-02	D-2211	B-91-30-3		50	30	20	668	2.83	0.14	997	76	202	16	**203**	**22**
XII-02	D-2212	B-91-30-5	4	400	50	20	668	2.80	0.14	922	74	193	11	**209**	**20**
XII-02	D-2213	B-91-30-6	5	500	50	20	668	2.80	0.14	909	75	191	27	**210**	**34**
XII-03	K-3276	B-99-57-8	13.5	660	30	20	534	4.03	0.06	970	45	100	4	**103**	**6**
XII-03	K-3280	B-99-57-12	13.5	1030	30	20	534	3.17	0.24	963	69	200	10	**208**	**18**
XII-03	K-3282	B-99-57-14	13.5	470	30	20	534	3.67	0.10	853	42	87	4	**97**	**7**
XII-03	K-3283x	B-99-57-15	13.5	390	30	50	2670	3.72	0.25	906	56	86	3	**95**	**7**
XII-03	K-3284	B-99-57-16	13.5	300	30	20	534	3.38	0.13	864	43	87	3	**101**	**6**
XII-03	K-3285x	B-99-57-17	13.5	60	30	50	2670	3.50	0.71	918	115	84	3	**92**	**12**
XII-04	D-2257	BG-90-37a	22	200	100	20	668	3.08	0.09	1024	51	205	19	**200**	**21**
XII-04	D-2258	BG-90-37b	22	300	100	20	668	3.03	0.09	980	48	189	20	**193**	**23**
XII-04	K-1992	BG-90-37a	22	100	50	20	445	3.32	0.25	1114	74	222	9	**199**	**16**
XII-04	K-1993	BG-90-37b	22	100	50	20	445	3.38	0.59	1116	133	213	19	**191**	**28**
XII-04	K-3262	B-99-56-2	29	50	30	26	534	3.47	0.21	1189	70	249	10	**210**	**15**
XII-05	K-1994	BG-90-38a	39	50	20	20	445	3.00	0.15	1011	75	182	2	**180**	**14**
XII-05	K-1995	BG-90-38b	39	50	20	20	445	3.33	0.17	1080	81	183	6	**170**	**14**
XII-05	K-3252	B-99-55-1	39	100	50	20	267	3.00	0.08	993	46	178	19	**179**	**21**
XII-05	K-3254	B-99-55-3	39	100	50	26	534	3.19	0.00	1048	46	190	12	**182**	**14**
XII-10	K-3181	B-99-37	40	50	30	20	289	3.42	0.01	1128	50	206	16	**183**	**16**

6. Extended summary and conclusions

U. RADTKE & G. SCHELLMANN

A new era of geological research began with MESOLELLA's (1967, 1968) pioneer work on Barbados. He was the first to demonstrate that the coral cap of Barbados, which covers about 85% of the island, comprises a complex sequence of coral limestones. MESOLELLA interpreted the characteristic terrace topography of the island as the result of a relatively continuous uplift. For the first time, $^{230}Th/^{230}U$ dating proved that reef units with different ages overlie each other, with the uppermost reef terraces being older than the lower terraces. MESOLELLA (1968), MESOLELLA et al. (1969), and BROECKER et al. (1968) established an absolute chronology through U-series dating of the three youngest reef units with ages of 82,000 years, 106,000 years, and 125,000 years. For the first time, these highstand sequences were related to palaeo sea levels. These sea-level reconstructions used data from four investigated traverses that were based on the assumptions of a constant and average uplift rate and a last interglacial sea-level maximum (127,000 BP, MIS 5e) at 6 m asl. Resulting palaeo sea-level values ranged from -13 m to -16 m around 82,000 years (MIS 5a) and from -10 m to -13 m around 105,000 years (MIS 5c) (see Tables 3.2, 3.3, and 3.4).

Since MESOLELLA and BROECKER (see above) assumed that each terrace was formed when summer solar radiation in the northern hemisphere was at its maximum, they concluded that their data supported the astronomical theory of Quaternary climate oscillations proposed by MILANKOVITCH (1941). Indeed, their Barbados results were extremely important for the revival of the MILANKOVITCH theory, which had fallen into disrepute by the mid 1960s. MILANKOVITCH revived the orbital theory of climate change in the 1910s and was strongly influenced by the ideas of the 19th century French astronomer J.A. ADHÉMAR and the Scottish scientist J. CROLL. By the 1920s, MILANKOVITCH´s theory of orbital forcing was generally complete and many scientists conducted field studies to test how well that theory explained past climatic variations. The theory was widely accepted until the 1950s, when results of the new radiocarbon method raised serious concerns about MILANKOVITCH's hypothesis. In particular, ^{14}C dating provided evidence for more glacial advances than could be accounted for by MILANKOVITCH´s theory. While the theory of orbital forcing was discredited again by 1965, it was revived in the late 1960s due to new data from deep sea cores where oxygen isotope records were dated as far back as 650,000 years.

The Barbados benchmark studies by MESOLELLA fell into this latter period. He was a member of R.K. Matthews' successful working group of geologists at Brown University. In the 1970s, this working group obtained remarkable results about the dating of the marine Quaternary stratigraphy of Barbados. In 1979, these results were compiled with special considerations to Middle Pleistocene reef units (BENDER et al. 1979). Palaeo sea levels were calculated for the last 640,000 years based on U-series ages for the last and penultimate interglacial reefs and based on He/U dating of the older reef tracts. Their interpretations provided evidence that the volumes of the polar and mountain ice masses during the interglacials of the last 700,000 years were comparable to those of the present. Derived conclusions were that sea level reached the present day value during these interglacials (see Chapter 3).

A new attempt to determine the absolute age of the fossil coral reef tracts of Barbados was presented by RADTKE et al. (1988) and RADTKE (1989) and was based on the relatively new Electron Spin Resonance (ESR) dating technique. RADTKE resampled the "classical" traverses Clermont Nose, Christ Church, Thorpe, and St. George´s Valley (see Chapter 3), which continued to play a central role in the reconstruction of the Quaternary geomorphological and geological evolution of the island.

Until the mid 1980s, alpha-spectrometric U-series dating was used to date carbonate fossils, which exceeded the dating range of the radiocarbon method. However, due to the limitations in precision and accuracy of the $^{230}Th/^{234}U$ dating technique, many important questions in palaeoclimatology were difficult to be addressed, as for example problems focusing on a possible double-peak sea-level maximum during MIS 5e around 127,000 years ago, or on the exact duration of MIS 5e. After 1987, these problems began to be addressed with direct measurements of U and Th by mass spectrometry that provided a spectacular improvement in the precision of coral dating due to the U-Th disequilibrium method.

Although the mass spectrometric U-series dating

of coral claims a high precision and a reasonable accuracy (e.g. EDWARDS et al. 1987a), early applications of this technique displayed obvious discrepancies and triggered subsequent work, which focused on potential error sources in the age determination. The main problem is the fact that even apparently pristine samples may have initial $^{234}U/^{238}U$ ratios that are higher than those of present-day seawater (c. 148 ‰). These problems have not yet been solved, although crosschecking with the ^{231}Pa method provides an efficient tool for testing the reliability of the U-Th ages. Thus, age estimates have probably not been affected by diagenetic alterations, if ^{230}Th and ^{231}Pa dates are concordant (e.g. GALLUP et al. 2002). Despite these problems, mass spectrometric dating of fossil coral from Barbados since the 1990s has continued to shed new light on important questions concerning the marine Quaternary record. In particular, the timing of Termination II (Chapter 3) is of special interest and recent results from Barbados suggest an age of 135,800 years for this event (GALLUP et al. 2002).

Intermediate summary 1:

After the benchmarking geomorphological and chronostratigraphical studies by MESOLELLA in the 1960s, research on the marine Quaternary of Barbados focused on improvements of the U-series methods and refinements of palaeo sea-level calculations. The U-series TIMS technique was developed in 1987. Since then, many samples from the "classical sites" have been remeasured. Although differences between the initial U ratios and those of present day seawater still raise questions about the accuracy of the TIMS U-Th age determination, TIMS dating has become an essential dating technique in Quaternary science.

The Electron Spin Resonance (ESR) technique for dating coral also plays an integral role in geochronological and morphostratigraphic studies carried out on Barbados during the last twelve years. The newly developed approach (D_E-D_{max} plot procedure) for determining the total absorbed radiation dose improves the precision of ESR dating of Quaternary coral (SCHELLMANN and RADTKE 2001a). It permits the differentiation not only between the main MIS 5, 7, 9, and 11, but also between sub-stages 5e, 5c, and 5a (e.g. SCHELLMANN and RADTKE 2001b). SCHELLMANN et al. (2004) recently demonstrated the high age consistency of ESR and TIMS U-series dating results by comparing data from paired Pleistocene coral samples collected from the emerged last interglacial coral reef terraces on Barbados (see Chapter 4). These results have important implications for the timing and extent of sea-level changes during MIS 5e, 5c, and 5a. Both dating methods indicate a distinct formation of up to three coral reef terraces during MIS 5e, at approximately 132,000 a (ESR) to 128,000 a (U/Th), at 128,000 a (ESR), and between c. 120,000 a (U/Th) and 118,000 a (ESR). It is also highly likely that three reef terraces were developed during MIS 5c between c. 103,000 a (U/Th) and 105,000 a (ESR). The formation of two separate coral reefs during MIS 5a was recognized for the first time on Barbados (SCHELLMANN & RADTKE 2001b). The older MIS 5a-2 reef terrace was dated to 85,000 a (ESR) and 84,000 a (U/Th), and the younger MIS 5a-1 terrace is approx. 74,000 a (ESR) or 77,000 a (U/Th) old (SCHELLMANN et al. 2004).

As shown by SCHELLMANN et al. (2004), ESR and TIMS U-series dates for individual Late Pleistocene coral reef deposits display high scattering (see Chapter 4). This indicates that time resolutions of both dating methods are currently limited to several thousand years and thus the ESR and U/Th age estimates for these periods of terrace formation are consistent. Furthermore, it is not possible to differentiate between single Late Pleistocene coral reef layers and reef deposits that have developed within time periods of less than 4,000 to 5,000 years, regardless of the dating technique used (ESR or TIMS U-series).

Further support for the validity of the ESR dating technique was provided in a recent study of Holocene coral samples from the Netherlands Antilles which were dated both with ESR and ^{14}C methods (RADTKE et al. 2003) and showed a convincing correlation. To summarize, ESR dating of fossil coral can be successfully applied to chronostratigraphic studies. However, although TIMS and ESR dating may be used independently as stand-alone dating techniques, the analysis of replicate samples should become a routine for both dating methods. A big advantage of ESR is that coral can be dated beyond the limits of the TIMS U-series techniques, up to at least 600,000 a.

The precision of ESR dating of corals and mollusc shells, and their potential in supporting chronostratigraphic studies on coral reefs, beach ridge systems, and eolianites was summarized recently by SCHELLMANN & RADTKE (2003).

Intermediate Summary 2:

Due to methodological improvements, the quality of ESR dating results has increased to such an extent that it is now comparable to that of ^{14}C and mass spectrometric U/Th dating results. Therefore, Electron Spin Resonance (ESR) dating of coral has become an efficient geochronological tool. The excellent correlation of TIMS and ESR data of paired last interglacial coral samples from different sites on Barbados provides confidence in the reliability of both techniques.

Many scientists who base their research on the classical „Barbados Model" assume a 6 ± 4 m higher sea level during the last interglacial c. 127,000 a ago (MIS 5e) (e.g. RADTKE, 1989 and references therein). Based on this assumption, sea level during the subsequent submaxima c. 105,000 a ka ago (MIS 5c) and c. 80,000 a ago (MIS 5a) should have been 10 to 20 m below present sea level.

The revised sea-level estimates presented here are based on the assumption that the southern part of Barbados has emerged at a more or less "constant" uplift rate of approx. 0.27 ± 0.02 m/1000 a, and that sea level was approx. 2 ± 2 m higher during the MIS 5e maximum compared to present sea level. Since present reef crest heights (Figure 4.24) were used for sea-level calculations, the estimates are approximations of former mean low tide water levels. The most tectonically stable part of the island and therefore the most suitable for determining palaeo sea-level observation is the south coast of Barbados to the east of Christ Church traverse, one of the so-called "standard traverses" (see Chapter 4; SCHELLMANN and RADTKE 2001b, 2002, and 2004). Fundamental problems, which are related to the assumption of constant uplift, are discussed below.

The two last interglacial sea-level maxima MIS 5e-3 and MIS 5e-2 were dated at c. 132,000 a (ESR) or c. 128,000 a (TIMS U/Th, T-5b coral reef terrace), and at c. 128,000 a (ESR, T-5a coral reef terrace), respectively (Chapter 4, SCHELLMANN et al. 2004). Sea level was around 2 ± 2 m above present during MIS 5e-3, and near present during MIS 5e-2 (see Chapter 4.4). Sea level dropped towards the end of MIS 5e-2 and reached –11 ± 2 m during the MIS 5e-1 reef growth at approximately 118,000 a to 120,000 a ago (T-4 coral reef terrace). During the MIS 5e interval, the three coral reef terraces T-5b, T-5a, and T-4 formed on the southern Barbados coast. The N4 terraces at Batts Rock Bay, west coast of Barbados, also formed during that time (Chapter 5). These findings correspond well with the established timing of MIS 5e sea-level changes elsewhere in the Caribbean. For example, mass-spectrometric U-series data by EDWARDS et al. (1997) and CHEN et al. (1991) collected on Barbados and Bahamas, respectively, generally indicated a maximum MIS 5e highstand between 132 or 128 ka ago, followed by a sea-level drop at about 123 to 120 ka ago.

The MIS 5c deposits investigated in this study included the three coral reef terraces T-3, T-2, and T-1b on the south coast (Chapter 4), as well as the N3 coral reef terrace and the abraded $N1_{[5]}$ coral reef deposit near Batts Rock Bay on the west coast of Barbados (Chapter 5). Neither the abundant ESR data nor the relatively few U/Th data allowed for a differentiation of the chronostratigraphy of these MIS 5c coral reef terraces (Figure 4.22; SCHELLMANN et al. 2004). Based on ESR data, they formed approx. 104,000 a to 105,000 a ago. This corresponds to the median value of 105,000 years calculated from the few U/Th dating results from MIS 5c coral samples from sample sites T-1b and T-3 on the south coast, and from $N1_{[5c]}$ and N3 on the west coast of Barbados (Chapter 4). Sea level reached three different relative highstands during MIS 5c around 105,000 a ago: c.-13 ± 2 m during MIS 5c-3; c.-20 ± 2 m during MIS 5c-2; and c.-25 ± 2 m during MIS 5c-1.

It is surprising that TIMS U-series data referring to timing and magnitude of sea-level changes in the Caribbean during MIS 5c are scarce. BARD et al. (1990) and EDWARDS et al. (1997) reported a relatively high sea level (c.–18 m) approx. 101,000 a and 104,000 a ago, respectively. These estimates were based on data from the discontinuously rising west coast of Barbados (SCHELLMANN & RADTKE 2002) and generally agree to the MIS 5c sea-level changes described above.

A double sea-level oscillation during MIS 5a correlated to the formation of two morphologically distinct coral reefs ($T\text{-}1a_1$ and $T\text{-}1a_2$) was identified on Barbados for the first time by SCHELLMANN & RADTKE (2001b). Both reef terraces were identified and mapped on the south coast of Barbados. ESR dating results from 41 coral samples from different sample sites yielded ages of approx. 74,000 a for $T\text{-}1a_1$ and approx. 85,000 a for $T\text{-}1a_2$ (Figure 4.22; SCHELLMANN and RADTKE, 2001b, 2002, 2004). These ages are generally consistent with the U/Th dating results from samples sites XI-04, XI-78, and XI-65 on the south coast of Barbados, which provided

median values of 76,700 a (T-1a$_1$) and 84,200 a (T-1a$_2$), respectively (Table 4.1, SCHELLMANN et al. 2004). An older MIS 5a coral reef terrace is developed at Batts Rock Bay on the west coast of Barbados. Coral samples from the N2 coral reef terrace at 20 m asl. provided an ESR age of approx. 85,500 a and median U/Th age of 84,500 a (Table 4.1), both indicating an association with an early MIS 5a-2 sea-level stand. These findings suggest a double sea-level oscillation during MIS 5a including an early MIS 5a-2 with a sea-level height of c.–21 ± 2 m dated at approx. 84,000 a (U/Th) or 85,000 a (ESR) and followed by a late MIS 5a-1 stand at c.–19 ± 2 m below present sea level dated at approx. 74,000 a (ESR) or 76,000 a (U/Th) (Figure 4.24).

The older MIS 5a sea-level stand at approx. 84,000 a to 85,000 a, is consistent with TIMS U-series data from the Worthing Terrace, Barbados, of approx. 83,300 a, 82,800 a and 88,200 a as reported by GALLUP et al. (1994), EDWARDS et al. (1997), and BARD et al. (1990b), respectively. In comparison, TOSCANO and LUNDBERG (1999) reported a MIS 5a sea-level stand of approx. -9 m below mean sea level (msl.) at 83,000 a, and of approx. -15 to -11 m (MSL) at 86,200 a to 80,900 a for the southeastern Florida carbonate margin. This agrees well with the timing of the older MIS 5a-2 sea-level stand on Barbados, although these sea-level calculations differ by some meters. However, these sea-level reconstructions conflict with a study on Bermuda conducted by LUDWIG et al. (1996), who assumed that sea level approx. 80,000 a ago was close to present sea level. CUTLER et al. (2002) presented a relatively high sea level at -24 m 76,200 a ago (based on two concordant TIMS U-series age determinations), which may correlate with the late MIS 5a-1 sea-level stand on Barbados.

Intermediate Summary 3:

Assuming a constant uplift rate of 0.276 m/ka on the south coast of Barbados, sea level reached its maximum during MIS 5e-3 and MIS 5e-2 between 132,000 a and 128,000 a ago, respectively. Subsequently, sea level dropped to c. -11 m below present sea level approx. 118,000 a to 120,000 a ago (MIS 5e-1). Sea level was generally lower during substage 5c compared to substage 5e. It reached three relative maxima at c. -13 m, -20 m, and -25 m during MIS 5c (approx. 105,000 a) and generated three distinct coral reef terraces in rapid succession. For the first time, a double sea-level oscillation was recognized on Barbados during MIS 5a: an early MIS 5a-2 (c. 85,000 a) with a sea level places at approx. -21 m, and a late MIS 5a-1 sub-stage (c. 74,000 a (ESR) or 77,000 a (U/Th) with a sea level approx. 19 m below present sea level.

The revised Barbados model presented here suggests that sea level seems to have oscillated more strongly during the last 400,000 years than commonly assumed. Evidence for these strong oscillations was provided by several sub-stages with palaeo sea-level elevations ranging from 10 m to 25 m below present sea level, which have been preserved on southern Barbados from the last two interglacial sea-level highstands (Figure 4.24: sub-maxima 5a-1, 5a-2, 5c-1, 5c-2, 5c-3, 7-1). The beginning of sea-level fall at the end of the relatively short last and penultimate interglacial transgression maxima - both of which probably lasted few tens of thousands of years only (Figure 4.24: 5e-3/5e-2, 7-2, and 7-3) - has been documented by morpho- and chronostratigraphically distinct coral reef formations. KU et al. (1990) described two "5e" terraces, which were morphologically separated: the classical "Rendezvous Hill Terrace" and the "Maxwell Terrace". However, alpha-spectrometric U-series dating was not able to yield any evidence for previously inferred separate highstands centering around 118,000 and 135,000 a. Instead, the obtained ages (120,000 a for Maxwell terrace and 117,000 a for Rendezvous Hill terrace), differ significantly from previously and subsequently published U-series results. The new investigations presented in this volume demonstrate that a double highstand during 5e can be identified morphologically as indicated by KU et al. (1990). Moreover, three morphologically and geochronologically (ESR) distinct 5e highstands were identified: T5b (5e-3) at 132,000 a; T5a (5e-2) at 128,000 a; and T4 (5e-1) ("Maxwell") at 118,000 to 120,000 a ago. Taking into account the very small difference in age and palaeo sea level, the two highstands 5e-3 and 5e-2 should be interpreted as minor oscillations during the MIS 5e maximum.

The analyses presented here would predict palaeo sea-level heights ranging from 8 m to more than 18 m for the third and fourth past interglacials (Figure 4.24, MIS 9 and 11), if they were based on the commonly held assumption that last interglacial sea level was 6 m higher than present sea level. However, these reconstructions would be inconsistent with oxygen isotope data obtained from deep sea cores, which imply that sea levels during the transgression maxima of the previous Middle Pleistocene interglacial time periods were comparable to Holocene and

last interglacial sea-level highstands. These oxygen isotope data can only be integrated with the sea-level reconstructions derived from the Barbados coral samples, if one assumes that the last interglacial sea level was comparable to present sea level or a maximum of 2 m higher (Figure 4.24). Therefore, the widely held assumptions of constant uplift and a last interglacial maximum sea level at 6 m are not supported by our study and appear to be incompatible.

Since Barbados does not seem to be significantly influenced by glacio- or hydro-isostatic effects (PELTIER 2002), the palaeo sea levels calculated here should be close to ice-equivalent eustatic values. For this reason Barbados has been an important focus of research on palaeo sea levels. However, a note of caution must be sounded. As mentioned above, palaeo sea-level estimates deduced from raised fossil coral reefs are generally based on the assumption that coral reef terraces have been uplifted at a constant rate. Palaeo sea levels calculated from the different traverses on the island are documented in many textbooks of Quaternary Geology and the results are frequently compared to data from other tropical fossil reef sequences such as those on Papua New Guinea (e.g. CHAPPELL et al. 1996, CUTLER et al. 2002) or Sumba Island (PIRAZZOLI et al. 1991), or to palaeo sea-level estimates derived from the measurement of the isotopic oxygen composition in deep sea foraminifers (SHACKLETON 1986).

However, MESOLLELLA (1968), STEARNS (1976), and BENDER et al. (1979) doubted the constant uplift model. MESOLELLA (1986) assumed that Barbados was uplifted at a near-linear rate between 500,000 and 127,000 years ago and that the near-linear uplift vanished after the maximum of the last interglacial. However, he admits that this assumption was not generally verifiable on Barbados. STEARNS (1976), one of the few critics of the "Barbados model", questioned the assumption of a constant uplift between 125,000 years and 80,000 years. He considered the "Barbados model" a preliminary approach, at best a fruitful first approximation to the problem of calculation Pleistocene palaeo sea levels. The model provided insufficient reliable information for the exact calculation of palaeo sea levels and for the implementation as a "standard measure" for coastal research elsewhere. BENDER et al. (1979) pointed out that a higher uplift rate had to be considered for the Christ Church area before 125,000 years. Despite these critiques, palaeo sea-level values obtained from Barbados are currently widely accepted and cited regularly as reference values.

Our research indicates that the assumption of a constant uplift on Barbados is flawed for several reasons:

(1) Reef stages from the last interglacial transgression maximum (MIS 5e) occur at heights ranging from 20 m to 60 m asl. Therefore, neotectonics must have differed spatially and, quite possibly, also temporally.
(2) Surfaces of individual older reef terraces east of South Point descend in elevation in an easterly direction towards the St. George Valley syncline. This indicates differential tectonic uplift rates (Chapter 4, Figure 4.23). Therefore, this region is not suited for palaeo sea-level estimates.
(3) The reef terraces within the vicinity of the Christ Church Traverse, which were used previously for global palaeo sea-level calculations, are warped anticlines and show clear evidence for differential tectonic uplift (Chapter 4, Figure 4.23).
(4) Similarly, the warped areas of the Clermont Nose Anticline indicate differential uplift and should not used for palaeo sea-level estimates either. There, the uplift rate before the last interglacial was much lower than that during the last interglacial (see below, Chapter 5).

The Clermont Nose traverse north of Bridgetown (west coast of Barbados) was chosen to demonstrate the great difficulties in palaeo sea-level reconstruction based on coastlines with a complicated tectonic history. As mentioned above, the reef terraces within the vicinity of the Clermont Nose Traverse, which have frequently been used for palaeo sea-level calculations, are warped anticlines. There, the uplift rate before the last interglacial was much lower than later uplift rates (see below and Figure 5.1). The maximum MIS 5e highstand of c. 127,000 a is preserved at c. 60 m asl. across the driveway of the University of the West Indies (Figure 5.2, locality VIII-01, N4 level). Localities VIII-10, VIII-20, VIII-21, and VIII -22 belong to penultimate interglacial sea-level highstand (c. 240,000 – 180,000 a) and reach altitudes of almost 90 m. The coral reef tract at 71 to 91 m was dated by GALLUP et al. (1994) with TIMS U-series at c. 200,000 years (Table 3.11) and confirmed this reef's classification as MIS 7. The geochronological evidence for the area 91 to 99 m asl. is not totally clear. Reef tracts may belong to oldest stage 7 or youngest stage 9 (see Fig. 5.1 for ESR, and Table 3.11 for TIMS). GALLUP et al. (1994) obtained a questionable age of 402,000 a for a sample at 100 m asl. ESR ages for locality VIII 25 (104 m asl.) cluster around 465,000 a. ESR ages of up to 500,000 a were obtained for VIII 26, the top of

Clermont Nose traverse along Gordon Cummins Highway (c.12-130 m asl.). Considering the systematic under-estimation of ESR ages for samples older than stage 7 (see Chapter 4.1.2), the highest reef tracts of Clermont Nose Traverse were formed at least during MIS 11 if not earlier.

The new results presented here are compelling. Prior to the last interglacial period, and most probably before the penultimate interglacial, the uplift rate in the area of the Clermont Nose Traverse was much lower compared to the rate during or after MIS 5. The uplift rate around 130,000 a was c. 0.44 m/1000 a and may have been similar at 200,000 a, if the palaeo sea level at that time was close to the present one or slightly lower (SIDDALL et al. 2003). Directly above the 90 m penultimate interglacial sediments, coral reefs get older at a rate of a few meters per interglacial. The calculated uplift rates for the highest part of Clermont Nose Traverse reach a max. of 0.24 m/1000 a but were probably lower. This indicates that uplift rates during these intervals were nearly twice those of the last interglacial. The timing of this dramatic change in tectonic behavior can only be estimated due to the lack of precise data between the highest part of the traverse and the coral of the penultimate interglacial at an altitude of 90 m. Based on evidence that marine sediments at c. 95 - 100 m belong to the third last interglacial around 300,000 a, the change in uplift velocity must have taken place sometime between 300,000 and 200,000 a. In conclusion, terraces in the vicinity of the Clermont Nose Anticline should not be used for sea-level calculations because they display indisputable evidence for differential uplift.

Intermediate summary 4:

The anticlinal warped areas of Clermont Nose and Christchurch Traverse are not suitable for Pleistocene sea-level reconstruction. It has been demonstrated that the regions around the classical traverses Christchurch and Clermont Nose have experienced differential rates of tectonic uplift, which make the commonly accepted assumption of constant uplift unreasonable. The uplift rate along Clermont Nose Traverse has changed between 0.24 and 0.45 m/1000a during the last 500,000 years.

This research demonstrated that detailed geomorphologic mapping and dating of fossil reef tracts is crucial for the identification of regions that were probably not affected by anticline or syncline warping (e.g. east of Christchurch Traverse, see Figure 4.23). Although the possibility that the rate of uplift has not even been constant over time in tectonically "safe" areas cannot be excluded, palaeo sea level calculated from the "more stable" parts of Barbados are of great importance to the pursuit of a regional Quaternary sea-level curve. The data are essential for geophysical models that calculate isostatic rebound effects.

In 1989, RADTKE wrote that "an evaluation of our present state of knowledge points to the fact that a valid solution for the sea-level record of the last 500,000 years will only become available in the next decade. Because of the chronostratigraphic problems that persist, it seems likely that the Early Pleistocene record will remain a "black box" for terrace and sea-level research" (RADTKE, 1989: p. 211). Although the last 12 years shone some light into the former black box of the Middle Pleistocene, the Early Pleistocene still remains quite challenging. However, progress of the last few years has been remarkable and sea-level changes of the last four interglacials have been estimated using different methods (e.g. SIDDALL et al. 2003) and are in discussion. Despite the critical reflections we have made, the results obtained on Barbados, are important for further global interpretation of sea-level change. Hopefully, these results will motivate researchers to look for similar phenomena at other localities. Determining temporal and spatial variations in rates of crustal uplift is a necessary prerequisite for any Pleistocene palaeo sea-level reconstruction based on coral reef terrace data. While the assumption of a constant uplift has an appealing simplicity, our work has demonstrated that, in Barbados at least, this assumption is not valid. The reconstruction of uplift rates and the associated identification of most suitable sites on Barbados for palaeo sea-level reconstruction was only possible through detailed analyses at numerous localities and through the combination of morphostratigraphy with multiple dating techniques. What remains is the challenge to identify comparable sites elsewhere on the globe in order to use site-to-site comparisons for the realistic quantification of global palaeo sea-level trends. Sea-level changes are one of the defining signatures of the Quaternary. Information on both timing and cause of global sea-level changes is the prerequisite for a better understanding of the correlation between geological processes and climatic change.

Literature

ADEY, W.H. (1986): Coralline algae as indicators of sea-level. - In: PLASSCHE, v. de O. (ed.): Sea-level research: a manual for the collection and evaluation of data: 229-280; Amsterdam.

ADEY, W.H. (1978): Algal ridges of the Caribbean sea and West Indies. – Phycologia, 17 (4): 361-367.

ADEY, W.H. & BURKE, R.B. (1977): Holocene bioherms of Lesser Antilles – geologic control of development. - Studies in Geology, 4: 67-81.

AHARON, P. & CHAPPELL, J. (1986): Oxygen isotopes, sea level changes and the temperature history of a coral reef environment in New Guinea over the last 100,000 years. – Palaeogeography, Palaeoclimatology, Palaeoecology, 56: 337-379.

AHMAD, N. & JONES, R.C. (1969): Genesis, chemical properties and mineralogy of limestone-derived soils, Barbados, West Indies. – Tropical Agriculture, 46: 1-15; Trinidad.

BAK, R.P.M. (1977): Coral reefs and their zonation in the Netherlands Antilles. – Studies in Geology, 4: 3-16.

BAK, R.P.M. (1976): The growth of coral colonies and the importance of crustose coralline algae and burrowing sponges in relation with carbonate accumulations. – Netherlands Journal of Sea Research, 10: 285-337.

BANNER, J.L., MUSGROVE, M.L. & CAPO, R.C. (1994): Tracing ground-water evolution in a limestone aquifer using Sr isotopes: Effects of multiple sources of dissolved ions and mineral-solution reactions. – Geology, 22: 687-690.

BANNER, J.L. WASSERBURG, G.J., CHEN, J.H. & HUMPHREY, J.D. (1991): Uranium-series evidence on diagenesis and hydrology in Pleistocene carbonates of Barbados, West Indies. – Earth and Planetary Science Letters, 107: 129-137.

BARD, E., ARNOLD, M., FAIRBANKS, R.G. & HAMELIN, B. (1993): ^{230}Th-^{234}U and ^{14}C ages obtained by mass spectrometry on corals. – Radiocarbon, 35 (1): 191-199.

BARD, E., FAIRBANKS, R.G. & HAMELIN, B. (1992a): How accurate are the U-Th ages obtained by mass spectrometry on coral terraces. – In: KUKLA, B. J. & WENT, E. (eds.): Start of a Glacial: 15-22; Berlin (Springer Verlag).

BARD, E., FAIRBANKS, R.G., ARNOLD, M. & HAMELIN, B. (1992b): ^{230}Th-^{234}U and ^{14}C ages obtained by mass spectrometry on corals from Barbados (West Indies), Isabela (Galapagos) and Mururoa (French Polynesia). – In: BARD, E. & BROECKER, W.S. (eds.): The Last Glaciation: Absolute and Radiocarbon Chronologies, NATO ASI Ser. I2: 103-110; Berlin, Heidelberg (Springer Verlag).

BARD, E., FAIRBANKS, R.G., HAMELIN, B., ZINDLER, A. & HOANG, C.T. (1991): Uranium-234 anomalies in corals older than 150,000 years. – Geochimica et Cosmochimica Acta, 55: 2385-2390.

BARD, E., HAMELIN, B., FAIRBANKS, R.G. & ZINDLER, A. (1990a): Calibration of the ^{14}C timescale over the past 30,000 years using mass spectrometric U-Th ages from Barbados corals. – Nature, 345: 405-410.

BARD, E., HAMELIN, B. & FAIRBANKS, R.G. (1990b): U-Th-ages obtained by mass spectrometry in corals from Barbados: sea-level during the past 130,000 years. – Nature, 346: 456-458.

BEAVEN, P.J. & DUMBLETON, M.J. (1966): Clay minerals and geomorphology in four Caribbean islands. – Clay Mineralogy, 6: 371-382.

BECKER, B., KROMER, B. & TRIMBORN, P. (1991): A stable isotope tree-ring timescale of the Late Glacial / Holocene boundary. – Nature, 353: 647-649.

BENDER, M.L. (1973): Helium-Uranium dating of corals. – Geochimica et Cosmochimica Acta, 37: 1229-1247.

BENDER, M.L., TAYLOR, F.W., MATTHEWS, R.K., GODDARD, J.G. & BROECKER, W.S (1979): Uranium-series dating of the Pleistocene reefs tracts of Barbados, West Indies. – Geological Society of America Bulletin, I 90: 577-594.

BENSON, L.V. & MATTHEWS, R.K. (1971): Electron microprobe studies of magnesium distribution in carbonate cements and recrystallized skeletal grainstones from the Pleistocene of Barbados, West Indies. – Journal of Sedimentary Petrology, 41: 1018-1025.

BIRD, J.B., RICHARDS, A. & WONG, P.P. (1979): Coastal subsystems of Western Barbados, West Indies. – Geografiska Annaler, 61 A (3-4): 221-236.

BLANCHON, P. & EISENHAUER, A. (2001): Multi-stage reef development on Barbados during the Last Interglacial. – Quaternary Science Reviews, 20: 1093–1112.

BLUME, H. (1974): The Caribbean Islands. – 464 p.; London.

BLUME, H. (1973): Die Westindischen Inseln. – 2nd ed.; Braunschweig.

BORG, L.E. & BANNER, J.L. (1996): Neodymium and strontium isotopic constraints on soil sources in Barbados, West Indies. – Geochimica et Cosmochimica Acta, 60 (21): 4193-4206.

BOTT, M.H.P. (1982): The Interior of the Earth. - 223 pp., Amsterdam (Elsevier).

BROECKER, W.S., THURBER, D.L., GODDARD, J., KU, T.L., MATTHEWS, K.L. & MESOLELLA, K.J. (1968): Milankovitch hypothesis supported by precise dating of coral reefs and deep-sea sediments. – Science, 159: 297-300.

BUDD, A. F. (2000): Diversity and extinction in the Cenozoic history of Caribbean reefs. – Coral Reefs, 19: 25-35.

CAREY, S. & SIGURDSSON, H. (1980): The Roseau ash: Deep-sea tephra deposits from a major eruption on Dominica, Lesser Antilles. – Journal of Volcanic Geothermal Research, 1: 67-86.

CHAPPELL, J., OMURA, A., ESAT, T., MCCULLOCH, M., PANDOLFI, J., OTA, Y. & PILLANS, B. (1996): Reconciliation of late Quaternary sea levels derived from coral terraces at Huon Peninsula with deep sea oxygen isotope records. – Earth and Planetary Science Letters, 141: 227-236.

CHAPPELL, J. & POLACH, H.A. (1991): Post-glacial sea level rise from a coral record at Huon Peninsula, Papua Neuginea. – Nature, 349: 137-140.

CHEN, J.H., CURRAN, H.A., WHITE, B. & WASSERBURG, G.J. (1991): Precise chronology of the last interglacial period: ^{234}U-^{230}Th data from fossil coral reefs in the Bahamas. – Geological Society of America Bulletin, 103: 82-97.

CUTLER, K.B., EDWARDS, R.L., TAYLOR, F.W., CHENG, H., ADKINS, J., GALLUP, C.D., CUTLER, P.M., BURR, G.S. & BLOOM, A.L. (2003): Rapid sea-level fall and deep-ocean temperature change since the last interglacial period. – Earth and Planetary Science Letters, 206: 253-271.

DAVIESS, S.N. (1971): Barbados; A major submarine gravity slide. – Geological Society of America Bulletin, 82 (9): 2593-2602.

DAY, M.J. (1993): Human Impacts on Caribbean and Central American Karst. – Catena Suppl. Bd., 25: 109-125.

DAY, M.J. (1983): Doline morphology and development in Barbados. – Annals of the Association of American Geographers, 73 (2): 206-219.

DEBROT, A.O., KUENEN, M.M.C.E. & DEKKER, K. (1998): Recent declines in the coral fauna of the Spaanse Water, Curaçao, Netherlands Antilles. – Bulletin of Marine Science, 63(3): 571-580.

DEGRAFF, J.V., BRYCE, R. JIBSON, R.W., MORA, S. & ROGERS, C.T. (1989): Landslides: Their extent and significance in the Caribbean. – In: BRABB, E.E. & HARROD, V. (eds.): Landslides: Extent and Economic Significance: 51-80; Rotterdam.

DENGO, G. & CASE, J.E. (1990) (eds.): The Caribbean region. - The Geology of North America, Vol. H. – The Geological Society of America, Boulder (Colorado).

DELANY, A.C., DELANY, A.CL., PARKIN, D.W., GRIFFIK, J.J., GOLDBERG, E.D. & REIMANN, B.E.F. (1967): Airborne dust collected at Barbados. – Geochimica et Cosmochimica, 31: 885-909.

DIA, A.N, COHEN, A.S., ONIONS, R.K. & SHACKLETON, N.J. (1992): Seawater Sr isotope variation over the past 300 kyr and influence of global climate cycles. – Nature, 356: 786-788.

DILLER, J.S. & STEIGER, G. (1902): Volcanic dust and sand from St. Vincent caught at sea and on Barbados. – Science, 15: 947-950.

DREWETT, P.L. (2002): Amerindian stories: An archaeology of early Barbados. – 28 pp.; Barbados.

DRUFFEL, E.R.M. (1997): Pulses of rapid ventilation in the North Atlantic surface ocean during the past century. – Science, 275: 1454-1457.

DULLO, W.-CHR. & MEHL, J. (1989): Seasonal growth lines in Pleistocene scleratinians from Barbados: record potential and diagenesis. – Paläontologische Zeitschrift, 63 (3/4): 207-214; Stuttgart.

DUNBAR, R.B. & COLE, J.E. (eds.) (1993): Coral records of Ocean - Atmosphere Variability. Report from the Workshop on Coral Paleoclimate Reconstruction, Nov. 5-8, 1992, La Parguera, Puerto Rico. – NOAA Climate and Global Change Program, Special Report No. 10: 38 p.

DUNCAN, P. (1975): Growth and form in the reef-building coral *Montastrea annularis*. – Marine Biology, 33: 101-107.

DUNCAN, P. M. (1863): On the fossil corals of the West Indian Islands - Part I. – Quarterly Journal of London Geological Society, 19: 406-458.

DUQUE-CARO, H. (1990): Neogene stratigraphy, paleoceanography, and paleobiogeography in northwest South America and the evolution of the Panama Seaway. – Palaeogeography, Palaeoclimatology and Palaeoecology, 77: 203-234.

EDWARDS, R.L., CHENG, J.H., MURRELL, M.T. & GOLDSTEIN, S.J. (1997): Protactinium–231 dating of carbonates by thermal ionization mass spectrometry: Implications for Quaternary climate change. – Science, 276: 782-786.

EDWARDS, R.L., CHEN, J.H. & WASSERBURG, G.J. (1987a): ^{238}U-^{230}U-^{234}U-^{232}Th systematics and the precise measurement of time over the past 500,000 years. – Earth and Planetary Science Letters, 81: 175-192.

EDWARDS, R.L., CHEN, J.H., KU, T.U. & WASSERBURG, G.J. (1987b): Precise Timing of the Last Interglacial Period from Mass Spectrometric Determination of Thorium-230 in Corals. – Science, 236: 1547-1553.

EISENHAUER, A., ZHU, Z.R., COLLINS, L.B., WYRWOLL, K.H. & EICHSTÄTTER, R. (1996): The Last Interglacial sea level change: new evidence from the Abrolhos islands, West Australia. – Geologische Rundschau, 85: 606-614.

ESAT, T.M., MCCULLOCH, T., CHAPPELL, J., PILLANS, B. & OMURA A. (1999): Rapid fluctuations in sea level recorded at Huon Peninsula during the Penultimate deglaciation. – Science, 283: 197-201.

FAIRBANKS, R.G. (1989): A 17,000 year glacio-eustatic sea level record: influence of glacial melting rates on the Younger Dryas event and deep-ocean circulation. – Nature, 342: 637-642.

FAIRBANKS, R.G. (1977): Geochemistry of marine skeletal carbonate for use in paleoenvironmental reconstructions. – Diss. Brown University: 193 p., Philadelphia.

study of mud volcanoes seaward of the Barbados accretionary wedge: sedimentology, structure and rheology. – Marine Geology, 145: 255-292.

LANDER, J.F., WHITESIDE, L.S. & LOCKRIDGE, P.A. (2002): A brief history of tsunamis in the Caribbean sea. – Science of Tsunami Hazards, 20 (2): 57-94.

LEWIS, J.B. (2002): Evidence from aerial photography of structural loss of coral reefs at Barbados, West, Indies. – Coral Reefs, 21: 49-56.

LEWIS, J.B. (1997): Abundance, distribution and partial mortality of the massive coral *Siderastrea sidera* on degrading coral reefs at Barbados, West Indies. – Marine Pollution Bulletin, 34 (8): 622-627.

LEWIS, J.B. (1960a): The coral reefs and coral communities of Barbados. W.I. – Canadian Journal of Zoology, 38: 1135-1145.

LEWIS, J.B. (1960b): The fauna of rocky shores of Barbados, West Indies. – Canadian Journal of Zoology, 38: 391-435.

LIGTHY, R.G., MACINTYRE, I.G. & STUCKENRATH, R. (1982): *Acropora palmata* reef framework: A reliable indicator of sea level in the Western Atlantic for the past 10,000 years. – Coral Reefs, 1: 125-130.

LIRMAN, D. (2000): Fragmentation in the branching coral *Acropora palmata* (Lamarck): growth, survivorship, and reproduction of colonies and fragments. – Journal of Experimental Marine Biology and Ecology, 251: 41-57.

LOW, S. & ZEIRA, S. (1972): ESR spectra of Mn^{2+} in heat-treated Aragonite. – American Mineralogist, 57: 1115-1124.

LUDWIG, K.R., MUHS, D.R., SIMMONS, K.R., HALLEY, R.B. & SHINN, E.A. (1996): Sea-level records at ~80 ka from tectonically stable platforms: Florida and Bermuda. – Geology, 24 (3): 211-214.

MACDONALD, R., HAWKESWORTH, C.J. & HEATH, E. (2000): The Lesser Antilles volcanic chain: a study in arc magmatism. – Earth Science Reviews, 49: 1-76.

MACINTYRE, I.G. (1972): Submerged reefs of the eastern Caribbean. – American Association of Petroleum Geologists Bulletin, 56: 720-738.

MACINTYRE, I.G. (1967): Submerged coral reefs, west coast of Barbados, West Indies. – Canadian Journal of Earth Sciences, 4 (3): 461-474.

MACINTYRE, I.G., RÜTZLER, K., NORRIS, J.N., SMITH, K.P., CAIRNS, S.D., BUCHER, K.E. & STENECK, R.S. (1991): An early Holocene reef in the western Atlantic: submersible investigations of a deep relict reef off the west coast of Barbados, W.I. – Coral Reefs, 10: 167-174.

MAH, A.J. & STEARN, C.W. (1986): The effect of hurricane Allen on the Bellairs fringing reef, Barbados. – Coral Reefs, 4: 169-176.

MCLEAN, R.F. (1967a): Origin and development of ridge furrow systems in beachrock in Barbados, West Indies. – Marine Geology, 5 (3): 181-193.

MCLEAN, R.F. (1967b): Measurements of beach rock erosion by some tropical marine gastropods. – Bulletin Marine Science, 17: 551-561.

MANN, P. (ed.) (1995): Geologic and Tectonic Development of the Caribbean Plate Boundary in Southern Central America. – Geological Society of America, Special Paper 295.

MARTINDALE, W. (1992): Calcified epibionts as paleoecological tools: examples from the Recent and Pleistocene reefs of Barbados. – Corals Reefs, 11: 167-177.

MARTIN-KAYE, R.H.A. (1969): A summary of the Geology of the Lesser Antilles. – Overseas Geology and Mineral Resources, 10 (2).

MARTIN-KAYE, R.H.A. & BADCOCK, J. (1966): Geological background to soil conservation and land rehabilitation measures in Barbados, W.I. – In: ROBINSON, E. (Ed.): Transactions of the Third Caribbean Geological Conference, Kingston, Jamaica, April 2-11, 1962: 131-153; Kingston.

MATTHEWS, R.K. (1990): Quaternary Sea-Level Changes. – In: Geophysics Study Committee (eds.): Sea-level changes: 88-103; Washington D.C. (National Academy Press).

MATTHEWS, R.K. (1986): The delta ^{18}O signal of deep-sea planktonic foraminifera at low latitudes as an ice-volume indicator. – South African Journal of Science, 82: 521-522.

MATTHEWS, R.K. (1973): Relative elevation of Late Pleistocene high sea level stands: Barbados uplift rates and their implications. – Quaternary Research, 3: 147-153.

MESCHEDE, M. (1998): The impossible Galapagos connection: geometric constraints for a near-American origin of the Caribbean plate. – Geologische Rundschau, 87: 200-205.

MESCHEDE, M. & FRISCH, W. (1998): A plate-tectonic model for the Mesozoic and Early Cenozoic history of the Caribbean plate. – Tectonophysics, 296 (3-4): 269-291.

MESOLELLA, K.J. (1968): The uplifted reefs of Barbados: Physical stratigraphy, facies relationship and absolute chronology. – Diss., Brown Univ., Part 1 & 2: 736 p.; Philadelphia.

MESOLELLA, K.J. (1967): Zonation of uplifted Pleistocene coral reefs on Barbados, West Indies. – Science, 156: 638-640.

MESOLELLA, K.J., SEALY, H.A. & MATTHEWS, R.K. (1970): Facies geometries within Pleistocene reefs of Barbados, West Indies. – American Association of Petroleum Geologists Bulletin, 54: 1899-1917.

MESOLELLA, K.J., MATTHEWS, R.K., BROECKER, W.S. & THURBER, D.L. (1969): The astronomical theory of climatic change: Barbados data. – Journal of Geology, 77: 250-274.

MEYERHOFF, A.A., TANER, J. & MORRIS, A.E.L. (1995): Caribbean Region/Karibische Region. – In:

KULKE, H. (ed.): Regional Petroleum Geology of the World. P.II. Africa, Australia and Antarctica. – Beiträge zur regionalen Geologie der Erde, 22: 455-470; Berlin, Stuttgart.

MILANKOVITCH, M. (1941): Kanon der Erdbestrahlung und seine Anwendung auf das Eiszeitenproblem. – Königlich-Serbische Akademie, Éditions Speciales, Tome CXXXIII, Section des Sciences Mathématiques et Naturelles, Tome 33; Belgrad.

MONTAGGIONI, L. (2000): Postglacial reef growth. – Earth and Planetary Sciences, 331: 319-330.

MUHS, D.R. (2001): Evolution of Soils on Quaternary Reef Terraces of Barbados, West Indies. – Quaternary Research, 56: 66-78.

MUHS, D.R., BUSH, C.A., STEWART, K.C., ROWLAND, T.R. & CRITTENDEN, R.C. (1990): Geochemical evidence of Saharan dust parent material for soils developed on Quaternary limestones of Caribbean and western Atlantic Islands. – Quaternary Research, 33: 157-177.

MUHS, D.R., CRITTENDEN, R.C., ROSHOLT, J.N., BUSH, C.A. & STEWART, K.C. (1987): Genesis of marine terrace soils, Barbados, West Indies: evidence from mineralogy and geochemistry. – Earth Surface Processes and Landforms, 12: 605-618.

MURRAY-WALLACE, C.V. & BELPERIO, A.P. (1991): The Last Interglacial shoreline in Australia - a review. – Quaternary Science Reviews, 10: 441-461.

MUNZINGER-ARCHIV (2002): Internationales Handbuch – Länder aktuell: Barbados. – Ravensburg.

NESBITT, H.W. & YOUNG, G.M. (1997): Sedimentation in the Venezuelan Basin, Circulation in the Caribbean Sea, and Onset of Northern Hemisphere Glaciation. – The Journal of Geology, 105: 531-544.

NEUMANN, A.C. & MACINTYRE, I. (1985): Reef response to sea level rise: keep-up, catch-up or give-up. – Proceedings, 5th Intern. Coral Reef Congress, Tahiti, Vol. 3: 105-110; Moorea (French Polynesia).

NURSE, L. & SEM, G. (2001): Small island states. - In: MCCARTHY, J., CANZIANI, O., LEARY, N., DOKKEN, D. & WHITE, K. (eds.), Climate Change 2001: Impacts, Adaptation and Vulnerability. – Cambridge (Cambridge University Press).

OKUNO, J. & NAKADA, M. (1999): Total volume and temporal variation of meltwater from last glacial maximum inferred from sea-level observations at Barbados and Tahiti. – Palaeogeography, Palaeoclimatology, Palaeoecology, 146: 283-293.

PANDOLFI, J.M. (2002): Coral community dynamics at multiple scales. – Coral Reefs, 21: 13-23.

PAUL, M. (1995): Geologic and tectonic development of the Caribbean plate boundary in Southern Central America. – The Geological Society of America, Spec. Paper, 295: XI-XXXII; Boulder (Colorado).

PELTIER, W.R. (2002): On eustatic sea level history: Last Glacial Maximum to Holocene. – Quaternary Science Reviews, 21: 377-396.

PERRY, C.T. (2001): Storm induced coral rubble deposition: Pleistocene records of natural reef disturbance and community response. – Coral Reef, 20: 171-183.

PFEFFER, K.-H. (1993): Zur Genese tropischer Karstgebiete auf den Westindischen Inseln. – Zeitschrift für Geomorphologie N.F., Suppl.-Bd. 93: 137-158; Berlin, Stuttgart.

PINDEL, J.L. & BARRETT, S.F. (1990): Geological evolution of the Caribbean Region. – In: DENGO, G. & CASE, J.E. (eds.): The Geology of North America, Volume H., The Caribbean Region. Geol. Soc. of North America: 405-432; Boulder.

PINGITORE, N.E. JR. (1976): Vadose and phreatic diagenesis: Processes, products and their recognition in corals. – Journal of Sedimentary Petrology, 46 (4): 985-1006.

PINGITORE, N.E. JR. & NICHOLAS, E. (1976): Diagenesis and porosity modification in *Acropora palmata*, Pleistocene of Barbados, West Indies. – Journal of Sedimentary Petrology, 46 (7): 985-1006.

PITTMAN, E.D. (1974): Porosity and permeability changes during diagenesis of Pleistocene corals, Barbados, West Indies. – Geological Society of America Bulletin, 85: 1811-1820.

POOLE, E.G. & BARKER, L.H. (1982): The geology of the Scotland District of Barbados. – Transactions, 9th Caribbean Geological Conference, Santo Domingo, Dominican Republic, 1980: 641-656; Santo Domingo.

PRIOR, D.B. & HO, C. (1972): Coastal and mountain slope instability on the islands of St. Lucia and Barbados. – Engineering Geology, 6: 1-18.

PROSPERO, J.M. & NEES, R.T. (1986): Impact of North African drought and El Niño on mineral dust in the Barbados trade winds. – Nature, 320: 735-738.

PROSPERO, J.M. & CARLSON, T.N. (1972): Vertical and areal distribution of Saharan Dust over the Western Equatorial North Atlantic Ocean. – Journal of Geophysical Research, 77 (27): 5255-5265.

PROSPERO, J.M., BONATTI, E., SCHUBERT, C. & CARLSON, T.N. (1970): Dust in the Caribbean atmosphere traced to an African dust storm. – Earth and Planetary Science Letters, 9: 287-293.

RADTKE, U. (1989): Marine Terrassen und Korallenriffe - Das Problem der quartären Meeresspiegelschwankungen. Erläutert an Fallstudien aus Chile, Argentinien und Barbados. – Düsseldorfer Geographische Schriften, 27: 245 p.; Düsseldorf (Germany).

RADTKE, U. & GRÜN, R. (1990): New findings on the reconstruction of Middle and Late Pleistocene sea-level change, Barbados, West-Indies. – Journal of Coastal Research, 6 (3): 699-708.

RADTKE, U. & GRÜN, R. (1988a). ESR dating of corals. – Quaternary Science Reviews, 7: 465-470.

RADTKE, U., GRÜN, R. & SCHWARCZ, H.P. (1988b): Electron spin resonance dating of the Pleistocene coral reef tracts of Barbados. – Quaternary Research, 29: 197-215.

RADTKE, U., SCHELLMANN, G., SCHEFFERS, A., KELLETAT, D., KASPER, H.U. & KROMER, B. (2003): Electron Spin Resonance and Radiocarbon dating of coral deposited by Holocene tsunami events on Curaçao, Bonaire and Aruba (Netherlands Antilles). – Quaternary Science Reviews, 22: 1309-1315.

RANDALL, R.E. (1970): Vegetation and environment on the Barbados coast. – Journal of Ecology, 58: 155-172.

RAPPAPORT, E.N. & FERNANDEZ-PARTAGAS, J.F. (1997): The deadliest Atlantic tropical cyclones, 1492 - present. – Internet: http://www.nhc.noaa.gov/pastdeadlya1.html.

RITTER, D.F., KOCHEL, R.C. & MILLER, J.R. (1995): Process Geomorphology. – 3rd Edition; Brown, Dubuque.

ROTH, J.M., DROXLER, A.W. & KAMEO, K. (2000): The Caribbean Carbonate Crash at the Middle to Late Miocene transition: Linkage to the establishment of the modern global ocean conveyor. – Proceedings of the Ocean Drilling Program, Scientific Results, 165: 249-273.

RUSSEL, R.J. (1966): Coral cap of Barbados. – Geografisch Tijdschrift, 2, 83(3): 289-302; Amsterdam.

RUSSEL, R.J. & MCINTIRE, W.G. (1965): Limestone terraces of Barbados. – Annals Association of American Geographers, 55 (4): 644.

SAINT, S.J. (1934): The coral limestone soils of Barbados. – Journal of Dept. of Science and Agriculture, 3: 1-37; Barbados.

SANDER, F. & STEVEN, D.M. (1973): Organic productivity of inshore and offshore water of Barbados: a study of the island mass effect. – Bulletin of Marine Science, 23 (4): 771-792.

SCATTERDAY, J. W. (1974): Reefs and associated assemblages off Bonaire, Netherlands Antilles, and their bearings on Pleistocene and Recent reefs models. – Proceedings of the Second International Coral Reef Symposium, 2. Great Barrier Reef Committee, Brisbane, Dec. 1974: 85-106.

SCHEFFERS, A. (2002a): Paleotsunamis in the Caribbean. Field evidences and datings from Aruba, Curaçao and Bonaire. – Essener Geographische Arbeiten, 33: 185 p.; Essen (Germany).

SCHEFFERS, A. (2002b): Paleotsunami evidences from boulder deposits on Aruba, Curaçao and Bonaire. – Science of Tsunami Hazards, 20 (1): 26-37.

SCHELLMANN, G. & KELLETAT, D. (2001): Chronostratigraphische Untersuchungen litoraler und äolischer Formen und Ablagerungen an der Südküste von Zypern mittels ESR-Altersbestimmungen an Mollusken- und Landschneckenschalen. – Essener Geographische Arbeiten, 32: 75-98; Essen (Germany).

SCHELLMANN, G. & RADTKE, U. (2004): A revised morpho- and chronostratigraphy of Late and Middle Pleistocene coral reef terraces on Southern Barbados (West Indies). – Earth-Science Reviews, 64: 157-187.

SCHELLMANN, G. & RADTKE, U. (2003): Die Datierung litoraler Ablagerungen (Korallenriffe, Strandwälle, Küstendünen) mit Hilfe der Elektronenspin-Resonanz-Methode (ESR). – Essener Geographische Arbeiten, 45: 95-113, Essen (Germany).

SCHELLMANN, G. & RADTKE, U. (2002) with a contribution by F. WHELAN: The coral reef terraces of Barbados - a guide. – Barbados 2002 – International Conference on "Quaternary Sea Level Change" with field trips and 4th annual meeting of IGCP Project 437 " Coastal Environmental Change during sea level highstands: A global synthesis with implications for management of future coastal change". INQUA Commission on Coastlines, IGU Commission on Coastal Systems. 26. October – 2. November 2002, Barbados (W.I.); 118 pp. with numerous figures and tables. – Bamberg (Dep. of Geography).

SCHELLMANN, G. & RADTKE, U. (2001a): Progress in ESR dating of Young and Middle Quaternary corals - a new approach of D_E determination. – Quaternary Science Reviews, 20: 1015-1020.

SCHELLMANN, G. & RADTKE, U. (2001b): Neue Ergebnisse zur Verbreitung und Altersstellung gehobener Korallenriffterrassen im Süden von Barbados. – Bamberger Geographische Schriften, 20: 201-224; Bamberg.

SCHELLMANN, G. & RADTKE, U. (1999): Problems encountered in the determination of dose and dose rate in ESR dating of mollusc shells. – Quaternary Science Reviews, 18: 1515-1527.

SCHELLMANN, G., RADTKE, U., POTTER, E.-K., ESAT, T.M., MCCULLOCH, T.M. (2004): Comparison of ESR and TIMS U/Th dating of marine isotope stage (MIS) 5e, 5c, and 5a coral from Barbados – implication for palaeo sea-level changes in the Caribbean. – Quaternary International, in press.

SCHELLMANN, G., RADTKE, U., POTTER, E.-K., ESAT, T.M., MCCULLOCH, T. & LAMBECK, K. (2002): Comparing ESR and TIMS U/Th age measurements of oxygen isotope stage 5c and 5a coral from Barbados. – LED 2002, 10th International Conference on Luminescence and Electron Spin Resonance Dating, 24.-28. June 2002, Reno (Nevada), Book of Abstracts.

SCHOMBURGK, R. (1848): The history of Barbados. – 722 p.; London.

SCHUHMACHER, H. (1991): Korallenriffe: Verbreitung, Tierwelt, Ökologie. – 4th ed., 275 p.; München (BLV).

SCOFFIN, T.P., STEARN, C.W., BOUCHER, D., FRYDL, P., HAWKINS, C.M., HUNTER, I.G. & MACGEACHY, J.K. (1980): Calcium carbonate budget of a fringing reef on the west coast of Barbados. – Bulletin of Marine Science, 30 (2): 475-508.

SEALEY, N. (1992): Caribbean world. A complete geography. – Cambridge.

SENN, A. (1948): Die Geologie der Insel Barbados, B.W.I. (Kleine Antillen) und die Morphogenese der umliegenden marinen Großformen. – Eclogae geologicae Helvetia, 40(2): 199-222; Basel.

SENN, A. (1946): Geological report of the British Union Oil Co. Ltd. on the geological investigation of groundwater resources of Barbados, B.W.I. (unpublished).

SENN, A. (1944): Remarks on the best procedure for testing the oil possibilities of Barbados, B.W.I., P. II: Geology. – British Union Oil Company, Ltd., Geol. Rep., 8.

SHACKLETON, N.J. & MATTHEWS, R.K. (1977): Oxygen isotope stratigraphy of Late Pleistocene coral terraces in Barbados. – Nature, 268: 618-620.

SHACKLETON, N.J. & OPDYKE, N.D. (1973): Oxygen isotope and paleomagnetic stratigraphy of equatorial Pacific core V28-238, oxygen temperature and ice volumes on a 10,000 and 100,000 year scale. – Quaternary Research, 3: 39-46.

SIDDALL, M., ROHLING, E.J., ALMOGI-LABIN, A., HEMLEBEN, CH., MEISCHNER, D., SCHMELZER, I. & SMEED, D.A. (2003): Sea-level fluctuations during the last glacial cycle. – Nature, 423: 853-858.

SIGURDSSON, H. & CAREY, S. (1991): Caribbean Volcanoes: A Field Guide. – Geological Association of Canada; Toronto.

SIGURDSSON, H., SPARKS, R.S.J., CAREY, S.N. & HUANG, T.C. (1980): Volcanogenic sedimentation in the Lesser Antilles Arc. – Journal of Geology, 88: 523-540.

SMITH, A.L. & ROOBOL, M.J. (1990): Mt. Pelée, Martinique; A study of an Active-Island-Arc Volcano. – Geological Society of America, Memoir 175: 105 p.

SPEED, R.C. (1990): Volume loss and defluidization history of Barbados. – Journal of Geophysical Research, 95 (B6): 8983-8996.

SPEED, R.C. (1983): Structure of the accretionary complex of Barbados, I: Chalky Mount. – Bulletin of the Geological Society of America, 84 (1): 92-116.

SPEED, R.C. (1981): Geology of Barbados: implications for an accretionary origin. – Oceanologica Acta, Suppl. 4: 259-267.

SPEED, R.C. & LARUE, D.K. (1982): Architecture and implications for accretion. – Journal of Geophysical Research, 87(B5): 3633-3643.

SPENCER, J.W.W. (1902): On the geological and physical development of Barbados. – Quart. J. London Geol. Soc., 58: 354-367; London.

SPENCER, T. & VILES, H. (2002): Bioconstruction, bioerosion and disturbance on tropical coasts: coral reefs and rocky limestone shores. – Geomorphology, 48: 23-50.

STEARN, C.W., SCOFFIN, T.P. & MARTINDALE, W. (1977): Calcium carbonate budget of a fringing reef in the west coast of Barbados. – Bulletin of Marine Science, 27 (3): 479-510.

STEARNS, C.E. (1976): Estimates of the position of sea-level between 140,000 and 75,000 years ago. – Quaternary Research, 6: 445-449.

STEARNS, C.E. & THURBER, D.L. (1965): Th-230/U-234 dates of Late Pleistocene marine fossils from Mediterranean and Moroccan littorals. – Quaternaria, 7: 29-42; Rome.

STEINEN, R.P. (1974): Phreatic and vadose diagenetic modification of Pleistocene limestone: Petrographic observations from subsurface of Barbados, West Indies. – The American Association of Petroleum Geologists Bulletin, 58 (6): 1008-1024.

STEINEN, R.P., HARRISON, R.S. & MATTHEWS, R.K. (1973): Eustatic low stand of sea level between 125,000 and 105,000 BP: Evidence from the subsurface of Barbados, West Indies. – Geological Society of America Bulletin, 84: 63-70.

STEINEN, R.P. & MATTHEWS, R.K. (1973): Phreatic vs. vadose diagenesis: Stratigraphy and mineralogy of a cored borehole on Barbados, W. I. – Journal of Sedimentary Petrology, 43 (4): 1012-1020.

STEINEN, R.P., MATTHEWS, R.K. & SEALY, H.A. (1978): Temporal variation in geometry and chemistry of the freshwater phreatic lens: The coastal carbonate aquifer of Christ Church, Barbados, West Indies. – Journal of Sedimentary Petrology, 48 (3): 733-742.

STODDART, D.R. (1990): Coral reefs and islands and predicted sea-level rise. – Progress in Physical Geography, 14: 521-536.

TAYLOR, F. (1974): The uplifted reef tracts of Barbados, West Indies: Detailed mapping and radiometric dating of selected areas. – M.S. Thesis Brown Univ., 235 p.; Philadelphia.

TAYLOR, F.W. & MANN, P. (1991): Late Quaternary folding of coral reef terraces, Barbados. – Geology, 19: 103-106.

TODD, D.L., KEENE, W.C. & MOODY, J.L. (2003): Effects of wet deposition on optical properties of the atmosphere over Bermuda and Barbados. – Journal of Geophysical Research, 108: 1-13.

TORRINI, R.J. (1986): Structure and Kinematics of the Oceanic Nappes of Barbados. – Transactions of the 11th Carribbean Geological Conference Barbados.

TORRINI, R.J. & SPEED, R. (1989): Tectonic wedging in

the forearc basin-accretionary prism transition, Lesser-Antilles forearc. – Journal of Geophysical Research, 94: 10549-10584.

TOSCANO, M.A. & LUNDBERG, J. (1999): Submerged Late Pleistocene reefs on the tectonically stable S.E. Florida margin: high-precision geochronology, stratigraphy, resolution of substage 5a sea-level elevation, and orbital forcing. – Quaternary Science Reviews, 18: 753-767.

TRECHMANN, C.T. (1937): The base and top of the coral-rock in Barbados. – Geological Magazin, 70 (878): 337-358; London.

TRECHMANN, C.T. (1933): The uplift of Barbados. – Geological Magazin, 70 (823): 19-47; London.

TRICART, J. (1968): Notes geomorphologiques sur la karstification en Barbade (Antille). Phénomès karstiques. – Centre de Recherches et Documentation Cartographiques et Géographiques. Memoires et Documents, New Series, 4 : 329-334.

TUSHINGHAM, A.M. & PELTIER, W.R. (1993): Implications of the radiocarbon timescale for ice-sheet chronology and sea-level change. – Quaternary Research, 39: 125-129.

VERNON, K.C. & CARROLL, C.M. (1965): Soil and Land Use Surveys No. 18, Barbados. – Publ. of Imperial College of Tropical Agriculture; Trinidad (West Indies).

VIDETICH, P.E. & MATTHEWS, R.K. (1989): Origin of discontinuity surfaces in limestones: isotopic and petrographic data, Pleistocene of Barbados, West Indies. – Journal of Sedimentary Petrology, 50 (3): 971-980.

WALTHER, R., BARABAS, M. & MANGINI, A. (1992): Basic ESR studies on recent corals. – Quaternary Science Reviews, 11: 191-196.

WANDELT, B. (2000): Geomorphologische Detailkartierung und chronostratigraphische Gliederung der quartären Korallenriffe auf Barbados (West Indies) unter besonderer Berücksichtigung des Karstformenschatzes. – Ph.D., University of Köln (Germany), (unpublished).

WATANABE, T., WINTER, A., OBA, T., ANZAI, R. & ISHIOROSHI, H. (2002): Evaluation of the fidelity of isotope records as an environmental proxy in the coral *Montastrea*. – Coral Reefs, 21: 169-178.

WATTS, D. (1970): Persistence and change in the vegetation of oceanic islands: an example from Barbados, West Indies. – The Canadian Geographer, XIV (2): 91-109.

WATTS, D. (1966): Man's influence on the vegetation of Barbados 1627 to 1800. – Occasional Papers in Geography No. 4; University of Hull Publications.

WEYL, R. (1966): Geologie der Antillen. – 410 p.; Berlin (Borntraeger).

WEYL, R.(1965): Erdgeschichte und Landschaftsbild in Mittelamerika. – Senckenbergische Naturforschende Gesellschaft, 175 p.; Frankfurt/M.

WHITING, B.M., MCFARLAND, D.P. & HACKENBERGER, S. (2001): Three-dimensional GPR study of a prehistoric site in Barbados, West Indies. – Journal of Applied Geophysics, 47: 217-226.

WILSON, M. (1997): The Caribbean environment. – 2nd ed.; Cambridge (England).

WORLD ALMANAC (2002): World almanac and book of facts 2002. – New York.

YOUNG, A. (1976): Tropical soils and soil survey. – Cambridge Geographical Studies; 9.

ZEUNER, F.E. (1959): The Pleistocene period. Its climate, chronology and faunal successions. – (2nd ed.); 447 p.; London.

ZEUNER, F.E. (1958): Dating the past. An introduction to geochronology. – (4th ed.); 516 p.; London.

ZEUNER, F.E. (1945): The Pleistocene period. Its climate, chronology and faunal successions. – 223 p.; London.

KÖLNER GEOGRAPHISCHE ARBEITEN

Herausgegeben vom

GEOGRAPHISCHEN INSTITUT DER UNIVERSITÄT ZU KÖLN

durch

H. BESLER H. BREMER E. BRUNOTTE F. KRAAS J. NIPPER U. RADTKE
K. SCHNEIDER G. SCHWEIZER D. SOYEZ O. TIMMERMANN D. J. WERNER

Schriftleitung: D. WIKTORIN

Heft 1 **KELLERSOHN**, Heinrich (1952):
Untersuchungen zur Morphologie der Talanfänge im mitteleuropäischen Raum. 104 S., 19 Abb., vergriffen.

Heft 2 **REITZENSTEIN**, Ursula (1953):
Das Ruhrkohlengebiet im Vest Recklinghausen zwischen Emscher und Lippe. 102 S., 13 Abb., vergriffen.

Heft 3 **BRUX**, Hedwig (1952):
Standortfragen der neueren Wohnsiedlungen am Beispiel der Städte Köln und Essen. 73 S., 2 Abb., vergriffen.

Heft 4 **KNAPP**, Rüdiger (1953):
Studien zur Vegetation und pflanzengeographischen Gliederung Nordwest-Italiens und der Süd-Schweiz. 59 S., 3 Abb., vergriffen.

Heft 5 **HERMES**, Karl (1955):
Die Lage der oberen Waldgrenze in den Gebirgen der Erde und ihr Abstand zur Schneegrenze. 277 S., 4 Karten u. 4 Tafeln in bes. Mappe, vergriffen.

Heft 6/7 **WEIGT**, Ernst (1955):
Europäer in Ostafrika - Klimabedingungen und Wirtschaftsgrundlagen. XIV u. 385 S., 37 Karten u. Fig., 30 Abb., vergriffen.

Heft 8 **DREHWALD**, Hans Rudolf (1955):
Zur Entstehung der Spillways in Nord-England und Süd-Schottland. Eine allgemeine und regionale Untersuchung. 82 S., 24 Karten u. Abb., vergriffen.

Heft 9/10 **UHLIG**, Harald (1956):
Die Kulturlandschaft - Methoden der Forschung und das Beispiel Nordostengland. VI u. 355 S., 2 Karten, 56 Abb., vergriffen.

Heft 11 **JANSEN**, Hans (1957):
Die sozial- und siedlungsgeographische Entwicklung im westlichen Jülicher Land. 116 S., 15 Karten, 16 Abb., vergriffen.

Heft 12 **WIEGELMANN**, Günter (1958):
Natürliche Gunst und Ungunst im Wandel rheinischer Agrarlandschaften. 220 S., 16 Karten, 11 Abb., vergriffen.

Heft 13 **ZSCHOCKE**, Reinhart (1959):
Siedlung und Flur der Kölner Ackerebene zwischen Rhein und Ville. 132 S., 10 Karten, 17 Abb., vergriffen.

Heft 14 **BIRKENHAUER**, Josef (1960):
Die Eifel in ihrer Individualität und Gliederung. 210 S., 16 Karten, 4 Profile, 16 Abb., vergriffen.

Heft 15 **KARGER**, Adolf (1963):
Die Entwicklung der Siedlungen im westlichen Slavonien. 120 S., 15 Karten, 4 Tafeln, (Franz Steiner Verlag GmbH, Wiesbaden) € 14.-

Heft 16 **ZSCHOCKE**, Herlig (1963):
Die Waldhufensiedlungen am linken deutschen Niederrhein. 82 S., 20 Karten, vergriffen.

Heft 17 **DÖRRENHAUS**, Fritz (1966):
Der Ritten und seine Erdpyramiden.
BECKER, Hans (1966):
Vergleichende Betrachtung der Entstehung von Erdpyramiden in verschiedenen Klimagebieten der Erde. X u. 112 S., 6 Karten, 16 Tafeln, 11 Fig., € 14.-

Heft 18 **BARTEL**, Jürgen (1966):
Baum und Strauch in der rheinischen Agrarlandschaft. 84 S., 8 Karten, 31 Abb., vergriffen.

Heft 19 **KLASEN**, Jürgen (1967):
Vergleichende Landschaftskunde der englischen Marschen. 331 S., 88 Abb., vergriffen.

Heft 20 **SIMONS**, Peter (1968):
Die Entwicklung des Anbaus und die Verbreitung der Nutzpflanzen in der ägyptischen Nilstromoase von 1800 bis zur Gegenwart. Eine agrargeographische Untersuchung. 218 S., 47 Karten, 36 Fotos, u. zahlr. Tab., € 6.-

Heft 21 **RICHTER**, Werner (1969):
Historische Entwicklung und junger Wandel der Agrarlandschaft Israels, dargestellt am Beispiel Nordgaliläas. 360 S., 65 Karten, 28 Abb., zahlr. Tab., vergriffen.

Heft 22 **ZSCHOCKE**, Reinhart (1969):
Siedlungsgeographische Untersuchungen der Gehöferschaften im Bereich von Saar-Ruwer-Prims. 79 S., 8 Karten, mehrere Tab., vergriffen.

Heft 23 **SCHMITZ**, Helge (1969):
Glazialmorphologische Untersuchungen im Bergland Nordwestspaniens (Galicien/Léon). 144 S., 7 Karten, 1 Profil, 26 Abb., € 10.-

Heft 24 **ZSCHOCKE**, Reinhart (1970):
Die Kulturlandschaft des Hunsrücks und seiner Randlandschaften in der Gegenwart und in ihrer historischen Entwicklung. XI u. 254 S., 34 Karten, 12 Abb., (Franz Steiner Verlag GmbH, Wiesbaden) vergriffen.

Heft 25 **SCHACHT**, Siegfried (1971):
Drei ausgewählte Reisbaulandschaften im westlichen Mittelmeergebiet (Küstenhof von Valencia, Sadobecken, Camargue). 199 S., 26 Abb., 29 Fotos, vergriffen.

Heft 26 **KOCH**, Wilfried (1971):
Funktionale Strukturwandlungen in Taiwan. Das Beispiel Luchou im Umland der Millionenstadt Taipei. 261 S., 10 Karten, 5 Abb., 35 Fotos, € 21.-

Sonderband FORSCHUNGEN ZUR ALLGEMEINEN UND REGIONALEN GEOGRAPHIE (1971):
Festschrift für Kurt Kayser zur Vollendung des 65. Lebensjahres. XXXIII u. 448 S., 31 Karten, 14 Fig., 36 Abb., (Franz Steiner Verlag GmbH, Wiesbaden) € 43.-

Heft 27 SCHLÜSSEL, Peter (1972):
Entwicklungen im Einflußbereich der Großstadt, dargestellt am Beispiel der Stadtrandgemeinde Lövenich bei Köln. 297 S., 16 Karten, 30 Fotos, zahlr. Tab., statistischer Anhang, € 19.-

Heft 28 KURSAWE, Hans-Dieter (1973):
Monheim, neue Stadtentwicklung zwischen den Großstädten. 263 S., 38 Abb., 14 Fotos, € 10.-

Heft 29 HENKEL, Gerhard (1973):
Die Wüstungen des Sintfeldes. Eine historisch-geographische Untersuchung zur Genese einer alten westfälischen Kulturlandschaft. 156 S., 28 Abb., 28 Fotos, vergriffen.

Heft 30 IM DIENSTE DER GEOGRAPHIE UND KARTOGRAPHIE (1973):
Symposium Emil Meynen. VI u. 107 S., 1 Karte, 3 Abb., 5 Fotos, € 7.-

Heft 31 BECKER, Hans (1974):
Das Land zwischen Etsch und Piave als Begegnungsraum von Deutschen, Ladinern und Italienern in den südlichen Ostalpen. 200 S., 20 Karten, 12 Fig., 29 Abb., € 29.-

Heft 32 NÖLLE, Fritz W. (1975):
Siegburg und Troisdorf. Die Entwicklung zweier Nachbarstädte an der unteren Sieg. XV u. 312 S., 52 Tab., 43 Abb., 14 Bilder, € 11.-

Heft 33 SABELBERG, Elmar (1975):
Der Zerfall der Mezzadria in der Toskana urbana. Entstehung, Bedeutung und gegenwärtige Auflösung eines agraren Betriebssystems in Mittelitalien. 260 S., 43 Abb., 16 Fotos, € 13.-

Heft 34 MATHEMATISCHE VORHERSAGEMODELLE ZUR GEWÄSSERGÜTE (1976):
SYMADER, Wolfhard: Multivariate Nährstoffuntersuchungen zu Vorhersagezwecken in Fließgewässern am Nordrand der Eifel.
RUMP, Hans Hermann: Mathematische Vorhersagemodelle für Pestizide und Schadstoffe in Gewässern der Niederrheinischen Bucht und der Nordeifel. 276 S., 1 Karte, 19 Abb., 48 Tab., € 10.-

Heft 35 STRAHL, Dorothea (1977):
Sozial-ökonomische Wertmaßstäbe und ihre Wandelbarkeit im ländlichen Raum. Untersucht an Beispielen aus dem Dollendorfer und Hillesheimer Kalkgebiet und der östlichen Hocheifel. 221 S., 1 Karte, 4 Beil., 5 Fig., € 10.-

Heft 36 BREMER, Hanna und **PFEFFER**, Karl-Heinz (Hrsg.) (1978):
Zur Landschaftsentwicklung der Eifel. Beiträge zur Geologie, Bodenkunde und Geomorphologie. 255 S., 40 Abb., 7 Tab., 6 Beil., vergriffen.

Heft 37 HEGNER, Rüdiger (1979):
Nichtimmergrüne Waldformationen der Tropen. Untersuchungen zu ihrer Typologie und Verbreitung. 410 S., 57 Abb., 64 Tab., € 15.-

Heft 38 ZENSES, Elisabeth (1980):
Reliefentwicklung in der nördlichen Eifel. 220 S., 17 Abb., 10 Karten, € 14.-

Heft 39 KUPPELS, Inge (1981):
Die Karstspalten der Schwäbischen Alb als Leitformen für die Morphogenese. 221 S., 13 Abb., 16 Tab., 12 Karten, vergriffen.

Heft 40 TOPOROWSKY, Norbert (1982):
Zentrale Orte und zentralörtliche Beziehungen in der Nordeifel und ihrem Bördenvorland vom Ende des 18. Jahrhunderts bis zur Gegenwart. VIII u. 218 S., 35 Tab., 8 Karten, vergriffen.

Heft 41 SCHMIDT, Siegfried (1982):
Wandlungen von Gefügemustern und Wirtschaftsformen im ländlichen Raum der südwestlichen Rheinbacher Lößplatte zwischen 1660 und 1830. 360 S., 10 Karten, 16 Tab., € 16.-

Heft 42 BURGER, Dieter (1982):
Reliefgenese und Hangentwicklung im Gebiet zwischen Sayn und Wied. 139 S., 83 Fig., 12 Tab., € 10.-

Heft 43 NICKE, Herbert (1983):
Reliefgenese des südlichen Bergischen Landes zwischen Wupper und Sieg. 286 S., 25 Abb., 2 Karten, 6 Profile, € 15.-

Heft 44 ARENTZ, Ludwig (1983):
Nährstoffe und Spurenelemente in Böden der Vulkaneifel. Eine landschaftsökologische Untersuchung mit Hilfe multivariater statistischer Verfahren. 247 S., 47 Abb., 16 Tab., € 12.-

Heft 45 EK, Camille und **PFEFFER**, Karl-Heinz (Hrsg.) (1984):
Le karst belge / Karstphänomene in Nordrhein-Westfalen. 583 S., 137 Abb., 23 Tab., 34 Fotos, € 23.-

Heft 46 JUNGE, Harald (1987):
Reliefgenerationen und Petrovarianz im Norden der Eifeler Nord-Süd-Zone. 245 S., 11 Tab., 32 Abb., 5 Tafeln, vergriffen.

Heft 47 ZEHNER, Klaus (1987):
Stadtteile und Zentren in Köln. Eine sozialgeographische Untersuchung zu Raumstruktur und räumlichem Verhalten in der Großstadt. IX u. 171 S., 17 Karten, 23 Tab., 16 Abb., vergriffen.

Heft 48 KUBINIOK, Jochen (1988):
Kristallinvergrusung an Beispielen aus Südostaustralien und deutschen Mittelgebirgen. 178 S., 10 Karten, 27 Abb., 7 Fotos, € 12.-

Heft 49 JANUS, Ursula (1988):
Löß der südlichen Niederrheinischen Bucht. 174 S., 3 Karten, 5 Tab., 31 Abb., € 12.-

Heft 50 ZENSES, Elisabeth (1989):
Kaltzeitliche Überformung des Altreliefs in Süd- und Zentral-Wales im Vergleich zur Nord-Eifel. 148 S., 13 Karten, 12 Tab., 33 Abb., € 12.-.

Heft 51 **BREITBACH**, Thomas (1989):
Basaltschuttdecken in der Hocheifel. Indikatoren pleistozäner Reliefüberprägung. Mit Vergleichsuntersuchungen im Hessischen Bergland. 265 S., 5 Tab., 41 Abb., € 15.-

Heft 52 **BORGER**, Harald (1990):
Bohnerze und Quarzsande als Indikatoren paläogeographischer Verwitterungsprozesse und der Altreliefgenese östlich von Albstadt (Schwäbische Alb). XII u. 209 S., 11 Karten, 18 Tab., 38 Abb., 35 Fotos, € 17.-

Heft 53 **FLORIAN**, Andrea-Johanna (1990):
Passagen. Ein Beispiel innerstädtischer Revitalisierung im Interessenkonflikt zwischen Stadtentwicklung und Einzelhandel. 223 S., 72 Tab., 14 Abb., € 15.-

Heft 54 **NUTZ**, Manfred (1991):
Räumliche Mobilität der Studierenden und Struktur des Hochschulwesens in der Bundesrepublik Deutschland. Eine Analyse des Entscheidungsverhaltens bei der Studienortwahl und der Einzugsgebiete der Universitäten. X u. 191 S., 29 Karten, 10 Tab., 23 Abb., € 16.-

Heft 55 **RIETHER**, Norbert (1991):
Geomorphologische Prozesse im Lichte von Sedimenten aus dem westlichen Sri Lanka. 236 S., 40 Tab., 104 Abb., € 17.-

Heft 56 **WÜRZ**, Axel (1992):
Die Vegetation der Moore Südtirols. IX u. 97 S., 54 Tab., 6 Abb., € 16.-

Heft 57 **NIPPER**, Josef & **NUTZ**, Manfred (Hrsg.) unter Mitarb. v. Dorothea **WIKTORIN** (1993):
Kriegszerstörung und Wiederaufbau deutscher Städte. Geographische Studien zu Schadensausmaß und Bevölkerungsschutz im Zweiten Weltkrieg, zu Wiederaufbauideen und Aufbaurealität. VIII u. 228 S., zahlr. Karten, Tab., Abb. u. Fotos, vergriffen.

Heft 58 **REUBER**, Paul (1993):
Heimat in der Großstadt. Eine sozialgeographische Studie zu Raumbezug und Entstehung von Ortsbindung am Beispiel Kölns und seiner Stadtviertel. X u. 154 S., 7 Karten, 7 Tab., 38 Abb., vergriffen.

Heft 59 **WEISS**, Günther (1993):
Heimat vor den Toren der Großstadt. Eine sozialgeographische Studie zu raumbezogener Bindung und Bewertung in Randgebieten des Verdichtungsraums am Beispiel des Umlandes von Köln. X u. 176 S., 6 Karten, 20 Abb., € 17.-

Heft 60 **SACHS**, Klaus (1993):
Ortsbindung von Ausländern. Eine sozialgeographische Untersuchung zur Bedeutung der Großstadt als Heimatraum für ausländische Arbeitnehmer am Beispiel von Köln. XII u. 138 S., 3 Karten, 8 Tab., 16 Abb., € 17.-

Heft 61 **GEBHARDT**, Hans & **SCHWEIZER**, Günther (Hrsg.) unter Mitarb. v. Paul **REUBER** (1995):
Zuhause in der Großstadt. Ortsbindung und räumliche Identifikation im Verdichtungsraum. Mit Beiträgen von H. Gebhardt, P. Reuber, K. Sachs, G. Schweizer, B.-A. Stegmann, G. Weiss, K. Zehner. VIII u. 107 S., zahlr. Karten, Tab. u. Abb., € 17.-

Heft 62 **ALISCH**, Matthias (1995):
Das äolische Relief der mittleren Oberen Allerniederung (Ostniedersachsen) - spät- und postglaziale Morphogenese, Ausdehnung und Festlegung historischer Wehsande, Sandabgrabungen und Schutzaspekte. IX u. 176 S., 5 Karten teilw. farbig, 13 Tab., 41 Abb., 10 Fotos, € 19.-

Heft 63 **BRUNOTTE**, Ernst; **IMMENDORF**, Ralf & **SCHLIMM**, Reinhold (1994):
Die Naturlandschaft und ihre Umgestaltung durch den Menschen. Erläuterungen zur Hochschulexkursionskarte Köln und Umgebung. Mit Beiträgen von A.J. Kalis & J. Meurers-Balke und Chr. Wallossek. VIII u. 123 S., 23 Karten, 1 farbige Kartenbeilage, 11 Tab., 20 Abb., € 18.-

Heft 64 **VERJANS**, Theo (1995):
Vergleichende vegetationskundlich-ökologische Studien in der alpinen Stufe des Latemar und Rosengarten (Prov. Bozen und Trient) auf der Grundlage pflanzensoziologischer und pedologischer Erhebungen. X u. 98 S., 45 Tab., 70 Abb., 12 Anlagen, vergriffen.

Heft 65 **WALLOSSEK**, Christoph & **WÜRZ**, Axel (Hrsg.) (1995):
Studien zur Biogeographie, Geoökologie und Umweltbelastung. VII u. 136 S., zahlr. Karten, Tab. u. Abb., € 17.-

Heft 66 **RADTKE**, Ulrich (Hrsg.) (1995):
Vom Südatlantik bis zur Ostsee - neue Ergebnisse der Meeres- und Küstenforschung. Beiträge der 13. Jahrestagung des Arbeitskreises Geographie der Meere und Küsten vom 25.-27. Mai 1995 in Köln. VI u. 242 S., zahlr. Karten, Tab., Abb. u. Fotos, € 19.-

Heft 67 **MANZ**, Hermann Heinrich (1995):
Der Wiederaufbau der Zentren der beiden Städte Magdeburg und Hannover nach dem Zweiten Weltkrieg. Ein Vergleich der politischen Hintergründe, der Aufbauziele, der Planungen und deren Realisation. IV u. 165 S., 67 Abb., 20 Fotos, € 17.-

Heft 68 **STEGMANN**, Bernd-Achim (1997):
Großstadt im Image. Eine wahrnehmungsgeographische Studie zu raumbezogenen Images und zum Imagemarketing in Printmedien am Beispiel Kölns und seiner Stadtviertel. XII u. 219 S., 10 Tab., 19 Abb., 6 Karten, vergriffen.

Heft 69 **SOYEZ**, Dietrich & **BAUER**, Jutta (Hrsg.) (1998):
Luftbildauswertung als angewandte Umweltforschung. VII u. 146 S., zahlr. Karten, Tab. u. Abb., € 18.-

Heft 70 **RADTKE**, Ulrich (Hrsg.) (1998):
Lumineszenzdatierung äolischer Sedimente. Beiträge zur Genese und Altersstellung jungquartärer Dünen und Lösse in Deutschland. VIII u. 124 S., zahlr. Karten, Tab. u. Abb., € 17.-

Heft 71 **HÖHMANN**, Marc (1999):
Flächenrecycling als raumwirksame Interaktion. Eine politisch-geographische Untersuchung über Entscheidungsstrukturen und Konfliktpotentiale räumlicher Veränderungen am Beispiel von Köln. VIII u. 125 S., 16 Abb., 7 Karten, 7 Fotos, € 17.-

Heft 72 **BUBENZER**, Olaf (1999):
Sedimentfallen als Zeugen der spät- und postglazialen Hang- und Talbodenentwicklung im Einzugsgebiet der Schwülme (Südniedersachsen). X u. 132 S., 53 Abb., 7 Karten, 16 Tab., € 18.-

Heft 73 **WIKTORIN**, Dorothea (2000):
Grundeigentum und Stadtentwicklung nach der Wende. Räumliche Wirkungen der Transformation von Grundeigentumsverhältnissen seit 1990 am Beispiel der Innenstadt und Äußeren Neustadt von Dresden. VIII u. 151 S., 20 Abb., 10 Tab., € 18.-

Heft 74 **WALLOSSEK**, Christoph (2000):
Der Buntschwingel (*Festuca varia* agg., *Poaceae*) im Alpenraum. Untersuchungen zur Taxonomie, Verbreitung, Ökologie und Phytosoziologie einer kritischen Artengruppe. XII u. 142 S., 45 Abb., 30 Tab., 19 Fotos, € 18.-

Heft 75 **KNUPP**, Marcus (2001):
Wochenmärkte im Jemen. Ein traditionelles Versorgungssystem als Indikator gesellschaftlichen Wandels. XIV u. 152 S., 11 Abb., 9 Karten, 29 Tab., 16 Fotos, € 18.-

Heft 76 **SOYEZ**, Dietrich & **SCHULZ**, Christian (Hrsg.) (2002): Wirtschaftgeographie und Umweltproblematik. VI u. 118 S., zahlr. Tab. u. Abb., € 18.-

Heft 77 **BOLLIG**, Michael, **BRUNOTTE**, Ernst & **BECKER**, Thorsten (Hrsg.) (2002):
Interdisziplinäre Perspektiven zu Kultur- und Landschaftswandel im ariden und semiariden Nordwest Namibia. VI u. 219 S., zahlr. Tab., Abb., Karten u. Fotos, € 25.-

Heft 78 **THÖNNESSEN**, Manfred (2002):
Elementdynamik in fassadenbegrünendem Wilden Wein (*Parthenocissus tricuspidata*). XII u. 113 S., 30 Abb. u. Fotos, 51 Tab., € 18.-

Heft 79 **SPRUNKEL**, Elke (2003): Vegetationskundlich-ökologische Untersuchungen in Kiesgruben des Kölner Stadtgebietes unter besonderer Berücksichtigung der Naturschutzproblematik im Verdichtungsraum. X u. 188 S., 45 Abb., 47 Tab., Anhang: 34 Tab., 8 Karten. CD-Rom Publikation, € 12.-

Heft 80 **BUBENZER**, Olaf (Hrsg.) (2003):
Studien zur Angewandten Geomorphologie und Landschaftsforschung. VI u. 110 S., 43 Abb., 10 Tab., € 18.-

Heft 81 **SCHELLMANN**, Gerhard **&** **RADTKE**, Ulrich, with contributions by Franziska Whelan (2004): The marine Quaternary of Barbados. XII u. 137 S., zahlr. Tab. u. Abb., € 30.-

Bezug: KÖLNER GEOGRAPHISCHE ARBEITEN
Geographisches Institut, Universität zu Köln
Albertus-Magnus-Platz, D - 50 923 K ö l n
Telefax 0221 / 470-4917
E-mail: ade85@uni-koeln.de

Palaeo sea level change is one of the most challenging issues in marine science. The knowledge about this topic has increased tremendously during the last forty years. However, numerous problems concerning concepts and theories of sea level change remain or have been detected recently.

Barbados has been the Mecca for sea level research since Mesolella's benchmark studies published in 1968. Numerous subsequent publications focused on the history of sea level change of Barbados. This textbook illustrates the history of sea level research on Barbados and presents new geomorphic and geochronologic investigations of Barbados' fossil coral reef terraces. The textbook comprises six chapters, ranging from a general overview to detailed morphostratigraphic descriptions. Furthermore, this publication presents perspectives for future research related to the reconstruction of palaeo sea levels and palaeo sea level change on Barbados and in the Caribbean.